

Attachment 5b

BAW-10219
REV. 04
DECEMBER 2000

**ELECTROSLEEVING QUALIFICATION
FOR PWR RECIRCULATING STEAM
GENERATOR TUBE REPAIR**

FRAMATOME TECHNOLOGIES, INC.
P.O. BOX 10935
LYNCHBURG, VA 24506-0935

COPY NO. 4

FTI NON-PROPRIETARY

This document is the non-proprietary version of the proprietary document BAW-10219P-04. In order for this document to meet the non-proprietary criteria, certain blocks of information were with-held based on the following criteria.

- (b) The information reveals data or material concerning FTI research or development plans or programs of present or potential competitive advantage to FTI.**
- (c) The use of the information by a competitor would decrease his expenditures, in time or resources, in designing, producing or marketing a similar product.**
- (d) The information consists of test data or other similar data concerning a process, method or component, the application of which results in a competitive advantage to FTI.**
- (e) The information reveals special aspects of a process method, component or the like, the exclusive use of which results in a competitive advantage to FTI.**

**BAW-10219
REV. 04
DECEMBER 2000**

**ELECTROSLEEVING QUALIFICATION
FOR PWR RECIRCULATING STEAM
GENERATOR TUBE REPAIR**

NON-PROPRIETARY

**FRAMATOME TECHNOLOGIES, INC.
P.O. BOX 10935
LYNCHBURG, VA 24506-0935**

FTI NON-PROPRIETARY

This document is the non-proprietary version of the proprietary document BAW-10219P-04. In order for this document to meet the non-proprietary criteria, certain blocks of information were with-held based on the following criteria.

- (b) The information reveals data or material concerning FTI research or development plans or programs of present or potential competitive advantage to FTI.**
- (c) The use of the information by a competitor would decrease his expenditures, in time or resources, in designing, producing or marketing a similar product.**
- (d) The information consists of test data or other similar data concerning a process, method or component, the application of which results in a competitive advantage to FTI.**
- (e) The information reveals special aspects of a process method, component or the like, the exclusive use of which results in a competitive advantage to FTI.**

RECORD OF REVISION

<u>Rev/Date</u>	<u>Section</u>	<u>Description</u>
04 12/2000	1.0	Added statement on UT peer review.
	3.0	Added update on Electrosleeve™ experience in Pickering, March 1999 UT results.
	4.0	Added code case to procedure qualification in Table 4.2.1.
	4.3	Added reference to Appendix B.
	5.1	Added "or" to Sleeve Length in Table 5.1.1 where two lengths are presented. Added regions to Figure 5.1.1.
	6.4	Revised number of data points from fatigue testing. Added description on development of design fatigue curve. Added additional high cycle data results and Design Fatigue Curve in Figure 6.4.1 Added Reference 13.34 for fatigue curve adjustment to define Design curve.
	6.5	Added Reference 13.83, (Argonne Labs Testing) to first paragraph.
	7.5	Revised number of samples for thermal shock.
	8.1	Added "44F, 51F, 51M" in Table 8.1.1. Added "Design Dimensions".
	8.4	Revised notes in Table 8.4.1 to state sleeve length in calculation.
	8.5	Added region information in second paragraph. Added nominal to sleeve thickness in Table 8.5.1 and 8.5.2. Removed footnote ⁽⁴⁾ which applied to Revision 3 of topical. Added 1.43 ΔP Allowable Defects, Table 8.5.2. Added regions to Figure 8.5.2. Added sleeve "ID Pit, Structural, Leakage" in Table 8.5.3. Added burst pressure information for ID pits.

RECORD OF REVISION (Cont'd)

<u>Rev/Date</u>	<u>Section</u>	<u>Description</u>
		Revised Table 8.5.4.
		Added Figure 8.5.3 and Table 8.5.5.
	9.5	Added Reference 13.49 (Argonne Labs, Corrosion Behavior Review).
	10.1.5	Information on honing. Enclosure 2, 5/20/98, Concern #14.
	10.8	Added alternative words to Waste Processing.
	11.0	Editorial revisions to reference EPRI Appendix J Peer reviews.
		Addition of OD length detection/sizing and OD SCC depth sizing.
	12.2.2	Additional description of ID pit. Added figure.
	12.4	Deleted Section 12.4 and renumbered 12.5 to 12.4.
		Revised tables for RMSE and 95% LCL.
		Revised Table 12.4.2 for 30% sleeve plugging limit and tube inspection for ID sleeve pits.
	13.0	Added revision level to 13.4.
		Added Reference 13.34 (Fatigue Curve).
		Added Reference 13.49 (Argonne Labs Corrosion Review)
		Added References 13.76 - 13.82 (EPRI Peer Review of UT Procedures).
		Added Reference 13.83 (Argonne Labs Report, NUREG1CR-6664 AM-99/23/August 2000.)
	B	Added Appendix B.

RECORD OF REVISION (Cont'd)

<u>Rev/Date</u>	<u>Section</u>	<u>Description</u>
03/ 10/98	ALL	The text has been completely rewritten and includes additional test results, analyses, and nondestructive examination qualification. The following Requests for Additional Information (referenced by NRC request date) have been incorporated.
		<u>RAI 7/2/96</u>
	Question 1	Section 6.5
	Question 2	Sections 6.6 and 8.6
	Question 3	Sections 6.6 and 7.4
	Question 5	Sections 10.4 and 11.8 (new sample sets)
	Question 6	Sections 11.8 and 11.9 (new sample sets)
		<u>RAI 7/25/96</u>
	Question 1	Section 11.9
	Question 2	Sections 11.8 thru 11.10 and Section 12 (new sample sets)
	Question 3	Sections 11.2.1 and 11.8 (new sample sets)
	Question 4	Section 11.8.5 (new sample set)
	Question 5	Table 12.5.2
	Question 6	Sections 6.3, 10.1.2, and 10.7
	Question 7	Sections 3 and 4
	Question 8	Sections 6.3, 10.1.2, and 10.2
	Question 9	Sections 10.3 and 10.4
	Question 10	Sections 10.3 and 10.4
	Question 11	Sections 3 and 11.10
		<u>RAI 12/17/96</u>
	Question 1	Sections 11.2.1, 11.7, and 11.9
	Question 2	Sections 8.5, 11.8 thru 11.10 (new sample sets) and Section 12
	Question 3	Section 11.2.1 and 11.8 thru 11.12 (new sample sets)
	Question 4	Section 11.8 (new sample sets) and Table 12.5.2
	Question 5	Sections 11.2.4 and 11.2.5
	Question 6	Sections 11.3 and 11.9
	Question 7	Sections 11.10 and Section 12
03/ 10/98		<u>RAI 4/28/97</u>
	Question 1	Sections 11.9, 11.11, and 11.12
	Question 2	Table 12.5.3
	Question 3	Table 11.9.3 and Section 11.9.10
	Question 5	Section 7.5

RECORD OF REVISION (Cont'd)

<u>Rev/Date</u>	<u>Section</u>	<u>Description</u>
	Question 6	Tables 11.9.2, 11.9.6, 11.9.7 and Section 11.9.3
	Question 7	Section 11.8.5 and Table 11.8.13 (new sample set)
	Question 9	Table 3.1
	Question 10	Sections 11.8 thru 11.12 (new sample sets) and Section 12
	<u>RAI 8/13/97</u>	
	Question 1	Sections 11.9 thru 11.11 and Section 12
	Question 2	Section 12
	Question 4	Section 11.7, 11.9, and 11.10
	Question 5	Section 11.9
	Question 6	Section 11.10
	<u>RAI 12/12/97</u>	
	Question 1	Sections 11.7.3, 11.9 and 11.11
	Question 4	Section 11.3.3 and 11.9.3
	Question 5	Section 11.7.3
	Question 7	Sections 5, 8, 10, 11, and 12 (primarily)
	Question 9	Section 11.4.2
	Question 10	Table 11.9.1
	Question 11	Section 11.9.3
	Question 12	Section 8.5 and Section 12
	Question 13	Sections 11.8 thru 11.11 (new sample sets)
	Question 14	Section 11.7.3 and 11.11
	Question 15	Section 11.10

While not all inclusive, the following changes provide technical information to clarify the qualification of the repair process.

3.0

Table 3.1 Updated nickel sleeve installation.

03/ 10/98

4.0

4.2 Added Reference to 5/8" tubing.
Table 4.2.1 Added Code Case N-569.

5.0

5.2 Expanded installation steps description, added process variable monitoring.

8.0

8.2

Table 8.5.1

Added information related to peripheral tube.

Revised to reflect structural limits for TSP peripheral tubes near wrapper wedge supports.

Figure 8.5.1

Added normalized burst pressure correlation.

9.0

9.2.2.4

Added Section.

9.4

Added Section.

10.0

10.1

Added reference to Code Case N-569.

10.3

Added Section.

10.4

Added Section.

10.8

Added Section.

12.0

New Section.

13.0

Was Section 12 in Rev. 01.

TABLE OF CONTENTS

	<u>PAGE</u>
1.0 EXECUTIVE SUMMARY	1-1
2.0 INTRODUCTION	2-1
3.0 BACKGROUND	3-1
4.0 DESIGN CRITERIA	4-1
4.1 Qualification Methodology	4-1
4.2 Design and Qualification Requirements	4-3
4.3 Sleeve Design Conditions	4-5
5.0 SLEEVE DESIGN	5-1
5.1 Design Description	5-1
5.2 Process Description	5-5
6.0 DESIGN VERIFICATION - MATERIAL PROPERTIES	6-1
6.1 Tensile Strength	6-1
6.2 Modulus of Elasticity	6-4
6.3 Ductility/Adhesion	6-6
6.4 Fatigue Life	6-8
6.5 Thermal Stability	6-10
6.6 Creep Properties	6-18
6.7 Burst Strength	6-29
6.8 Thermodynamic Properties	6-31
7.0 DESIGN VERIFICATION - MECHANICAL TESTING	7-1
7.1 Locked Tube Testing	7-1
7.2 Fatigue Testing	7-4
7.3 Testing of Degraded Sleeves	7-8
7.4 Creep-Fatigue Experimental Analysis	7-18
7.5 Leak Testing of Minimum Bond Length	7-21
7.6 Tube-to-Tubesheet Pull-Out Load Testing	7-21
7.7 Mechanical Testing Summary	7-22
8.0 DESIGN VERIFICATION - ANALYSES	8-1
8.1 Pressure Boundary Thickness	8-1
8.2 Fatigue Test Loads	8-3
8.3 Flow-Induced Vibration	8-11
8.4 Thermal/Hydraulic	8-13
8.5 Sleeve Structural Limits	8-15

TABLE OF CONTENTS (Cont'd)

	<u>PAGE</u>
8.0 DESIGN VERIFICATION - ANALYSES (Cont'd)	
8.6 Creep Analysis	8-25
8.7 Design Summary	8-37
9.0 DESIGN VERIFICATION - CORROSION	9-1
9.1 General Corrosion Properties	9-1
9.2 Primary Side Corrosion Evaluation	9-9
9.3 Secondary Side Corrosion Evaluation	9-23
9.4 Exposure to Mercury at Room Temperature	9-50
9.5 Corrosion Evaluation Summary	9-51
10.0 SLEEVE INSTALLATION	10-1
10.1 Installation Procedure	10-1
10.2 Process Verification	10-3
10.3 Electrosleeving Chemical Procurement and Quality Assurance Process	10-4
10.4 Electrosleeving Process Detrimental Materials Control	10-5
10.5 Installation System/Tooling	10-6
10.6 ALARA	10-10
10.7 Sleeving Experience	10-12
10.8 Waste Processing	10-13
11.0 NONDESTRUCTIVE EXAMINATION	11-1
11.1 NDE Requirements	11-1
11.2 NDE Methodology Evaluation	11-4
11.3 Ultrasonic Testing Background	11-8
11.4 Ultrasonic System Description	11-11
11.5 UT Acquisition Parameters	11-16
11.6 UT Data Presentation	11-17
11.7 UT Analysis Techniques	11-21
11.8 Qualification Program for Longitudinal Wave UT	11-31
11.9 Qualification Program for Shear Wave UT	11-57
11.10 UT Qualification Results	11-70
11.13 NDE Qualification Conclusions	11-73
12.0 PLUGGING LIMIT DEFINITION	12-1
12.1 Repair Limit for Uniform Thinning Degradation	12-2
12.2 Repair Limit for Sleeve Pitting and Disbond	12-3
12.3 Repair Limit for Cracking Degradation	12-6
12.4 Electrosleeve™ Plugging Limits	12-8

TABLE OF CONTENTS (Cont'd)

	<u>PAGE</u>
13.0 REFERENCES	13-1
Appendix A PWR DESIGN INFORMATION	A-1
Appendix B SITE SPECIFIC LICENSING AMENDMENT REQUEST SUMMARY	B-1

LIST OF TABLES

	<u>PAGE</u>	
3.1	Steam Generator Nickel Plating and Electrosleeving Experience	3-7
4.2.1	Summary of Applicable Codes and Standards	4-4
5.1.1	Steam Generator Tube and Electrosleeve™ Nominal Dimensions	5-1
5.2.1	Process Variables	5-6
6.1.1	ASME Code, Section III, Minimum Design Strength Values	6-3
6.4.1	Fatigue Testing Results	6-10
6.5.1	Summary of Microhardness Determination on Strain-Annealed Electrosleeves	6-17
6.6.1	Creep Test Specimens - Constant Axial Load Creep Test	6-23
6.7.1	FTI Burst Test Results at Room Temperature	6-30
6.7.2	OHT Burst Test Results at 581°F	6-30
7.1.1	Locked Tube Test Results	7-3
7.1.2	Calculated Loads for Locked Tubes	7-3
7.2.1	Fatigue Testing Specimens	7-6
7.2.2	Summary of Minimum Bond Fatigue Test Load Ranges	7-7
7.3.1	Plugging Criteria Fatigue Test Specimens	7-11
7.3.2	Circumferential Defect Fatigue Test Loads	7-12
7.3.3	Axial Defect Fatigue Test Loads	7-14
7.3.4	Fatigue Inspection Interval [] ^{c,e}	7-15
7.3.5	Plugging Criteria Burst Specimens	7-17
7.4.1	Creep-Fatigue Testing Results	7-19
8.1.1	Tube/Sleeve Dimensions	8-2
8.1.2	Primary Membrane Stress Intensity Range	8-3
8.2.1	Summary of Minimum Bond Fatigue Test Load Ranges	8-7

LIST OF TABLES (Cont'd)

	<u>PAGE</u>
8.2.2 [^c] Fatigue Test Loads	8-9
8.2.3 [^c] Fatigue Test Loads	8-11
8.3.1 Sleeve Flow-Induced Vibration Analyses Results	8-12
8.4.1 Thermal/Hydraulic Effects of Sleeves in Steam Generator Tubes	8-14
8.5.1 Electrosleeve™ Structural Limits Level A Conditions	8-16
8.5.2 Electrosleeve™ Structural Limits Level D Conditions	8-17
8.5.3 Electrosleeve™ Draft Reg. Guide 1.121 Structural Limits Burst and Leakage Limits	8-19
8.5.4 Electrosleeve™ Structural Acceptance Standard	8-22
8.5.5 Electrosleeve™ ID Pitting Bursting Structural Limits	8-24
8.6.1 [^c] Electrosleeve™ Installed in the Tube Free Span	8-30
8.6.2 [^c] Electrosleeve™ Installed at Top of Tubesheet	8-32
8.6.3 [^c]	8-35
8.7.1 Acceptable Wall Thicknesses for an Installed Sleeve	8-37
9.1.1 Summary of Literature Survey - Nickel and Alloy 600 General Corrosion Rates in Various Environments	9-2
9.2.1 Primary Side Matrix Chemistry	9-9
9.2.2 Primary Side Chemistry Comparison	9-11
9.3.1 Secondary Side Matrix Chemistry	9-25
9.3.2 Secondary Side Chemistry Comparison	9-26
9.3.3 Summary of Crack Propagation Tests	9-28
9.3.4 Maximum SCC Penetrations in Alloy 600 Control Specimens	9-33
9.3.5 Secondary Side Capsule Tests	9-37
9.3.6 Summary of Heat Transfer Sludge Corrosion Tests	9-40

LIST OF TABLES (Cont'd)

	<u>PAGE</u>	
9.3.7	Composition % Weight of Sludge Mixture and Other Chemical Species Used to Fill the Sludge Simulant Holders	9-43
9.5.1	Summary of Material Susceptibility (Accelerated) Tests	9-53
9.5.2	Summary of Primary Water Corrosion Testing	9-55
9.5.3	Summary of Secondary Side Corrosion Tests	9-56
10.6.1	Sleeve ALARA Evaluation (100 sleeves) Average Area Dose Rates Electroformed Sleeve Exposure	10-11
11.3.1	Transducer and Flaw Type Comparison	11-10
11.8.1	Parent Tube OD Pit Sample Set	11-33
11.8.2	Parent Tube OD Pit Sizing Results	11-34
11.8.3	Sleeve OD Pit Data Set	11-37
11.8.4	Sleeve OD Pitting Results - 3/4" Tube	11-38
11.8.5	Sleeve OD Pitting Results - 7/8" Tube	11-38
11.8.6	Disbond Sample Set	11-41
11.8.7	Two Pitch Extent Sizing Error Bounds	11-42
11.8.8	Disbond Circumferential Extent Sizing Results	11-43
11.8.9	Disbond Axial Extent Sizing Results	11-44
11.8.10	ID Pit Sample Set	11-47
11.8.11	ID Pit Sample Set Detection Results	11-49
11.8.12	ID Profilometry Sample Set	11-51
11.8.13	ID Profilometry Sample Set Sizing Results	11-53
11.8.14	Combined Wall Thickness Data Set	11-55
11.8.15	Combined Wall Thickness Results	11-56
11.9.1	Axial ODSCC Extent Sample Set Pre-Sleeve Results	11-60

LIST OF TABLES (Cont'd)

	<u>PAGE</u>	
11.9.2	Axial ODSCC Extent Sample Set Post-Sleeve Results	11-61
11.9.3	Circumferential ODSCC Extent Sample Set Pre-Sleeve Results	11-62
11.9.4	Circumferential ODSCC Extent Sample Set Post-Sleeve Results	11-63
11.9.5	Axial ODSCC Depth Sample Set Pre-Sleeve Results	11-66
11.9.6	Axial ODSCC Depth Sample Set Post-Sleeve Results	11-67
11.9.7	Circumferential ODSCC Depth Sample Set Pre-Sleeve Results	11-68
11.9.8	Circumferential ODSCC Depth Sample Set Post-Sleeve Results	11-69
11.10.1	Summary of Flaw Detection	11-71
11.10.2	Summary of Sizing Performance	11-72
12.1.1	Repair Limits for Uniform Thinning (Includes 100% Through-Wall Degradation in Tube) Based on UT Sizing RMSE	12-3
12.2.1	Repair Limits for OD Pitting (Includes 100% Through-Wall Degradation in Tube) Based On UT Sizing RMSE	12-4
12.3.1	RSME Repair Limits for Axial Cracks >3/4" and 360° Circumferential	12-7
12.3.2	95% LCL Repair Limits for Axial Cracks >3/4" and 360° Circumferential Cracks	12-7
12.4.1	Minimum Repair Limits Using EPRI Approved Appendix J Techniques	12-8
12.4.2	Electrosleeve™ Plugging Limits	12-10
12.4.3	Repair Limit Based on UT Sizing RMSE	12-10 12-11
12.4.4	Repair Limit Based on UT 95% LCL	12-12 12-13

LIST OF TABLES (Cont'd)

		<u>PAGE</u>
A.1	W-D Design Information	A-2
A.2	W-E Design Information	A-6
A.3	CE SYS 80 Design Information	A-10
A.4	Westinghouse 7/8" Tubing S/G Design Information	A-13
A.5	Combustion Engineering 3/4" x 0.048" Tubing S/G Design Information	A-18
A.6	W-F Design Information	A-25

LIST OF FIGURES

	<u>PAGE</u>	
3.1	Electroplated Tubes Pulled From Doel-2	3-4
5.1.1	Electrosleeve™ Pressure Boundary	5-2
5.1.2	Typical RSG TSP and TS Sleeve Arrangement	5-4
6.1.1	Material Test Specimen Designs - Tensile, Fatigue, Young's Modulus Specimens	6-2
6.1.2	Typical Tensile Properties vs. Temperature	6-3
6.2.1	Elastic Modulus vs. Temperature	6-5
6.3.1	Reverse Bend Specimen	6-7
6.4.1	Electrosleeve™ Material Fatigue Test Data	6-9
6.5.1	Material Test Specimen Designs - Thermal Stability Specimens	6-11
6.5.2	Electrosleeve™ Thermal Stability Test Results at 650°F	6-12
6.5.3	Electrosleeve™ Exothermic Peak Values (using DSC Method)	6-13
6.5.4	Kissinger Plot for Activation Energy	6-14
6.5.5	Expected Thermal Destabilization Mechanism	6-15
6.5.6	Electrosleeve™ Activation Energy vs. Temperature	6-16
6.6.1	Standard Creep Specimen	6-19
6.6.2	Circumferentially Notched Creep Specimen	6-20
6.6.3	Mechanical Test Specimen Designs - Minimum Bond Fatigue and Burst Specimens	6-21
6.6.4	Creep Test Results	6-25
6.6.5	Electrosleeve™ Typical Fracture Surface Fractography	6-27
7.1.1	Typical Locked Tube Mockup Test Rig	7-2
7.2.1	Mechanical Test Specimen Designs (Minimum Bond Fatigue and Burst Specimens)	7-5
7.3.1	Mechanical Test Specimen Designs (Plugging Criteria Fatigue Specimens)	7-10

LIST OF FIGURES (Cont'd)

	<u>PAGE</u>
7.3.2 Mechanical Test Specimen Designs (Plugging Criteria Burst Specimens)	7-16
7.4.1 Typical Creep-Fatigue Surface Fractography	7-20
8.2.1 Peripheral Tubes Affected by TSP-to-Wrapper Supports	8-5
8.5.1 Normalized Burst Pressure vs. FTI and EPRI Burst Pressure Correlations	8-18
8.5.2 Typical Electrosleeve™ Pressure Boundary	8-21
8.5.3 Electrosleeve™ ID and OD Pit Structural Limits	8-24
8.6.1 [] ^c Strain (%) vs. Time	8-26
8.6.2 Tube Defects Modeled in [] ^c	8-28
8.6.3 ANSYS vs. [] ^c Test Data	8-33
8.6.4 [] ^{b,c}	8-34
9.3.1 Secondary Side Capsule Tests	9-30
9.3.2 Capsule Furnace Setup	9-35
9.3.3 Capsule Testing For Faulted Secondary Side Environments	9-36
9.3.4 Refreshed Autoclave Loop	9-41
9.3.5 Steam Generator Electrosleeved Tube Mockup For Sludge and Faulted Chemistry Tests	9-42
10.5.1 Electrosleeve™ Installation System Schematic	10-8
10.7.1 Electrosleeve™ Installation Experience	10-13
11.1.1 Electrosleeve™ NDE Regions	11-2
11.3.1 UT Wave "V" Path	11-9
11.4.1 UT-360 System Diagram - Data Station	11-13
11.4.2 UT-360 System Diagram - Containment	11-14
11.4.3 UT-360 System Diagram - Probe Head	11-16
11.6.1 Typical C-Scan Map	11-20

LIST OF FIGURES (Cont'd)

	<u>PAGE</u>
11.6.2 Typical A-Scan Presentation	11-21
11.7.1 Mode Conversion Method Example	11-27
11.7.2 Full Skip Normalization Method	11-30
12.2.1 Schematic of ID Pit	12-5

LIST OF ACRONYMS/TERMS

A/D	Analog to Digital Converter
ADB	Acceptable Disbond
AECB	Atomic Energy Control Board
ALARA	As Low As Reasonably Achievable
ANSYS	ANSYS Analysis System Software (Finite Element Mode)
ASME	American Society of Mechanical Engineers
ASME B&PV	American Society of Mechanical Engineers, Boiler and Pressure Vessel Code
ASTM	American Society of Testing Materials
AVT	All Volatile Treatment
AX EDM	Axial EDM Notch
BAT	Best Available Technology
CD	Concentrate/Dryer Unit
CE	Combustion Engineering
CE SYS 80	Combustion Engineering System 80 RSG
CFR	Code of Federal Regulations
COA	Certificate of Analysis
COC	Certificate of Conformance
DE	Destructive Examination
DFO	Differential Focus Optical
DI	Deionized Water
DOR	Depth of Reflection
DSC	Differential Scanning Calorimetry
DSM	Degradation-Specific Management
E	Modulus of Elasticity
ECT	Eddy Current Testing
EDM	Electrode Discharge Machining
EFPY	Effective Full Power Years
EMAT	Electromagnetic Acoustic Transducer
EPRI	Electric Power Research Institute
FESEM	Field Emission Scanning Electron Microscopy
FIV	Flow-Induced Vibration
FSM	Fluid-Elastic Stability Margin
FSN	Full Skip Normalization
FTI	Framatome Technologies, Incorporated
GB	Grain Boundary

HP	Hewlett-Packard
HTMA	High Temperature Mill Annealed
ID	Inside Diameter
IGA	Intergranular Attack
IGSCC	Intergranular Stress Corrosion Cracking
ISI	In-Service Inspection
LCL	Lower Confidence Limit
LOCA	Loss of Coolant Accident
LOW	Lake Ontario Water
LTMA	Low Temperature Mill Anneal
MCRR	Ministry of Consumer and Commercial Relations
MCS	Mode Converted Signal
MSDS	Material Safety Data Sheet
MSLB	Main Steam Line Break
MULTEQ	FORTTRAN Software developed by EPRI (Multiple Equations)
MUX	Multiplex
MWT	Mean Wall Thickness
NCR	Nonconformance Report
NDD	No Detectable Degradation
NDE	Nondestructive Examination
NIC	NDE Integrated Control
NRC	Nuclear Regulatory Commission
OBE	Operational Bases Earthquake
OD	Outside Diameter
ODSCC	Outside Diameter Stress Corrosion Cracking
OHT	Ontario Hydro Technologies, Inc.
OTSG	Once Through Steam Generator
P_b , P_{burst}	Internal Burst Pressure,
$P_{collapse}$	External Collapse Pressure
P_m	Primary Stress
POD	Probability of Detection
PWR	Pressurized Water Reactor
PWSCC	Primary Water Stress Corrosion Cracking
QA	Quality Assurance
QADP	Quality Assurance Data Package
QCIR	Quality Control Inspection Report
RAI	Request for Additional Information (NRC acronym)

LIST OF ACRONYMS/TERMS (Cont'd)

RCS	Reactor Coolant System
RG 1.121	NRC Draft Regulatory Guide 1.121
RMSE	Root Mean Squared Error
RO	Reverse Osmosis
RSG	Recirculating Steam Generator
RT	Room Temperature
RUB	Reverse U-bend
RWR	Remaining Wall Resolution
SCC	Stress Corrosion Cracking
SG	Steam Generator
S_m	Allowable Stress Intensity
SPS	Sleeve Procedure Specification
SSE	Safe Shutdown Earthquake
ST	Sleeved Tube
S_u , $S_{ultimate}$	Ultimate Tensile Strength
S_y , S_{yield}	Yield Strength
TIG	Tungsten Inert Gas
TOF	Time of Flight
T_p	Exothermic Peak Temperature
TS	Tubesheet
TSP	Tube Support Plate
TSS	Tubesheet Sleeve
TTS	Top of Tubesheet
TW	Through-Wall
UF	Ultra-Filtration
UT	Ultrasonic Testing
VHN	Vickers Microhardness Number
VT	Virgin Tube
W-51	Westinghouse Model 51 RSG
W-D	Westinghouse Model D RSG
W-E	Westinghouse Model E RSG
W-F	Westinghouse Model F RSG
WT	Witness Tube
%TW	Percent Through-Wall

1.0 EXECUTIVE SUMMARY

Nickel plating has been used as a repair and preventive-maintenance technique for metal components, including nuclear steam generator tubing, affected by primary water stress corrosion cracking. The Electrosleeve™⁽¹⁾, which takes advantage of the chemical and material properties of nickel, represents the next generation of steam generator repair. A process and resulting sleeve have been developed to repair Alloy 600 tubing in recirculating steam generators (RSGs) designed by Combustion Engineering or Westinghouse.

The Electrosleeve™ is a layer, or sleeve, of high-purity nickel (>99.5%) that is electrochemically deposited on the inner surface of the tube. Since the nickel bonds directly to the tube, the repair is leak tight. Further, the process does not deform the parent tube or affect its material microstructure; therefore, stress relieving is not required after the sleeve has been installed. The Electrosleeve™ can be placed in any tube of the RSG and anywhere within the tube except in the U-bend.

Installing the Electrosleeve™ uses a four-step process. The first step is cleaning the inside surface of the tube. Depositing a very thin layer of nickel (nickel strike) is the second phase of the process. This step prevents repassivation of the bonding surface and establishes a transition layer between the parent tube and the Electrosleeve™. Forming the sleeve is the third step; the fourth involves nondestructively examining (NDE) the sleeve using ultrasonic testing (UT).

Framatome Technologies, Inc. (FTI) has qualified the Electrosleeve™ by characterizing its material properties, performing structural analyses, and mechanical and corrosion tests to verify its performance in the operating environment of a steam generator. The material properties of the ultra-fine-grained nickel sleeve were characterized by testing as recommended by the ASME Boiler and Pressure Vessel Code, Section III Appendices and ASTM specifications. These tests established the sleeve's tensile strength, ductility, modulus of elasticity, fatigue and creep characteristics, thermal stability, burst strength, and thermal-dynamic properties.

The results from the above-mentioned tests were used in subsequent structural analyses and mechanical-qualification tests. Criteria were also established to set the extent to which a sleeve can be degraded before the tube must be repaired or removed from service.

The qualification process also required that an accurate and repeatable NDE method be used to verify the sleeve's proper installation. Typically, eddy current testing (ECT) is used to examine repairs in steam generators. FTI, however, found that the electroformed nickel affected the ECT results. Therefore, various NDE techniques were assessed to determine the best type for this application. UT provides the most accurate tool for verifying the sleeve's position and integrity. The qualification of the ultrasonic examination techniques were successfully peer reviewed and found to meet the requirements of the EPRI PWR Steam Generator Examination Guidelines, which is the industry-mandated document for NDE of steam generator tubing.

The development and qualification program has shown that the Electrosleeve™ and associated inspection process meet all of the requirements for application in steam generator repair.

⁽¹⁾ Electrosleeve™ is a trademark of Ontario Hydro Technologies, Inc.

2.0 INTRODUCTION

To repair recirculating steam generators (RSGs) with degraded Alloy 600 tubing, the Electrosleeve™⁽¹⁾, an electroformed sleeve, was developed and qualified. This report documents the design analyses, mechanical testing, corrosion evaluation, nondestructive examination, installation process, and ALARA (As Low As Reasonably Achievable) aspects of the sleeve design.

Sleeving is a method used to repair defective steam generator tubes to keep them in service. Typically, sleeves were designed with sleeve-to-tube joints that were either welded, brazed, rolled, and/or hydraulically expanded. However, these joints created another set of problems in the tubes, which often required performing post-installation stress relief. Therefore, the focus of sleeve design shifted to repair methods that would produce minimal residual effects on the parent tube. The result was the electroplated sleeve, an electrodeposition of conventional (large-grained) nickel (>99% pure) on the inner surface of the tube. This sleeve, while not a complete structural repair, required no welding or deformation of the parent tube, yet provided the leak limiting benefits of previous sleeve repair options.

The Electrosleeve™ represents the next generation of steam generator tube repair. It is an electroformed sleeve consisting of ultra-fine-grained nickel electrochemically deposited on the inner surface of a degraded tube to form a structural repair. The electrochemical deposition of nickel provides a continuous metallurgical bond between the tube and sleeve that eliminates all leak paths and crevices. The nickel utilized in the Electrosleeve™ repair process, once deposited, is referred to as a nanostructured material. Nanostructured sleeve material has a grain structure with mean diameters of less than 300 nanometers (nm). This grain structure provides unique properties including enhanced corrosion and wear properties along with improved hardness, strength, ductility, and thermal stability that exceed those of conventional nickel electroplating. The grain structure (~250 grains/0.001 inch) produces the enhanced strength while the microalloying sets the thermal stability.

The Electrosleeve™ provides a structural, leak-tight seal while minimizing residual stresses on the parent tube. Because the electroformation of the nickel imparts low stresses on the parent tube, installing the sleeve does not deform the parent tube or change the microstructure; thus, the design does not require post-installation stress relief. In addition to maintaining the tube in service, the continuous metallurgical bond

maintains the heat transfer area over the length of the sleeve. The strength and installation also provide a free path through the sleeve for future needs. Thus, the structural repair using an Electrosleeve™ minimizes thermal-hydraulic losses and maximizes heat transfer performance.

⁽¹⁾ Electrosleeve™ is a registered trademark of Ontario Hydro Technologies, Inc. (OHT).

3.0 BACKGROUND

Recirculating steam generators (RSGs) were typically fabricated with tubing made of mill-annealed nickel-chromium-iron (Ni-Cr-Fe) Alloy 600. The cracking of low-temperature mill-annealed (LTMA) tubes due to high tensile stresses was identified in the late 1970's and early 1980's. Primary water stress corrosion cracking (PWSCC) occurred in low row U-bends and in the expansion roll transitions of tubing expanded into the tubesheet. U-bend stress relief [13.9] and preventive shot peening [13.8] were developed for plants identified as having a high potential for PWSCC. However, the French and Belgians reported that shot peening was not as effective when performed after the plant was in operation as when performed prior to the plant operation [13.10]. The decrease in performance was attributed to the presence of small cracks that initiated during operation prior to the peening operation. Thus, other repair methods were required to keep tubes in service.

Subsequently, plants began experiencing degradation by outside diameter stress corrosion cracking (ODSCC) at both roll and explosive expansion transitions. In addition, secondary side corrosion began to emerge at the tube support plate (TSP) intersections. The types of tubes experiencing various degradation modes included high-temperature mill-annealed (HTMA) tubes as well.

Identification of these degradation mechanisms led to the development of numerous sleeve designs in the industry. The overall objective of these sleeve designs was to provide a structural repair by spanning the degraded region of the tube. The typical sleeve design was the tube-within-a-tube concept, with structural joints formed by various means at each end of the sleeve. The joints required permanent deformation of the sleeve and tube for welded (leak-tight) or mechanical (leak-limiting) sleeve installation. The tube deformation produced residual stress in the tube. In addition to the deformation residual stresses, welded joints produced residual stresses in the heat-affected zone. These joints had to be stress relieved to reduce the potential of any type of stress corrosion cracking (SCC). For a mechanical joint, stress relief can negate the leak-limiting capability of the joint; therefore, some residual stress must remain to ensure the integrity of the joint.

Since the original installation of many of these sleeves, some tubes have been found locked (restrained) at the TSPs due to mechanisms such as the buildup of corrosion products. This impairs the ability to perform an effective stress relief (approximately

1400°F for five minutes) of tube-sleeve joints. In some of these instances, rather than reducing stress, stress relief could lead to either localized yielding or buckling of the tube (low yield stress at 1400°F) or a redistribution of residual stresses. If the joint yields axially because the thermal growth caused by the stress relief is restrained by the locked tube support, the thermally induced deformation will result in a residual tensile stress as the temperature from the stress relief heater returns to ambient.

In 1993, Laborelec-Belgium confirmed the effect of residual stresses with an intensive SCC testing program of steam generator tubes repaired with welded sleeves. This study evaluated all types of welding: tungsten inert gas (TIG) overlap or fillet, laser, and kinetic [13.43]. The study concluded that the risk of developing new cracks in the parent tube at the upper joint of a welded tube-sleeve assembly was high for a tubing material highly susceptible to PWSCC. The risk was a concern because of the circumferential orientation of the new cracks and the difficulty of detecting them in the complex geometry of the joint.

To eliminate these concerns, Framatome Technologies, Inc. (FTI) in cooperation with OHT, developed the Electrosleeve™. The process deposits a layer of nearly pure nickel (with traces of phosphorus) on the inside diameter of degraded tubes to provide a structural, leak-tight repair that requires no stress relief. The Electrosleeve™ will span defects within the tube at the baffle plates, the tube support plates, at or near the secondary face of the tubesheet, or in free-span regions of steam generators. Further information on the technology can be found in Reference 13.66 where it is concluded that homogenous nickel-phosphorus alloys displayed corrosion resistance superior to their crystalline counterparts. Comparisons of corrosion performance indicate that Ni-P alloys are superior to pure nickel and to 316L stainless steel at high (> 0.45 volts) potential.

Electrodeposition of pure nickel, a stable material, is a precursor technology closely related to Electrosleeve™ that, as documented by Dini [13.67], has been discussed and researched extensively. (This reference provides a comprehensive background on processes, testing, and troubleshooting in electrodeposition technology.) Since 1985, Framatome (Europe) has been using nickel electroplating as a remedial technique to repair steam generator tubing with PWSCC. The primary goal of this technique is to arrest the degradation process of the tube wall by depositing a layer of nickel plating capable of bridging PWSCC in a steam generator tube. This process has also been used to seal the roll transition area to inhibit or prevent the initiation of PWSCC. Some of

these repairs have been performed over through-wall flaws. The through-wall flaw was defined by observed leakage.

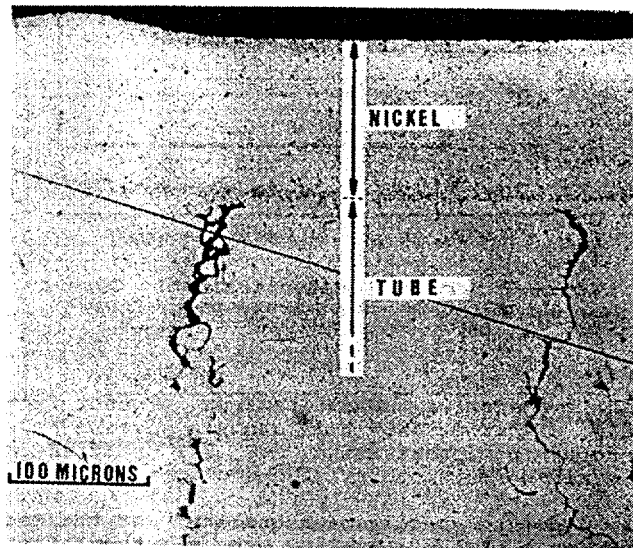
To evaluate the performance of the electroplated nickel sleeves, two tubes with through-wall cracks were pulled from Doel-2 after nine months and two years of operation, respectively. The tubes were ultrasonically tested and destructively examined (Figure 3.1). The results verified that the cracking did not propagate into the nickel sleeve. (Reference 13.56 shows the metallographic sections of these tubes.)

At the EUROCORR '96 conference, Laborelec representatives presented additional information about the Belgian experience on repairing steam generator tubes [13.69]. The operating experience of plants with nickel-plated tubes compared favorably to other sleeve repair techniques (mechanical, welded, and laser-welded sleeving).

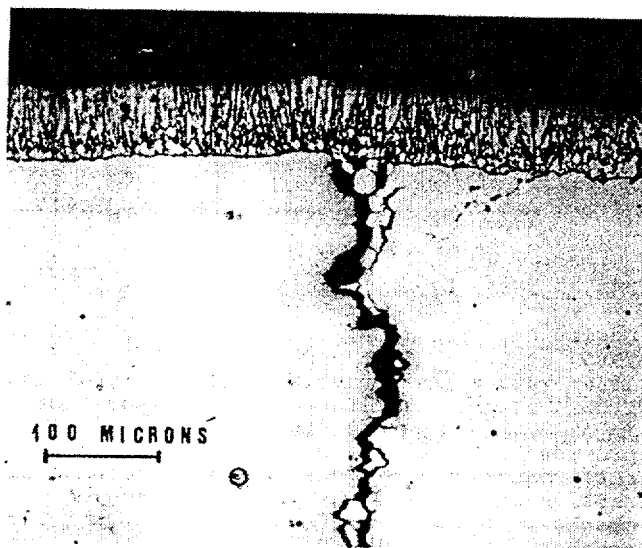
In North America, operating experience with nickel plating has been equally favorable. The Framatome nickel-plating technique was first used in the U.S. at Baltimore Gas & Electric's Calvert Cliffs Unit 1 in 1994 [13.37], where one hundred eighteen (118) pressurizer heater nozzles were plated to a thickness of 8 mils. The same technology was used again in 1998 at Florida Power & Light's St. Lucie Unit 1 to plate one hundred twenty (120) pressurizer heater nozzles to a thickness of 10 mils. A 10-mil layer of nickel was qualified to seal a 1/2-inch through-wall crack for more than 120 fatigue cycles.

The Electric Power Research Institute (EPRI) has documented the use of electroplated nickel to successfully repair European steam generator tubes affected by PWSCC [13.12]. From 1985-1992, Framatome successfully installed electroplated nickel in more than 1,000 tubes at various plants in Europe [13.39]. The repair method has been successfully used to prevent cracking as well as to repair existing 100% through-wall cracks within the parent tube. Greater than 95% of these electroplated nickel sleeves remained in service for the life of the steam generator, with no compromising degradation or cracking. (A small percentage of tubes have been plugged since the first large commercial application in 1988 at Doel-2, but none were due to any defect or degradation of the nickel sleeving.)

FIGURE 3.1
ELECTROPLATED TUBES PULLED FROM DOEL-2



Tube 18/51 pulled after 9 months of service



Tube 21/59 pulled after 2 years of service

OHT successfully installed the next generation of nickel-plated sleeve, the Electrosleeve™, in various steam generators in the Pickering plants. Initially, the sleeves were installed as part of the development phase, and the parent tubes were either plugged or pulled for evaluation. The first ever production scale Electrosleeving campaign was executed at PND Unit 5 during the period April 25 to May 4, 1994. The campaign consisted of a total 46 sleeves including in-boiler and out-boiler witness sleeves. The "Trustie" ultrasonic testing (UT) system was used to determine the Electrosleeve thickness and the bond integrity to the parent tube. The initial inspection performed after the Electrosleeving indicated that 44 sleeves were acceptable as per the quality assurance criteria outlined in the station procedures and material and process approved documents. It is important to note that the steam generator tubing material of PND 'B' is Monel 400 and that an unusually thick and tenacious oxide layer was present on the tubes. This oxide is believed to have resulted from the stress relief thermal treatment of the steam generators. The activation step applied during the Unit 5 electrosleeve process involved acid activation *without* anodic polarization.

Fourteen (14) of the eighteen (18) in-boiler sleeves were left in operation and four (4) were immediately pulled for destructive examination. These Electrosleeves and the 28 witness sleeves were tested for chemical composition and mechanical integrity. All sleeves met or exceeded chemical and physical specification requirements. These requirements included yield and tensile strength and ductility determinations. Bend tests were utilized for the measurement of the Electrosleeve/parent tube adhesion. On the basis of these physical test results it was concluded that the remaining 14 in-boiler sleeves possessed the required properties for pressure boundary replacement. The Atomic Energy Control Board granted approval to leave these sleeves in operation.

In April 1995, as required by the Canadian Nuclear Safety Commission (CNSC), all fourteen in-boiler Electrosleeves were inspected by UT. After approximately one year of operation, the results of the inspection revealed an acceptable performance of the installed sleeves. This was evidenced by the overall continuity of sleeve-to-tube bonding and consistency in sleeve thickness with originally values installed. However, two tubes showed two small areas of disbond. One of these disbonds comprised an area at the limit of UT inspectability ($< 1\text{mm}^2$); and the second tube had an area slightly larger at approximately $6 \times 8\text{mm}$. This discontinuity represented 0.7% of the total area of the Electrosleeve.

The root cause of these disbonds was identified as residual patches of oxide which separated from the alloy substrate upon temperature cycling. It is only when the oxide patches are small that the Electrosleeve/oxide bond is stable. It was concluded that the disbond would only occur after one temperature cycle. The qualification results demonstrated that the Electrosleeve/Monel bond was metallurgical and that the bond strength was unaltered after more than five hundred thermal cycles from room temperature to operating temperature.

In March 1999 UT inspection results showed no measurable changes in any of the fourteen (14) Electrosleeves since the 1995 inspection. The data confirmed that twelve electrosleeves were fully bonded and that the small areas of disbond of the remaining two showed no change from the 1995 inspection. The UT results confirmed the thickness of all the Electrosleeves.

Pickering Electrosleeve Performance: Electrosleeves have now been in operation at Pickering, Unit 5 steam generators for more than six years. The results of the three UT inspections performed during this period have shown a satisfactory performance of Electrosleeves under the operating environmental conditions of this unit. The comparison of the UT Electrosleeve maps for each tube clearly reveals no corrosion of the material or any other type of degradation. The experience at Pickering clearly demonstrates that electrosleeving of steam generator tubes is a viable permanent repair technology.

In 1995, FTI installed nine electrosleeves in a steam generator at Oconee Unit 1. These sleeves were installed as part of the development program to gain experience with the sleeving equipment and field procedures. All of the sleeves were successfully installed as confirmed by ultrasonic testing (UT). Since the Electrosleeve™ was not licensed in the U.S. at that time, these tubes were subsequently plugged. Table 3.1 provides a summary of Framatome nickel plating and Ontario Hydro electrosleeving experience in operating steam generators.

Two U.S. utilities have independently hired consultants to provide additional technical review of the Electrosleeve™ qualification program. These consultants participated in technical presentations and received copies of the topical report (December 1995 and March 1996). Both consultants found the electrosleeving process acceptable.

The term "Electrosleeve™" specifically refers to nanocrystalline microalloyed nickel that is electrochemically deposited on the steam generator tube. Electrosleeving material has the necessary strength and thermal stability to qualify as a structural repair. Nickel plating refers to the process currently used in Europe that utilizes a thin (~0.004 inch) layer of nickel to either prevent PWSCC or to inhibit further growth of existing PWSCC. Nickel plating uses high purity nickel, but the material does not have nanocrystalline structure and is not microalloyed for thermal stability. Nickel plating, as currently used in Europe and adapted for pressurizer heater nozzles, is not qualified as a structural repair.

TABLE 3.1
STEAM GENERATOR NICKEL PLATING AND ELECTROSLEEVEING EXPERIENCE

PLANT/VENDOR	YEAR	TUBES NI-PLATED	TUBES IN-SERVICE	ACTIONS TAKEN	COMMENTS
Doel-2 (Framatome)	1985	10	1	3 plugged, 3 pulled, and 3 repaired (1990)	R&D field baseline program; large through-wall cracks; some leaked due to micro nickel pits; lab exam results: bridged cracks, no internal corrosion
Doel-2 (Framatome)	1986	81	56	13 plugged, 3 pulled, and 9 repaired (1990)	R&D field baseline program; large through-wall cracks; some leaked due to nickel hardness (nickel cracked over Alloy 600 cracks > 0.39 inch)
Doel-2 ⁽¹⁾ (Framatome)	1988	33	33		First commercial application; large through-wall cracks; visual inspections in 1988, 1989, and 1990 with a 40X baroscope; conclusions: no leaks, no visible corrosion, no erosion
Doel-3 ⁽²⁾⁽⁶⁾ (Framatome)	1988	11	11 ⁽⁷⁾		Large through-wall cracks in parent tubing; UT inspected in 1988 (baseline), 1989, 1990, and 1991; conclusion: cracks have not propagated into nickel plating
Ringhals-3 ⁽³⁾⁽⁶⁾ (Framatome)	1990	10	10 ⁽⁷⁾		UT (long. and circum.) baseline in 1990 to qualify UT relative to ET; UT 1991 and 1992; conclusion: cracks have not propagated
Doel-2 ⁽⁴⁾ (Framatome)	1990	345	337	8 plugged (not related to nickel plating)	Local re-expansion (2 inches) in the tubesheet entirely protected by Ni-plating on 4 inches (2 mils thick); visual and ET inspected in 1990 (baseline)
Tihange-2 ⁽⁵⁾ (Framatome)	1992	602	602 ⁽⁷⁾		Plating in parallel on all three SGs
Pickering-6 (OHT)	May 1993	1	0		Trial run of Electrosleeve™ Process not approved yet by AECB and MCCR so tubes plugged.
Pickering-8 (OHT)	October 1993	9	0		9 electrosleeves installed in B05 and B011; process not approved yet by AECB and MCCR so tubes plugged.
Pickering-1 (OHT)	Nov 1993	8	0		8 electrosleeves installed in 3 tubes; 3 sleeves unacceptable due to disbanded areas. Process not approved yet by AECB and MCCR so tubes plugged.
Pickering-5 (OHT)	May 1994	46	14	4 tubes pulled	90% electrosleeves acceptable. 28 of 46 sleeves installed in mockup located on SG platform. As of August of 1998, all 14 electrosleeved tubes in SG are still in operation.
Tihange-2 (Framatome)	1993 1995	565 118	565 ⁽⁷⁾ 118 ⁽⁷⁾		On all three SGs. More than 500 tubes in 1993 and 118 tubes in 1995 electroplated.
Tihange-2 (Framatome)	1996	600	600 ⁽⁷⁾		600 tubes electroplated in May 1996 outage. SG change-out performed in 1998.
Oconee-1 (FTI/OHT)	1995	9	0	All 9 electrosleeved, then plugged	9 electrosleeves installed in SG tubes, process not yet approved by NRC, 9 tubes plugged.

NOTES:

- (1) Crack sizes at Doel-2: 0.2 to 0.3 inch; frequently up to 0.5 inch
 (2) Crack sizes at Doel-3: 0.4 inch
 (3) Crack sizes at Ringhals-3: 0.1 to 0.2 inch
 (4) No cracks; high work hardened area

- (5) Crack sizes at Tihange-2: 0.35 to 0.47 inch
 (6) Steam generator replacement was made at Doel-3 in 1993, in Ringhals-3 in 1995 & in Thiange-2 in 1998.
 (7) Tubes in service refers to the remaining duration of service until SG change-out.

4.0 DESIGN CRITERIA

The design criteria used to evaluate the Electrosleeve™ are detailed in this section. These criteria define the design and qualification requirements of the Electrosleeve™.

4.1 Qualification Methodology

The first step in qualifying the Electrosleeve™ for use in repairing degraded pressurized water reactor (PWR) steam generator tubing involved specifying the requirements, regulatory or others, that are imposed on the sleeve in its installed condition. If the current standard did not apply explicitly to the Electrosleeve™, then it was still followed as a guideline. Next, the material properties of the Electrosleeve™ were determined per the ASME Boiler and Pressure Vessel Code and the ASTM guidelines. For this topical report, the term "ASME Code" refers to the ASME Boiler and Pressure Vessel Code (ASME B&PV). The terms may be used interchangeably.

The following methodology was used to qualify the Electrosleeve™:

- Define the design requirements for the steam generator tube repair,
- Develop the applicable material properties per the requirements of the ASME Code, Section III [13.2],
- Prepare a design analysis of the tube repair per the requirements of the ASME Code, Section III [13.2], and
- Evaluate the tube repair to the requirements of the Nuclear Regulatory Commission (NRC) Draft Regulatory Guide 1.121 (RG 1.121) [13.6].

The design requirements for the Electrosleeve™ are defined in Section 4.2.

The tests done to establish the material properties are presented in Section 6.0. The material properties were developed per the following methodology:

- Determine the allowable stress intensity value (S_m) per the methodology of ASME Code, Section III, Appendix III-2110(b).

- Perform tensile testing per ASTM E8 and E21 [13.13, 13.14],
 - Perform creep testing per ASTM E139 [13.22],
 - Perform bend testing per ASTM E290 [13.20], and
 - Verify the thermal stability of the electrochemically deposited nickel at the design temperature of 650°F.
-
- Determine the design fatigue curve for the electrochemically deposited nickel and apply the appropriate ASME Code, Section III safety factors (2 on stress, 20 on cycles).
 - Determine the appropriate fatigue strength reduction factors applicable to the "as-formed" surface finish.
 - Determine the additional physical properties associated with the ultra-fine-grained nickel material.

The design analyses for the Electrosleeve™ were performed using ASME Code, Section III as a guideline and followed the methodology outlined below:

- Determine the minimum required sleeve thickness using ASME Code, Section III, Subsection NB as a guide. The design stress intensity value determined in Section 6.0 was used.
- Determine the structural loading associated with the tube repair including repair of locked tubes and tubes with 100% through-wall defects. Evaluate the structural loads and installed sleeve configurations per the stress and fatigue limits in ASME Code, Section III.
- Determine the minimum sleeve attachment length using the experimental analysis techniques of ASME Code, Section III, Appendix II.

Additional qualification evaluations included:

- Flow-Induced Vibration (FIV),
- Corrosion (Primary and Secondary Side Environments),
- Nondestructive Examination Techniques, and
- RG 1.121 Evaluation.

The purpose of this report is to show that the Electrosleeve™ is qualified to structurally repair the RSG tubing designs in service today. Qualification testing and/or analysis was performed on three sizes of tubing (1 1/16", 3/4", and 7/8"). In the cases where a bounding condition and size were determined, the results were expanded to encompass the other sizes of tubing. Material test results are presented for 1/2" and 5/8" size tubing along with results for 1 1/16", 3/4", and 7/8" Alloy 600 tubes.

4.2 Design and Qualification Requirements

The electroformed sleeve is designed for application in PWR steam generators with tubing having the following nominal dimensions:

- 1 1/16" OD x 0.040" wall,
- 3/4" OD x 0.042"/0.043"/0.048" walls, and
- 7/8" OD x 0.050" wall.

A sleeve has also been designed (described in a separate topical) for once through steam generator (OTSG) 5/8" OD x 0.037" wall tubes.

The operating conditions of the RSGs form the design basis for the operating conditions of the sleeve. The sleeve must meet the following design requirements:

- Span defects in the parent tube at top of tubesheet (TTS) and TSP locations,
- Provide a structural repair for the parent tube at these locations,
- Provide a leak-tight seal for primary to secondary side water, and
- Minimize residual stress in the parent tube to minimize the possibility of primary and secondary side intergranular stress corrosion cracking (IGSCC).

The design and qualification of the sleeve utilized applicable industry codes and standards as summarized in Table 4.2.1. The ASME Code is the basic governing document for numerous aspects of the design including determining test loads, performing structural analyses, procuring material, establishing the sleeve procedure qualification, and preparing the sleeve procedure specification (SPS) (Section 10.0).

TABLE 4.2.1
SUMMARY OF APPLICABLE
CODES AND STANDARDS ⁽¹⁾

APPLICATION	CRITERIA
Structural Design of the Sleeve - Sleeve/Tube Loads - Analyses	ASME B&PV Code, Section III [13.2]
Sleeve Plugging Limit	NRC Draft Reg. Guide 1.121 [13.6]
Material Procurement	ASME B&PV Code, Sections II and III [13.1, 13.2] Section XI, Code Case N-569 [13.4]
Electroformed Sleeve Material Qualification	ASME B&PV Code, Section XI, Code Case N-569 [13.4] ASME Standards [13.13-13.28]
Sleeve NDE	ASME B&PV Code, Sections V and XI [13.3, 13.4] Code Case N-504-1 [13.7] Section XI, Code Case N-569 [13.4]
Procedure Qualification	ASME B&PV Code Case N-569 [13.4], EPRI Checklist [13.11]

NOTES:

- (1) The ASME B&PV Code Section III does not address nanocrystalline nickel material. Therefore, these Code sections were followed as a guideline for developing the Electrosleeve™

At present, nickel is not identified as an approved material in the Code for ASME, Section III, Class I, systems. However, electrodeposition has been identified in ASME, Section XI, Code Case N-569, as a tube repair method. Therefore, material testing (as recommended by Code Case N-569) has been performed per the guidance of ASME, Section III and ASTM to establish material design properties. Similarly, the sleeve procedure qualification has been performed following the guidance of ASME, Section XI, Code Case N-569.

4.3 Sleeve Design Conditions

The design and operating conditions for the RSG are imposed on the sleeves. The tables in Appendix A detail the operating conditions for which the sleeve has been designed. Analyses and tests were performed for the worst-case bounding conditions. The sleeve has been designed to encompass the following types of steam generators:

- Westinghouse Models D, E, F, 33, 44, 44F, 51, and 51M.
- Combustion Engineering (CE) Models 67, 80, 3410, Ft. Calhoun.

Design transients for steam generators were used to establish loading transients for the sleeve. Section 8.0 discusses how these transients were used to establish the sleeve loading transients and cycles. Operating pressure and thermal loading ranges were used to establish the worst-case conditions, considering both unlocked and locked tube conditions. For the locked tube condition, the tubes were considered locked at all tube support plates, which is the most conservative assumption.

Appendix B is a summary of plant specific conditions that may be identified in Licensing Amendment Requests.

5.0 SLEEVE DESIGN

The physical design of the Electrosleeve™ is described in this section. A brief description of the installation and a list of the key process parameters are also included.

5.1 Design Description

An electroformed sleeve is an electrochemical deposition of ultra-fine-grained nickel material on the inside diameter of a degraded steam generator tube. Table 5.1.1 summarizes the dimensions of an installed Electrosleeve™ in the RSG designs. Because the thickness of the sleeve depends on the rate of deposition, the actual sizes of installed sleeves may vary. If the installed sleeve does not meet the target design parameters, justification or testing must be performed as required to leave the sleeve in service.

TABLE 5.1.1
STEAM GENERATOR TUBE AND ELECTROSLEEVE™
NOMINAL DIMENSIONS

STEAM GENERATOR	TUBE OD (INCH)	TUBE WALL (INCH)	NOMINAL SLEEVE WALL (INCH)	SLEEVE LOCATION	SLEEVE LENGTH (INCH)
Westinghouse F	0.688	0.040	┌ c,e7 └ J	Tubesheet (TS)	┌ c,e7
				Midspan, TSP	└ J
Westinghouse D, E	0.750	0.043	┌ c,e7 └ J	TS	┌ c,e7
				Midspan, TSP	└ J
CE SYS 80	0.750	0.042	┌ c,e7 └ J	TS	┌ c,e7
				Midspan, TSP	└ J
All CE SGs (except CE SYS 80)	0.750	0.048	┌ c,e7 └ J	TS	┌ c,e7
				Midspan, TSP	└ J
Westinghouse 33, 44, 44F, 51, & 51M	0.875	0.050	┌ c,e7 └ J	TS	┌ c,e7
				Midspan, TSP	└ J

For the purposes of qualifying this repair process, any reference to the length of a sleeve refers to the length between the tapered transitions including the minimum bond lengths. The tapered transitions are not considered part of the pressure boundary region of the sleeve (Figure 5.1.1).

FIGURE 5.1.1
ELECTROSLEEVE™ PRESSURE BOUNDARY

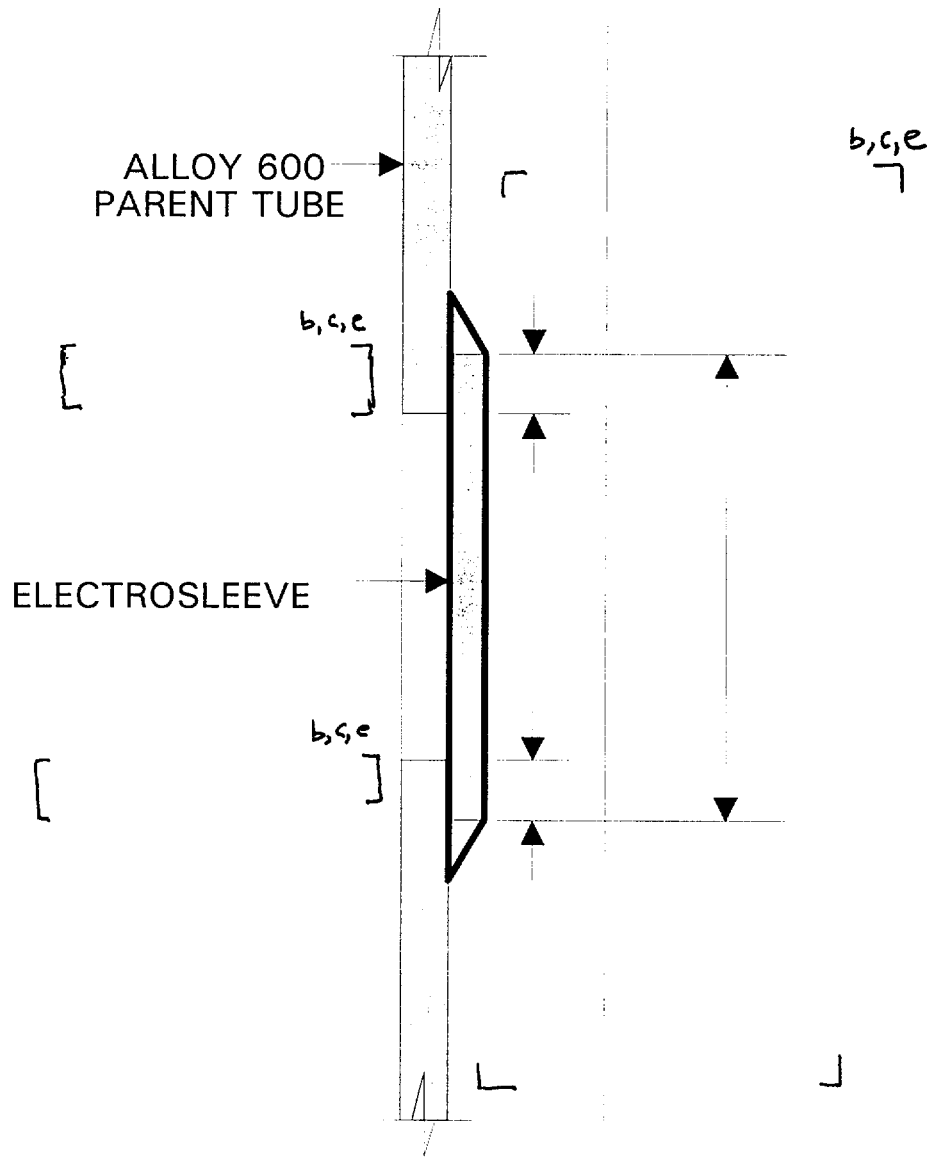
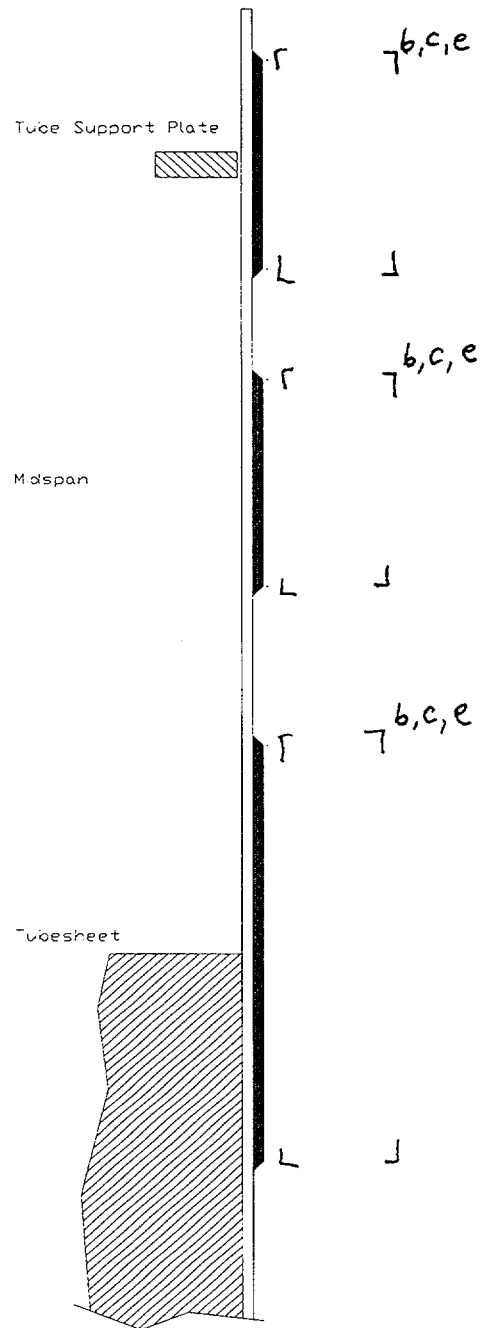


Figure 5.1.2 depicts a typical installed Electrosleeve™. The sleeve is designed to repair tubes by spanning the degraded region. The sleeve can be installed at any straight section of tubing including the expansion transitions, all of the TSP intersections, and the free-span areas. The electroformed repair is leak-tight because the nickel is bonded to the tube.

FIGURE 5.1.2
TYPICAL RSG TSP AND TS SLEEVE ARRANGEMENT



The material used for the sleeve is high purity nickel (>99.5%). Nickel has excellent bonding characteristics with the Alloy 600 base metal. The Electrosleeve™ composition does not release activated species such as cobalt and has excellent material properties, including ductility, as discussed in Section 6.0 of this report.

The design enables the sleeve to act as the primary pressure boundary and maintains its structural integrity under operating and accident conditions. Installation of the sleeve has no effect on the parent-tube material microstructure. Residual stresses generated in the tube are low, thereby eliminating post-installation stress relief.

5.2 Process Description

The process steps for installing an Electrosleeve™ are summarized below with a more detailed description presented in Section 10.0.

- Tube marking and position definition
- Mechanical tube cleaning
- Electrosleeve™ probe positioning
 - []^{c,e}
 -
 - []^{c,e}
 - []^{c,e}
 - Electroforming []^{c,e}
 - []^{c,e}
 - Flush with DI water
- Probe removal
- Nondestructive Examination (Ultrasonic/Eddy Current)

After the tubes are marked and the position defined, the tubes are mechanically cleaned with a vacuum-assisted rotating scraper or hone. The cleaning removes loose oxides in order to reduce the level of radioactive contamination of the waste streams. A specially designed probe is then installed at the desired location and remains in place for the following steps: acidic cleaning and activation, nickel strike, and nickel forming. Acid cleaning and activation prepares the tube surface by electroetching or "dissolving" the surface oxide layer to improve the contact and adherence of the nickel layer to the tube inside diameter (ID). The nickel strike is a transition layer between the parent tube and

the Electrosleeve™, which is deposited during the subsequent forming step. Only the Strike and Watts steps are involved with the formation of the sleeve.

As shown in Table 5.2.1, a number of parameters are monitored and controlled to ensure proper sleeve installation. In addition, a witness tube (WT) located on the steam generator platform can be electroformed in parallel with the actual steam generator tubes. The WT can then be examined to verify correct electroforming has occurred in the tubes.

TABLE 5.2.1
PROCESS VARIABLES

PARAMETER	RECOMMENDED MONITORING	RECOMMENDED DATA STORAGE FREQUENCY
┌		c,e┐
└		┘

6.0 DESIGN VERIFICATION - MATERIAL PROPERTIES

The Electrosleeve™ is a nanocrystalline material installed in situ on the tube inside surface using an electrochemical deposition process. This section describes the tests performed to establish the properties of the Electrosleeve™ material. ASTM and ASME standards were used in the development and qualification of the material. The material properties of the electrochemically deposited nickel material are independent of the parent tube inside diameter and thickness as shown by supporting data presented in the following sections. For the purposes of this section and other design verification sections of this report, a specimen is defined as a tube with an Electrosleeve™ installed on the inside diameter.

6.1 Tensile Strength

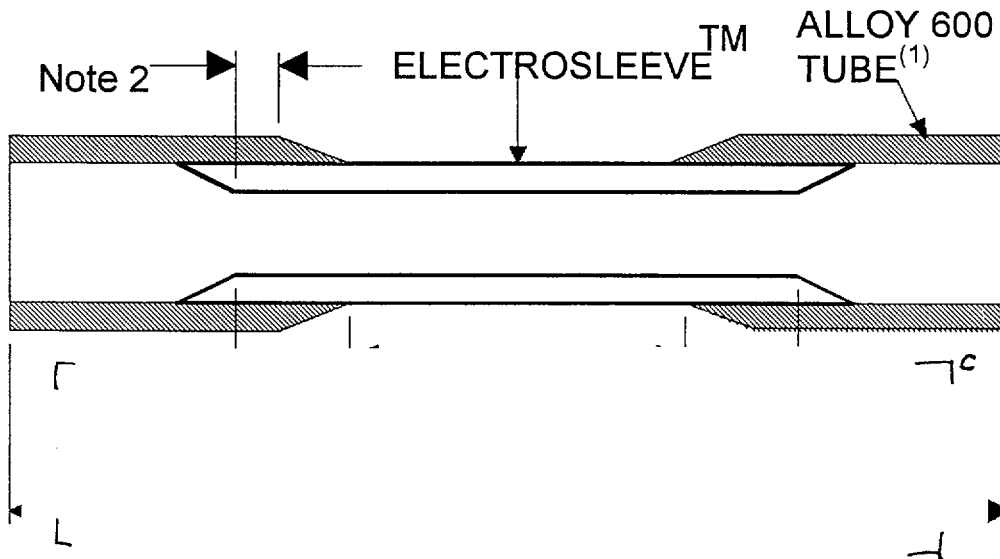
Tensile tests were performed at [^{b,c}] temperature [^{b,c}] to determine yield strength, ultimate strength, and elongation of the electrochemically deposited nickel material. [^{b,c}] specimens were tested to ensure statistically significant results. FTI tested four sizes of Alloy 600 tubes:

- 5/8" OD x 0.034" wall,
- 3/4" OD x 0.043" wall,
- 3/4" OD X 0.048" wall, and
- 7/8" OD x 0.050" wall.

Additionally, OHT performed tensile tests of ultra-fine-grained nickel material deposited in 1/2" OD x 0.049" wall Monel 400 tubes [^{b,c}].

The test specimens were fabricated as shown in Figure 6.1.1 and tested per ASTM procedures [13.13, 13.14]. The results of the tensile tests were tabulated for each of the temperatures tested by FTI and combined with the results of OHT. These data were evaluated per the ASME Code Section III to establish the design properties for the nanocrystalline nickel material at a range of temperatures, including operating temperatures.

FIGURE 6.1.1
 MATERIAL TEST SPECIMEN DESIGNS⁽¹⁾
TENSILE, FATIGUE, YOUNG'S MODULUS SPECIMENS



NOTES:

(1) Electro sleeves were installed in the following tube sizes for testing:

- 5/8" OD x 0.034" wall
- 3/4" OD x 0.043" wall
- 3/4" OD x 0.048" wall
- 7/8" OD x 0.050" wall

(2) Nominal sleeve-to-tube bond length:

5/8" OD tubes: [

3/4" and 7/8" OD tubes: [

$I^{c,e}$
 $I^{c,e}$

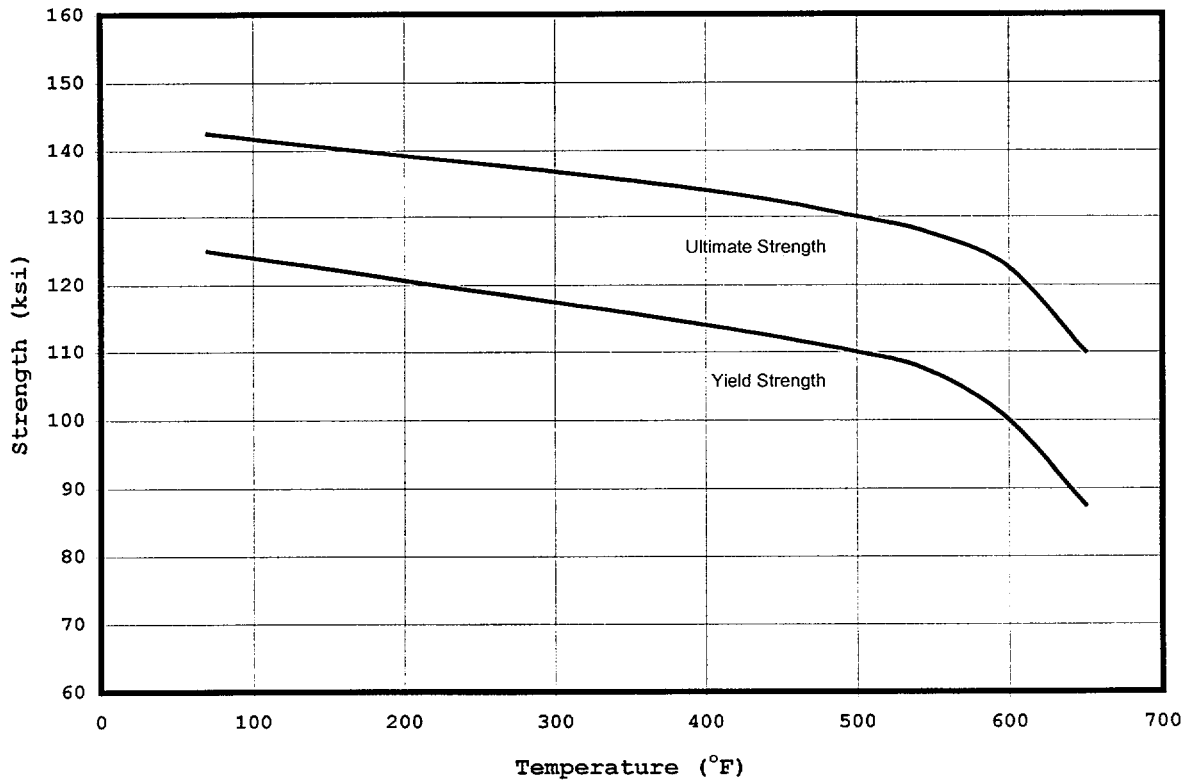
The ASME Code, Section III minimum design strength values at various temperatures are tabulated in Table 6.1.1. The typical yield and ultimate strength versus temperature curves are shown in Figure 6.1.2.

TABLE 6.1.1
ASME CODE, SECTION III, MINIMUM DESIGN STRENGTH VALUES

[Experimentally Determined per References 13.2 and 13.4]

Temperature (°F)	S _{yield} (ksi)	S _{ultimate} (ksi)	S _m (ksi)
650	60.0	90.0	30.0
600	70.0	100.0	33.3
100	100.0	130.0	43.3

FIGURE 6.1.2
TYPICAL TENSILE PROPERTIES VS. TEMPERATURE



6.2 Modulus of Elasticity

[]^b specimens were tested to determine the modulus of elasticity for the material per ASTM procedure [13.15]. Of those, FTI tested four Alloy 600 tube sizes with installed electrosleeves:

- 5/8" OD x 0.034" wall,
- 3/4" OD x 0.043" wall,
- 3/4" OD x 0.048" wall, and
- 7/8" OD x 0.050" wall.

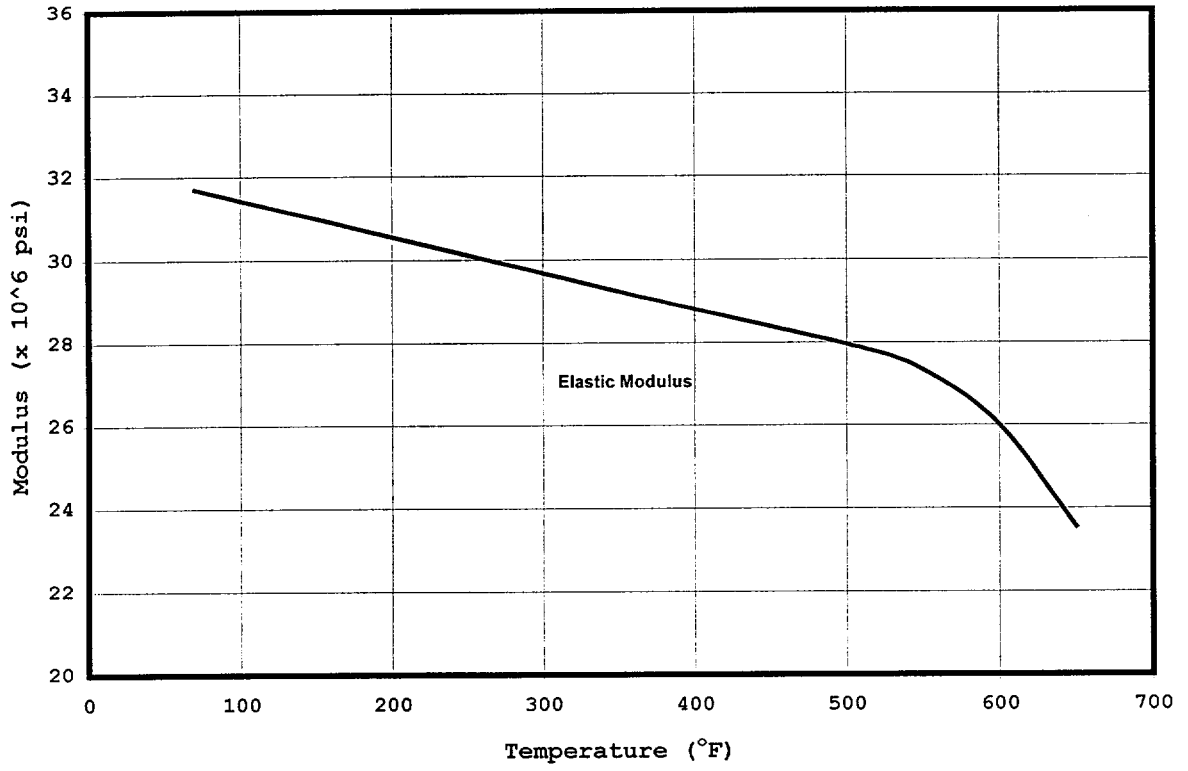
The specimen design is illustrated in Figure 6.1.1.

The specimens were loaded uniaxially with load and strain measured at []^b distinct points within the elastic region. A linear regression was performed on the data points. The loading and regression process was repeated twice and averaged. The same specimen was then heated to a different temperature and the loading was repeated.

Modulus of elasticity (Young's Modulus) testing []^{b,c,e}

The testing showed that the modulus of elasticity for the electrochemically deposited nickel material does not depend on the size of the tube. Figure 6.2.1 presents the typical testing results for Young's Modulus versus temperature for all tube sizes. The variation in the average testing result for Young's Modulus versus the ASME Code value for Nickel 201 (Ni₂₀₁) over the typical RSG operating temperature range (70°F to 625°F) is approximately 6%. These results show the Young's Modulus value for Ni₂₀₁ is representative of the Electrosleeve™ nanocrystalline nickel material. Thus, the Young's Modulus of Ni₂₀₁ is used [13.2].

FIGURE 6.2.1
ELASTIC MODULUS VS. TEMPERATURE



6.3 Ductility/Adhesion

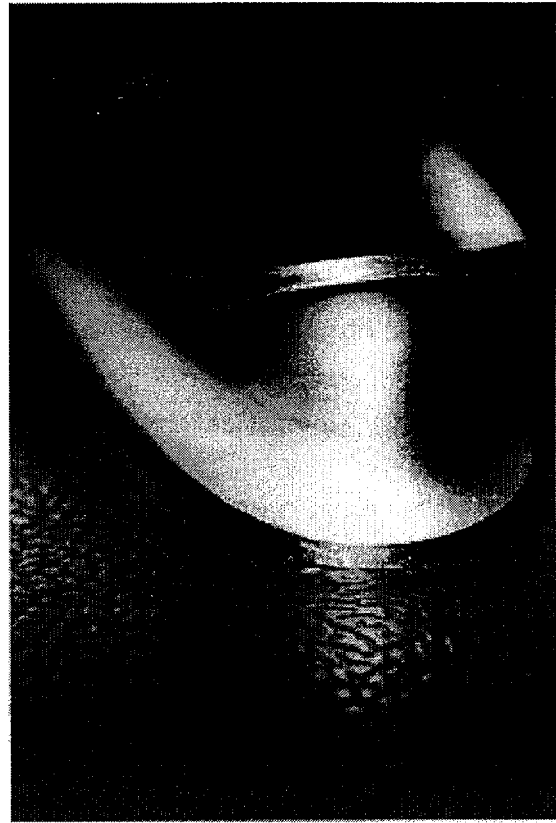
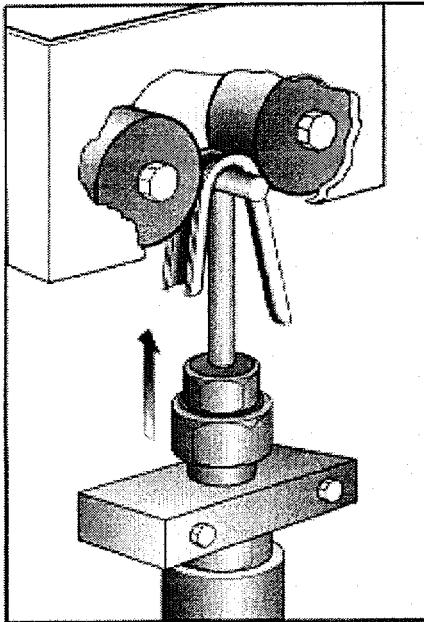
The bonding strength of the electrodeposited nickel to the tube generally depends on sufficient cleanliness of the parent tube material and an adequate nickel pre-film layer.

A vacuum-assisted rotating and translating hone or scraper is used to clean the tube surface. An electrochemical surface activation step follows the mechanical cleaning step to remove any remaining oxides []^d the tube material. The exposed clean tube surface is immediately pre-filmed with nickel to prevent the surface from passivating before the sleeve is installed. Process controls and monitoring of variables, such as applied current and voltage, provide assurance that the process cleaning and pre-filming are within specified ranges.

The Alloy 600 cleaning/surface activation process was qualified using furnace-oxidized tubing. The activation step alone was then used to clean the surface of pulled steam generator tube samples to verify that this step, without mechanical cleaning, would remove the tube surface oxides. The activation and pre-film steps are discussed in detail in Section 10.0. UT inspection verified that the electrosleeves were 100% bonded when inspected by UT.

Ductility is a controlled material property dependent on the deposition parameters. To verify the ductility and adhesion of the electrochemically deposited nickel material, []^{b,c} specimens were tested per ASTM procedure [13.20, 13.21]. Specimens were fabricated by electrosleeving a tube and then cutting it longitudinally in half. The specimens were then bent over a []^{c,e} mandrel with the nickel sleeve outside diameter in tension, as shown in Figure 6.3.1. After being bent, the sleeves were visually inspected for areas of separation and cracking. None of the qualification specimen installed per normal process procedures showed any defects. Therefore, the ductility and adhesion characteristics of the electrochemically deposited nickel material were verified and deemed acceptable (Reference 13.4). The ductility of the electrochemically deposited nickel material is further demonstrated by the ductile failures the material exhibited during the tensile tests (Section 6.1), creep tests (Section 6.6), and burst tests (Section 6.7).

FIGURE 6.3.1
REVERSE BEND SPECIMEN



The above illustrations - from left to right - show a drawing of the reverse bend test set-up and a photograph of a reverse bend specimen.

6.4 Fatigue Life

The work presented here represents the only documented systematic study of the fatigue performance of nanostructured materials. A comprehensive review [13.45] of the literature as to how grain size (i.e., ≥ 10 micrometers (μm)) affects the fatigue performance of conventional nickel and nickel-based alloys found that as grain size decreased, the resistance to fatigue crack initiation increased as did the fatigue crack propagation rate.

These results indicate nanostructured materials are expected to display superior high cycle fatigue performance (initiation controlled process) and possibly somewhat compromised low cycle fatigue resistance (propagation controlled process).

Fatigue testing was performed on [^{b,c}] electrosleeved tube specimens to establish a design fatigue curve. FTI tested four Alloy 600 tube sizes with installed electrosleeves:

- 5/8" OD x 0.034" wall,
- 3/4" OD x 0.043" wall,
- 3/4" OD x 0.048" wall, and
- 7/8" OD x 0.050" wall.

In addition, OHT performed fatigue testing on thirty-eight (38) electrosleeved tube specimens using 1/2" OD x 0.049" wall Monel 400 tubes.

Specimens with the as-plated inside surface condition and specimens with a machined inside surface were tested. All of the specimens were machined on the OD to remove the tube and the sleeve OD was polished.

Fatigue testing was performed in accordance with ASTM procedures [13.16 - 13.19]. The testing was performed with fully reversed strain, or load, on each specimen ($R = -1$) [13.19] from full axial tension to full axial compression. Ranges of frequencies were tested to encompass the expected subjective conditions an actual sleeve would experience.

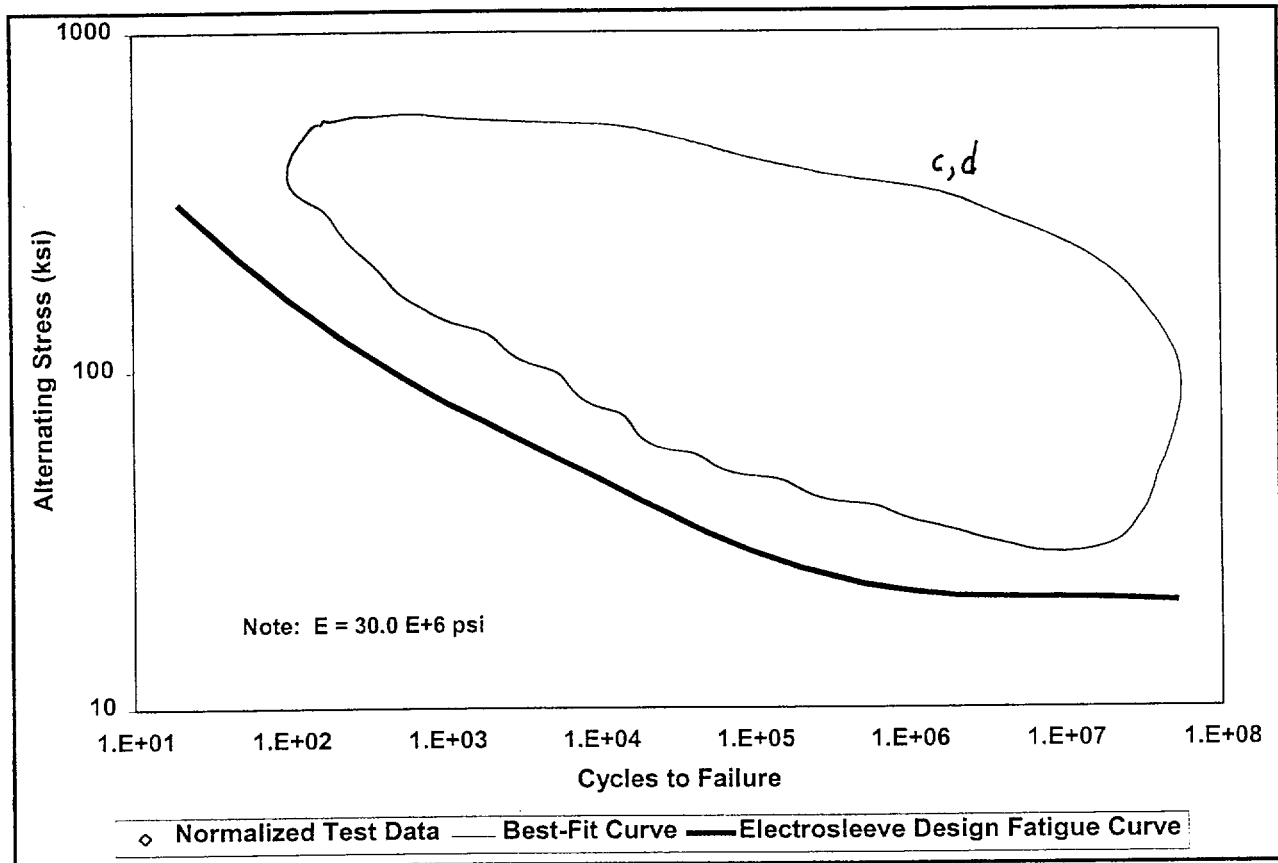
Fatigue testing of the Electrosleeve™ material was conducted at both room and elevated temperatures. Table 6.4.1 shows the material maintains its fatigue resistance in the temperature range tested.

TABLE 6.4.1
FATIGUE TESTING RESULTS

TEMPERATURE (°F)	STRAIN AMPLITUDE (%)	CYCLES TO FAILURE
Γ		b, c, d Γ
⊥		⊥

Strain amplitude data for each test specimen were tabulated, multiplied by the elastic modulus to convert to stress, and plotted against the cycles-to-failure. All of the as plated and high temperature test data were normalized to the machined ID test results at room temperature. The normalized test results are shown on Figure 6.4.1. The stress versus cycles-to-failure values for all specimens were fitted to a curve obtained by applying a least squares fit. The best fit curve through the normalized test data, Figure 6.4-1, does not contain a ASME code safety factor. The design curve was obtained from the best-fit curve by applying a factor of two on stress or a factor of twenty on cycles, whichever was more conservative at each point [13.34]. Combining the results of both of these adjusted curves resulted in a single, bounding design fatigue curve. Figure 6.4.1 illustrates the fatigue data for the Electrosleeve™ material using a modulus of elasticity (E) of 30.0×10^6 psi.

FIGURE 6.4.1
ELECTROSLEEVE™ MATERIAL NORMALIZED FATIGUE TEST DATA



6.5 Thermal Stability

Thermal stability of the Electrosleeve™ material is important because of long-term (forty years) thermal exposure to operating temperatures as high as 626°F along with upset excursions up to the design temperature of 650°F. The principal strengthening mechanism for the Electrosleeve™ material is the Hall-Petch mechanism (i.e., grain refinement) [13.60, 13.61]. Previous studies have shown that nanocrystalline nickel may exhibit a driving force for grain growth several orders of magnitude greater than that for conventional polycrystalline nickel materials [13.62]. Therefore, the primary thermal effect on the Electrosleeve™ material would be a reduction in mechanical strength. Additional discussion on thermal stability and burst testing is presented in Reference 13.83.

The effect of annealing time [^{b,c,d}] on the Vickers Hardness Measurements (VHN) of the Electrosleeve™ material was determined. Electrosleeve™ material with the following alloys were evaluated:

- Nanocrystalline pure nickel,
- Nanocrystalline nickel [^{c,e}] and
- Nanocrystalline nickel [^{c,e}]

[^{b,c}] electrosleeved tubes were used to fabricate [^{b,c}] test specimens (three fabricated from each tube). Figure 6.5.1 shows the test specimen configuration. Each test configuration used five test specimens. The hardness values reported are at the mid-wall location of the Electrosleeve™ material. Each data point represents a minimum of four readings from each of the five specimens. VHN values are in accordance with ASTM procedure [13.23]. The Electrosleeve™ materials used had a plated hardness [^{d,e}]

FIGURE 6.5.1
MATERIAL TEST SPECIMEN DESIGNS
THERMAL STABILITY SPECIMENS

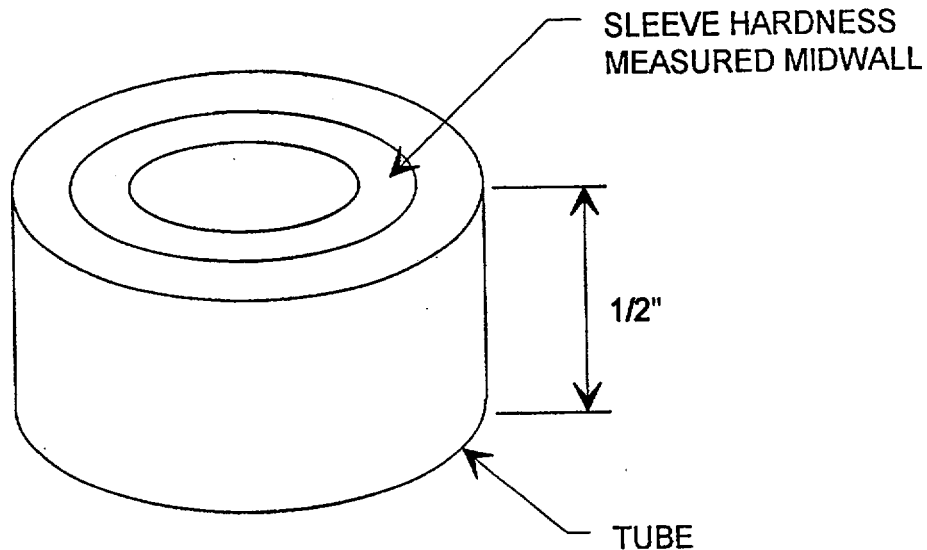
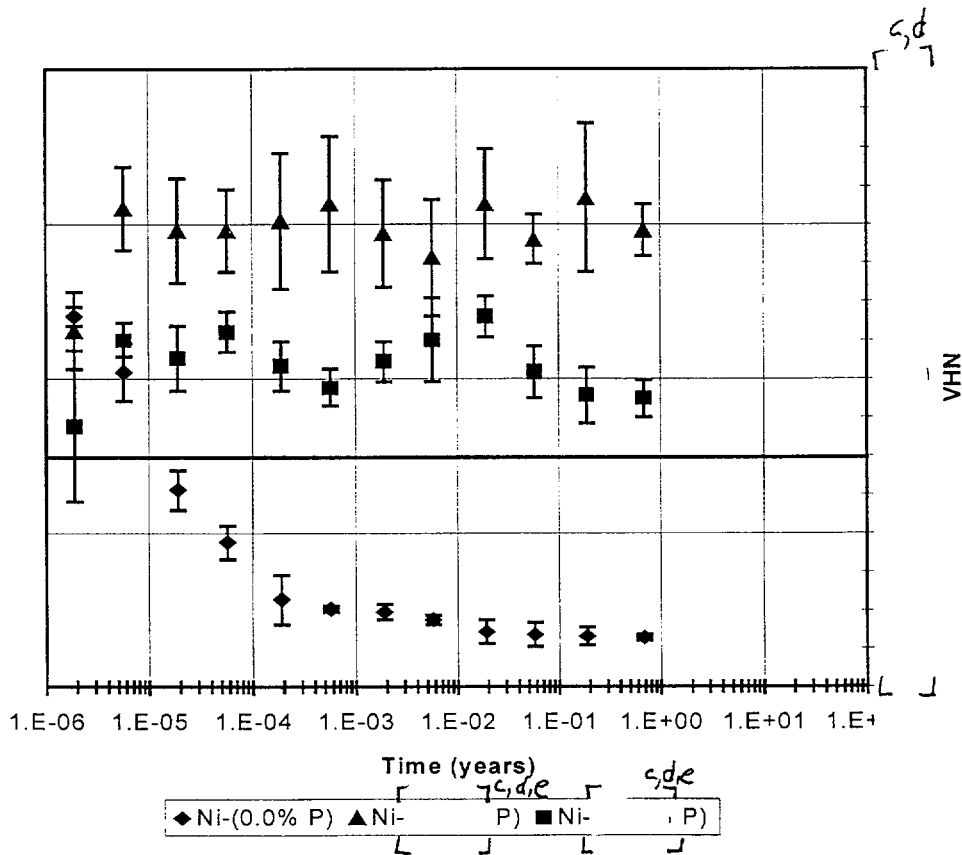


Figure 6.5.2 shows that pure nanocrystalline nickel decays rapidly ^c within the first few hours of annealing. This reduction is representative of rapid grain growth leading to a resultant grain size consistent with that of conventional polycrystals (i.e., 10 - 30 μm). The nanocrystalline nickel containing ^{d,e} phosphorus ^b shows no evidence of hardness decay within the total test period evaluated (i.e., approximately 10 months). The influence of minor solute additions on retarding grain growth in nanostructured nickel was previously documented [13.62, 13.63] and attributed to:

- Solute drag effects on the grain boundaries,
- Reduction in grain boundary (GB) energy from solute segregation, and
- Zener drag effects associated with the possible formation of nano-precipitates [13.62, 13.63, 13.74].

FIGURE 6.5.2
ELECTROSLEEVE™ THERMAL STABILITY TEST RESULTS AT 650°F



The margin of safety for the thermal stability of the Electrosleeve™ material was determined using differential scanning calorimetry (DSC) measurements. Figure 6.5.3 is a typical DSC scan for the Electrosleeve™ material. The DSC scan detected an exothermic peak at approximately 580°C (1076°F). The results of the DSC analysis shown in Figure 6.5.4 are in the form of a Kissinger plot [13.64]. In the peak temperature (T_p) range of 560°C - 580°C (1040°F - 1076°F) with heating rates ranging from 30 - 100 K/min., the shifts in the exothermic peaks are shown to yield an apparent activation energy of 59 kcal/mole.

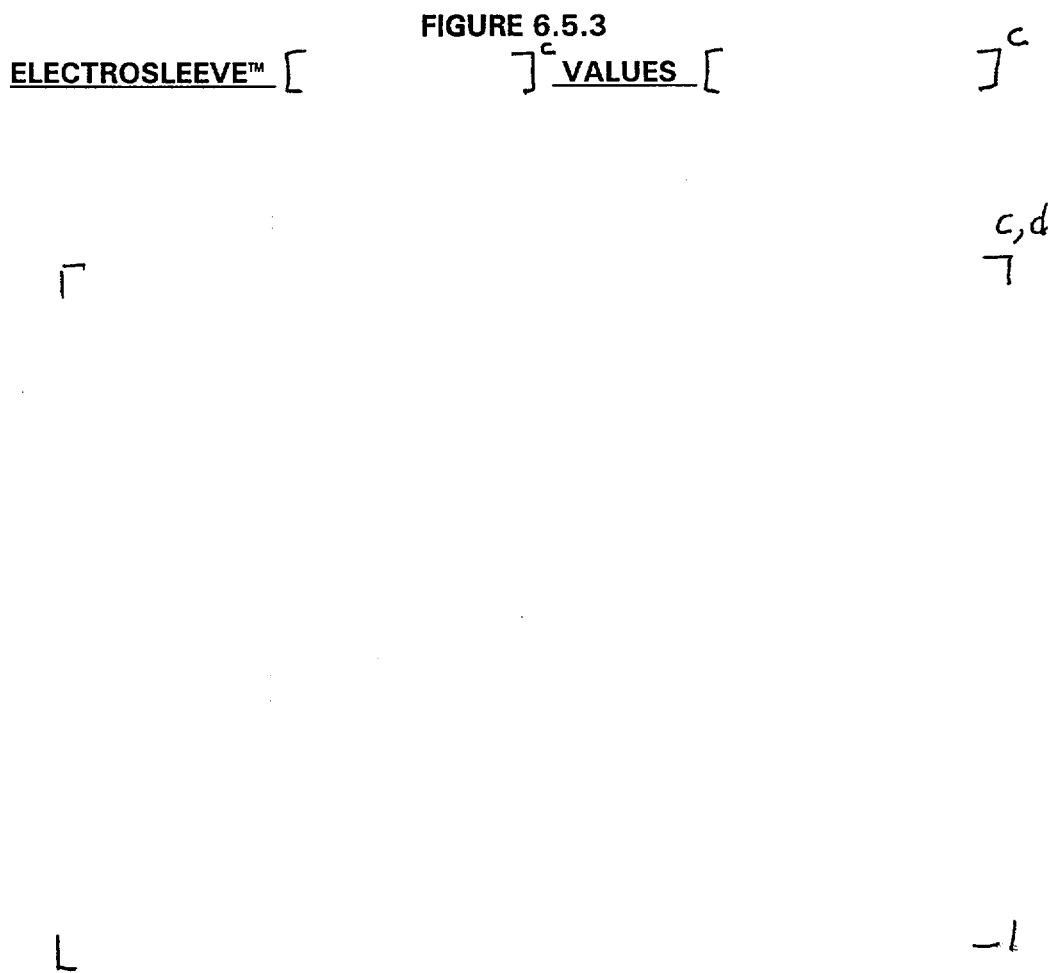
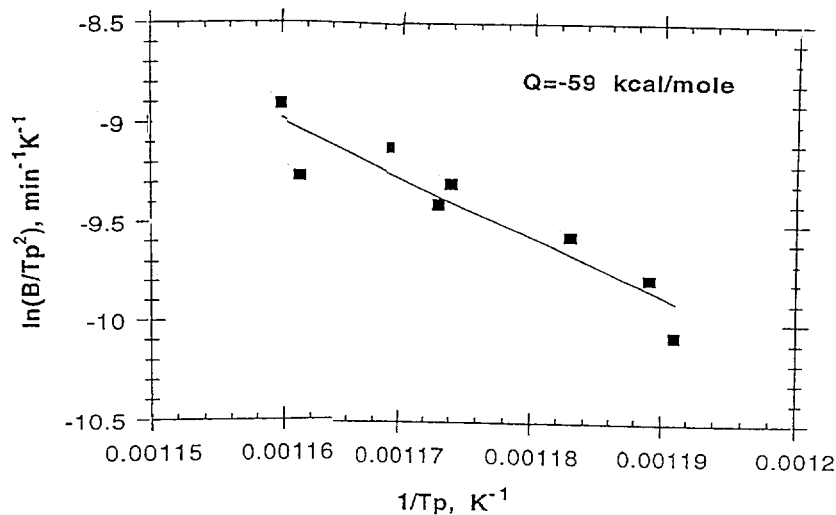


FIGURE 6.5.4
KISSINGER PLOT FOR ACTIVATION ENERGY



By using DSC, Mehta, et. al., evaluated the thermal stability of a (Ni - 1.2 wt% P) alloy having an average grain size of 10 nm [13.65]. The exothermic peak was found to be 360°C (680°F) and the activation energy was found to be approximately 52 kcal/mol. These values were attributed to the onset of rapid grain growth associated with a transition from solute drag as the primary stabilizing influence at lower temperatures to a weaker grain boundary pinning by Ni_3P precipitates at the elevated temperatures. The higher values of activation energy and peak temperature reported for the Electrosleeve™ material are primarily attributed to a larger grain size (i.e., 100 nm) leading to a reduced driving force for grain growth.

Figure 6.5.5 shows schematically the expected mechanism for thermal destabilization of the Electrosleeve™ material. At temperatures below T_p (i.e., approximately 560°C or 1040°F), the Electrosleeve™ material structure is primarily stabilized by the presence of continuous phosphorous at the grain boundaries. At temperatures above T_p , the precipitate Ni_3P can form readily and results in phosphorous depletion at grain boundaries. Grain boundaries can then migrate; however, depending upon temperature, they may be pinned by the Ni_3P . At higher temperatures, the grain boundaries may break away from the precipitates and grain growth may continue. The process described predicted increasing activation energy with decreasing temperature. Some evidence for this phenomenon is seen in Figure 6.5.6 which shows activation energy values determined from microhardness measurements performed on thermally

aged Electrosleeve™ material in the temperature range of 400°C - 600°C (752°F - 1112°F). The Arrhenius dependence (i.e., the reciprocal of time for the onset of hardness decay) is the basis of the activation energy shown in Figure 6.5.6.

FIGURE 6.5.5
EXPECTED THERMAL DESTABILIZATION MECHANISM

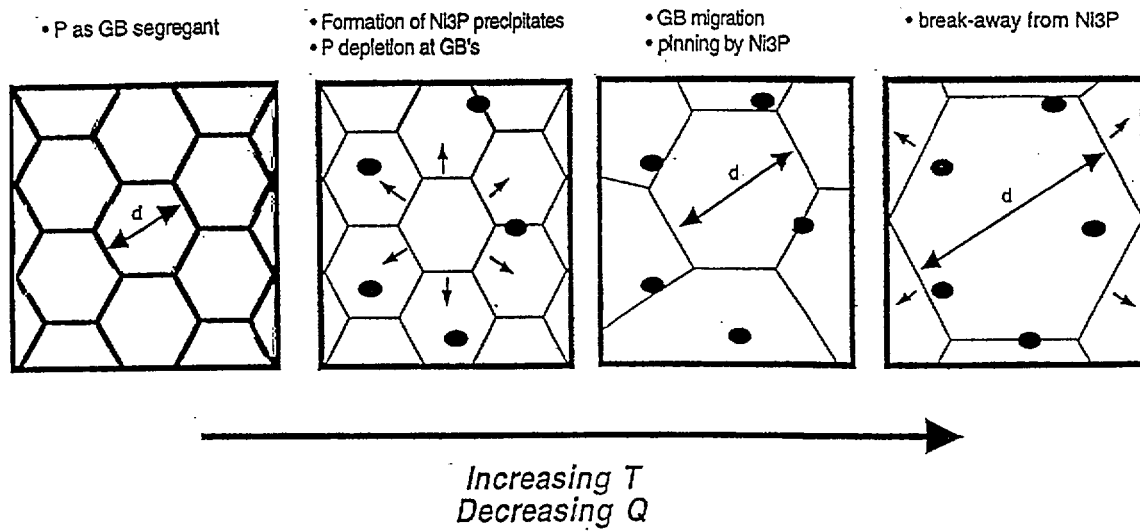
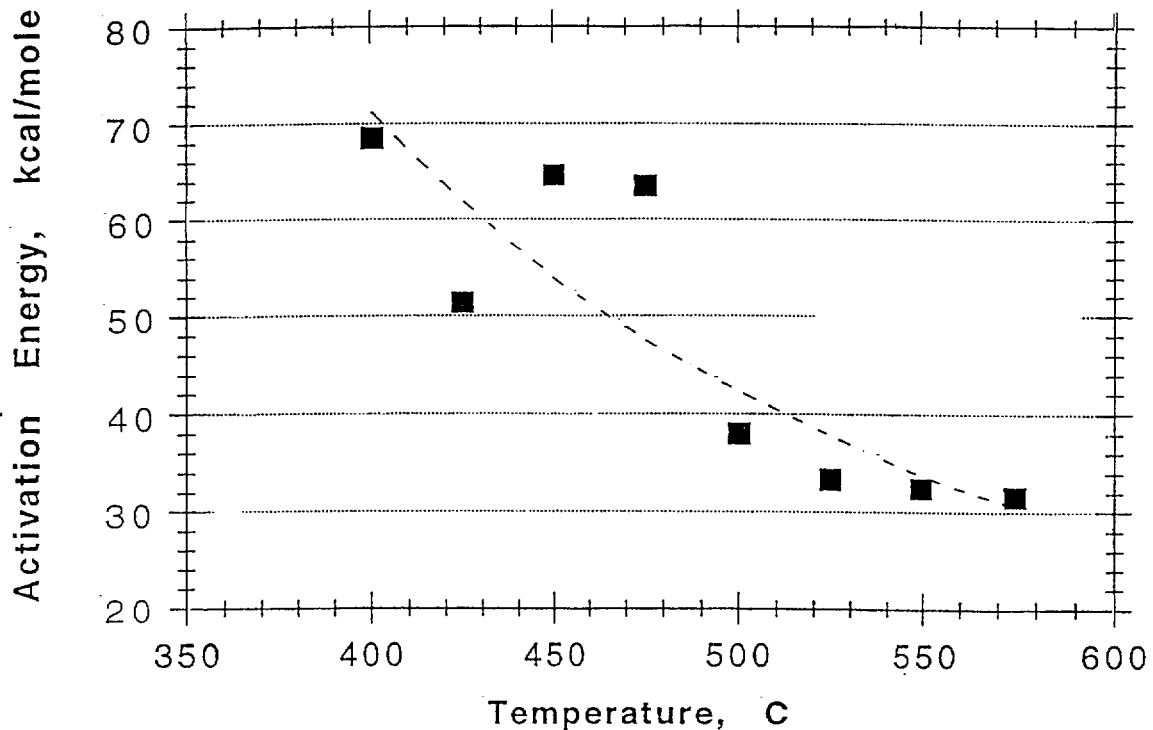


FIGURE 6.5.6
ELECTROSLEEVE™ ACTIVATION ENERGY VS. TEMPERATURE



While DSC analysis provides an approximate assessment of thermal stability associated with rapid grain growth processes the values of activation energy displayed in Figure 6.5.6 are more representative of the actual service conditions of an installed Electrosleeve™ in a steam generator. Figure 6.5.6 shows that, for long-term exposure to temperatures of approximately 350°C (662°F), the activation energy for grain growth of the Electrosleeve™ material is above 70 kcal/mole. This proves the excellent thermal stability of the Electrosleeve™ material at operating temperatures.

The testing results summarized in Figure 6.5.2 demonstrate that the Electrosleeve™ material is fully stable at the PWR design temperature of 650°F and at the lower operational temperatures. Additional testing at 675°F verified thermal stability. However, thermal destabilization will not result in catastrophic deterioration of the Electrosleeve™ material. Thermal destabilization will occur as a gradual reduction in the mechanical properties similar to conventional Ni₂₀₁.

Resistance to Strain-Induced Recrystallization

Due to the cold-work stored energy, strained materials tend to undergo recrystallization accompanied by a commensurate decrease in mechanical strength at temperatures well below those required for the onset of normal grain growth. C-ring specimens of electrosleeved Alloy 600 tubing subjected to 1.0%, 1.5%, and 2.0% nominal strain were used to assess the susceptibility of Electrosleeve™ material to strain-induced recrystallization. These strain values were into the plastic regime. The specimens were then thermally treated at 662°F for 1,500 and 3,000 hours.

After the specimens were thermally treated, the microhardness was determined in the sleeve region near the Alloy 600 interface where the maximum deformation is expected. The results are summarized in Table 6.5.1.

TABLE 6.5.1
SUMMARY OF MICROHARDNESS DETERMINATION
ON STRAIN-ANNEALED ELECTROSLEEVES

APPLIED STRAIN (%)	HARDNESS AT 1,500 hrs. (VHN)	HARDNESS AT 3,000 hrs. (VHN)
1.0	362 ± 60	374 ± 76
1.5	354 ± 6	318 ± 9
2.0	314 ± 12	373 ± 60

The results showed no evidence that recrystallization occurred in any of the specimens since the hardness of recrystallized nickel is expected to be less than 150 VHN. The hardness values are consistent with the normal variance in hardness noted with plated material.

6.6 Creep Properties

The effect of decreasing grain size on creep deformation has been well documented with steady-state creep rates generally increasing with decreasing grain size. However, with the exception of the work presented here, to date there have only been a few studies on the creep performance of nanostructured materials. Wang and co-workers recently demonstrated that nanocrystalline nickel with a grain size of less than 40 nm can exhibit grain boundary sliding deformation at room temperature [13.46]. At average grain sizes greater than 40 nm, dislocation mechanisms (i.e., power law creep) were shown to be operative.

Intrinsic intergranular creep cracking is the predominant mode of premature creep failure for engineering materials. A recent study showed that geometric constraints associated with decreasing grain size could render nanostructured materials highly resistant and possibly immune to this mode of creep failure [13.47]. This resistance is likely manifested as:

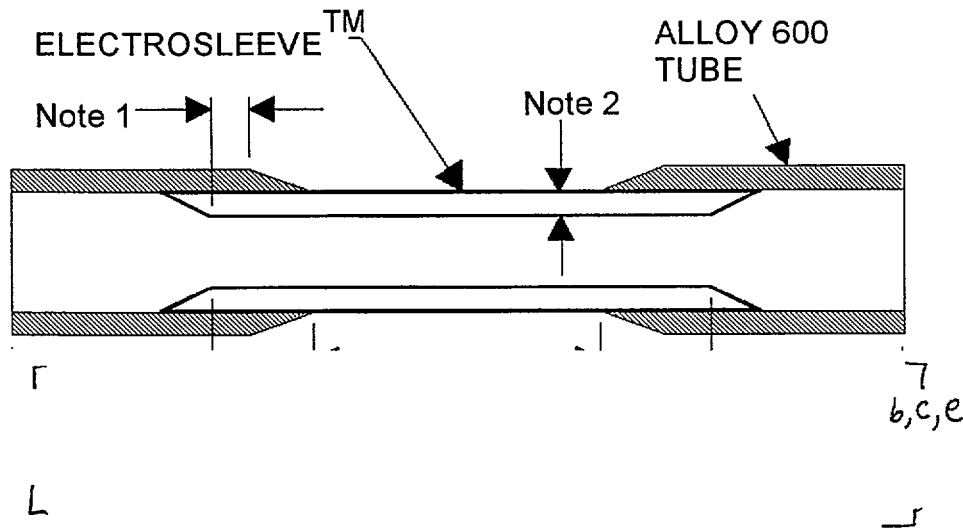
- The exclusive appearance of ductile fracture features in failed creep specimens,
- Minimal time-dependent total strain at failure, and
- Extended creep life despite possibly enhanced steady-state creep rates.

A series of constant load creep tests was performed using ASTM E139 [13.22] as a guideline to determine the creep behavior of the Electrosleeve™ material. Creep testing determines deformation as a function of time and the time to fracture at an elevated temperature when sufficient load is present. Constant-load creep testing is performed in a controlled environment at constant temperature. The measured deformation for a defined gauge length provides a strain-versus-time data presentation that represents the creep phenomena. Selecting a mathematical equation to model this phenomena is a significant challenge. The applicable literature presents many options for modeling creep [13.30, 13.31, and 13.38] and finite element codes [13.32] have creep calculation capability for analysis. Section 8.6 presents an evaluation of the data and analysis. Figures 6.6.1 and 6.6.2 are typical fabrication drawings of the creep test specimens.

Four types of creep specimens were tested:

- Standard Specimen: This specimen (Figure 6.6.1) was a standard tensile specimen. The tube was machined to produce a nominal gage length. This specimen was used to establish creep rates.

FIGURE 6.6.1
STANDARD CREEP SPECIMEN

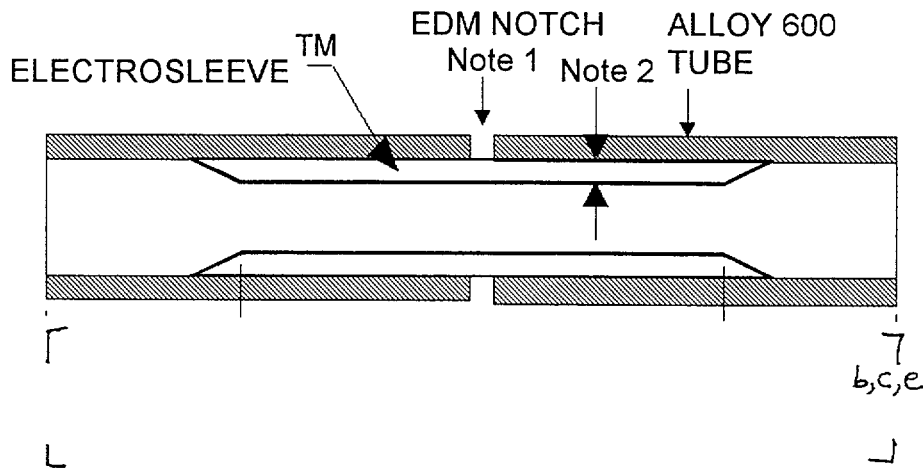


NOTES:

- (1) The sleeve-to-tube bond length was nominally $[\quad]^e$ long, except for the minimum bond specimen, which had a $[\quad]^e$ bond length.
- (2) The wall thickness of the sleeve varied from $[\quad]^e$ depending on the specimen.

- Circ. Notched Specimen: This specimen (Figure 6.6.2) was a "best effort" creation to evaluate factors associated with notch sensitivity. The specimen was fabricated by machining a 360° circumferential, 100% through-wall EDM notch in the Alloy 600 parent tube. The width of the notch was specified as []^{b,c} with a radius at the bottom of the EDM notch of []^{b,c} or less.

FIGURE 6.6.2
CIRCUMFERENTIALLY NOTCHED CREEP SPECIMEN

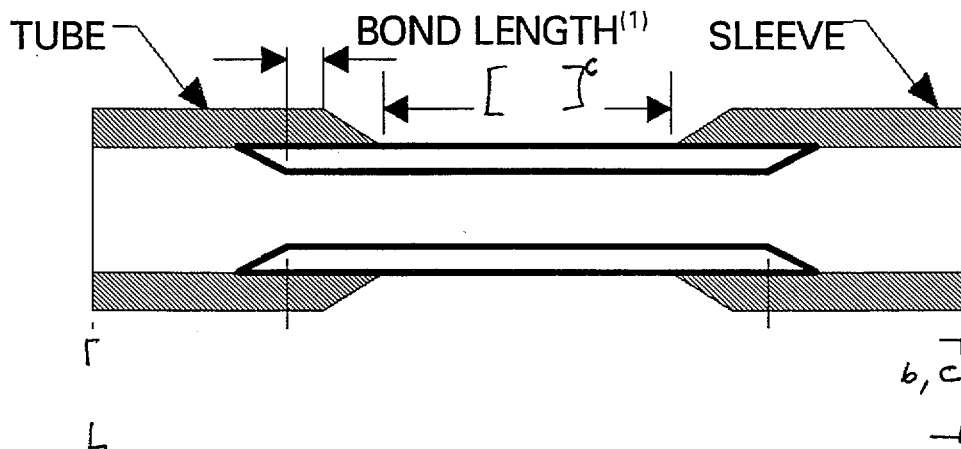


NOTES:

- EDM notch specimens had a 360° circumferential notch, []^{b,e}
- The wall thickness of the sleeve varied []^{c,e} depending on the specimen.

- Minimum Bond Specimen:** This specimen (Figure 6.6.3) was fabricated by machining the tube and sleeve such that only a small sleeve-to-tube bond length existed (nominally $[]^{c,e}$ inch, minimum $[]^{c,e}$ inch). This specimen was used to evaluate any interaction between a minimum bond and creep. This specimen was subjected to experimental fatigue tests consisting of axial load cycling and thermal cycling prior to creep testing. Refer to Section 7.4 for a description of these tests.

FIGURE 6.6.3
MECHANICAL TEST SPECIMEN DESIGNS
MINIMUM BOND FATIGUE AND BURST SPECIMENS



NOTES:

- (1) The sleeve to tube bond length for the minimum bond fatigue specimens was nominally $[]^{c,e}$

- C-Ring Specimen: These specimens were fabricated from an installed Electro sleeve™ and were loaded to OD tensile strains of []^{b,c}. The specimens were put into a []^{b,c} NaOH (caustic) corrosion test []^{b,d} (see Section 9.3.1.2). The specimens exhibited 100% through-wall SCC cracks in the Alloy 600 tube. The Alloy 600 cracks were blunted at the nickel surface. No cracking was observed in the nickel material. While the primary purpose of this test was to show corrosion resistance, it also served to show creep cracking did not occur at an SCC crack tip under high stress.

Table 6.6.1 lists the creep test specimens. Tests performed at temperatures []^{b,c} were used to evaluate the influence of temperature. Figure 6.6.4 presents typical creep test []^d. The standard specimen geometries exhibited ductile failures with typical elongation []^{c,d}.

TABLE 6.6.1 (Cont'd)
CREEP TEST SPECIMENS

CONSTANT AXIAL LOAD WITH PRESSURE CREEP TEST⁽¹⁾⁽²⁾

┌					┐	c,d
└					┘	

CREEP TEST SAMPLE PREPARATION FOR FATIGUE

┌					┐	c,d
└					┘	

NOTES:

- (1) All creep testing for material verification is complete.
- (2) All tests were performed at constant temperature and constant load.
- (3) Specimen types are defined as follows:
 - a. Standard: Standard creep test specimen per Figure 6.6.1.
 - b. Circ Notch: A 360°, 100% through-wall notch machined on the tube ([])^{b,c} per Figure 6.6.2.
 - c. Min. Bond: The sample had a nominal sleeve to tube bond length []^{b,c} per Figure 6.6.3.
- (4) Microstructural exam result: fully ductile morphology; no evidence of intergranular-sliding, voids, cavitation, or fracture.
- (5) Prior to constant load creep test, this sample was fatigue cycled for a loading sequence equivalent to 40 effective full power years (EFPY) with a factor of []^d on the number of test cycles.
- (6) Sample removed from creep test to perform fatigue test.
- (7) This creep test was discontinued since sufficient data had been accumulated for the specimen.
- (8) Strain was not measured due to specimen design.

FIGURE 6.6.4
CREEP TEST RESULTS

c,d
7

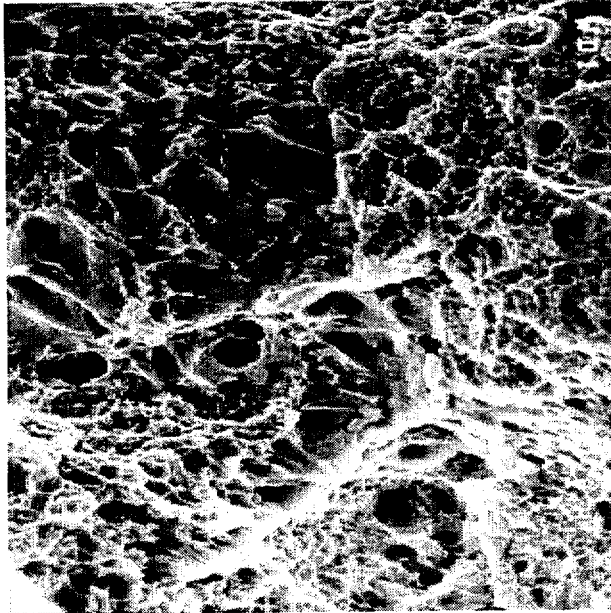
┌

└

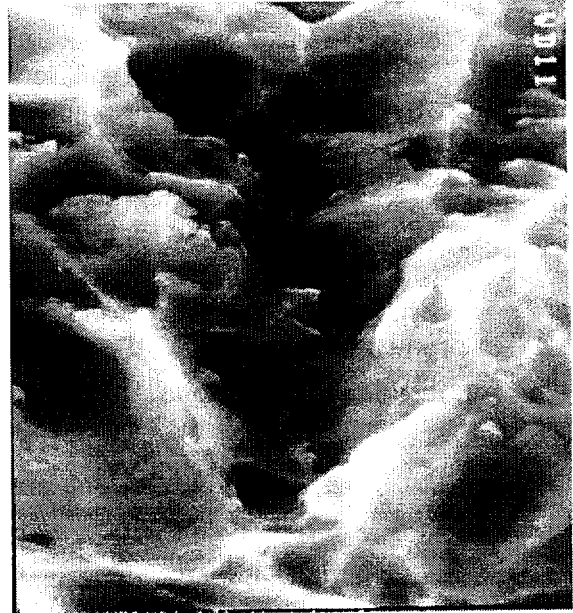
└

Creep fracture faces on specimens designated 34-060, CT-007, and 34-023 were examined by high resolution field emission scanning electron microscopy (FESEM) to elucidate the nature of the fracture mode. The high-resolution capability of the FESEM was utilized to identify any possible contributions from grain boundaries to the fracture processes of the ultra-fine-grained Electrosleeve™ material (approximately 100 nm grain size). Figure 6.6.5 shows photomicrographs of the fracture faces of specimens 34-053 and CT-007 at magnifications ranging from 5000X to 110,000X.

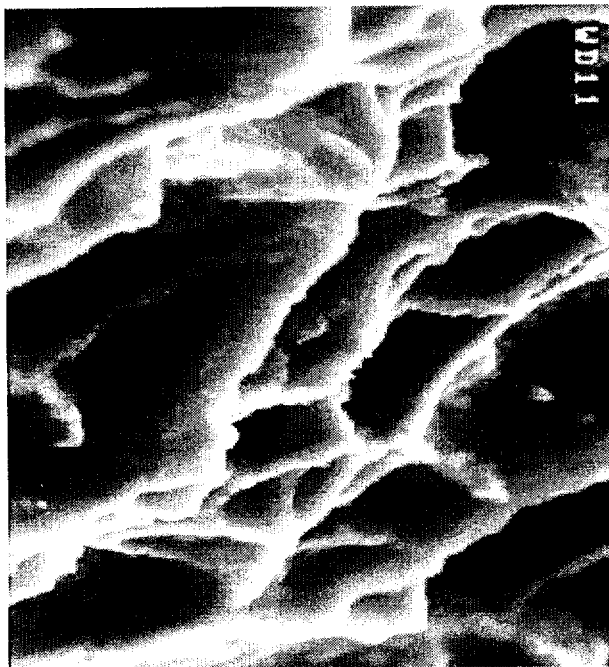
FIGURE 6.6.5
ELECTROSLEEVE™ TYPICAL FRACTURE SURFACE FRACTOGRAPHY



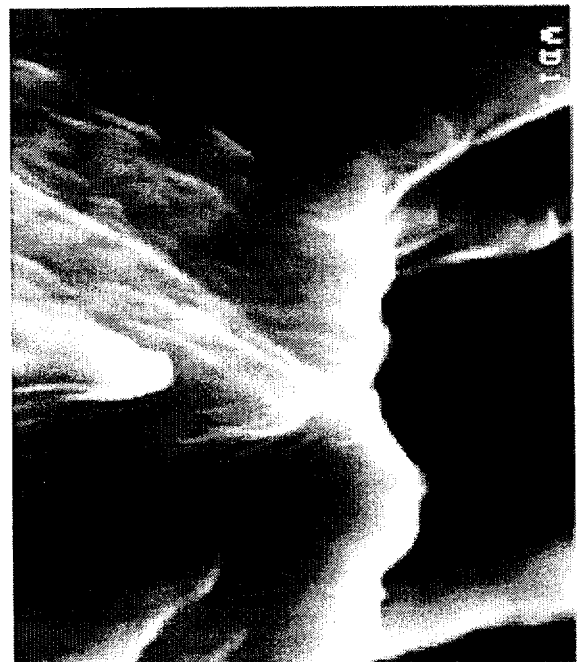
Magnified 5,000X
Serial No. 34-023



Magnified 30,000X
Serial No. 34-023



Magnified 30,000X
Serial No. CT-007



Magnified 110,000X
Serial No. CT-007

The creep fracture faces examined had some unique differences in loading conditions:

- CT-007 was a standard tension specimen that failed in tension.
- 34-023, a minimum bond sample, was first exposed to fatigue loadings and then creep tested to failure.
- 34-060, an EDM circumferential notch sample, was exposed to an axial load in conjunction with internal pressure and then creep tested to failure.

Photomicrographs recorded at magnifications of approximately 5000X show that the fracture faces of all specimens examined are entirely ductile in nature and possess classical microvoid coalescence features. Inspection at higher magnification (>70,000X) reveals the ultrafine grain structure of the material. No evidence of grain boundary cavitation or fracture was evident in any of the fracture faces examined. Indeed, the grain boundary regions appear "raised" relative to the grain interiors, whereas intergranular fracture would typically yield "ditched" grain boundary regions.

In summary, fractographic analysis of specimens 34-060, CT-007, and 34-023 demonstrated that creep failures are entirely ductile in nature with no evidence of operative intergranular failure mechanisms.

Extrinsic creep cracking is the creep-assisted propagation of a pre-existing flaw (crack) in the material of interest (e.g., Electrosleeve™). Although the resistance of nanostructured materials to extrinsic creep cracking has yet to be addressed elsewhere, considerable evidence exists that the bi-material interface comprising the nanostructured Electrosleeve™ and Alloy 600 parent tubing poses a formidable barrier to crack penetration and propagation. Sugimura, et. al., have considered the general case of crack propagation in a bi-material system in which the two materials have similar elastic properties but different plastic properties (i.e., yield strength) [13.48]. The authors show by both geometric considerations and experimental data that when a crack in the material having the lower yield strength (e.g., Alloy 600) approaches a bi-material interface, crack tip shielding will occur, which inhibits crack penetration into the material of higher yield strength (e.g., Electrosleeve™). Further evidence for the extrinsic creep cracking resistance of the Electrosleeve™ was obtained from the caustic SCC test results as presented in Section 9.3.1.2. These results demonstrate that SCC-induced sharp cracks in Alloy 600 were "blunted" upon encountering the

Electrosleeve™ for extended periods of time under both high stress and elevated temperature conditions (i.e., creep conditions).

6.7 Burst Strength

Burst testing was performed on eleven (11) Electrosleeve™ specimens. Figure 6.6.3 shows the specimen design. Each specimen had a machined gauge length to accurately test the burst characteristics of the electrochemically deposited nickel material.

The specimens were pressurized using a hydraulic pressure generator at room temperature. Per EPRI guidelines [13.68], the specimens were internally pressurized at a rate of 200 to 2000 psi per second. Table 6.7.1 shows the results for the different sizes of specimens tested. For supplemental information, Table 6.7.2 contains OHT results for burst testing at a temperature of 581°F for electrosleeved specimens installed in 1/2" x 0.049" Monel 400 tubes. The data indicate that the electroformed sleeve material burst pressure can be calculated by classical burst pressure formulas such as:

$$P_a = 2tS_u / D_o$$

where:

P_a	=	calculated minimum burst pressure
t	=	actual thickness
S_u	=	actual ultimate tensile strength
D_o	=	outside diameter

6.8 Thermodynamic Properties

Testing performed on nanocrystalline nickel [13.33] showed that the measured temperature-dependent properties (linear coefficient of thermal expansion and isobaric heat capacity) of nanocrystalline nickel produced by electrodeposition compared well with the results obtained for conventional polycrystalline nickel material. Therefore, the physical properties of Ni₂₀₁ from Reference 13.2 were used to determine the coefficient of thermal expansion, thermal conductivity, specific heat, and density of the nanocrystalline material.

7.0 DESIGN VERIFICATION - MECHANICAL TESTING

The Electrosleeve™ qualification program combined analysis and mechanical testing to meet the sleeve qualification requirements presented in Section 4.0. This section summarizes the mechanical testing; Section 8.0 presents the analysis results. Together, Sections 7.0 and 8.0 demonstrate that the installed Electrosleeve™ is qualified for application in all RSG designs and their operating conditions.

7.1 Locked Tube Testing

Locked tube testing was performed to measure the loads induced on a locked parent tube as a result of the electrosleeving installation process. Four mockups were tested: three measuring 3/4" x 0.043" wall and one that measured 7/8" x 0.050" wall. Each mockup had tubes that were roll expanded and welded into the TS and TSP, reinforced with tie rods, instrumented with strain gages and thermocouples, and sleeved in the TS and freespan. Figure 7.1.1 depicts a typical mockup used in the locked tube testing.

Table 7.1.1 shows the results for a 4-inch long Electrosleeve™ installed in the freespan.

TABLE 7.1.1
LOCKED TUBE TEST RESULTS

TUBE OD (INCHES)	LOCKED TUBE SPAN TEST LENGTH (INCHES)	TESTING AVERAGE AXIAL TENSION LOAD (LBS)	TUBE AXIAL TENSILE STRESS (KSI)
3/4	┌		┐ ^{d,}
7/8	└		┘ ^e

The results of the locked tube testing for the 3/4" and 7/8" tubes were used to calculate a typical locked tube loading for the 11/16" tube. The loads were then normalized to a typical span length for each tube size. The tube axial stress outside the sleeved region was also calculated.

The calculated results for a [^{b,c}] Electrosleeve™ installed completely within the tube span are presented in Table 7.1.2.

TABLE 7.1.2
CALCULATED LOADS FOR LOCKED TUBES

TUBE OD (INCHES)	TYPICAL LOCKED TUBE SPAN LENGTH (INCHES)	TYPICAL LOCKED TUBE AXIAL TENSION LOAD (LBS)	TYPICAL LOCKED TUBE AXIAL TENSILE STRESS (KSI)
11/16	┌		┐ ^{b,c,}
3/4			┘ ^{d,e}
7/8	└		┘

To determine the effect of different sleeve lengths or of multiple installed sleeves within a particular span, the axial span load and stress may be ratioed by the actual length of the installed sleeve(s) versus the [^{b,c}] length. These stresses are considered low and thus not significant.

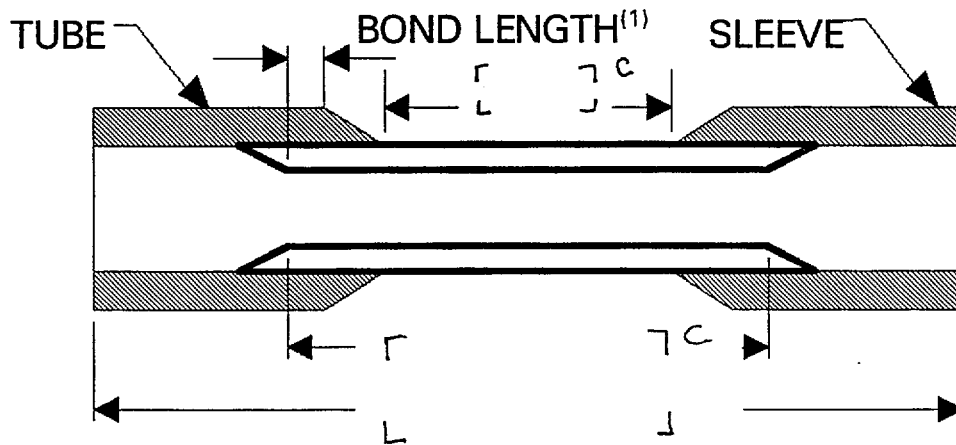
7.2 Fatigue Testing

Section III of the ASME B&PV Code does not provide design rules for sleeves fabricated in situ by electrochemically deposited material. In such cases, the ASME B&PV Code, Section III, Appendix II [13.2] allows the use of experimental stress analysis to substantiate the critical, or governing, stresses. The adequacy of the installed material and its bond to the tube to withstand operational pressure and thermal cyclic loadings was demonstrated by means of fatigue testing per the ASME B&PV Code, Section III, Article II-1500 [13.2].

The Electrosleeve™ is designed to accommodate all loads that any steam generator tube can experience due to normal plant conditions and all anticipated transients specified for the steam generator. Appendix A summarizes the expected transient conditions that were used to qualify the Electrosleeve™ design. The fatigue testing loads associated with these transients are reported in Section 8.2.

The minimum bond specimen illustrated in Figure 7.2.1 (this figure is the same as Figure 6.6.3) addresses the situation where significant degradation and metal loss of the parent tube occurs (e.g., wastage, gross intergranular attack (IGA)). The sample was machined so that the minimum acceptable bond length between the tube and Electrosleeve™ was present. The nominal bond length in the samples was []^{b,c}, while some samples had a []^{b,c} bond. The testing described below verified that the Electrosleeve™ and the minimum bond length will carry the loads imposed in service for the various steam generator designs.

FIGURE 7.2.1
 MECHANICAL TEST SPECIMEN DESIGNS
 MINIMUM BOND FATIGUE AND BURST SPECIMENS⁽²⁾



NOTES:

- (1) The sleeve to tube bond length for the minimum bond fatigue specimens was nominally $[] \cdot b \cdot c$
- (2) The tube and sleeve sizes for the test specimens are given in Table 7.2.1 and Section 7.3.

Eight specimens were tested, two of each tube size, as described below:

TABLE 7.2.1
FATIGUE TESTING SPECIMENS

NUMBER OF TEST SPECIMENS	TUBE SIZE	SLEEVE WALL THICKNESS (INCHES)
2	5/8" OD x 0.034" wall	┌
2	3/4" OD x 0.043" wall	┌ b, c, e
2	3/4" OD x 0.048" wall	┌
2	7/8" OD x 0.050" wall	└

The minimum bond fatigue test specimens were tested with loadings that represent the design life of an installed sleeve and are given in Table 7.2.2.

TABLE 7.2.2
SUMMARY OF MINIMUM BOND FATIGUE TEST LOAD RANGES⁽¹⁾⁽²⁾

Γ		7

b,c,d

L

1

In accordance with the methodology outlined in ASME Section XI, these test specimens were subjected to temperature and pressure cycles to demonstrate structural integrity. Thermal cycling was performed to determine if the differences in the thermal expansion coefficients for the sleeve and the tube would adversely affect the sleeve-to-tube joint. The thermal cycling involved heating the specimens []. The pressure cycling involved internally pressurizing the specimens []. The sleeve-to-tube joint was ultrasonically examined after test completion to verify that the Electrosleeve™ did not separate from the tube.

The axial cycling was performed at room temperature to the test loads described in Section 8.2. The test loads were based on the highest set of operating tube loads anticipated, considering locked or unlocked tubes at the tube support plates. The test loads and cycles were increased to account for the number of test specimens per the requirements of ASME Code, Section III, Appendix II.

The acceptance criteria used for the axial cycle testing were for the specimens to complete the required cycling with no failure. Failure is defined "as a propagation of a crack through the entire thickness, such as would produce a measurable leak in a pressure retaining member" [13.2]. This criterion applies to the exposed Electrosleeve™ material as well as the sleeve-to-tube bond.

As the fatigue tests were completed, the specimens were examined visually and tested ultrasonically for bond or sleeve failure. [] specimens were acceptable with no evidence of degradation or leakage.

7.3 Testing of Degraded Sleeves

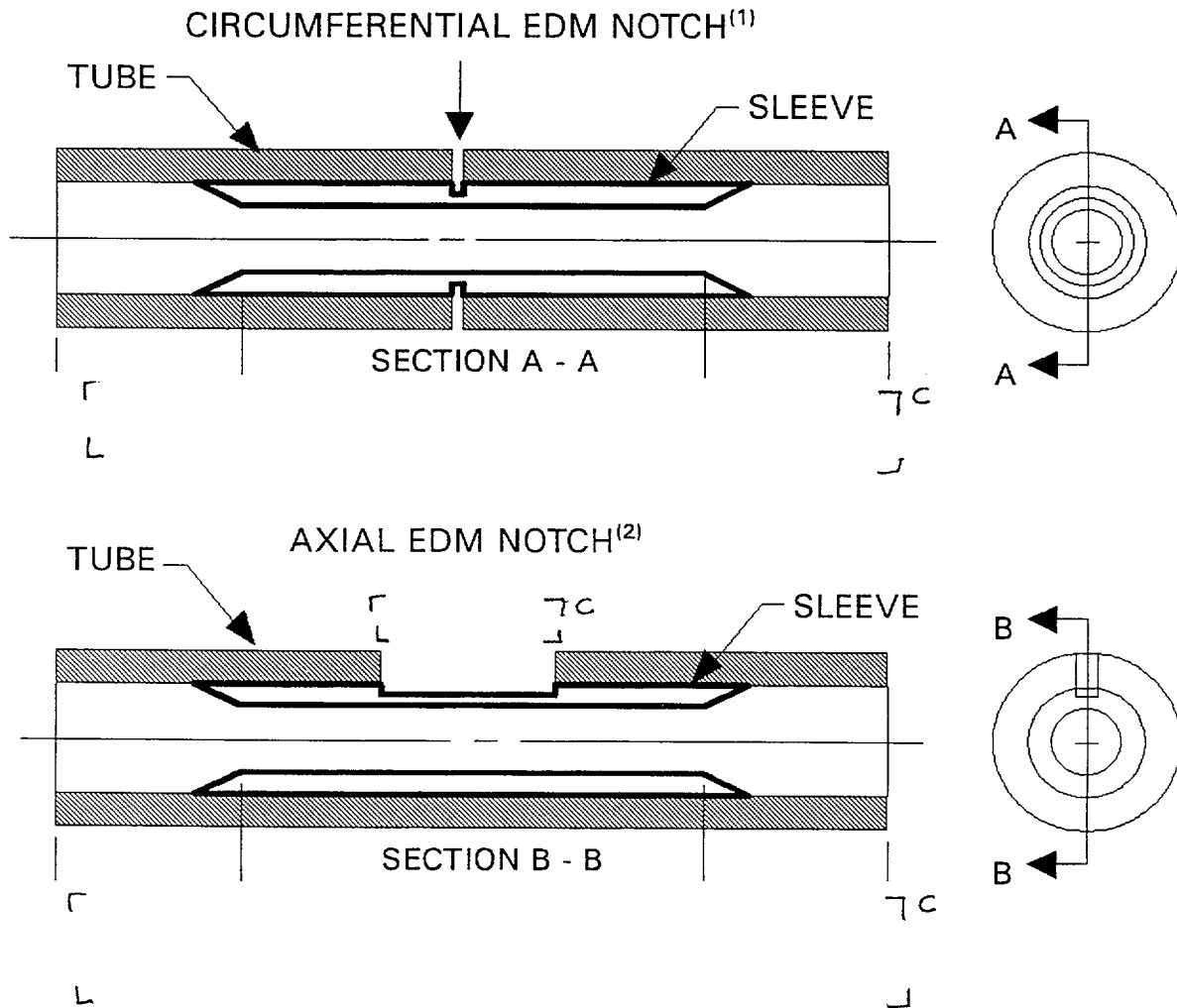
A series of fatigue tests was performed on mechanically degraded sleeves to establish plugging criteria per the guidelines of the NRC Draft Regulatory Guide 1.121 [13.6]. Test specimens with [] EDM notches were used as a "best effort" for this testing. The EDM notched specimens had a radius []. This testing was done to support development of plugging criteria as discussed in Section 12.0. Two types of tests were performed on the degraded sleeves, fatigue and burst.

7.3.1 Plugging Criteria Fatigue Tests

The analysis for a degraded sleeve considered two types of flaws, a 360° circumferential flaw and an infinitely long axial flaw. The flaws were considered to extend []^c through-wall of the parent tube and []^{b,c,e} into the wall thickness of the sleeve.

Based on these flaws, cyclic test loads were developed to represent design basis transients (Section 8.2). Eight test specimens were fabricated and subjected to these test loads. The specimens were fabricated as shown in Figure 7.3.1 and are listed in Table 7.3.1. Tables 7.3.2 and 7.3.3 define the test loads. The sleeves with axial defects were tested by cycling internal pressure. Similarly, the sleeves with circumferential defects were tested with cyclic axial loads. The required loads for the 11/16" OD tube are shown for comparison.

FIGURE 7.3.1
 MECHANICAL TEST SPECIMEN DESIGNS
 PLUGGING CRITERIA FATIGUE SPECIMENS



NOTES:

- (1) The circumferential EDM notch extended 360° around the specimen and []^{b,c} into the wall thickness of the sleeve. []^{b,c}
- (2) The axial EDM notch was []^{b,c} long and extended []^{b,c} into the wall thickness of the sleeve. []^{b,c}

TABLE 7.3.1
PLUGGING CRITERIA FATIGUE TEST SPECIMENS

b, c, e

Γ			Γ
L			J

NOTES:

(1) Refer to Figure 7.3.1 for a sketch of the defect.

TABLE 7.3.2
CIRCUMFERENTIAL DEFECT FATIGUE TEST LOADS

11/16" OD X 0.040" TUBE SIZE ⁽¹⁾		
INTERIOR LOCKED TUBE LOAD SET FOR 40 EFPY		
AXIAL LOAD SET (lbs)	AXIAL LOAD RANGE (lbs)	TOTAL TEST CYCLES
[]
		^c
PERIPHERAL LOCKED TUBE LOAD SET FOR 40 EFPY		
AXIAL LOAD SET (lbs)	AXIAL LOAD RANGE (lbs)	TOTAL TEST CYCLES
[]
		^c

3/4" OD x 0.042"/0.043"/0.048" TUBE SIZE		
INTERIOR LOCKED TUBE LOAD SET FOR 40 EFPY		
AXIAL LOAD SET (lbs)	AXIAL LOAD RANGE (lbs)	TOTAL TEST CYCLES
[]
		^c
PERIPHERAL LOCKED TUBE LOAD SET TESTED ⁽²⁾		
AXIAL LOAD SET (lbs)	AXIAL LOAD RANGE (lbs)	TOTAL TEST CYCLES
[]
		^c

TABLE 7.3.2 (Cont'd)
CIRCUMFERENTIAL DEFECT FATIGUE TEST LOADS

7/8" OD x 0.050" TUBE SIZE		
INTERIOR LOCKED TUBE LOAD SET FOR 40 EFPY		
AXIAL LOAD SET (lbs)	AXIAL LOAD RANGE (lbs)	TOTAL TEST CYCLES
] C
PERIPHERAL LOCKED TUBE LOAD SET TESTED ⁽²⁾		
AXIAL LOAD SET (lbs)	AXIAL LOAD RANGE (lbs)	TOTAL TEST CYCLES
] C

NOTES:

- (1) The fatigue qualification for an 11/16" tube was performed by comparison of these test loads and the testing performed using the 3/4" and 7/8" OD tubes.
- (2) All test specimens were cycled to failure or 40 EFPY (whichever occurred first) using a load set representing an interior locked tube and were then conservatively cycled through the load set representing a peripheral locked tube. Each specimen had a 360°, []^{b,c} through-wall defect in the sleeve. The total test cycles shown for the peripheral tube represent the minimum time to failure.

TABLE 7.3.3
AXIAL DEFECT FATIGUE TEST LOADS

PARENT TUBE SIZE	PRESSURE RANGE (psi)	TOTAL TEST CYCLES
11/16" tube ⁽¹⁾ x 0.040" wall	r	7 b,c,d
3/4" tube ⁽²⁾⁽³⁾ x 0.042", 0.043", 0.048" wall		
7/8" tube ⁽²⁾⁽³⁾ x 0.050" wall	L	J

NOTES:

- (1) The fatigue qualification for an 11/16" tube size was performed by comparison of the test loads and the testing performed using 3/4" and 7/8" OD tubes.
- (2) The total test cycles shown represent the minimum failure time for any specimen of this type tested.
- (3) Each specimen had a 1 inch long axial, [^{b,c}] through-wall (TW) defect in the sleeve. 100% of the tube was removed. See Figure 7.3.1.

The test loads were developed to allow testing to proceed in steps with each step representing two years of operating life. The test steps were repeated until the specimens failed or reached forty (40) years of service life. The failure point can be used to define the inspection interval for the defective sleeve. Failure of the sleeves with axial defects was defined as detecting leakage through the sleeve defect. Failure of the sleeves with circumferential defects was defined as structural breakage at the flaw.

Table 7.3.4 shows the results of the defective sleeve fatigue tests. An Electrosleeve™ with a []^{b,c} through-wall defect has a maximum inspection interval of:

TABLE 7.3.4
FATIGUE INSPECTION INTERVAL

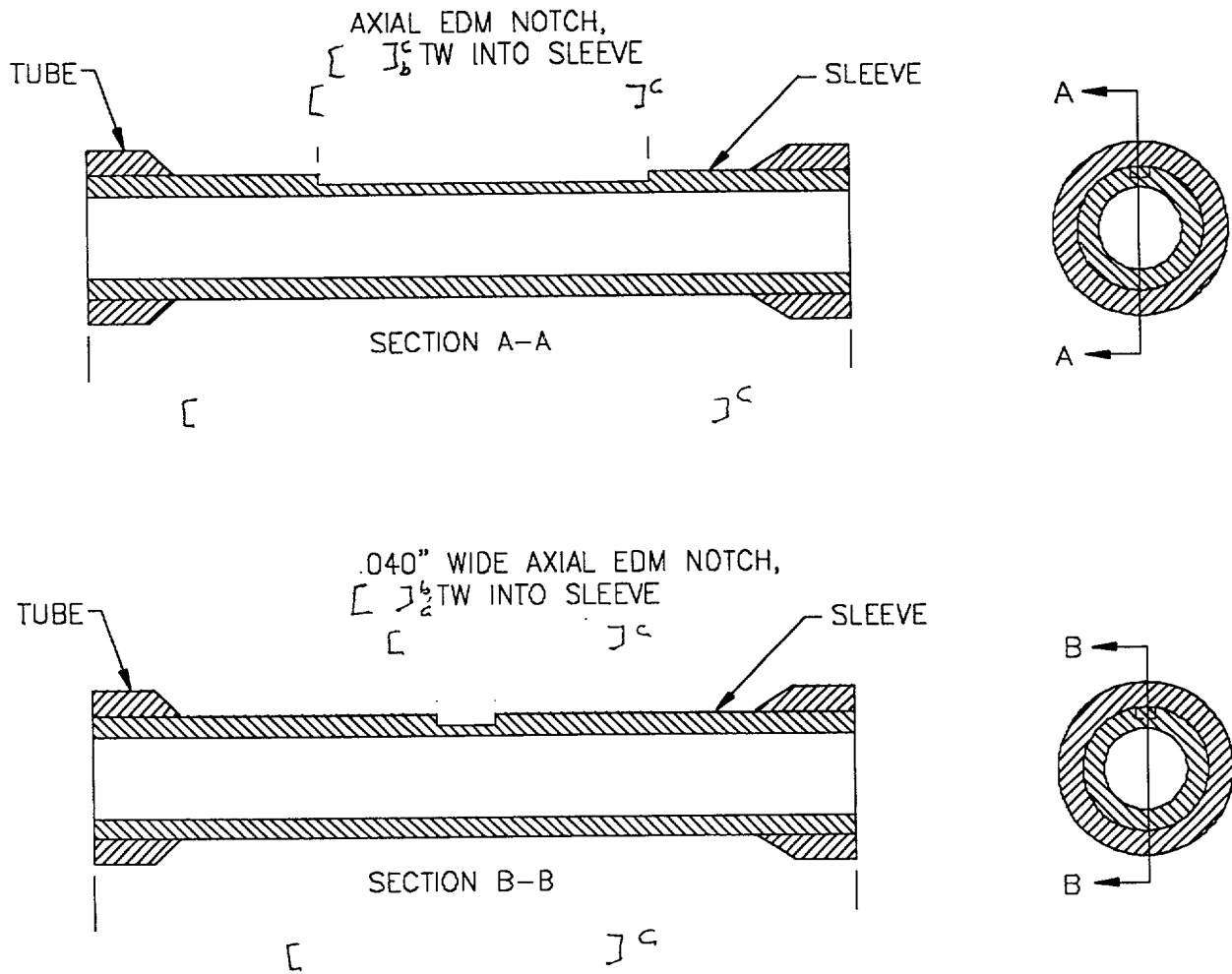
TUBE SIZE	DEFECT TYPE	FATIGUE INSPECTION INTERVAL (EFPY)
3/4" x 0.042/0.043/0.048"	┌	└
7/8" x 0.050"		b,c,e
3/4" x 0.042"/0.043"/0.048"		
7/8" x 0.050"	└	┌

7.3.2 Plugging Criteria Burst Testing

The tube burst pressure must be greater than the limiting pressure defined by three times normal operating differential pressure or 1.43 times the worst case faulted differential pressure per Draft Regulatory Guide 1.121 [13.6]. Burst tests were performed on sleeved tubes to demonstrate that this margin is available in sleeves with defects.

Test specimens were fabricated with two types of flaws in the sleeve, axial and pitting flaws. The flaws extended []^{b,c} to []^{b,c} into the sleeve wall. Figure 7.3.2 depicts the test specimens. Five specimens were burst tested. The tests were performed at room temperature and at operating temperature.

FIGURE 7.3.2
MECHANICAL TEST SPECIMEN DESIGNS
PLUGGING CRITERIA BURST SPECIMENS



The specimens, along with burst test results, are listed in Table 7.3.5.

TABLE 7.3.5
PLUGGING CRITERIA BURST SPECIMENS⁽²⁾

SPECIMEN NUMBER	TUBE SIZE	SLEEVE DEFECT	TEST TEMP. ⁽³⁾ (°F)	CALCULATED BURST PRESSURE (ksi)	BURST PRESSURE (ksi)
754225-78-059	7/8" OD x 0.050"	┌			┌ b, c, d
754225-78-060	7/8" OD x 0.050"				
754225-78-063	7/8" OD x 0.050"				
754225-78-064	7/8" OD x 0.050"				
754225-78-065	7/8" OD x 0.050"	└			└

NOTES:

- (1) Refer to Figure 7.3.2 for a sketch of the axial defect.
- (2) Tube wall was completely removed from the test specimens. The sleeve thickness for these specimens was []^{b, c, d} inch.
- (3) The actual test temperature is reported (RT = Room Temperature).
- (4) % through-wall = Percent through-wall of the sleeve.

7.4 Creep-Fatigue Experimental Analysis

[^{b,c}] specimens were tested to determine the effect of creep-fatigue interaction. The test results (Table 7.4.1) showed sufficient margin in the design of the Electrosleeve™ to accommodate the combined effects of fatigue and creep that an installed Electrosleeve™ could experience in a steam generator. Additionally, the fracture faces of specimens []^b were examined. Photomicrographs at relatively low magnification (Figure 7.4.1) show that the fracture-face features of the specimens were entirely ductile. Further, the fractographic analysis of specimens 766037-CT-006 and 766037-34-051 revealed the creep failures to be entirely ductile with no evidence of operative intergranular failure mechanisms.

TABLE 7.4.1
CREEP-FATIGUE TESTING RESULTS

Sample	Tube Size	Creep/Fatigue Testing
[]	3/4" x 0.043" [Figure 6.6.1]	1. [] creep test [] 2. 40 EFPY W-D model locked tube load fatigue test at 650°F. 3. [] fatigue tested [] to failure []
[]	7/8" x 0.050" (Minimum bond sample with 1/4" sleeve-to-tube bond) [Figure 7.2.1]	1. [] thermal cycles [] 2. 40 EFPY fatigue test using locked tube loads [] 3. [] creep test [] 4. 40 EFPY fatigue test using locked tube loads [] 5. [] fatigue tested [] [] to failure []
[]	3/4" x 0.043" [Figure 6.6.2]	1. [] creep tested [] 2. [] [], constant load fatigue test [] 3. []

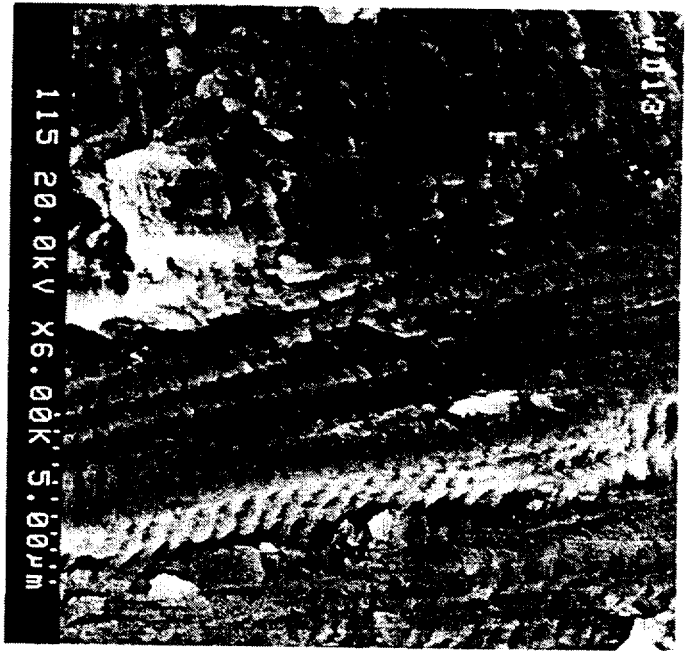
all []^{b,c,d}

FIGURE 7.4.1
TYPICAL CREEP-FATIGUE SURFACE FRACTOGRAPHY

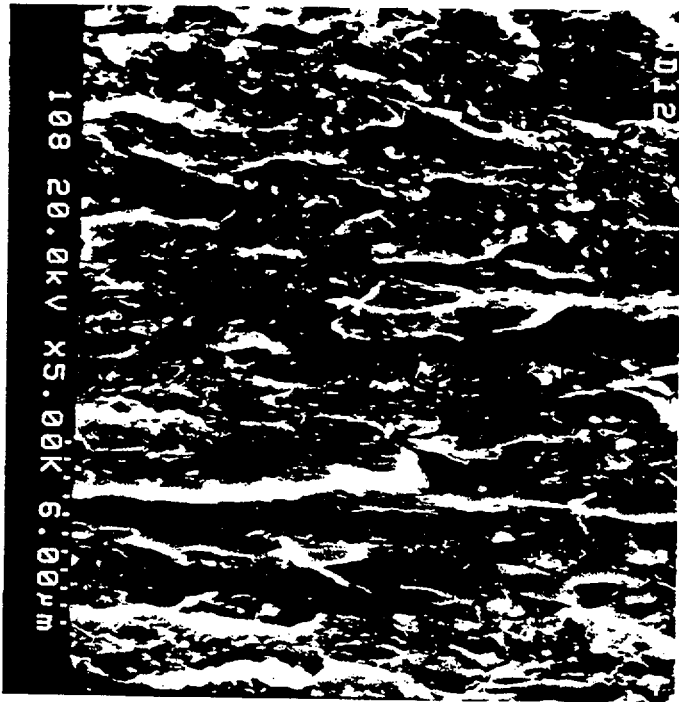
Serial No. [J^c



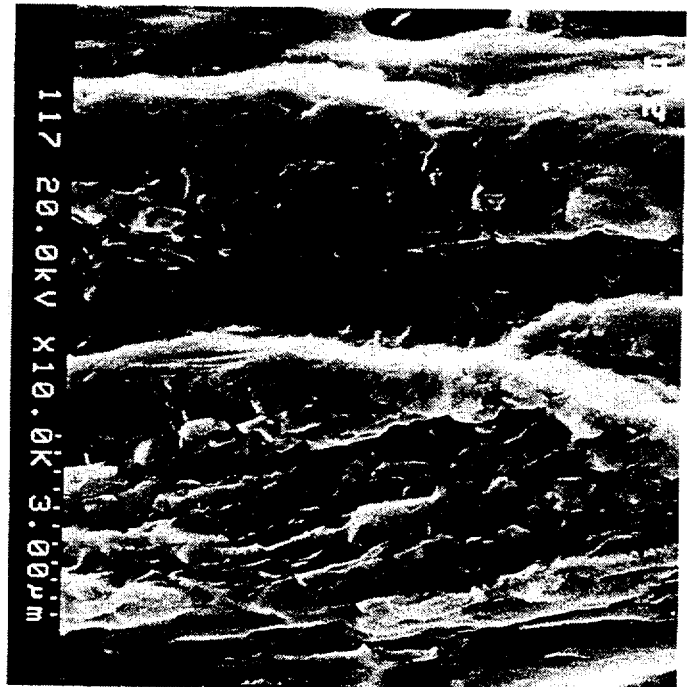
Serial No. [J^c



Serial No. [J^c



Serial No. [J^c



7.5 Leak Testing of Minimum Bond Length

Leak testing was performed at room temperature on []^{b,c} electrosleeved 11/16" OD Alloy 600 tubes. After the sleeves were installed, the specimens were UT inspected. Then, the tube material was removed as shown in Figure 7.2.1. The specimens were subjected to a primary side hydrotest at 4200 psig and then to a thirty (30) minute leak test at 2500 psig. No visible leakage was observed.

In addition, after the minimum bond fatigue testing described in Section 7.2 was completed, a 7/8" OD sample was subjected to rapid thermal shock cycles. The specimen was heated above 600°F and then the inside surface of the electrosleeved tube was subjected to a high-velocity cold-water flush. The specimen cooled to room temperature in approximately 5 to 10 seconds. After experiencing ten thermal shock cycles, the specimen was UT inspected and showed no loss of bonding. The specimen was then subjected to a primary-side hydrotest at 4200 psig followed by a thirty (30) minute leak test at 2500 psig. No visible leakage was observed.

These test results are consistent with the design objectives of a "sealed" sleeve installation and support the total bonding verified by the UT inspection.

7.6 Tube-to-Tubesheet Pull-Out Load Testing

The repair of a degraded tube at the top of a tubesheet can affect the strength of the tube-to-tubesheet contact engagement in the tubesheet bore. To evaluate the post-sleeved engagement strength, samples were fabricated to evaluate the axial tube pull-out load. Tube specimens were roll expanded into the full length of four-inch tubesheet blocks. Four tubes were rolled into tubesheet mockups (i.e., two with 3/4" x 0.043" wall tubes and two with 7/8" x 0.050" wall tubes). An []^{b,c} Electrosleeve™ was installed (centered over the []^{b,c} tubesheet block) into one of each size mockup. The sleeve extended []^{b,c} past each end of the tubesheet block. The center []^{b,c} length of each mockup was cut away. The sleeve extended []^{b,c} past each end of the tubesheet block. Thus, the []^{b,c} mockups yielded []^{b,c} sleeved and []^{b,c} unsleeved samples.

All []^{b,c} samples were then heat treated at 650°F for ten hours. The tube section was then pulled out of the tubesheet block (pull test performed at room temperature) and the removal load for the sleeved specimens was compared to the removal load for the similar unsleeved samples. The addition of the Electrosleeve™ increased the average joint strength of the four test specimens by approximately 10%. This increase in joint strength is attributed to the added stiffness of the composite tube section to resist the Poisson effect of the axial tube loading. Since the coefficient of thermal expansion of nickel is higher than that of the Alloy 600 or the carbon steel tubesheet, the joint strength will also increase at operating temperature.

Thus, the installation of the Electrosleeve™ does not require any change in the effective tube-to-tubesheet rolled joint length. The installation of the Electrosleeve™ should also increase the tube-to-tubesheet joint strength for other tube expansion methods.

7.7 Mechanical Testing Summary

The mechanical design verification tests were performed to show that the Electrosleeve™ is structurally capable of withstanding actual in-service loading conditions. The results of the conservative tests reported in this section envelop the expected worst case conditions.

The burst tests demonstrate that the Electrosleeve™ is ductile and has burst characteristics similar to undegraded tubes. The burst tests also showed that a sleeved tube with a []^{b,c} through-wall defect in the sleeve will withstand faulted condition loadings.

The locked tube tests showed that the electro sleeving process is unaffected by locked tubes. Further, no significant loads are generated in the parent tube from the installation process.

The series of experimental fatigue tests confirmed the structural integrity of the electrochemically deposited nickel sleeve material, with the following conclusions being drawn:

- Testing tubes with 100% through-wall defects showed the sleeve would last for its specified design life.

- Testing tubes with 100% through-wall defects, including []^{b,c} through-wall defects in the sleeve, showed that a sleeve with a []^{b,c} defect would last longer than the specified five year inspection interval.
- A nominal bond length []^{b,c} will carry all loading conditions and prevent leakage.
- Thermal, pressure, and axial loads have no detrimental effects on either the bond or the sleeve strength characteristics.

8.0 DESIGN VERIFICATION - ANALYSES

Design analyses were performed for the Electrosleeve™ to verify it conforms to the qualification requirements identified in Section 4.0. The design analyses consist of:

- Pressure boundary minimum thickness calculation,
- Analyses to support fatigue testing per Appendix II of the ASME Code,
- Analyses of flow-induced vibration of sleeved tubes,
- Analyses of the effect of a sleeve on heat transfer and primary fluid flow,
- Analyses of a degraded sleeve, and
- Analysis of creep.

The analyses were performed on the different sizes of steam generator tubing outlined in Section 4.0. The results are presented in Sections 8.1 through 8.6.

8.1 Pressure Boundary Thickness

Based on the material test results for the electroformed nickel material, a design stress intensity value (S_m) of 30 ksi at 650°F was established in Section 6.1. This S_m value was used to evaluate the structural adequacy of the various sleeve sizes for pressure thickness and external pressure in accordance with the ASME B&PV Code. Using the primary side design pressure (per NB-3324 [13.2]), the minimum sleeve thickness for each design is given in Table 8.1.1.

TABLE 8.1.1
TUBE/SLEEVE DIMENSIONS

PLANT	NOMINAL TUBE SIZE		ELECTROSLEEVE™		
	OD (inch)	Thickness (inch)	Nominal OD (inch)	Minimum Thickness (inch)	Nominal Thickness (inch)
Westinghouse RSG Model F	11/16	0.040	┌		7 b,c,e
CE RSG System 80	3/4	0.042			
Westinghouse RSG Models D & E	3/4	0.043			
All CE RSGs (Except Sys 80)	3/4	0.048			
Westinghouse RSG Models 33, 44, & 51	7/8	0.050	└		└

The allowable external pressure for the sleeve and tube was calculated per classical collapse pressure equations for each sleeve size. Based on these calculations, the sleeve has a greater external pressure capability than the tube. Thus, the sleeve exceeds the strength of the original tube for external pressure loadings.

The design primary stress intensities for each steam generator design were calculated assuming that the tube was completely removed from the sleeve. The maximum stress intensities (Table 8.1.2) meet the primary stress (P_m) limits.

TABLE 8.1.2
PRIMARY MEMBRANE STRESS INTENSITY RANGE

PARENT TUBE SIZE	SLEEVE STRESS CRITERIA	MAXIMUM PRIMARY STRESS INTENSITY RANGE (ksi)	ASME CODE ALLOWABLE STRESS ⁽¹⁾ (ksi)
11/16" OD x 0.040" wall	$P_m \leq S_m$	$P_m = [\quad]^{b,c}$	30.0
3/4" OD x 0.042"/0.043" wall	$P_m \leq S_m$	$P_m = [\quad]^{b,c}$	30.0
3/4" OD x 0.048" wall	$P_m \leq S_m$	$P_m = [\quad]^{b,c}$	30.0
7/8" OD x 0.050" wall	$P_m \leq S_m$	$P_m = [\quad]^{b,c}$	30.0

NOTES:

- (1) Stress values are for design pressure at 650°F for the sleeve. The analysis conservatively assumes the tube is not present.

8.2 Fatigue Test Loads

Section III of the ASME B&PV Code does not provide design rules for sleeves fabricated by electrochemical deposition of material. In such cases, the ASME B&PV Code, Section III, Appendix II [13.2] allows the use of experimental stress analysis to substantiate the critical, or governing, stresses. The adequacy of the installed material and its bond to the tube to withstand operational pressure and thermal cyclic loading was demonstrated by means of fatigue testing per the ASME B&PV Code, Section III, Article II-1500 [13.2].

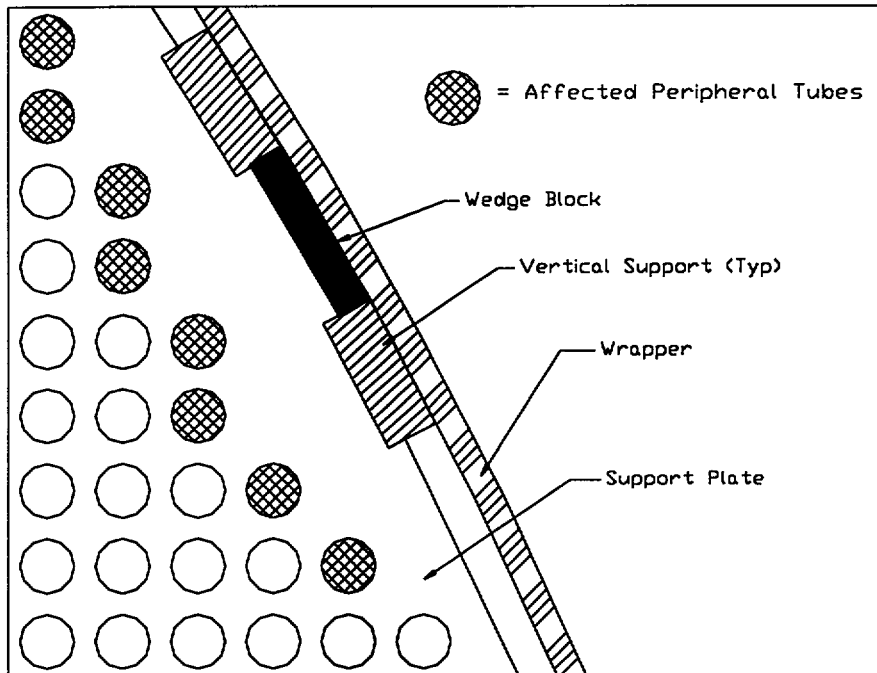
- Specimen 1: The minimum bond specimen was fabricated by machining away the tube and sleeve such that a small sleeve-to-tube bond length exists (nominally $\left[\right]^{b,c}$ inch). These specimens were subjected to experimental fatigue tests consisting of axial load cycling, thermal cycling, and pressure cycling. Refer to Section 7.2 for a description of these tests.
- Specimen 2: This specimen was used to evaluate circumferential cracks. The tube was removed over a $\left[\right]^{b,c}$ length and a full circumferential EDM notch was then machined in the exposed sleeve 30% through-wall. The radius at the bottom of the EDM notch was 0.003 inch or less. Refer to Section 7.2 for a description of these tests.
- Specimen 3: This specimen was used to evaluate axial cracks. The tube was removed over a $\left[\right]^{b,c}$ length and a $\left[\right]^{b,c}$ long EDM notch was then machined in the exposed sleeve $\left[\right]^{b,c}$ through-wall. The radius at the bottom of the EDM notch was $\left[\right]^{b,c,d}$ inch or less. Refer to Section 7.2 for a description of these tests.

The Electrosleeve™ is designed to accommodate all loads that the steam generator tube may experience due to normal plant conditions and all anticipated transients specified for the steam generator. The tables presented in Appendix A summarize the expected transient conditions used in the design of the sleeves for the different sizes of tubes.

Calculations were prepared for each sleeve design to determine a conservative maximum loading for a sleeve in any steam generator tube based on the transients listed in Appendix A. These calculations include pressure, thermal gradient, thermal differential, and seismic loading.

The loads were evaluated for tubes either locked or unlocked at the tube support plates. The tube loading calculated for a locked tube enveloped the tube loads calculated for a tube in the unlocked condition. As a result, the fatigue loading evaluation considered the tubes to be locked at all tube support plates. The locked tube axial loads increase near TSP vertical restraints similar to the TSP-to-wrapper support in Figure 8.2.1. The tubes most affected are the first tubes in each row closest to the TSP support.

FIGURE 8.2.1
PERIPHERAL TUBES AFFECTED BY TSP-TO-WRAPPER SUPPORTS



Loads due to thermal and pressure transients were calculated for [^{b,c}] sleeved tube cases using the transients listed in Appendix A. Where possible, transients were grouped together and the number of cycles adjusted accordingly. The structural model for each of these cases considered a tube with sleeves installed at the top of the tubesheet and at least three TSP locations. [^{b,c,e}]

The sleeved

tube conditions considered are:

- Sleeved periphery tube (severed and unsevered), and
- Sleeved interior tube (severed and unsevered).

The loading analysis model for the periphery tube case (Figure 8.2.1) considered the following boundary conditions:

- The tube is coupled to the tubesheet and to each of the TSPs,
- Each TSP is fixed to the wrapper,
- The wrapper is fixed to the shell, and
- The tube is either severed or unsevered between the sleeve attachment bonds.

The loading analysis model for the interior tube case considered the following boundary conditions:

- The sleeved tube and its adjacent tubes are coupled to the tubesheet and to each of the TSPs, and
- The tube is either severed or unsevered between the sleeve attachment bonds.

The specific combination of geometry and operating conditions, that resulted in the highest load for a given transient grouping, was used in the mechanical test program. The load ranges were calculated based on the following conditions:

- A single peripheral tube is sleeved at 70°F after it initially locked to the support plate at 100% power conditions. Only this tube was assumed to interact with the wrapper and shell.
- Interior sleeved tubes were influenced only by adjacent tubes and not by the shell and wrapper.

The calculated axial tube loads for all transients were combined into a set of test load ranges. The required number of test cycles was determined per ASME Appendix II [13.2] and was based on the number of test assemblies and various factors relating the test conditions to the actual operating conditions.

The fatigue load testing sequence for Specimen 1 is shown in Table 8.2.1 (same as Table 7.2.2) for the recirculating steam generators. The load testing sequences were utilized in the tests described in Section 7.2.

TABLE 8.2.1
SUMMARY OF MINIMUM BOND FATIGUE TEST LOAD RANGES⁽¹⁾⁽²⁾

5/8" OD x 0.037" TUBE SIZE LOADS (lbs)	LOAD RANGE (lbs)	TEST CYCLES
┌		┐ b,c,d
└		┘

3/4" OD x 0.042"/0.043"/0.048" TUBE SIZE LOADS (lbs)	LOAD RANGE (lbs)	TEST CYCLES
┌		┐ b,c,d
└		┘

7/8" OD x 0.050" TUBE SIZE LOADS (lbs)	LOAD RANGE (lbs)	TEST CYCLES
┌		┐ b,c,d
└		┘

NOTES:

- (1) The loading listed represents the worst case combination, (i.e., peripheral tube, 40 year service life, Transient + FIV + OBE Loads).
- (2) The ASME Appendix II, Testing Factors have been applied to these loads and cycles based on the number of test specimens and test conditions.

Fatigue testing was performed (Section 7.2) to determine the life of an Electrosleeve™ with a part through-wall defect in a degraded tube. This testing included tubes and sleeves with circumferential and axial crack-like defects (i.e., EDM machined defects). These specimens were subjected to testing representative of the design life of the steam generator.

Fatigue test loads were calculated for the sleeve specimens to represent the operating pressure and thermal stress ranges for the steam generator life. To simulate the normal operating transient stresses, an equivalent load was calculated to account for the thermal stress gradient and the differential pressure versus stress present in the sleeve. This additional load was determined based on the pressure versus thermal membrane and bending stress. The equivalent loading was combined with loads due to pressure and thermal expansion differences to give the test loading. This test load created an equivalent membrane and bending stress in the tube/sleeve at the defect location representative of normal fatigue transient loadings. Both 3/4" OD and 7/8" OD sleeved tube specimens were tested. The test loadings and total cycles required in the fatigue tests in Section 7.2 are listed in Tables 8.2.2 and 8.2.3 (Tables 8.2.2 and 8.2.3 are the same as Tables 7.3.2 and 7.3.3, respectively).

TABLE 8.2.2
FATIGUE TEST LOADS

11/16" OD X 0.040" TUBE SIZE ⁽¹⁾		
INTERIOR LOCKED TUBE LOAD SET FOR 40 EPFY		
AXIAL LOAD SET (lbs)	AXIAL LOAD RANGE (lbs)	TOTAL TEST CYCLES
[b,c,d]
PERIPHERAL LOCKED TUBE LOAD SET FOR 40 EPFY		
AXIAL LOAD SET (lbs)	AXIAL LOAD RANGE (lbs)	TOTAL TEST CYCLES
┌		
L		

3/4" OD x 0.042"/0.043"/0.048" TUBE SIZE		
INTERIOR LOCKED TUBE LOAD SET FOR 40 EPFY		
AXIAL LOAD SET (lbs)	AXIAL LOAD RANGE (lbs)	TOTAL TEST CYCLES
┌		┌ b,c, d
L		└
PERIPHERAL LOCKED TUBE LOAD SET TESTED ⁽²⁾		
AXIAL LOAD SET (lbs)	AXIAL LOAD RANGE (lbs)	TOTAL TEST CYCLES
┌		┌ b,c, d
L		└

TABLE 8.2.3
]^c FATIGUE TEST LOADS

PARENT TUBE SIZE	PRESSURE RANGE (psi)	TOTAL TEST CYCLES
11/16" tube ⁽¹⁾ x 0.040" wall	┌	┐ b, c, d
3/4" tube ⁽²⁾⁽³⁾ x 0.042", 0.043", 0.048" wall		
7/8" tube ⁽²⁾⁽³⁾ x 0.050" wall	└	┘

NOTES:

- (1) The fatigue qualification for an 11/16" tube size was performed by comparison of the test loads and the testing performed using 3/4" and 7/8" OD tubes.
- (2) The total test cycles shown represent the minimum failure time for any specimen of this type tested.
- (3) Each specimen had a 1 inch long axial, []^{b,c} TW defect in the sleeve. 100% of the tube was removed. See Figure 7.3.2.

8.3 Flow-Induced Vibration

The flow-induced vibration (FIV) analyses evaluated fluid-elastic stability margins (FSM) and random vibration response for the nickel sleeve. For all of the steam generator designs analyzed, sleeves were assumed to be installed at all TSPs and TTS locations in both the hot and cold legs. The fluid-elastic stability margins and the responses to small-scale turbulence were examined. Possible vortex shedding was not considered to be a problem. No credit was taken for increased local damping due to sleeves. The FIV analyses were performed using Connor's constants, percent damping, and added mass coefficient as listed in Table 8.3.1. The percent damping value used is based on FTI testing data.

[]^c **TABLE 8.3.1**
FLOW-INDUCED VIBRATION ANALYSES RESULTS⁽³⁾

SG DESIGN	VIRGIN TUBE (VT) or SLEEVED TUBE (ST)	FLOW STABILITY MARGIN (FSM) ⁽¹⁾⁽²⁾			RANDOM VIBRATION PEAK FATIGUE STRESS (psi, rms)		SLEEVE FATIGUE USAGE FACTOR
		HOT LEG	U BEND	COLD LEG	TUBE	SLEEVE	
CE SYS 80	VT	┌					┐ b,c,d
	ST						
Westinghouse Model D and E	VT						
	ST						
Westinghouse Model F	VT						
	ST						
CE Model 67, CE ANO-2, and CE Model 3410	VT						
	ST						
CE (Fort Calhoun)	VT						
	ST						
Westinghouse Models 33, 44 and 51	VT						┐
	ST	└					

NOTES:

(1) FIV Acceptance Criteria

┌

┐ b,d

(2) FIV Constants and Coefficients

└

┐

┌

┐ b,d

└

┐

(3) Worst case tube in RSGs analyzed.

The FIV tube model included the hot leg, U-bend, and cold leg tubing between the tubesheets. This model allows cross flow loads to be applied to the U-bend tubing for evaluating the tube support plate sleeves. The cases considered are virgin and sleeved tubes. The results of all of the FIV analyses are presented in Table 8.3.1. The bounding cases for each similar design are presented in the Table. For the 7/8" OD tube designs, the Westinghouse Model 51 RSG is bounding, and for the 3/4" OD tube Westinghouse designs, the D5 is bounding. Specific analyses were performed for the Combustion Engineering (CE) System 80, ANO-2 (original SG design prior to SG replacement in 2000), and Fort Calhoun RSG designs to bound all CE RSG designs. The analyses indicate that the Electrosleeve™ is acceptable for installation in all RSGs with respect to FIV considerations.

8.4 Thermal/Hydraulic

The effect of an Electrosleeve™ installation on steam generator performance was analyzed for heat transfer, flow restriction, and steam generation capacity. Several cases were considered in the evaluation, either a single sleeve in a tube or multiple sleeves in a single tube. All steam generators designs were considered in these analyses. In addition, cases in which the sleeved tubes were distributed asymmetrically among the RSGs were considered.

The analyses show that the thermal/hydraulic effects of electrosleeving are minimal. The effects of installed electrosleeves on primary flow are presented in Table 8.4.1 for each of the steam generator designs. The results are presented as an equivalent number of sleeves installed having the same impact as plugging one tube.

TABLE 8.4.1
THERMAL/HYDRAULIC EFFECTS OF
SLEEVES IN STEAM GENERATOR TUBES

% FLOW REDUCTION AND TUBE SLEEVE/PLUG RATIOS FOR RSG PLANT TYPES (CASE WITH TUBES PER RSG AFFECTED)				
PLANT	CASE 1 ⁽¹⁾		CASE 2 ⁽²⁾	
	% FLOW REDUCTION	SLEEVE/PLUG RATIO	% FLOW REDUCTION	SLEEVE/PLUG RATIO
Westinghouse Model D	┌			c,d,e┐
Westinghouse Model E				
Westinghouse Model F				
CE System 80				
CE Model 67				
CE Model RSG (Ft. Calhoun)				
CE Model RSG Model 3410				
Westinghouse Model 33				
Westinghouse Model 44				
Westinghouse Model 51	└			┘

NOTES:

- (1) Case []^c = Hot leg Tubesheet []^c Sleeve (TSS)
 (2) Case []^c = Hot leg []^c TSS, and []^c TSP []^c sleeve

In summary, the thermal/hydraulic analyses of the Electrosleeve™ show:

- A smaller, unrecoverable pressure drop due to maintaining a larger sleeve ID, and
- A minimal effect on heat transfer since the sleeve is in direct contact with the tube.

8.5 Sleeve Structural Limits

NRC Draft Regulatory Guide 1.121 (RG 1.121) [13.6] provides guidance for determining the degradation limits for PWR steam generator tubes. Since the sleeve replaces a portion of the original tube, the structural limits for a degraded sleeve were determined using this guideline. The required minimum sleeve wall thickness was calculated for the defined sleeve pressure boundary length only. The tapered sections of the sleeves are not included in the structural assessments.

Three criteria for normal operating conditions (level A) and four criteria for faulted conditions (level D) were evaluated in the sleeve/tube bonding joint and in the straight sleeve section. The minimum wall thickness required to accommodate three times the normal operating pressure differential or 1.43 times the limiting accident pressure differential was determined from the tests described in Section 6.7.

The analysis results in Tables 8.5.1 and 8.5.2 show that any sleeve exhibiting a uniform thinning flaw []^{b,c} through-wall at a location where the tube has a 100% through-wall flaw meets the RG 1.121 criteria. However, the circumferential extent of the uniform thinning flaw for tube locations near vertical restraints, such as the TSP-to-wrapper support shown in Figure 8.2.1, is limited. The circumferential degradation limit for these tube locations varies based on the plant-specific main steam line break (MSLB) loading and degradation depth. A plant may choose not to sleeve these tube locations or to remove an installed sleeve from service if circumferential through-wall tube cracking occurs.

TABLE 8.5.1
ELECTROSLEEVE™ STRUCTURAL LIMITS LEVEL A CONDITIONS

CRITERIA	MAX ΔP (psi)	NOMINAL TUBE		ALLOWABLE DEFECT IN THE (NOMINAL) SLEEVE THICKNESS ⁽¹⁾	
		OD (inch)	THICKNESS (inch)	% SLEEVE WALL	(mils)
$P_m \leq S_y$ Interior Tubes	1600	11/16	0.040	7	b, c, d 7
	2000	3/4	0.042		
	1600	3/4	0.043		
	2000	3/4	0.048		
	1600	7/8	0.050		
$P_m \leq S_y$ Peripheral Tubes ⁽²⁾	1600	11/16	0.040		
	2000	3/4	0.042		
	1600	3/4	0.043		
	2000	3/4	0.048		
	1600	7/8	0.050		
$3\Delta P \leq P_{burst}$	1600	11/16	0.040		
	2000	3/4	0.042		
	1600	3/4	0.043		
	2000	3/4	0.048		
	1600	7/8	0.050	L	-1

NOTES:

- (1) Assumes 100% uniform thinning of the tube wall at the same location as the sleeve uniform thinning flaw.
- (2) Applies to tubes adjacent to TSP vertical supports (i.e. TSP-to-wrapper wedge locations).
- (3) Circumferential degradation extent of tube locations (Note 2) is limited as discussed in Section 8.5.

TABLE 8.5.2
ELECTROSLEEVE™ STRUCTURAL LIMITS LEVEL D CONDITIONS

CRITERIA	MAX ΔP (psi)	NOMINAL TUBE		ALLOWABLE DEFECT IN THE (NOMINAL) SLEEVE THICKNESS ⁽¹⁾	
		OD (inch)	THICKNESS (inch)	% SLEEVE WALL	(mils)
$P_m \leq 0.7 S_u$	2650	11/16	0.040	┌	b,c,d ┐
	2500	3/4	0.042		
	2650	3/4	0.043		
	2585	3/4	0.048		
	2650	7/8	0.050		
$1.43 \Delta P \leq P_{burst}$	2650	11/16	0.040		
	2500	3/4	0.042		
	2650	3/4	0.043		
	2585	3/4	0.048		
	2560	7/8	0.050		
$\Delta P \leq 0.9 P_{collapse}$	2650	11/16	0.040		
	2500	3/4	0.042		
	2650	3/4	0.043		
	2585	3/4	0.048		
	2560	7/8	0.050		
$P_m + P_b \leq$ (lesser of $3.12 S_m$ or $0.91 S_u$)	2650	11/16	0.040	└	┘
	2500	3/4	0.042		
	2650	3/4	0.043		
	2585	3/4	0.048		
	2560	7/8	0.050		

NOTES:

- (1) Assumes there is 100% uniform thinning of the tube wall at the same location as the sleeve uniform thinning flaw.

FTI developed a burst pressure correlation to determine the burst structural limits for part through-wall and 100% through-wall flaws. The FTI burst pressure correlation was developed by using both FTI burst tests and industry test data. The FTI burst tests were performed with various lengths and depths of EDM notches as well as with and without electrosleeves. Figure 8.5.1 shows the normalized burst pressure for Alloy 600 tubes versus the predicted normalized burst pressure using both the FTI and EPRI [13.73] burst correlations. The burst test results for electrosleeves show close agreement to the FTI burst pressure correlation. Table 8.5.3 provides a summary of the allowable part through-wall flaw for each sleeve size listed in Table 5.1.1.

**FIGURE 8.5.1
NORMALIZED BURST PRESSURE**

Γ

7
b,c,d

L

J

TABLE 8.5.3
ELECTROSLEEVE™ DRAFT REG. GUIDE 1.121 STRUCTURAL LIMITS
BURST AND LEAKAGE LIMITS⁽⁴⁾⁽⁵⁾

Indication Type	11/16" OD x 0.040" Tube	3/4" OD x 0.042"/ 0.043" Tube	3/4" OD x 0.048" Tube	7/8" OD x 0.050" Tube
	<i>b,c,d</i> Sleeve Thickness %TW ⁽³⁾	<i>b,c,d</i> Sleeve Thickness %TW ⁽³⁾	<i>b,c,d</i> Sleeve Thickness %TW ⁽³⁾	<i>b,c,d</i> Sleeve Thickness %TW ⁽³⁾
Uniform Thinning ⁽²⁾⁽⁴⁾	┌			<i>b,c,d</i> ┐
OD Pit ⁽⁴⁾				
Structural Leakage				
ID Pit ⁽⁶⁾				
Structural Leakage ⁽⁷⁾				
Axial Crack ≤ 3/4 inch ⁽⁵⁾				
Axial Crack > 3/4 inch ⁽¹⁾⁽⁵⁾				
360° Circumferential Crack ⁽²⁾⁽⁵⁾	└			┘

NOTES:

- (1) A slight reduction in the structural limit occurs for axial crack lengths $\left[\begin{matrix} b, c \\ \end{matrix} \right]$.
- (2) The circumferential degradation extent for tubes adjacent to the TSP periphery vertical supports (Figure 8.2.1) is limited as discussed in Section 8.5.
- (3) The % through-wall in the above table is of the sleeve nominal thickness.
- (4) The structural limit for OD pitting and uniform thinning were determined using the ΔP values as shown on Tables 8.5.1 and 8.5.2.
- (5) The structural limit for crack-like defects was determined using the larger of either three times the normal operating pressure differential at 100% power or 1.43 times the limiting accident pressure differential as listed in Appendix A for each tube size.
- (6) ID sleeve pit, fabrication anomaly, not degradation.
- (7) To preclude leakage from a $\left[\begin{matrix} c \\ \end{matrix} \right]$ ID pit during normal, upset, and accident conditions, $\left[\begin{matrix} c \\ \end{matrix} \right]$ of the nominal tube thickness is required, see Table 8.5.4.

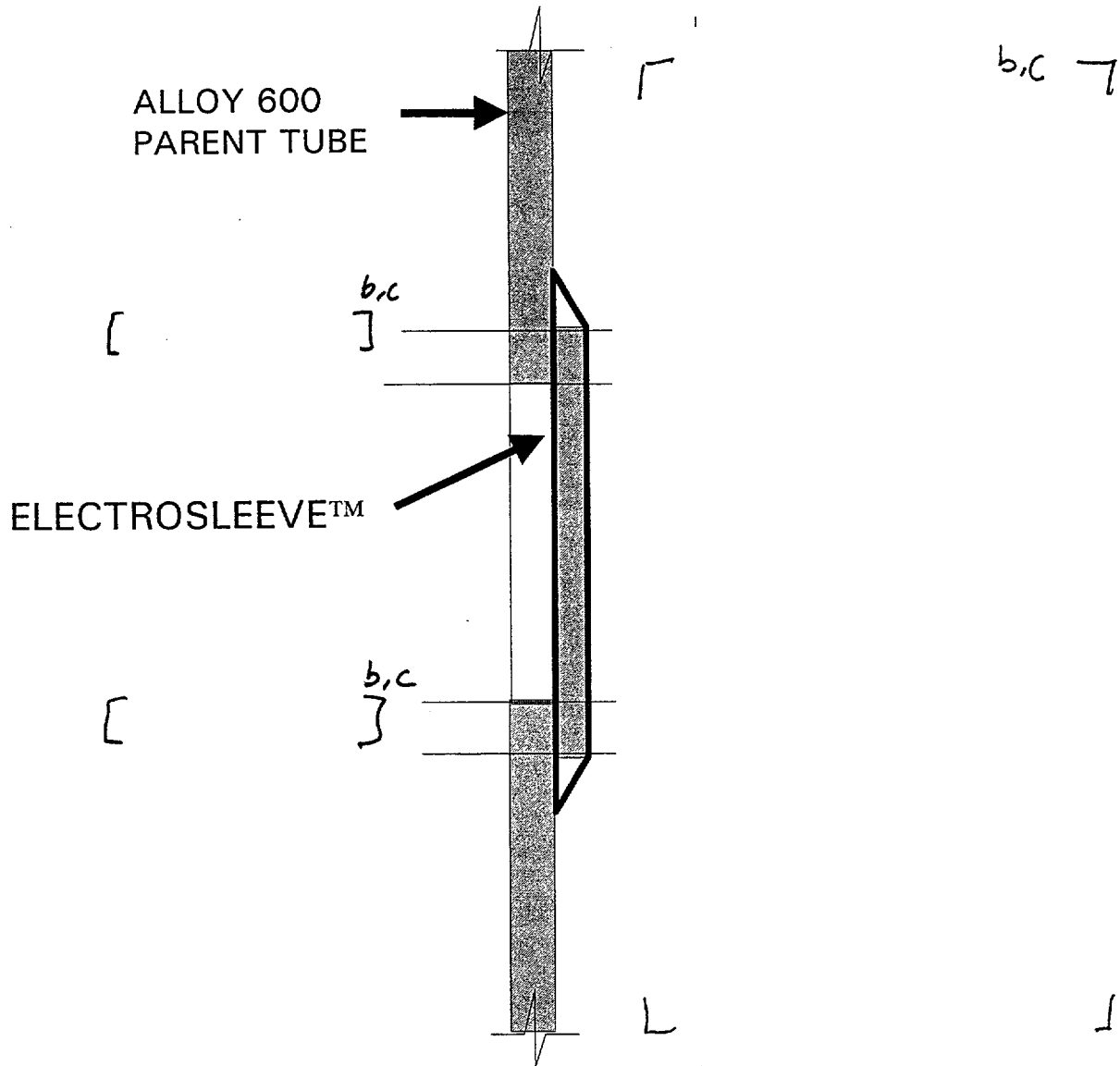
FTI also determined the burst structural limit for a 100% through-wall pit. This burst pressure limit was determined using FTI burst test results of Alloy-600 tubes with part through-wall and 100% through-wall pits of various diameters. Using the burst pressure correlation, an analysis was performed to determine the burst pressure for pits that were 100% through the sleeve wall and that did not have any structural support from the parent tube. The lower tolerance limit on flow stress was used. The analysis determined that a []^{b,c} diameter pit in the Electrosleeve™ met all of the structural requirements of RG 1.121. A remaining ligament for OD pits of []^{b,c} of the sleeve nominal thickness meets the structural requirements of RG 1.121 and precludes any leakage during any normal, upset and accident conditions. Figure 8.5.3 shows the burst pressure limit for various sizes of 100% through-wall pits and the leakage pressure limit for an OD pit []^{b,c} through-wall of the Electrosleeve™.

A 100% through-wall sleeve pit with a diameter []^{b,c} coincident with a 100% through-wall tube crack will typically not exhibit leakage that exceeds the usual plant leakage limit (150 gpd) during either normal or faulted operating conditions. A []^{b,c} bond width between any through-wall tube degradation and a sleeve ID pit precludes the potential for any leakage. Table 8.5.5 shows the thickness of undegraded tube that would be required to preclude leakage at the burst pressure for an Electrosleeve™ (with no support from the tube) for an ID pit that is 100% through-wall of the Electrosleeve™. For a []^{b,c} diameter ID pit, []^{b,c} of the adjacent tube thickness surrounding an area []^{b,c} in any direction would be required. Note that the burst limit for a []^{b,c} diameter 100% through-wall pit is []^{b,c}. An undegraded tube thickness of []^{b,c} of the nominal tube wall provides sufficient structural capacity to preclude leakage due to the differential pressure during any plant's normal, upset and accident conditions (e.g., Level D Condition differential pressure of 2650 psi).

Fatigue test results, presented in Section 7.3, indicate that any sleeve with a crack-like flaw, []^{b,c} through-wall of the sleeve exhibits a margin against fatigue failure that greatly exceeds the RG 1.121 fatigue requirements. The test results are applicable whether the tube wall is removed from the sleeve OD or if the tube has a 100% through-wall flaw. Additionally, a conservative fracture mechanics evaluation for a thinned sleeve with a deep, []^{b,c} through-wall, infinite length axial flaw was performed. The axial flaw propagation depth from this analysis is less than []^{b,c} of the nominal thickness sleeve over eighteen (18) months of operation. This growth value is used in the plugging limit evaluations in Section 12.0.

The structural limits for the three distinct regions of the tube affected by the installation of the Electrosleeve™ are summarized in Table 8.5.4. The three distinct regions of the tube are illustrated in Figure 8.5.2 (same as Figure 5.1.1).

FIGURE 8.5.2
ELECTROSLEEVE™ PRESSURE BOUNDARY



Notes: Pressure Boundary is denoted by shaded areas.

TABLE 8.5.4
ELECTROSLEEVE™ STRUCTURAL ACCEPTANCE STANDARD

REGION ⁽⁴⁾	COMPONENT	ACCEPTABLE STRUCTURAL DEGRADATION
A	TUBE	<ul style="list-style-type: none"> Plant Technical Specification Requirements
	SLEEVE	<ul style="list-style-type: none"> All Indications are acceptable
B	TUBE	<ul style="list-style-type: none"> Plant Technical Specification Requirements
	SLEEVE ⁽¹⁾	<ul style="list-style-type: none"> Minimum thickness (Table 8.1.1) No leak path Minimum bond length []^{b,c} ID pit 100% through-wall
C	TUBE	<ul style="list-style-type: none"> All Indications are acceptable <p>(Special Evaluation or Contingency Resolutions)⁽²⁾</p> <ul style="list-style-type: none"> For an Electrosleeve™ ID pit left in service, a minimum of []^{b,c} of the nominal tube wall (from the tube ID) extending at least around the pit shall be free of tube degradation.
	SLEEVE ⁽¹⁾	<ul style="list-style-type: none"> Minimum thickness (Table 8.7.1) Uniform thinning []^{b,c} Axial crack []^{b,c} Axial crack []^{b,c} 360° Circumferential crack []^{b,c} OD pit []^{b,c} <p>(Special Evaluation or Contingency Resolutions)⁽²⁾</p> <ul style="list-style-type: none"> ID pit 100% through-wall with a tube bond []^{b,c}

NOTES:

- (1) The Electrosleeve™ nominal thickness was used to calculate % through-wall.
- (2) Installation minimum thickness, disbond process violations, ID pits, and nodules require a Non-Conformance Report (NCR) resolution with the Owner’s concurrence to justify acceptability for service.
- (3) Note that the circumferential degradation extent for tubes adjacent to the TSP periphery vertical supports (Figure 8.2.1) is limited as discussed in Section 8.5.
- (4) See Figure 11.1.1 for definition of Regions A, B, and C.
- (5) Assumes 100% of the tube is removed.

FIGURE 8.5.3

ELECTROSLEEVE™ ID and OD PIT STRUCTURAL LIMITS
(Applicable to all tube sizes)

b, c, d, e
└

└

L

└

8.6 Creep Analysis

ASME Code Case N-47 [13.5] established design rules for Section III, Class 1 components for the conditions when the metal temperature exceeds those established by Section III. The design rules in the code case [13.29] are designed to guard against:

- Ductile rupture from short term loadings,
- Gross distortion,
- Creep rupture from long term loadings, and
- Creep fatigue failure.

The analysis results presented in Section 8.1 and the mechanical testing in Section 7.0 demonstrate ductile rupture from short term loadings are not a concern. The other design aspects are discussed below.

8.6.1 Gross Distortion

During creep, a specimen under load will undergo permanent deformation over time. The amount of deformation will vary based on stress, time, and temperature. The majority of the creep tests described in Section 6.6 were performed at $[\quad]^{b,c}$ under a number of different loads. Additional tests were performed at $[\quad]^{b,c}$ and $[\quad]^{b,c}$ to evaluate the influence of temperature.

The creep response of the Electrosleeve™ material was modeled using an equation often referred to as the Garofalo equation [13.38]. The creep test results formula used is:

$$\left[\quad \right]^{b,c,d}$$

Where: $\left[\quad \right]$ $\left[\quad \right]^{b,c,d}$

L J

The material constants for the creep equation were determined by fitting the curve to the results from constant load tests (Figure 8.6.1). The temperature correction term was conservatively based on published data for Nickel 200.

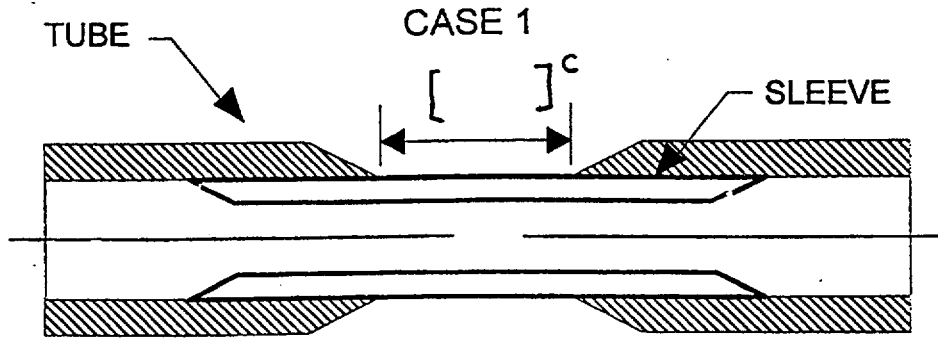
[^c] **FIGURE 8.6.1**
STRAIN (%) VS. TIME⁽¹⁾

b,c,d

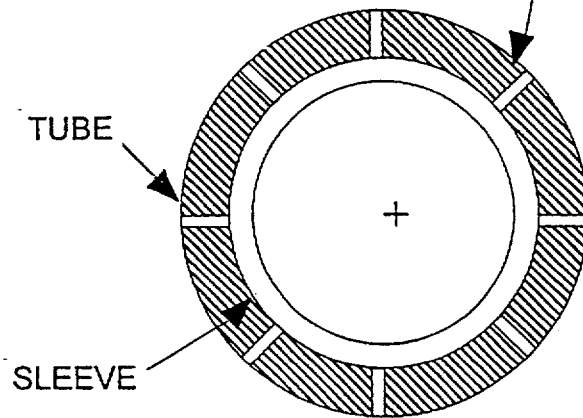
The computer program ANSYS was then used to create a finite element model using various tube/defect geometries to calculate the total creep strain. The following cases were considered and are illustrated in Figure 8.6.2:

- $[\quad]^c$ uniformly spaced defects, $[\quad]^{b,c}$ wide, infinite length;
- 360° circumferential defect; $[\quad]^{b,c}$ wide;
 - in the free span,
 - at the secondary tubesheet face,
 - at the secondary tubesheet face within a sludge pile; and
- Parent tube removed for 360° over a $[\quad]^c$ length.

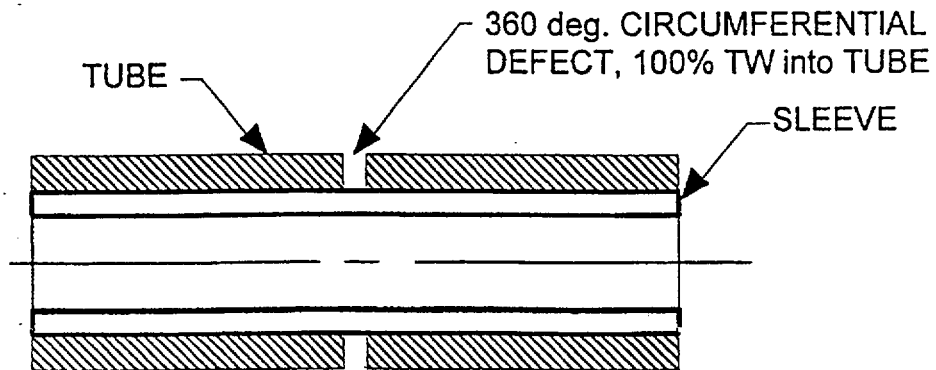
FIGURE 8.6.2
TUBE DEFECTS MODELED []^c



[]^c CASE 2
INFINITELY LONG
AXIAL DEFECTS
100% TW into TUBE



CASE 3



With the exception of a sleeve at the secondary tubesheet face, each case was assumed to be a freespan tube defect to maximize the thermal gradient stress across the tube/sleeve interface. In each case, the tubing defect was modeled to extend 100% through-wall to the tube/sleeve interface.

The finite element analysis imposed the steady state loads generated during 100% power and transient fatigue loads. The transient loads included the loads generated under the worst case locked tube scenario.

The analysis results for various times are summarized in Tables 8.6.1 and 8.6.2, and the results are displayed graphically in Figure 8.6.3. Converting the calculated creep strains into expected deformations in the steam generator demonstrates the Electrosleeve™ is not subject to any gross distortions.

[
 TABLE 8.6.1
] ELECTROSLEEVE™
INSTALLED IN THE TUBE FREE SPAN⁽³⁾

FREE SPAN DEFECT TYPE: TUBE REMOVED ⁽²⁾				
TUBE SIZE (inches)	TOTAL TIME (hours) ⁽¹⁾	MEMBRANE (%)	MEMBRANE + BENDING (%)	LOCAL (%)
11/16	┌			b,c,d ┐
3/4				
7/8				
	└			┘

FREE SPAN DEFECT TYPE: 360° CIRCUMFERENTIAL CRACK ⁽²⁾				
TUBE SIZE (inches)	TOTAL TIME (hours)	MEMBRANE (%)	MEMBRANE + BENDING (%)	LOCAL (%)
11/16	┌			b,c,d ┐
3/4				
7/8				
	└			┘

(See notes on next page)

[^c]
TABLE 8.6.1 (Cont'd)
ELECTROSLEEVE™
INSTALLED IN THE TUBE FREE SPAN⁽³⁾

FREE SPAN DEFECT TYPE: 8 INFINITE LENGTH AXIALS ⁽²⁾				
TUBE SIZE (inch)	TOTAL TIME (hours) ⁽¹⁾	MEMBRANE (%)	MEMBRANE + BENDING (%)	LOCAL (%)
11/16	┌			b,c,d┐
3/4				
7/8				
	└			└

NOTES:

- (1) [
- (2) Defects are 100% through the tube wall. Refer to Figure 8.6.2.
- (3) Results include locked tube transient loading.
- (4) [

] b,c

] b,c

FIGURE 8.6.3
ANSYS VS. []^{b,c} TEST DATA

c,d 7

┌

L

8.6.2 Creep Rupture

Over the last half century, considerable research and effort has been spent developing methods to predict creep rupture. Many of these techniques involve time-temperature parameters whereby short-term tests at high temperature are used to predict long term exposure to lower temperatures. Analysis of data for a variety of aluminum-, iron-, nickel-, titanium-, cobalt-, and copper-based alloys led Monkman and Grant to the following empirical relationship [13.35]:

$$\log t_r + m \log (m_{cr}) = C$$

Where:

- t_r = time to rupture
- m_{cr} = minimum creep rate
- m and C = material constants that differ among alloy groups, but are nearly fixed values for different lots within the same alloy group

In a comparison between various extrapolative techniques, the Monkman-Grant relationship was more accurate than that provided by any of five different time-temperature parameters [13.36]. The Monkman-Grant relationship for the Electrosleeve™ is illustrated in Figure 8.6.4.

FIGURE 8.6.4

b, c, d

┌

└

┐

Using the relationship illustrated in Figure 8.6.4, the ANSYS constants discussed earlier, normal operating temperature, and differential pressure, a conservative time-to-rupture analysis for a sleeve with the tube removed can be performed. Table 8.6.3 shows the time-to-rupture for the sleeve sizes in this topical:

TABLE 8.6.3

[]^{b,c}

STEAM GENERATOR DESIGN	T-HOT (°F)	HOOP PRESSURE STRESS (KSI)		TIME TO RUPTURE (HRS)
CE SYS 80 W-E	┌			b,c┐
W-D W-F				
CE (0.048 wall)				
W-51	L			└

The analyses summarized in the above table are conservative for the following reasons:

- Operating T-hot is higher than the average metal temperature of the Electrosleeve™,
- Radial thermal expansion imparts a compressive stress on the sleeve ID that limits creep deformation,
- The temperature correction used for the ANSYS material constants is conservative, and
- The calculation does not assume any support from the parent tube, tube support plate, or tubesheet.

With these conservatisms, the simplified estimate of creep rupture time agrees with the more rigorous ANSYS analysis to demonstrate that creep rupture is not a concern at operational temperatures and pressures.

8.6.3 Creep Fatigue Failure Evaluation

The ASME Section III Appendices [13.2] contain rules for experimental stress analysis to determine whether or not a component can withstand the cyclic loading required for its intended application. A specific requirement is for the test sample to have the same composition and to be subjected to identical mechanical working and heat treatment as the actual component. The purpose of identical processing is to produce mechanical properties equivalent to those of the material in question.

This experimental design philosophy has been expanded to address creep-fatigue. Test samples were creep tested to strains equal to and exceeding that expected in actual steam generator service (Section 7.4). The samples were then subjected to cyclic testing in accordance with the ASME Code. The tests demonstrated that the Electrosleeve™ has substantial fatigue life after creep deformations equal to and greater than that expected in service.

The testing summarized in Section 7.4 included the following safety margins:

- The ASME methodology includes a safety factor based on the number of samples being tested. With only one sample being tested, the required safety margins were maximized. Testing additional samples would have reduced the required fatigue loads and/or cycles.
- One of the samples went through fatigue testing before and after the creep exposure.

For the expected creep deformations and transient loading in steam generator tubing, the Electrosleeve™ is not subject to failure by the combined effects of creep and fatigue.

8.6.4 Creep Summary

The creep deformations in the Electrosleeve™ are extremely small at operational temperatures and loads. Testing and analysis demonstrate no failures from gross distortion, creep rupture, or creep fatigue will occur under the steam generator operating conditions.

8.7 Design Summary

The Electrosleeve™ has been qualified for installation in the following steam generator designs:

- Westinghouse Models 33, 44, 51, D, E, and F;
- CE Models 67, 3410, and System 80;
- CE SG at Ft. Calhoun.

The Electrosleeve™ is qualified for installation over all tube defect types including IGA, circumferential cracks, axial cracks, pitting, and other similar defects. The Electrosleeve™ is qualified for installation in tube freespan regions, at tube expansion transitions, and at tube support plate regions. The sleeve is a structural repair of the parent tube. Installation in tube locations adjacent to the TSP vertical supports is limited as discussed in Section 8.5. The installed minimum and nominal sleeve wall thicknesses are shown in Table 8.7.1.

TABLE 8.7.1
ACCEPTABLE WALL THICKNESSES FOR AN INSTALLED SLEEVE

TUBE SIZE	INSTALLED SLEEVE MINIMUM WALL THICKNESS (INCH)	INSTALLED SLEEVE NOMINAL WALL THICKNESS (INCH)
1 1/16" OD x 0.040" wall	┌	b,c,e┐
3/4" OD x 0.042/0.043/0.048" wall		
7/8" OD x 0.050" wall	└	┘

The field process is designed and operated to install a sleeve with the average wall thickness equal to or greater than the nominal thickness. A minimum thickness may occur due to tube ovality or sleeve tube concentricity.

Testing indicates that a [^{b,c}] nominal bond length between the sleeve and tube will carry all structural loads. For conservatism, the bond length for field acceptance will be set at a minimum of [^{b,c,e}]. Figure 8.5.2 illustrates the bond length and pressure

boundary. The minimum bond length of [^{b,c}] at both sleeve ends provides adequate structural attachment to a parent tube. Bonding of the Electrosleeve™ to the degraded tube region (i.e., tube between the two minimum bond attachments) is not required to meet the structural design requirements (Figure 8.5.2).

Testing has demonstrated that a sleeve repair with a 30% through-wall defect in the sleeve wall and a tube 100% through-wall defect occurring at the same location may be expected to last at least 26 EFPY. Thus, an inspection interval of 5 years was established.

9.0 DESIGN VERIFICATION - CORROSION

The objectives of the corrosion evaluation are to determine the susceptibility of the Electrosleeve™ material to known Alloy 600 degradation mechanisms such as stress corrosion cracking (SCC) and to evaluate the corrosion potential of the Electrosleeve™ material in environments that may exist in an operating steam generator.

The corrosion evaluation was performed by first addressing general corrosion characteristics and then evaluating primary and secondary side environments. Operating experience is presented in Section 3.0.

9.1 General Corrosion Properties

Nickel and nickel alloy materials are used in many corrosion applications, especially in caustic environments. In fact, "most tough corrosion problems involving caustic and caustic solutions are handled with nickel" [13.57, pg. 243]. Because of the widespread use of nickel, the corrosion resistance of high purity nickel has been thoroughly investigated and documented. This research is directly applicable to the Electrosleeve™ since the electroformed sleeve consists of high purity (>99.5%), nanocrystalline nickel material.

9.1.1 Literature Survey of Nickel Corrosion

A general literature review was performed comparing the corrosion behavior of Alloy 600 and pure nickel [13.40] in various environments. Corrosion rates are summarized in Table 9.1.1.

TABLE 9.1.1
SUMMARY OF LITERATURE SURVEY
NICKEL AND ALLOY 600 GENERAL CORROSION
RATES IN VARIOUS ENVIRONMENTS

ENVIRONMENT	CORROSION RATE (mils per year)	
	Nickel/Ni-200	Alloy 600
WATER, Distilled, High Purity 200°F 160°F CO ₂ /air Fresh Water Sea Water	0.001 0.02 - 0.2 <1.0 Minor Pitting	0.001 No data No data
ACIDS, Boiling Sulfuric 5%,214°F 10%,216°F 19%,219°F 50%,253°F 75%,360°F 96%,560°F Hydrochloric 10%-30%,Aerated, 86°F 10%-30%,Deaerated, 86°F 30%,Deaerated, 86°F Phosphoric <40% Room Temp >40% Room Temp Elevated Temp Organic Acids Deaerated Aerated	34 120 110 >1000 910 >1000 ~80 ~10 ~70 <1 <1 150 - 220 Low High	249 390 640 >1000 >1000 860 No data ~10 ~100 <0.1 <2 High Low Low
ALKALIS Caustic Soda Other Alkalis Ammonia (400°C - 600°C) Ammonium Hydroxide (>1%)	Low Low High Low	Low Low Low No Data
SALTS Reducing Neutral/Alkaline Oxidizing	Varied, Low Low, <5 Mostly High	Varied, Low Varied, Low Varied, Low - High

Chemical environments, including liquid metals, are presented in Reference 13.57 relative to the cracking tendencies.

In general, both nickel and its alloys effectively resist attack in acid, neutral, and alkaline conditions. The presence of highly oxidizing species has been found to decrease this resistance in some chemical environments. For example, both nickel and nickel alloy corrosion has been observed in an acidic and highly oxidizing environment containing sulfur species. A galvanic attack between pure nickel and Alloy 600 or Monel 400 material will not occur in steam generator environments due to the low potential difference generated by the formation of a coupling of these two materials.

9.1.2 Comparison of Nickel Plating and Electrosleeve™

Nickel plating has been successfully used to repair steam generator tubes since 1985 [13.39]. This experience is summarized in Section 3.0 (Table 3.1). The nickel plating utilized has typically been thin walled (5-8 mils) compared to the thicker walled (> 25 mils) Electrosleeve™ repair method. The nickel plating is intended to be a corrosion resistant "patch" rather than a structural repair.

Both electrosleeves and nickel plating are >99.5% pure nickel. Phosphorus is micro-alloyed in the Electrosleeve™ to add thermal stability. Nickel plating has a conventional polycrystalline grain structure whereas the electrosleeving process produces a nanocrystalline microstructure. The relative grain boundary volume is smaller in polycrystalline materials than in nanostructures. Therefore, alloy elements, such as phosphorus that migrates to the grain boundaries, tend to be present at much higher concentrations at the grain boundaries of polycrystalline structures. As a consequence, the small phosphorus content in the Electrosleeve™ material would be more evenly distributed in its microstructure than in its corresponding coarser grained counterpart. Because of this difference in microchemistry, nanostructures are more resistant to intergranular corrosion phenomena (IGA, SCC) than their microcrystalline counterparts.

The corrosion properties of nanostructures were evaluated in a literature survey. Most of the corrosion evaluations conducted to date have been laboratory studies involving potentiodynamic polarization techniques. The studies typically show comparable general corrosion resistance in nanostructured materials relative to their conventional counterparts.

The effect of phosphorus on the corrosion resistance of nickel is complex since it depends on the environmental conditions. However, at phosphorus concentrations of less than 0.9%, the corrosion behavior of the alloy is similar to that of pure nickel [13.50]. Thermodynamic computations have been performed to assess the stability of nickel (Ni) and nickel-phosphorus (Ni-P) alloys in high temperature aqueous media [13.44]. Potential-pH diagrams constructed for Ni and Ni-P alloys (with P concentrations $\leq 25\%$ by weight) at temperatures up to 200°C show that the presence of P does not noticeably alter the normal thermodynamic stability domains (i.e., potential-pH) for Ni. Since numerous soluble (and insoluble) P-bearing species (usually PO_4 type) can be formed, high P concentrations may affect corrosion kinetics; however, the presence of P is not expected to compromise the excellent thermodynamic stability of Ni and its oxides in high temperature water.

The general conclusion from this comparison is that the Electrosleeve™ material will perform the same as steam generator nickel plating in regards to corrosion behavior. Specific tests to evaluate the corrosion characteristics of the Electrosleeve™ material were performed as discussed below.

9.1.3 General Corrosion Tests of Electrosleeve™

Corrosion tests were performed on Electrosleeve™ samples to confirm general corrosion properties for the material. The environments used were severe and were not representative of normal or faulted steam generator chemistry. However, the environments will attack Alloy 600. Thus, these tests are meant to characterize Electrosleeve™ material, not to predict the life in a steam generator.

The corrosion mechanisms tested included IGA, SCC, pitting, and crevice corrosion. Standard ASTM test procedures were followed.

9.1.3.1 Boiling Sulfuric Acid IGA Test

The boiling sulfuric acid-ferric sulfate test [13.24] is a standard ASTM method to detect the susceptibility of wrought, nickel-rich, chromium-bearing alloys to IGA. This method uses ferric chloride in 50% boiling sulfuric acid. The test is aggressive to nickel based materials with little or no chromium due to the oxidizing nature of the ferric ion.

For this test, five Electrosleeve™ specimens, one-inch long, were exposed to 50% boiling sulfuric acid containing ferric chloride for 1.5 hours.

The Electrosleeve™ specimens were removed from the test solution and examined by transverse cross-section for evidence of IGA. No IGA was found. This was expected since the Electrosleeve™ material is intrinsically resistant to IGA due to its nanocrystalline grain size which minimizes variations between grain boundary chemistry and grain interiors.

9.1.3.2 Polythionic Acid SCC Test

The polythionic acid test [13.25] is a standard ASTM method used to evaluate the relative resistance of stainless steels and related materials to SCC. The test is applied to wrought products, castings, and weld metals by immersion in a solution containing polythionic acid at room temperature. Cracking of austenitic stainless steels (Type 302 and 304) would be expected in 1 hour or less in this solution. The Electrosleeve™ test period was 46 hours. The environment may also produce areas of intergranular attack; however, the test was not used for intergranular attack.

Five Electrosleeve™ specimens, one-half inch long, were tested. Five additional electrosleeved tube samples were tested as C-rings. These C-ring specimens had the Electrosleeve™ in tension on the inside surface to evaluate the effect of applied stress. All C-ring samples were stressed to produce sleeve yielding.

After exposure to the corrosion environment, transverse cross-sections were examined metallographically. There was no evidence of SCC in the Electrosleeve™ material.

9.1.3.3 Magnesium Chloride SCC Test

The boiling magnesium chloride test [13.26] is a standard ASTM method employed to evaluate the relative resistance of wrought, cast, and welded stainless steels and related alloys to SCC. The test can detect the effects of composition, heat treatment, surface finish, microstructure, and stress on the susceptibility of these materials to chloride SCC. The test is carried out in a solution of magnesium chloride (about 45%) which boils at 311°F (155°C) for a duration of 3 hours.

Five Electrosleeve™ specimens, one-half inch long, were tested. Five additional electrosleeved tube samples were tested as C-rings. These C-ring specimens had the Electrosleeve™ in tension on the inside surface to evaluate the effect of applied stress. All C-ring samples were stressed to produce sleeve yielding.

After exposure to the corrosion environment, transverse cross-sections were examined metallographically. There was no evidence of SCC in the Electrosleeve™ material.

9.1.3.4 Sodium Chloride SCC Test

The sodium chloride SCC test [13.27] is a standard ASTM method used to characterize the SCC resistance of aluminum, ferric, and other alloys exposed to alternating immersion or wetting and drying conditions. The typical cycle time is 10 minutes immersion in the solution and 50 minutes drying in air. This test is an accelerated test to evaluate the resistance to SCC and is not intended to predict performance in specialized chemical environments.

Five Electrosleeve™ specimens, one-half inch long, were tested. Five additional electrosleeved tube samples were tested as C-rings. These C-ring specimens had the Electrosleeve™ in tension on the inside

surface to evaluate the effect of applied stress. All C-ring samples were stressed to produce sleeve yielding.

The test specimens were exposed for 21 days to a 3.5% sodium chloride (NaCl) solution at room temperature with alternate wetting and drying.

Metallographic examination of the specimen cross-sections revealed no SCC.

9.1.3.5 Ferric Chloride Pitting and Crevice Corrosion Test

The ferric chloride test [13.28] is a standard ASTM method used to evaluate the resistance of stainless steels, nickel-base, chromium-bearing, and related alloys to pitting and crevice corrosion. This test is an accelerated test designed to cause the breakdown of type 304 stainless steel at room temperature. The test evaluates pitting and crevice corrosion.

Pitting Corrosion

Five Electrosleeve™ specimens, one-half inch long, were exposed to the test solution of 6% ferric chloride in water at room temperature. The ferric chloride used in this test provides an aggressive, strongly oxidizing, acidic environment to accelerate the test process. The specimens were exposed to the solution for 72 hours.

Examination of cross sections of the samples showed no evidence of pitting on the Electrosleeve™. As observed in other test results, the effect of the ultra-fine-grained size of the Electrosleeve™ material is a resistance to pitting corrosion.

Crevice Corrosion

The same solution used in the pitting step is used in the crevice corrosion test. Sandwiching a Teflon rod between two electrosleeved tube halves created crevice specimens. A total of five crevice specimens were exposed to the test solution for a period of 72 hours at room temperature.

Some crevice corrosion was observed in four of the ten half-tube samples (two per crevice specimen). The remaining six half-tube samples showed no evidence of crevice corrosion. Some attack of the Electrosleeve™ material was expected in this highly oxidizing acidic environment. With six of the ten specimen surfaces showing no crevice corrosion, it is concluded that even in this severe test environment, the Electrosleeve™ material shows good resistance to crevice corrosion.

9.1.3.6 Summary of Characterization Tests

Standard ASTM tests were used to characterize performance of the material relative to corrosion mechanisms. The results of these tests revealed no susceptibility to IGA in the boiling sulfuric acid test. No cracks were found in the samples exposed to the polythionic acid, boiling magnesium chloride, or alternate immersion tests. The ferric chloride test showed that the samples had no susceptibility to pitting corrosion and only slight susceptibility to crevice corrosion.

The performance of nanocrystalline micro-alloyed Electrosleeve™ material was found to be acceptable in these tests and similar to that expected of high purity polycrystalline nickel.

9.2 Primary Side Corrosion Evaluation

In general, corrosion in the primary system of a PWR is minimized by careful control of the environmental characteristics. The reactor coolant system (RCS) is a closed system that does not come in contact with outside contaminant sources. The environment is further controlled by limiting the presence of contaminants to low levels as required by plant technical specifications. The RCS chemistry control parameters and expected limiting values for the various modes of operation are given in Table 9.2.1. The corrosion of nickel and nickel based alloys is minimal during power operation due to:

- The addition of dissolved hydrogen which acts as a reducing agent,
- Controlling the dissolved oxygen content to 100 ppb,
- The pH at temperature is maintained slightly alkaline, and
- Nickel solubility is low at operating temperatures (approximately 550-650°F (288-343°C)).

TABLE 9.2.1
PRIMARY SIDE MATRIX CHEMISTRY

PARAMETERS								
Plant Mode	Boron (ppm)	Lithium (ppm)	Oxygen (ppm)	Temperature (°F)	Hydrogen Peroxide (ppm)	Hydrogen (cc/kg)	Chloride (ppm)	Fluoride (ppm)
1	0-2000	2.2-3.5	<0.1	$T_{hot} - T_{cold}$	0	25-35	<0.15	<0.15
2 3 4	2000-3000	0-3.5	<0.1 (>250°F)	$T_{hot} - T_{cold}$ T_o 200	0	0-35	<0.15 (>250°F)	<0.15 (>250°F)
5	3000	0	0-3	<200	<10	0	<1	<1
6	3000	0	8	Ambient	0-6	0	<1	<1

To evaluate corrosion performance of the Electrosleeve™ material in the primary side environment, the following conditions were addressed:

- Full Power Operating Conditions
 - Borated Primary Water
 - Pure Water with Hydrogen

- Shutdown Conditions
 - Boric Acid
 - Crud Burst

- Parent Tube PWSCC
 - Residual Stresses in Parent Tube
 - Ability of Sleeve to Stop PWSCC

Table 9.2.2 contains a summary of the primary side principal chemistry parameters in a typical PWR and their values during testing.

TABLE 9.2.2
PRIMARY SIDE CHEMISTRY COMPARISON

PARAMETERS												
	Boron (ppm)		Lithium (ppm)		Oxygen (ppm)		Temperature (°F)		Hydrogen Peroxide (ppm)		Hydrogen (cc/kg)	
	Plant	Test	Plant	Test	Plant	Test	Plant	Test	Plant	Test	Plant	Test
1 (>5%)	0-2000	650 - 2500	2.2-3.5	0-2	<0.1	<0.01	T _{hot} - T _{cold}	662	0	0	25-35	40-45
2		2500		0	<0.1	<0.01		176				
3 (0-5%)	2000-		0-3.5				200 - 610	302	0		0-35	
4	3000							482				
5 (<200°F)	3000	2500	0	0	0-8	NA	<200	194	<10	10 - 100	0	0
6 (Refueling))	3000	1200	0	0	8	8	Ambient	75	0-6		0	

Framatome (Europe) has performed numerous corrosion tests on steam generator tube nickel plating to demonstrate performance in this environment [13.39]. As previously discussed, the corrosion behavior of high purity standard nickel plating and high purity Electrosleeve™ nickel forming is comparable. Thus, the data on steam generator tube nickel plating is directly applicable.

9.2.1 Full Power Operating Conditions

Corrosion testing was performed on nickel plating in environments that included pure water and primary water chemistry conditions [13.39]. Highly stressed hard rolled transition zones or highly stressed reverse U-bend (RUBs) specimens were used in the testing. Also, samples were subjected to temperature and pressure cycling in pure water to induce deformations in the nickel layer.

9.2.1.1 Pure Water Testing

The objective of this test was to determine the cracking resistance of highly stressed nickel plating in pure water and to compare it to Alloy 600.

RUB specimens were tested in an autoclave at the following conditions:

- Environment: pure water [

],^{b,c}

[

],^{b,c}

- Temperature: [

],^{b,c}

- Pressure: [

],^{b,c}

- Test Period: [

],^{b,c}

The RUB specimens used in this test were as follows:

- Two specimens without nickel plating,
- Three specimens with { ^{b,c} } of nickel plating,
- Three specimens with { ^{b,c} } of nickel plating, and
- Three specimens with { ^{b,c} } of nickel plating.

NOTE: The heat of Alloy 600 material used in this test has been shown to crack in less than 500 hours in deaerated pure water environments.

After 2,000 hours, the test specimens were examined and, as expected, the unplated specimens contained numerous cracks. Following 4,000 hours, a second examination of the specimens was performed. Cracking was not observed on any of the nickel plated specimens regardless of the plating thickness at either the 2000 hour or 4000 hour examinations.

The conclusion of this test is that a nickel sleeve will not crack in pure water and will protect Alloy 600 against cracking. The thicker Electrosleeve™ (>25 mils) offers greater protection to the Alloy 600.

9.2.1.2 Primary Water Testing

The objective of this test was to determine the cracking resistance of highly stressed nickel plating in primary water and to compare it to Alloy 600.

Two Alloy 600 RUB test specimens with 4 mils (100 μm) of nickel plating, along with unplated Alloy 600 RUB control specimens, were placed in an autoclave at the following test conditions [13.39]:

- Environment: {

} ^{b,c}

Two nickel plated Alloy 600 test strips were tested in an open beaker at the following conditions:

- Environment: []^{b,c}
[]^{b,c}
- Temperature: []^{b,c}
- Test Period: []^{b,c}

At the end of the test period, the specimens were examined and weighed. The measured weight loss was negligible []^{b,c}. This minimal measured weight loss is equivalent to a corrosion rate

Then, two nickel plated Alloy 600 test strips were tested in an open beaker at the following conditions:

- Environment: []^{b,c}
 - Temperature: []^{b,c}
 - Test Period: []^{b,c}
- []^{b,c}

At the end of the test period, the specimens were examined and weighed. There was no measurable weight loss.

9.2.2.2 Boric Acid - Elevated Temperatures

A group of tests were performed on nickel plated Alloy 600 tubes in a boric acid environment at elevated temperatures. These tests address the potential for corrosion of nickel plating from boric acid trapped within Alloy 600 cracks. The tests also partially address Mode 5 conditions.

Nickel plated tubing specimens were placed in Alloy 600 capsules, welded shut, placed in a furnace at room temperature, and tested at the following conditions:

- Environment: [

],^{b,c}

- Temperatures: [

],^{b,c}

- Test Period: [

],^{b,c}

[

],^{b,c}

solution. The oxygen level for Mode 5 is 0-8 ppm, and temperature is less than 200°F. Thus, the test did not address worst case oxygen levels for Mode 5 but did encompass the temperature and typical boron concentration.

The specimens were removed from the oven and examined at the end of the test period. No corrosion of the nickel plating was observed for the three test temperatures.

9.2.2.3 Shutdown Crud Burst/Cleanup

During a typical plant shutdown for a maintenance or refueling outage, an RCS crud burst is induced through an adjustment to the coolant pH and oxidant level. For this, the plant is borated to the refueling concentration, the lithium and dissolved hydrogen removed, and hydrogen peroxide (up to 10 ppm) may be added when the temperature has decreased to less than 200° F. This condition is typically maintained for a period of 12 hours to reduce the crud inventory in the RCS prior to continuing the refueling activities. This condition was evaluated by testing Electrosleeve™ specimens at the following conditions:

- Environment: [

],^{b,c}

- Temperatures: [

],^{b,c}

- Test Period: [

],^{b,c}

- Test Specimens: [

].^{b,c}

specimens were tested at each concentration. At the end of the test period, the specimens were examined and weighed. [

].^{b,c,d} No localized attack was observed on the Electrosleeve™ surface. There was no significant difference in the hydrogen peroxide concentrations.

[

].^{b,c,d}

9.2.2.4 Low pH and Shutdown Chemistry Conditions

The use of the Electrosleeve™ as a repair requires the corrosion test to envelop the expected chemical conditions during shutdown as well as during operation.

Mode 5 Corrosion Testing

Electrosleeve™ specimens were tested in the following environment:

- Boron: []^{b,c}
- Oxygen: []^{b,c}
- pH: []^{b,c}
- Temperature: []^{b,c}

These conditions were selected to envelop expected plant conditions during shutdown with the controlling elements being the boron and the dissolved oxygen.

The samples were first exposed to a [] environment [] with examinations made at intermediate times. The examinations revealed that the samples had passivated []^{b,c,d} and the weight loss had essentially stopped (within the precision of the weight loss measurement).

The temperature was lowered to ambient []^{b,c,d}. The test was maintained []^{b,c,d} and no additional weight loss was observed. The conclusion from this test is that no detectable degradation is expected in the Electrosleeve™ due to shutdown chemistry conditions.

Electrosleeve™ in Low pH Conditions

To simulate a low pH excursion during shutdown, a test using sulfuric acid to lower the pH to 4.0 was performed. The samples from the Mode 5 test were used in the following environment:

- Boron: []^{b,c}
- Oxygen: []^{b,c}
- pH: []^{b,c}
- Temperature: []^{b,c}

Intermediate examinations were made revealing that, after a short period of time, the samples passivated and no further weight loss was detected. This test supports earlier test results that demonstrate little or no corrosion of the electrosleeves is expected due to normal shutdown chemistry conditions.

The conclusion from this test is that even with an artificially lowered pH, virtually no additional degradation occurred in the Electrosleeve™ samples.

9.2.3 Parent Tube SCC

Two tests have been performed to evaluate SCC in the parent tube. The first test verified that a nickel plated layer would prevent SCC in the parent tube at highly stressed regions by providing a protective layer.

A test was also performed with electrosleeves to verify that high residual tensile stresses are not induced into the parent tube at the ends of the sleeve.

9.2.3.1 Stress Corrosion Cracking Protection

PWSCC susceptible Alloy 600 specimens containing stresses greater than 30 to 35 ksi tested in 10% NaOH (caustic) solution were shown to rapidly induce stress corrosion cracking. Steam generator roll transition mockups were used to evaluate the effect of nickel plating on SCC [13.39]. The Alloy 600 tubes were rolled using a five-step rolling process, which resulted in two roll transition regions in each mockup. The specimens were tested at the following conditions:

- Environment: []^{b,c}
- Temperature: []^{b,c}
- Pressure: []^{b,c}
- Test Period: []^{b,c}

The test solution was injected in the mockups which were then internally pressurized.

[]^{b,c} mockups were tested:

- []^{b,c,d}
- []
- []
- []

Mockups were pre-cracked 100% through-wall in a sodium tetrathionate solution (at room temperature) prior to being plated. These mockups were plated []^{b,c,d}.

Unplated Alloy 600 tubing produced 50% through-wall cracks after 120 hours and 100% through-wall after 240 hours.

[

b,c,d
]. The

mockups plated with 100 or 150 μm (4.0 or 5.9 mils) of nickel showed no attack or damage to the nickel plating.

Thus, a nickel plating thickness of 4.0 mils or greater provides protection of the parent tube from PWSCC. An Electrosleeve™ will offer improved protection because nanostructured materials provide greater resistance to SCC. The design thickness for the Electrosleeve™ is greater than 25 mils which provides a greater level of corrosion resistance.

9.2.3.2 Stress Corrosion Cracking (Effect of Stress)

A primary concern with standard steam generator sleeving has been the introduction of residual tensile stresses into the Alloy 600 parent tube due to the sleeving process. Such tensile stresses lead to PWSCC in the parent tube while the sleeve typically does not experience SCC. Electrosleeving has the advantage of not introducing these high residual tensile stresses to the tube.

The objective of this corrosion test is to demonstrate the absence of significant residual stresses imparted on the Alloy 600 tube after electrosleeving. A second objective is to demonstrate the resistance of the Electrosleeve™ to SCC.

The corrosion test environment was as follows:

- Environment: [
- Temperature: [
- Pressure: [
- Test Period: [

] b,c

] b,c

] b,c

] b,c

These corrosion specimens are from the locked tube tests described in Section 7.1. The 3/4" OD tubing, EPRI heat 96834, was known to be susceptible to SCC in caustic environments. [

^{b,c,e}
]

The measured installation stress due to locked tubes was nominally 3.0 ksi tensile. Alloy 600 will not produce PWSCC in the steam generator environment or SCC in a caustic environment for these stress levels.

The sleeved tubes were cut from the locked tube mockup and placed in the autoclave. [

^{b,c,d}
], the test was intended to

evaluate residual stress.

[^{b,c}] C-rings, fabricated from the same heat of Alloy 600 without an installed Electrosleeve™, were included in the test as control specimens. The C-rings were electropolished to remove approximately 0.5 mil from each surface and loaded to a nominal 0.5% strain.

The specimens were removed from the autoclave and examined. Stress corrosion cracking was observed in all [^{b,c}] C-rings ranging in [^{b,c,d}]. The susceptibility of the Alloy 600 to SCC was confirmed in the test condition.

No SCC was observed along the length of the [^{b,c}] electrosleeved specimens. Thus, high residual tensile stresses were not induced into the parent tube at the ends of the sleeve. In addition, there was no degradation of the Electrosleeve™ material.

9.2.4 Summary of Primary Side Tests

Corrosion testing of high purity nickel in pure water and primary water environments at accelerated temperatures indicate that the Electrosleeve™ is not expected to experience corrosion degradation at steam generator operating conditions.

Shutdown crud burst testing determined that the general corrosion of the Electrosleeve™ over a 40 year life [

] b,c

If boric acid is trapped in the crevice of an existing tube crack and the Electrosleeve™ is installed, tests indicate that no corrosion attack of the sleeve is expected.

The wall thickness of an Electrosleeve™ (>25 mils) exceeds the minimum required thickness to protect the tube from initiating or propagating SCC in highly stressed regions. In addition, SCC is not expected to occur in the Alloy 600 parent tube at the ends of the Electrosleeve™.

9.3 Secondary Side Corrosion Evaluation

Evaluating the corrosion performance of a material for secondary side environments is more difficult than evaluating the primary side performance due to the wide range of chemistry conditions that may be encountered. Steam generator upset chemistry conditions may result from condenser in-leakage, ion exchange resin regenerant chemicals (caustic and acid) from condensate polishing and makeup demineralizer systems, acidic sulfur species from resin ingress, chlorides, and corrosion product iron and copper.

The effect of these contaminants is further compounded by the concentrating mechanisms associated with heat transfer and boiling in the steam generators. The generally accepted steam generator and secondary system chemistry program is All Volatile Treatment (AVT). In this program, there are no solids intentionally added to the steam generators for chemistry control. Only volatile chemicals such as ammonia and hydrazine are used for corrosion control.

Corrosion of the Electrosleeve™ in the secondary side environment of a PWR is minimized by the following environmental characteristics:

- Hydrazine is added to scavenge oxygen,
- Feedwater dissolved oxygen is < 5 ppb,
- The feedwater pH is maintained in the alkaline range (≥ 8.8) by adding ammonia or other amines,
- Nickel solubility is low at operating temperatures (approximately 550-650°F [288-343°C]),
- Plant operating procedures call for operator action in the event of severe chemistry excursions to minimize time at the event, and
- Exposure of the sleeve to the secondary side is minimal. This is due to the Alloy 600 degradation being tight SCC or IGA. In addition, no crevice is created between the sleeve OD and tube ID.

If exposed to the secondary side bulk water, there are no corrosion concerns for the Electrosleeve™ provided that the water chemistry is within the recommended specifications. Table 9.3.1 provides secondary side chemistry values and Table 9.3.2 provides a summary of the secondary side principal chemistry parameters in a typical PWR. However, considering that the main reason to utilize electrosleeves is to arrest Alloy 600 cracking, the Electrosleeve™ must withstand the environment that locally forms at the crack tip.

TABLE 9.3.1
SECONDARY SIDE MATRIX CHEMISTRY⁽¹⁾

PARAMETERS								
Plant Mode	Sulfate (ppb)	Sodium (ppb)	Chloride (ppb)	Copper (ppb)	Oxygen (ppb)	Temperature (°F)	Boron (ppm)	Iron (ppb)
1	<20	<20	<20	<1 (FW)	<5 (FW)	$T_{hot} - T_{cold}$	<10	<5 (FW)
2 3 4	<100	<100	<100	N/A	<100	$T_{hot} - T_{cold}$ to 200	<10	N/A
5	<1000	<1000	<1000	N/A	<100 (FW)	<200	<1	N/A
6 (Refuel)	<1000	<1000	<1000	N/A	<100 (Source)	Ambient	<1	N/A

NOTES:

(1) Lead (Pb) limits not established.

TABLE 9.3.2
SECONDARY SIDE CHEMISTRY COMPARISON⁽¹⁾

PARAMETERS																
Plant Mode	Sulfate (ppb)		Sodium (ppb)		Chloride (ppb)		Copper (ppb)		Oxygen (ppb)		Temperature (° F)		Boron (ppm)		Iron (ppb)	
	Plant	Test	Plant	Test	Plant	Test	Plant	Test	Plant	Test	Plant	Test	Plant	Test	Plant	Test
1(>5%) ⁽²⁾	<20	0 - 3E5	<20	0 - 3E7	<20	0 - 2E7	<1 (FW)	6E6 +sludge	<5 (FW)	<5 - 3E9	T _{hot} - T _{cold}	265-305	<10	0	<5 (FW)	sludge
2 3 (0-5%) 4	<100		<100		<100		N/A		<100				<10		N/A	
5 (<200°F)	<1000		<1000		<1000		N/A		<100 (FW)		<200		<1		N/A	
6 (RF)	<1000		<1000		<1000		N/A		<100 (Source)		Ambient		<1		N/A	

NOTES:

- (1) Lead (Pb) limits not established.
- (2) Test used 1 gram of lead (Pb).

The performance of the Electrosleeve™ in severe secondary side environments was evaluated by exposing the sleeve to extreme environments at elevated temperatures. This was addressed by exposing highly stressed tube/Electrosleeve™ samples in an environment known to cause SCC in Alloy 600. Arrest of cracking at the Alloy 600/Electrosleeve™ interface demonstrates the corrosion resistance. The environments included high concentrations of active species:

- Chloride in acidic and alkaline media,
- Sulfate in acidic and alkaline media, and
- High/low redox conditions.

The chemistry of these extreme environments may be approached in a localized region of the secondary side. However, the acidity and redox potential values for these tests were chosen to accelerate the material degradation and are not present in an operating unit.

Evaluation of worst case conditions under sludge piles was also tested. These tests were performed in refreshed autoclaves which incorporate steady state heat transfer conditions. These tests simulate the steam generator operation. As in an operating unit, the heat transfer process concentrates chemical solutions. The tests were accelerated by increasing the bulk water concentrations of the contaminants by factors greater (typically 1000x) than those expected in an operating unit excursion event.

The objective of these tests was to conservatively evaluate the degradation of the Electrosleeve™ material when exposed to extreme environments (e.g., caustic, acidic, fresh water in-leakage, etc.) under simulated operating conditions that involve heat transfer in a confined geometry (e.g., sludge pile). While several postulated chemistry environments have been presented in the literature, Reference 13.55, the testing performed using the Electrosleeve™ material with the heat transfer effects envelops most chemical conditions.

9.3.1 SCC Propagation Tests

To evaluate the crack arrest capability of electrodeposited nickel, two tests were conducted. The first test demonstrated the ability of nickel-plated steam generator tubes containing through-wall cracks to maintain their integrity in a secondary side environment (chemistry and pressure conditions). The second test demonstrated the ability of highly strained electrosleeves to arrest ODSCC in Alloy 600 tubing.

A summary of the test conditions and results for these crack property tests is contained in Table 9.3.3.

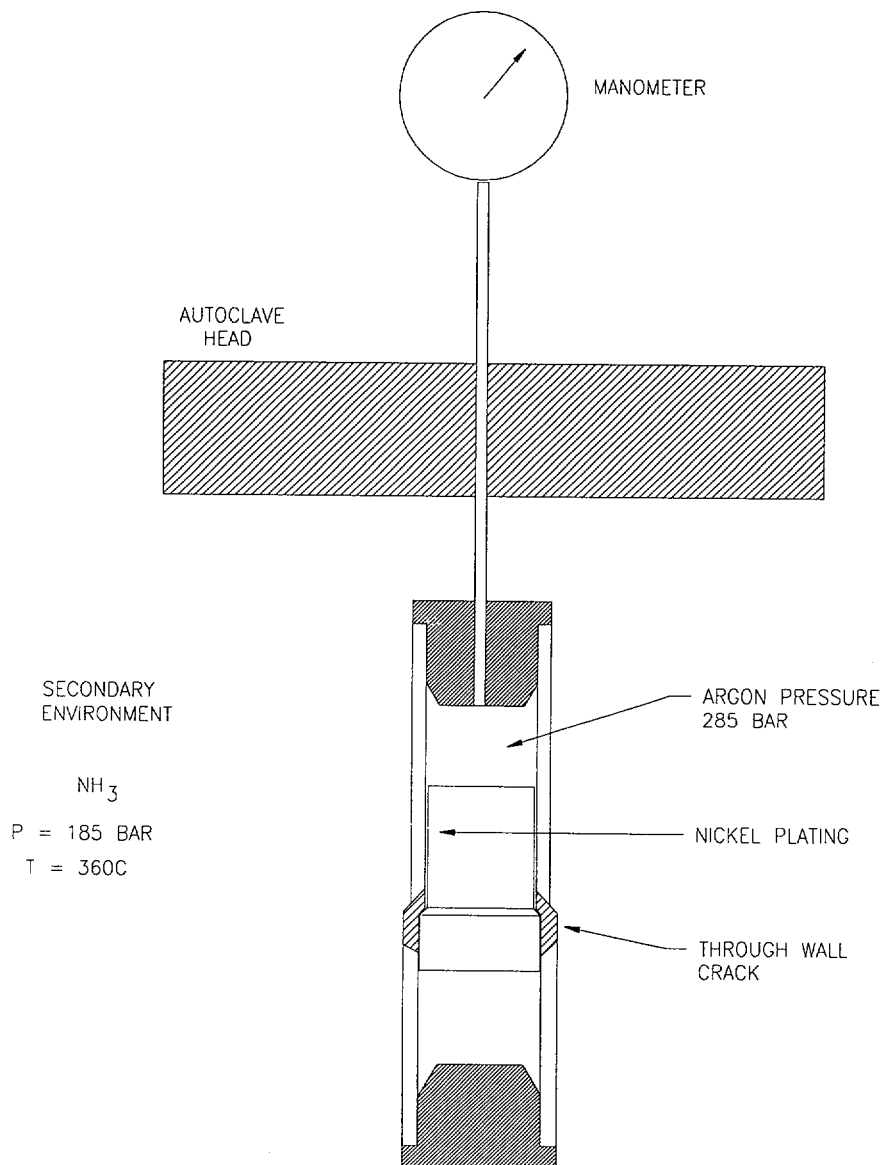
TABLE 9.3.3
SUMMARY OF CRACK PROPAGATION TESTS

TEST PURPOSE	TEST ENVIRONMENT		RESULTS
SCC Propagation Tests (Pre-cracked S/G Tubing)	┌		┐ b,c,d
SCC Propagation Tests (Stressed C-rings)	└		┘

9.3.1.1 Precracked Steam Generator Tubing Test

Steam generator tubing, containing OD initiated cracks (including through-wall cracks), was nickel plated and tested in a mockup (see Figure 9.3.1). The purpose of the test was to determine whether through-wall cracks in nickel plated steam generator tubes will continue to propagate through the nickel plating when exposed to secondary side conditions [13.39].

FIGURE 9.3.1
SECONDARY SIDE CAPSULE TESTS



The test conditions were as follows:

- Environment: []
- Temperature: []^{b,c}
- Differential Pressure: []^{b,c}
- Test Period: []^{b,c}

Three nickel plated pre-cracked tubes were exposed to these conditions for the test duration. Ultrasonic examinations conducted []^{b,c,d} indicated no increase in the depth of the cracks when compared to pre-test examination data. Thus, with the pre-cracked tubes, the electroplate provided tube integrity.

9.3.1.2 Crack Arresting C-Ring Test

Alloy 600 steam generator tubing with and without an installed Electrosleeve™, in the form of highly stressed C-rings, was used to evaluate the ability of the Electrosleeve™ to arrest a crack propagating from the tube OD. Testing was performed in a 10% NaOH (caustic) environment that is known to cause SCC in susceptible Alloy 600 material.

The test conditions were as follows:

- Environment: []^{b,c}
- Temperature: []^{b,c}

• Pressure: [

] b,c

• Test Period: [

] b,c

Testing was performed using [] C-ring specimens;
[] b,c from each of the following four tube types:

- Bare Alloy 600 tubes,
- Electrosleeved Alloy 600 tubes,
- Bare electrosleeves, and
- Nickel 200 tubes (3/4" OD x 0.049" wall)

The specimens were prepared from 3/4" OD Alloy 600 tubing (EPRI heat number 96834) that has been shown to be susceptible to SCC in this environment.

All C-rings were electropolished to remove approximately 0.5 mil from each surface. To place the Electrosleeve™ in tension in the final C-ring configuration, the electrosleeved tube specimens were machined to an Alloy 600 nominal tube wall of 10 mils. C-ring specimens were then stressed to 1.0%, 1.5%, and 2.0% strain.

Dimensional analysis of the test specimens (bare Electrosleeve™, Nickel 200, Alloy 600, and electrosleeved Alloy 600) following the 3,000 hour test confirmed all C-rings maintained tensile stresses throughout the test period.

The bare Electrosleeve™ material and Nickel 200 showed no evidence of SCC under the conditions tested.

The Alloy 600 displayed severe intergranular SCC following the 3,000 hour exposure. Table 9.3.4 presents crack depth and strain levels.

TABLE 9.3.4
MAXIMUM SCC PENETRATIONS
IN ALLOY 600 CONTROL SPECIMENS

APPLIED STRAIN (%)	AVERAGE OF MAXIMUM CRACK DEPTHS (mils)	STANDARD DEVIATION (mils)
1.0	┌	┐ b,c,d
1.5		
2.0	└	┘

[^{b,c}], the lowest applied strain yields considerable variability in the maximum extent of SCC. However, all applied strains produced maximum crack lengths in excess of the nominal 10 mil thickness of the Alloy 600 tubing used with the electrosleeved specimens.

All of the tested electrosleeved C-ring specimens [^{b,c}] displayed the SCC penetrations through [^{b,c,e}] wall Alloy 600 tubing. The SCC growth stopped at the Electrosleeve™ material.

Based upon exposure time, the cracks were likely to have remained "blunted" at the Electrosleeve™ interface. [

^{b,c,d}] No evidence of either sleeve disbonding or crack propagation along the interface was noted in any of the test specimens.

In summary, the conclusions from this test are:

- Bare Electrosleeve™ material behaves in a manner consistent with Nickel 200 and displays complete immunity to caustic SCC,
- Propagating SCC in Alloy 600 is "blunted" by the Electrosleeve™, and

- The high stress conditions at the "blunted" Alloy 600 cracks do not result in Electrosleeve™ disbonding or interfacial cracking.

9.3.2 Capsule Tests

The objective of this test was to characterize the corrosion performance of the Electrosleeve™ material in confined conditions of extreme bulk water chemistry.

Test conditions were as follows:

- Environment: Demineralized water; 2,000 psi oxygen overpressure or deaerated (by bubbling nitrogen through the solution prior to the test),
- Temperature: 508°, 536°, 580°, & 608°F (265°, 280°, 305°, & 320°C),
- Test Period: 750 hours (approximately 31 days).

Five-inch long sections of Monel 400 tubing containing three-inch long electrosleeves were used to manufacture the capsules.

The electrosleeved tubing capsules were sealed with Monel 400 nut/cap assemblies on both ends. One end of the capsule contained a pressure transducer to identify any through-wall leakage. The capsules were then placed into a furnace and heated to the respective test temperatures (see Figures 9.3.2 and 9.3.3). A total of twenty-four (24) different temperature and environmental combinations were tested. Table 9.3.5 presents the tests and the results.

FIGURE 9.3.2
CAPSULE FURNACE SETUP

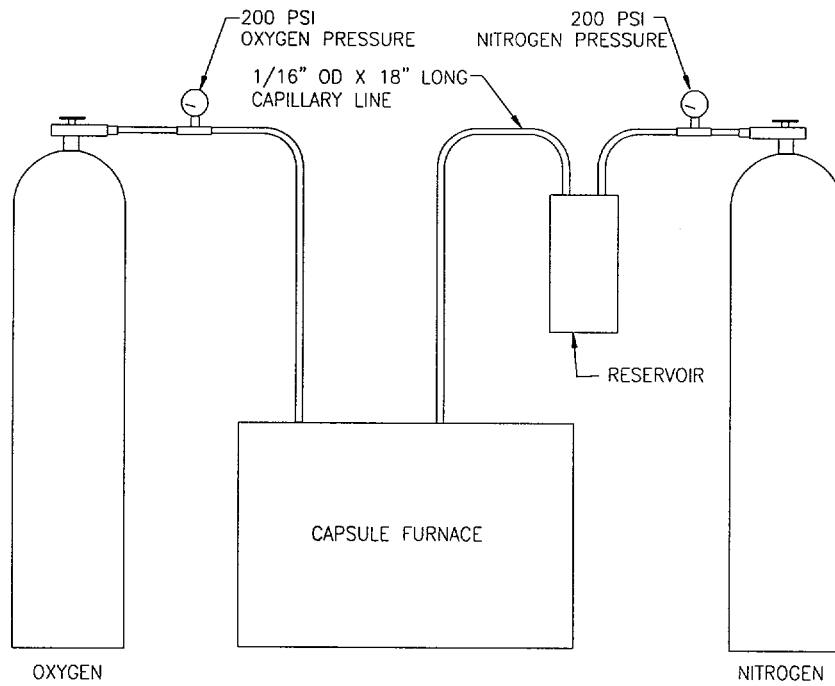
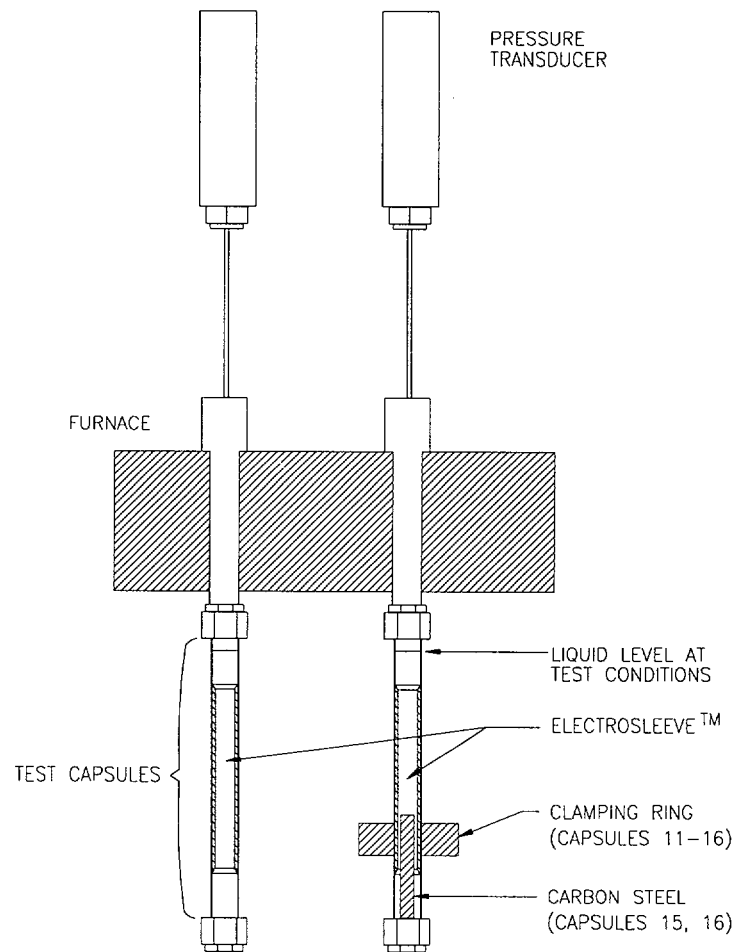


FIGURE 9.3.3
CAPSULE TESTING FOR FAULTED SECONDARY SIDE ENVIRONMENTS



The tests performed with 2,000 psi oxygen (~3,000 ppm) are extremely conservative and are not intended to be representative of the oxygen content of the secondary side chemistry.

Destructive examination of the capsule specimens (see Table 9.3.5) provided the following correlations between the chemical environments and the extent of Electrosleeve™ degradation.

[

].^{b,c,d}

Under severely oxidizing conditions, [.]^b, which contained sulfuric acid, experienced sleeve degradation. Capsules []^b, which had added sodium hydroxide, exhibited none to minimal attack.

[

].^{b,c,d}

In general, caustic environments were not aggressive to the sleeve material.

Neutral chemistries, [

].^b

had no measurable sleeve degradation.

No evidence of cracking of the Electrosleeve™ was found in the regions of capsules []^b, which were externally stressed. [

].^{b,c,d}

combination of Pb and high caustic was aggressive to the carbon steel but not aggressive to the Electrosleeve™.

The conclusion from these tests is that the Electrosleeve™ material will be attacked under highly acidic with highly oxidizing environments. The sleeve is resistant to caustic environments and to attack without oxygen. The highly

oxidizing condition (2,000 psi oxygen) is not present on the secondary side of the steam generator or within the Alloy 600 cracks.

9.3.3 Heat Transfer Sludge Corrosion Tests

The objective of these corrosion tests was to assess the corrosion performance of an Electrosleeve™ when a large area is exposed to extreme chemistry conditions under a sludge pile.

These tests address the formation of dynamic crevice environments that form in operating steam generators and yield information on the performance of the Electrosleeve™ material under these environments. However, in the steam generator, the sleeve is not exposed to these environments over large areas. Typically, the only portion of the sleeve exposed would be the tips of the cracks in the Alloy 600 tube.

Heat transfer corrosion tests allow the direct comparison of bulk water environments between the operating unit and the laboratory test. The test design involved heat transfer simulation similar to the hot leg of a steam generator and simulation of a sludge pile around the tube.

Accelerated conditions were chosen to assess the chemistry limits of the material performance. The three bulk water environments selected addressed three different operating scenarios of feedwater contamination: condenser cooling water, sodium hydroxide, and sulfuric acid. The latter species are used as ion exchange resin regenerants that may be accidentally produced in the event of operational malfunctions in the water treatment or condensate polishing systems. Normally these events are short, lasting on the order of a few hours. The present water chemistry specifications call for remedial action in such events which may even necessitate immediate unit shutdown. A summary of heat transfer corrosion tests is contained in Table 9.3.6.

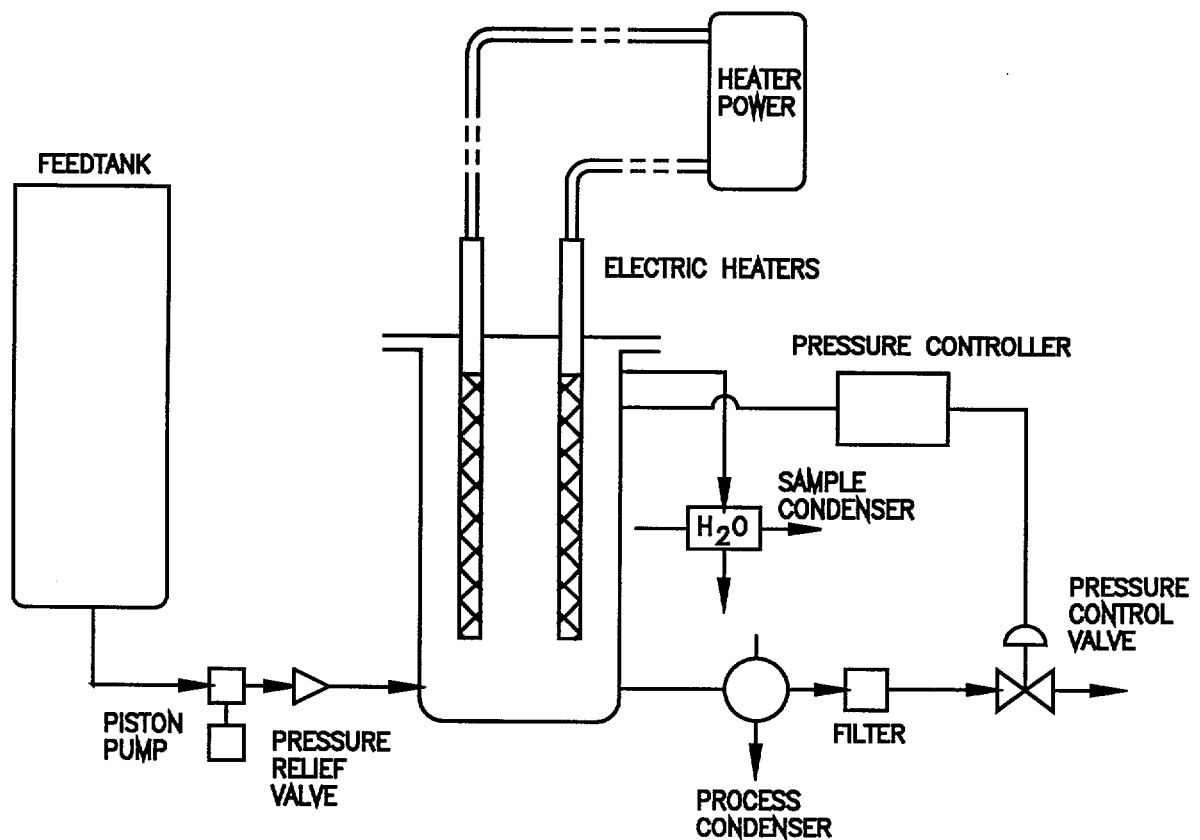
TABLE 9.3.6
SUMMARY OF HEAT TRANSFER SLUDGE CORROSION TESTS

┌			┐
			b, c, d
└			┘

Experimental

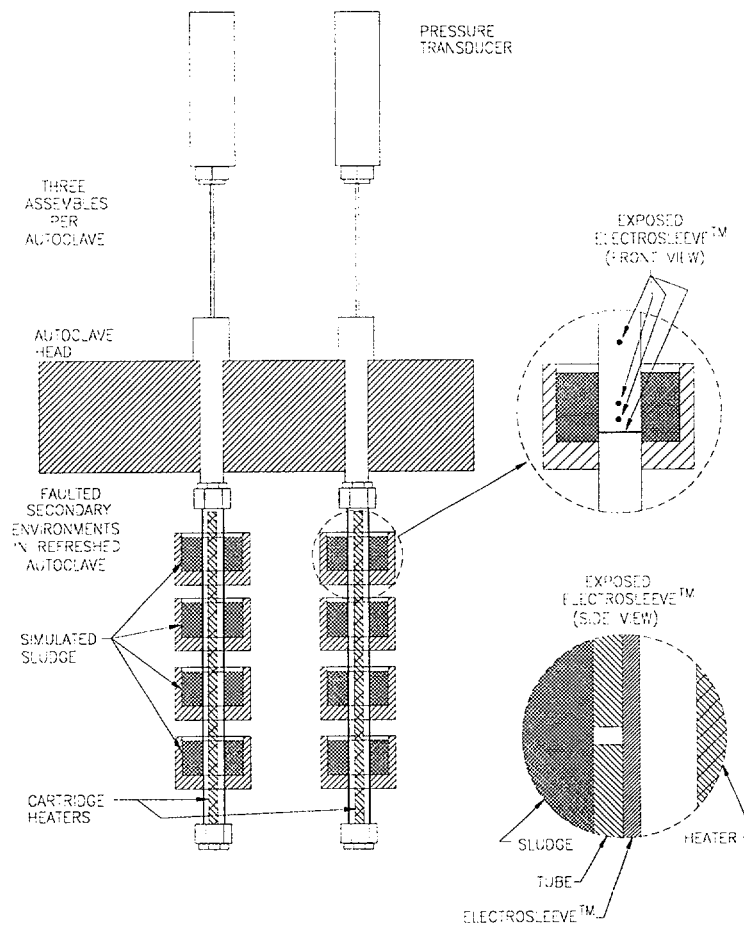
Figure 9.3.4 is a schematic of the refreshed autoclave loop that was used in these tests. The tests were conducted in [] Alloy 600 autoclaves. Three internally heated tube mockups were fastened to the autoclave cover. Each mockup had a cartridge heater and the tube was internally pressurized with helium []. The pressure simulates operating hoop stresses and enhances heat transfer with minimal occurrence of tube hot spots. The heat flux was controlled to simulate operating conditions.

FIGURE 9.3.4
REFRESHED AUTOCLAVE LOOP



The tube was hard rolled into [^{b,c}] carbon steel holders. Figure 9.3.5 presents the mockup arrangement.

FIGURE 9.3.5
STEAM GENERATOR ELECTROSLEEVED TUBE MOCKUP
FOR SLUDGE AND FAULTED CHEMISTRY TESTS



Each holder was filled with a mixture of fossil boiler sludge consisting of ~70% magnetite and ~30% metallic copper with additional added species. The composition of the sludge mixtures are listed below:

TABLE 9.3.7
COMPOSITION % WEIGHT OF SLUDGE MIXTURE AND
OTHER CHEMICAL SPECIES USED TO FILL THE SLUDGE SIMULANT HOLDERS

┌							┐ b,c,d
└							┘

Each tube was electrosleeved [_{b,c}]. The tube in the sludge holder contained a circumferential groove, nominally 1/8-inch wide, and four drilled holes, 1/16-inch diameter. One drilled hole, 1/16-inch diameter, was placed in the freespan of the tube between the holders. This arrangement ensures maximum heat flux through the sleeve. Figure 9.3.5 details the groove and drilled hole that exposed the Electrosleeve™ to the secondary side chemistry.

Electrochemical Environments

The feedwater chemistry for these tests simulated three different types of in-leakage. The in-leakage types were:

- Fresh Water (condenser cooling water),
- Caustic (sodium hydroxide), and
- Acid (sulfuric).

The under-deposit chemistries produced by these solutions generically included the scenarios of high pH, low pH, and condenser cooling water ingress. The tests were accelerated by using concentrations approximately 1000X greater than in an anticipated event. Moreover, the redox potential of the solution was raised by increasing the concentration of dissolved oxygen (by a factor of 1000X). This increase caused the region under the sludge to be aggressive to the tubing. Additional acceleration was obtained by the presence of aggressive species in the simulated sludge [13.51, 13.52, 13.53].

Feedwater solutions were prepared by mixing the targeted species with deionized water. Lake Ontario Water (LOW) was used as fresh water. For LOW, MULTEQ [13.42] predicts an alkaline pH concentration. The dissolved oxygen concentration was prepared by sparging the feedwater with the appropriate nitrogen/oxygen mixture.

9.3.3.1 Fresh Water Ingress Test

This test addressed the condition in which a chronic and massive condenser cooling water intrusion occurs during operation. The test parameters were as follows:

• Feedwater: [] b,c

• pH: [] b,c

• Temperature: [

] b, c

L

]

• Pressure: [

] b, c

• Test Periods: [

] b, c

Results

Tube assemblies were removed for examination [

] b, c, d

No attack of the Electrosleeve™ material or the Monel 400 parent tube material was observed [

] b, c, d

Test Significance

Under extreme accelerated conditions which simulate the under deposit environment in an operating unit, the Electrosleeve™ performance is excellent. [

] b, c, d

The test severity was greatly increased by the high dissolved oxygen concentration, which imposes high redox potential particularly under the sludge pile where local anodic regions may be prevalent due to

the possibility of forming differential oxygen cells as a result of localized steaming. The concentration capability of the sludge piles has been demonstrated (hideout return phenomena in operating units) and measured in lab experiments. The tube surface and the Electrosleeve™ were exposed to solutions with high impurity concentrations under the sludge pile. The solution concentration increased with time to several orders of magnitude greater than the bulk water [13.54].

Behavior predicted from thermodynamic considerations and assessed by the capsule tests was consistent with the Electrosleeve™ material. MULTEQ predicts alkaline environments based upon the concentration of the bulk chemistry (LOW) used in the test. Even for high values of redox, the Electrosleeve™ nickel was passive.

9.3.3.2 Acid Ingress

This test addressed the condition of a massive continuous acid ingress in a steam generator during operation. Test parameters were as follows:

• Feedwater: [

] b,c

• Temperature: [

] b,c

• Pressure: [

] b,c

] b,c

• Test Period: [

] b,c

Results

[

] b,c,d

Destructive examination of the regions under the sludge showed corrosion attack on the Electrosleeve™ material and the tube substrate. The extent of attack []^{b,c} examined was approximately the same which indicates that the degradation occurred during the initial, high oxygen period. The observed degradation was general corrosion with some regions of localized attack.

Test Significance

The test addressed an unbuffered, continuous, large acid ingress in a steam generator. The severity of the test was increased due to the acid concentration being a factor of 1,000X over any credible realistic scenario (typically less than 300 ppb free acid). [

] b,c,d

Such a scenario is not realistic if an operator were to follow the EPRI Secondary Chemistry Guidelines [13.41]. An acid intrusion would immediately trigger corrective actions, including plant shutdown, which would essentially eliminate the heat flux induced concentrating mechanisms generated during the tests described above.

The severity of the test was augmented by increasing the dissolved oxygen concentration, thus increasing the redox potential, especially under the sludge pile.

The results confirmed that a combination of highly acidic and highly oxidizing conditions are aggressive to the Electrosleeve™. [

.]^{b,c,d}, when the redox was lowered by decreasing the dissolved oxygen concentration, the Electrosleeve™ performed satisfactorily. This effect confirmed the trend observed in the capsule testing.

The heat transfer test was more severe than the corresponding capsule test because there is a continuous addition of acid to the heat transfer surfaces and the concentration of contaminants under the sludge pile. MULTEQ calculations determined low (less than 1.0) solution pH values at concentration factors of 1,000X which was rapidly reached under the sludge pile. The material potential impressed by the solution redox was transpassive as in the capsule test.

In credible acidic excursions expected in operating steam generators, the Electrosleeve™ material demonstrates resistance to corrosion.

9.3.3.3 Caustic Ingress

This test addresses the condition of a massive continuous caustic ingress in a steam generator during operation. The test parameters were as follows:

- Feedwater: [

] ^{b,c}

- Temperature: [

] b,c

- Pressure: [

] b,c

- Test Period: [

] b,c

Results

Examination of the tube in the areas under the sludge piles revealed no attack of the Electrosleeve™ or the tube after [] exposure [

] b,c,d

Test Significance

Under extreme caustic conditions, the test confirmed acceptable performance of the Electrosleeve™. The excursion scenario was highly accelerated in terms of the total caustic concentration and the solution redox potential. The degradation observed [] was consistent with the data obtained in the capsule testing and in agreement with the thermodynamic data.

9.3.4 Secondary Side Corrosion Rate

[

] b,c,d

[

J. b, c, d

As previously discussed, the main objective of the corrosion testing was to demonstrate the effectiveness of the Electrosleeve™ repair at remedying the SCC degradation problem. The heat transfer tests demonstrated that the Electrosleeve™ can also perform under anticipated, realistic operating scenarios if exposed to such chemistries.

9.4 Exposure to Mercury at Room Temperature

9.4.1 Environment Assisted Cracking

A literature search was conducted on environment assisted cracking of pure nickel materials. A number of environments, highly unlikely to exist in a PWR, were identified that might produce stress corrosion type flaws in the Electrosleeve™. A number of sources, captured in Reference 13.57, indicate that pure nickel is not resistant to liquid mercury. Reference 13.58 states that the nickel weight loss in the presence of 600°F heated mercury is 900 mg/inch² in 30 days of exposure. The expected depth of penetration of the stress corrosion cracks in the normal crystalline nickel is reported to be, in the same conditions as above, between 10 and 90 mil.

9.4.2 Experimental Procedure

A liquid mercury attack experiment of Electrosleeve™ was defined similar to an ASTM G-38 test [13.59]. Stressed areas of C-Rings were submerged in liquid mercury at room temperature.

[

J. b, c, e

9.4.3 Results

[^{b,c}] the C-Rings presented the following results:

- []
- No recordable indications were found using liquid penetrant examination, and ^{b,c,e}]
- Using an analytical scale [^{b,c,d}] no weight loss [^{b,c}] was observed. ^{b,c,d}]

[] ^{b,c,d}]

9.5 Corrosion Evaluation Summary

Qualification of the corrosion properties of the Electrosleeve™ was performed using a three phased program. The first phase involved a literature review and selection of tests, including ASTM standard tests, to determine the susceptibility of the Electrosleeve™ to known forms of Alloy 600 damage such as IGA and SCC. The second phase focused on corrosion testing in specific primary side environments that are known to be detrimental to Alloy 600 tubing. The third phase focused on secondary side environments including alkaline, neutral, and acidic in the presence of oxidizing and reducing species and, in many cases, at extreme conditions to accelerate the corrosion processes. A review of the data to show nickel is very resistant to corrosion and SCC has been performed by Argonne Labs, Reference 13.49.

A comparative review of the general corrosion characteristics of nickel and Alloy 600 demonstrates that Alloy 600 is typically more resistant to general attack in highly oxidizing acidic solutions but is more susceptible to IGA and SCC. This agrees with experience in the steam generator environment where IGA and SCC are the predominant modes of degradation for Alloy 600 tubes.

Testing performed on electrosleeves included caustic and ASTM standard tests to determine the susceptibility of the material to IGA and SCC. These tests demonstrated resistance of the Electrosleeve™ material to IGA or SCC. The sleeve was shown to protect the Alloy 600 tube from SCC on the primary side and to stop SCC from propagating into the Electrosleeve™ from the secondary side of the tube (see Table 9.5.1).

TABLE 9.5.1
SUMMARY OF MATERIAL SUSCEPTIBILITY (ACCELERATED) TESTS

TEST PURPOSE	TEST ENVIRONMENT	SPECIMEN DESCRIPTION	RESULTS
Susceptibility to IGA	Boiling 50% Sulfuric Acid-Ferric Sulfate at RT; Standard ASTM Method; [] b,c	┌ 7 b,c,d	No evidence of IGA.
Stress Corrosion Cracking (SCC) Test ASTM G 35	% Solution of Polythionic Acid at RT; Standard ASTM Method; [] b,c		No evidence of SCC of Electrosleeve™ material
Stress Corrosion Cracking (SCC) Test ASTM G 36	Boiling 45% MgCl ₂ at 311°F for 3 hrs; Standard ASTM Method; [] b,c		No evidence of SCC in the Electrosleeve™ material; No evidence of pitting or cracking on plated surface
Stress Corrosion Cracking (SCC) Test ASTM G 44	3.5 % Solution of NaCl at RT with alternate wetting & drying of specimens; [] b,c Standard ASTM Method; [] b,c		No evidence of SCC
Stress Corrosion Cracking (SCC) Test	10% Solution of NaOH at 662°F; [] b,c		The unplated Alloy 600 mockups cracked 50% through-wall after 120 hrs exposure; and 100% after 240 hrs. No evidence of stress corrosion cracking in the mockups with [] Electrosleeve™. b,c,d
Stress Corrosion Cracking (SCC) Test (Effect of Stress)	10% Solution of NaOH at 662°F; [] b,c		No evidence of SCC was found on any of the electroslieved specimens. [] b,c,d
Pitting & Crevice Corrosion Test ASTM G 48	6% Ferric Chloride Solution at RT Pitting Test - [] b,c Crevice Test - [] b,c	└ └	Some slight general corrosion on Electrosleeve™ material, but no evidence of pitting. [] b,c,d

NOTES:

(1) These mockups were pre-cracked through-wall with a room temperature sodium tetrathionate solution prior to being plated.

Both circumferential and axial SCC conditions have been repaired with nickel plating. The nickel plating has also been installed over Alloy 600 tube cracks that are 100% through-wall. Thus, the nickel plating has been exposed to primary side environments as well as secondary side environments (via the tube cracks) [13.56]. This is exactly the same manner that the Electrosleeve™ will be exposed to the two environments. The performance of the nickel plating in foreign plants has been excellent in 10 years of service.

Corrosion testing was conducted on both nickel plating and electrosleeves to evaluate the Electrosleeve™ material performance in primary and secondary environments. Primary side tests included pure water, primary water, and boric acid. A summary of these tests is contained in Table 9.5.2. Secondary side tests included heat transfer conditions, sludge, and confined geometry (crevices) with the associated concentrating mechanisms evaluated. A summary of these tests is contained in Table 9.5.3.

TABLE 9.5.2
SUMMARY OF PRIMARY WATER CORROSION TESTING

TEST PURPOSE	TEST ENVIRONMENT	RESULTS
Primary Water during Normal Operation	┌ └ b,c	No corrosion or degradation of Nickel plating
Primary Water during Shutdown (Aerated)		Negligible Corrosion of Nickel Plating [] b,c,d
Primary Water during Shutdown (Deaerated)		Negligible Corrosion of Nickel Plating [] b,c,c'
Concentrated Boric Acid (To simulate boric acid trapped within cracks)		No corrosion or degradation of Nickel plating
Saturated Boric Acid (Aerated without Oxygen replenishment)		[] some pitting observed. Nickel Hydroxide formation on the surface of specimens [] b,c,d
Saturated Boric Acid (Aerated with Oxygen replenishment)		Very deep through-wall pitting observed [] b,c,d
Primary Water SCC		Unplated control specimens heavily cracked after [] b,c Nickel plated specimens did not exhibit SCC, no corrosion or pitting observed
Pure Water SCC		Unplated control specimens heavily cracked Nickel plated specimens did not exhibit SCC, regardless of plating thickness
Caustic SCC in Roll Transitions Areas		Unplated tubes cracked [] [] b,c,d No cracking was observed with [] of Nickel plating
Caustic Residual Stress Test in Locked Tube Arrangement		No cracking was observed, especially in the transition regions, on the specimens
Temperature and Pressure Cycling in Pure Water	┌ └	No leakage observed No loss of adhesion observed Cracks well bridged by Nickel plating

TABLE 9.5.3
SUMMARY OF SECONDARY SIDE CORROSION TESTS

TEST PURPOSE	TEST ENVIRONMENT		RESULTS
Sludge and Faulted Chemistry Tests (Caustic Excursions)	┌	┐ b,c	No corrosion of Electrosleeve™ [] ┐ b,c,d
Sludge and Faulted Chemistry Tests (Acid Excursion)			[] ┐ b,c,d
Sludge and Faulted Chemistry Tests (Condenser In-leakage)			Negligible Corrosion of Electrosleeve™ [] ┐ b,c,d
SCC Propagation Tests (Precracked S/G Tubing)			Ultrasonic examination before and after testing showed no increase in crack depths
SCC Propagation Tests (Stressed C-rings)			[] ┐ b,c ┐: No cracking observed in Electrosleeve™; [] ┐ b,c,d
Electrosleeved Capsule Tests			[] ┐ b,c,d
Electrosleeved Capsule Tests			[] ┐ b,c,d
Electrosleeved Capsule Tests			[] ┐ b,c,d ┐: high caustic tests showed relatively high corrosion rates, but much lower than acidic/oxidizing tests
Electrosleeved Capsule Tests	┌	┐	[] ┐ b,c,d

The following conclusions were reached based on the results of these tests and on comparison to expected conditions:

- Nickel plating is effective in protecting Alloy 600 steam generator tubing from PWSCC. High purity electrodeposited nickel material is not susceptible to SCC or IGA in either the primary water environment or the secondary water environment.
- Electrosleeve™ general corrosion is negligible in primary water environments under expected operating and shutdown conditions.
- Electrosleeve™ corrosion is negligible in secondary environments. Additionally, the nature of tight cracks in Alloy 600 tubing limits exposure of the sleeve to the secondary side.
- Installation of electrosleeves does not introduce high residual stresses in the parent tube at the leading and trailing edges of the sleeve.

In conclusion, general corrosion, crevice corrosion, pitting, SCC, or IGA of the Electrosleeve™ material is not a concern in PWR environments. The in-service experience of electrodeposited nickel materials supports this conclusion.

10.0 SLEEVE INSTALLATION

10.1 Installation Procedure

The sleeve procedure specification (SPS) defines the generic requirements for field installation of the Electrosleeve™. The SPS was prepared following the guidelines of the ASME Code, Section XI, Code Case N-569 for steam generator tube sleeving and identifies the essential and non-essential variables for the process. The following is a summary of the installation procedure. Installation tooling, ALARA practices, and chemical procurement are also discussed.

10.1.1 Pre-Installation Tube Eddy Current Inspection

An ECT inspection of the tubes is performed to identify which tubes are to be repaired and to verify that no pluggable defects exist outside the area to be sleeved. This step is a standard part of a steam generator ECT inspection outage.

10.1.2 Surface Cleaning/Preparation (Woods)

Mechanical cleaning of the tube ID is performed in the sleeving region to remove loose oxides and reduce contamination levels. Cleaning removes a substantial amount of radioactive contaminants prior to the Woods surface activation process. Mechanical cleaning is accomplished by rotating and translating a hone or scraper on the tube ID in the sleeving region.

After removing the cleaning tip from the tube, the electroforming probe is inserted into the tube to the sleeving elevation. This step may involve installing multiple probes in different tubes, enabling several sleeves to be installed at the same time. The probe has integral seals to keep the solutions confined to the desired electroforming region, called the "plating cavity".

Final cleaning and preparation of the tube is accomplished by using the Woods electrolyte solution. Typically, this is a low pH nickel chloride and dilute hydrochloric acid solution. The surface is activated by circulating the Woods solution through the plating cavity. [

Je

The activation step is aggressive on edges such as ID crack surfaces, producing chamfered edges at the crack. The removal of a small amount of material permits the electroforming step to deposit material into the crack and produce a bridge across the ID of the crack.

10.1.3 Pre-Filming (Strike)

The pure nickel Strike is an electroplated pre-layer applied to the surface of the tube before introducing the Watts electroforming solution. The nickel chloride based Strike solution is circulated through the plating cavity and forward current is applied to deposit the Strike layer. This step prevents repassivation of the tube material between the Woods activation and the Watts electroforming steps and facilitates the adhesion of the Electrosleeve™ to the parent tube. A nitrogen purge and deionized water rinse is then performed to remove residual chlorides that may contaminate the Watts electroforming solution.

10.1.4 Electroforming (Watts)

The Electrosleeve™ is deposited on the tube during this step of the process. The Watts solution is circulated through the plating cavity while forward current is applied to deposit the nanostructured material. The anode is non-consumable; therefore, all of the nickel deposited is from the nickel sulfate solution circulated through the probe. [

]^{CL}

The probes and plating cavity are then purged with nitrogen and given a final rinse with deionized water. This completes the sleeve installation process and the electroforming probes are removed from the tubes.

10.1.5 Post-Installation NDE

A post-installation UT inspection is conducted to examine the bond between the sleeve and the parent tube and to verify sleeve thickness and length. Section 11.0 of this report presents additional information on NDE as it pertains to electro sleeving.

The surface finish of the sleeve is evaluated as part of the initial UT inspection. If the surface roughness exceeds one-tenth of the wave length, the surface finish of the sleeve can attenuate the sound propagation into the sleeve. For a 10 MHz transducer and a coupling velocity of 0.058 inch per micro second, one-tenth wavelength is 0.00058 inch or ~ 600 micro-inches. If the surface is unacceptable, a honing process has been qualified. The objective of the honing process is to improve the surface finish in order to reduce the attenuation in the UT signal to acceptable levels.

The surface finish improvement has been qualified using a flexible honing tool. Typically, the abrasive material is tungsten carbide. The abrasive (points) globules have an independent suspension that is self-centering, and self-aligning to the sleeve ID. The resilient flexible honing tool, with soft-cutting action, removes and flattens the peaks produced by the electrodeposition process; free of cut, torn, and folded metal. The honing process is controlled [

] ^{b,c,e}

[

] ^{b,c,e}

Thus the hone "deburs" the peaked finish very rapidly without significant metal removal.

Additionally, the material exposed by the process is metallurgically the same as the material considered in corrosion testing discussed in Section 9.3 (i.e. coupon samples were machined to expose the material to environments).

10.2 Process Verification

10.2.1 Process Qualification Requirements

ASME Section XI Division 1, Code Case N-569, provides accepted rules for process qualification. Essential and non-essential process variables are defined (FTI imposes an expanded list of essential variables) and consecutive qualification samples are produced. The samples are then subjected to non-destructive and destructive examinations to prove that the target material properties have been met. Non-destructive examinations consist of ECT prior to installation and UT examination after sleeves are installed. Destructive examinations include bend tests, hardness, and material composition analysis.

Process operating limits are defined in the qualification documents. Process controls and on-line monitoring during the electrodeposition process allow operators and quality control personnel to confirm the process variables. System operator qualification requirements are well defined by the Code Case. For example, operator inactivity for a six month period would require personnel re-qualification.

10.2.2 Field Installation

Typical system operation in a power plant will generate witness tube/sleeve samples prior to installation of sleeves in the steam generator. This system is capable of producing witness sleeves simultaneous with installed Electrosleeve™ specimens and thus provides significant assurance that material properties are being met. The witness tube can be sleeved with one of the electroforming probes used for sleeve installation in the steam generator, [

]e

The witness tube sleeve is examined for bonding, surface finish, and thickness. [

]e

Hardness, chemistry, or mechanical testing may be used to obtain information related to sleeve strength.

The following are typical variables monitored during the installation of the Electrosleeve™:

- Flow rate
- Pressure
- Temperature
- Solution pH
- Voltage
- Current
- Process Time

All essential process variables, as listed in the SPS, are monitored and recorded as specified.

10.3 Electrosleeving Chemical Procurement and Quality Assurance Process

The electrosleeving chemical procurement procedure specifies the steps to be taken for the procurement and inventory control of chemicals to be used in this process.

[

] ^{b,c,e}

[

] c,e

The documentation for the chemicals used is provided to the customer in the form of a data package to support transportation, receipt, and control at the plant site.

[

] c,e

[

] c,e

10.4 Electrosleeving Process Detrimental Materials Control

Detrimental materials are maintained by control and independent analysis of all process chemicals. [

] c,d,e

An allowable level of detrimental materials in procured chemicals was defined and integrated into the chemical procurement procedure. [] e

[

]e

[

]d,e

[

]e

10.5 Installation System/Tooling

The installation of the electroformed sleeve is accomplished remotely by tooling attachments mounted on a manipulator. Typical manipulators that may be used for sleeving include: ROGER™, COBRA™, and FLEXIVERA™ manipulators. The sleeve installation tooling minimizes the personnel radiation exposures in accordance with ALARA principles.

The sleeving system utilizes a series of skids and trailers. Each skid contains a different portion of the fluids and chemicals required to successfully perform the sleeving process. The system contains a supply manifold to deliver the solutions from the skids to the probes. The probes are connected to a return manifold that collects the solution as it returns from the probes and directs it back to the appropriate skid.

The sequential steps of the electroforming process are computer controlled. Figure 10.5.1 depicts a schematic of the system.

The electroforming probe consists of a tubular anode []^e. The integral probe seals hold the probe in position. []

] ^{c,e}

FIGURE 10.5.1
ELECTROSLEEVE™ INSTALLATION SYSTEM SCHEMATIC

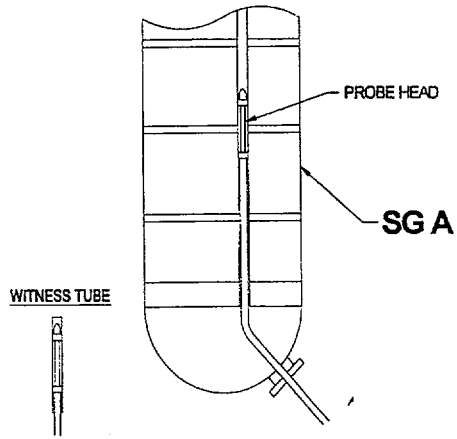


FIGURE 10.5.1 (Cont'd)
ELECTROSLEEVE™ INSTALLATION SYSTEM SCHEMATIC

┌

c,e
└

L

└

10.6 ALARA

The ALARA evaluation has been prepared using the process steps for electrosleeving in conjunction with radiation dose fields representative of Westinghouse Model D steam generators. The exposure estimate is based on sleeving []^c in a single steam generator channel head. This quantity is representative of a typical sleeving campaign and provides a useful standard for comparison. Table 10.6.1 provides detailed information regarding the assumed radiation fields as well as estimated exposures for the various sleeving activities and the total estimated process exposure.

Remote manipulators will be used for the electrosleeving process. Since the manipulator is typically installed at an earlier time to support inspection or repair, the estimate provided does not include exposure associated with manipulator installation or removal. [

] c,e

[

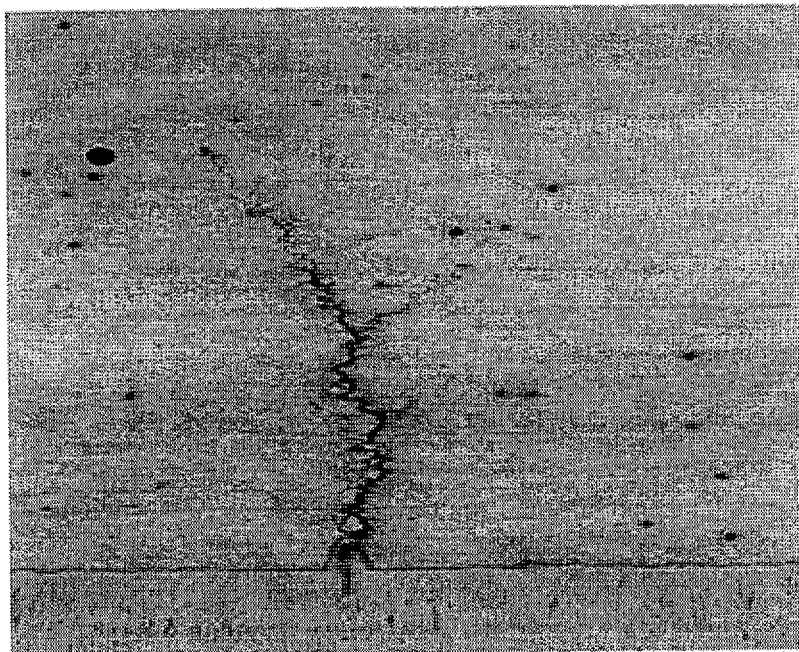
] c,e

10.7 Sleeving Experience

As part of the qualification process, a number of tube conditions were evaluated to demonstrate the process capabilities. Sleeves were successfully installed into tubes with the following conditions:

- Contaminated 5/8" tubes, cleaning process evaluation,
- Contaminated, sensitized, in-service tubes (Oconee Unit 1; 9 tubes),
- Shot peened tubes,
- Dented tubes (see Figure 10.7.1),
- Cracked tubes (see Figure 10.7.1),
- Top of tubesheet roll transitions with 100% through-wall PWSCC cracks (laboratory induced), and
- Tube support plate sections from a retired steam generator.

FIGURE 10.7.1
ELECTROSLEEVE™ INSTALLATION EXPERIENCE



Sleeving in a cracked tube

10.8 Waste Processing

The spent solutions and chemical contaminated rinses generated by electrosleeving will be processed using the best available technology (BAT). Any waste sludges that are generated by the use of BAT will be considered hazardous and radioactive as defined by 40CFR261.31 (F006).

FTI developed an Electrosleeve™ waste processing system that may be used which utilizes two parallel processes. One treats the rinse water generated during the Electrosleeve™ process application, and the other treats the spent process solutions (i.e., Woods, Strike, and Watts). The rinse water generated during the Electrosleeve™ process is treated using a combination of ultra-filtration (UF) and reverse osmosis (RO). The spent process solutions are treated using a concentrate/dryer (CD) unit. The two parallel processes provide for volume reduction, maximum water recovery and purification, and solidification of the solvent mixed waste stream.

11.0 NONDESTRUCTIVE EXAMINATION

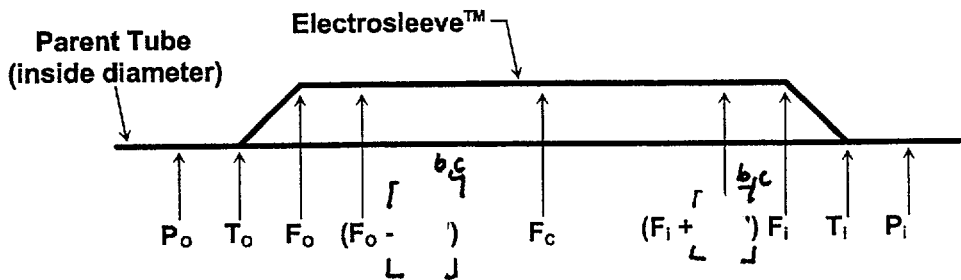
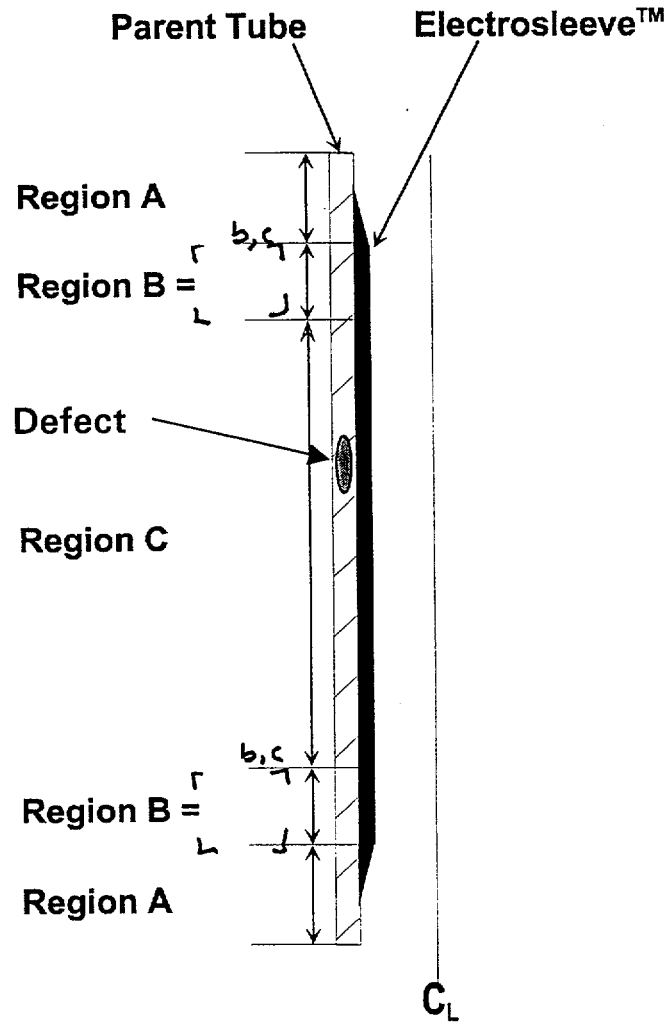
The nondestructive examination (NDE) technologies evaluated to perform the examinations of an Electrosleeve™ are presented in this section. NDE inspection is required to provide specific dimensional information of an installed sleeve as well as in-service monitoring. The NDE inspection technique must provide a means to determine the sleeve thickness, the position of the sleeve relative to the intended repair location, the presence of the sleeve-to-tube bond, quality of the sleeve installation, and depth/extent of flaws in the parent tube. Taking into account the above requirements, an evaluation was performed to select and qualify an inspection technique.

While eddy current testing (ECT) is an established NDE method for steam generator tube inspection, ultrasonic testing (UT) has been selected as the NDE inspection method for the Electrosleeve™. UT has advantages relative to eddy current. The fundamental method of using sound propagation and reflection provides the advantages of thickness measurement, bond verification, and superior flaw detection. In addition, UT has no sensitivity to permeability variations found in high purity nickel.

11.1 NDE Requirements

Three regions of a sleeved tube (Figure 11.1.1) were defined to clearly describe NDE requirements, capabilities, and qualification. In these regions, the primary pressure boundary transfers from the parent tube to the sleeve and back to the tube. The three regions and the inspection requirements for each region are discussed below.

FIGURE 11.1.1
ELECTROSLEEVE™ NDE REGIONS



11.1.1 Sleeve Regions

The tube is the pressure boundary in the taper region (Region A). Thickness measurements in Region A are required at the locations marked P_o and P_i , where the P represents parent tube and "o" and "i" represent the outlet and inlet of the sleeve installation probe flow, respectively. The zero thickness transitions (T_o or T_i) occur at the first presence of nickel plating.

The bond length, which transfers the pressure boundary from the parent tube to the sleeve, is Region B. This region extends from the start of a taper transition (F_o or F_i) for a full thickness length L . The full sleeve thickness transition occurs at the first measurable decrease in thickness from the average sleeve wall thickness. The combined parent tube/sleeve wall is the pressure boundary for this region.

The full thickness portion of the sleeve between the full thickness taper reinforcement regions is the mid-span or Region C. This section of the sleeve spans the parent tube flaw and is normally bonded over the entire region. However, the sleeve is the pressure boundary. Thickness measurements in the mid-span region are required at the locations marked F_i [], F_c , and F_o [] where F represents the full thickness, "c" represents the center, and "o" and "i" represent the outlet and inlet, respectively.

11.1.2 Basic Electrosleeve™ NDE Requirements

The NDE examination must be capable of characterizing the Electrosleeve™ repair with respect to the following criteria:

- Installation
 - Sleeve positioning relative to flaw or support structure - process verification
 - Sleeve-to-tube bonding – process verification
 - Sleeve Thickness – process verification

- Sleeve ID Pitting – process verification
- In-Service
 - Sleeve OD Pitting – associated with 100% through-wall flaw in parent tube
 - Parent Tube Cracking – flaw growth, depth, or extent
 - Parent Tube Volumetric Wall Reduction – flaw growth, depth, or extent

11.2 NDE Methodology Evaluation

A number of NDE companies, laboratories, and academic institutions have participated in a project to develop and evaluate new techniques for examination of the Electrosleeve™. This section presents a discussion for each technology considered.

11.2.1 Eddy Current

Some form of eddy current examination will be used to identify tube candidates for installation of an Electrosleeve™. However, eddy current testing has not been widely used in the examination of nickel plated tube repairs due to the lack of penetration in the highly permeable nickel. There are significant problems with the use of eddy current techniques for examination of the Electrosleeve™ repair. The main difficulties are the discrimination of sleeve geometry from degradation, the accurate depth sizing of crack-like flaws, and the detection of less significant degradation.

Saturation Probes

Non-rotating saturation probes were evaluated early in the testing and demonstrated difficulty in detection of flaws in the sleeve end transitions. The saturation field may have improved the detection of parent tube flaws within Region C; however, these flaws are of less concern within this region.

A magnetic-bias, rotating plus point probe was found to produce more noise and a lower signal-to-noise response than a nonmagnetic-bias probe. Thus, the magnetic-bias plus point probe was eliminated as a viable examination technology for the Electrosleeve™.

Pulsed Eddy Current

The use of pulsed eddy current was evaluated. Pulsed eddy current demonstrated a significant improvement in the technology, but the improved system still did not possess sufficient resolution to separate parent tube flaws from flaws that breached the Electrosleeve™.

Rotating Coil Methods

Several rotating coil probe designs, including pancake coils, MICA coils, plus point coils, and differential pancake coils, were evaluated. Each of these probe types has demonstrated detection of significant parent tube or sleeve flaws at some level of sensitivity. One of these rotating coil designs could possibly perform the extent sizing of certain degradation types. As part of the rotating coil test program, multiple frequencies and mixing capabilities were also evaluated. Despite the extensive testing, the rotating coil techniques have not demonstrated the ability to verify the structural integrity of the Electrosleeve™ separate from the parent tube.

Swept Frequency Methods

The use of an eddy current swept frequency algorithm has been proposed. However, the technique is not commonly available and has not been evaluated.

11.2.2 Magnetic Methods

One alternate approach for the validation of the Electrosleeve™ repair was to examine the nickel layer by itself. This would require an examination method that is insensitive to the Alloy 600 parent tube, which is nonmagnetic. Several magnetic examination methods were evaluated.

Remote Field Probes

Remote field eddy current methods have been used for the examination of magnetic materials. An excitation coil is used to induce a field into the magnetic material. The permeable tube material will conduct the induced field to a location remote from the excitation coil. A second receiver coil responds to the remotely induced field. Material variations between the two coils produce changes in the received signal.

Significant artifact signals were noted with a remote field technique. The technique has significant difficulty due to the presence of the carbon steel tubesheet or support plates.

Flux Leakage

Flux leakage techniques have also been used for the examination of magnetic material. A field is induced into a magnetic material and any changes in the permeability of the material will cause a local flux distortion.

Flux leakage examination was attempted on the Electrosleeve™ repair. While there is some promise for this technique in freespan regions, flux leakage is also affected by the presence of carbon steel in the tubesheet and support plates.

11.2.3 Electromagnetic Acoustic Transducers (EMAT)

A magnetic field combined with an eddy current coil can be used to induce an acoustic pulse in a material. The eddy currents react with the magnetic field to produce a shock wave. As with any UT system, this acoustic energy is used to inspect the subject material. The primary difference with the EMAT system is that no liquid couplant is required to transmit the acoustic energy into the material. This technique is not currently being evaluated because there are no commercially available transducers that will fit into steam generator tubing.

11.2.4 UT Examination

UT is conducted by transmitting sound into the tube wall and acquiring the returning echo from a reflective surface (i.e., tube OD surface, sleeve to parent tube interface (disbond), crack corner reflector, etc.). Ultrasonic examination is excellent for detecting flaws and measuring thickness in seamless and longitudinally welded pipe and tubing [13.70]. The time of flight (TOF), speed of sound in the material, and amplitude of the returning echo yield information about the reflecting surface and the distance of the reflector from the transducer. The examination modes used during the sleeve examinations are longitudinal wave normal beam (i.e., zero degree) and shear wave angle beam testing.

11.2.5 NDE Technology Summary

An NDE technique is required to discriminate sleeve geometry from degradation, to depth size crack-like flaws, and to detect less significant degradation. As the qualified NDE method, UT techniques will be presented in detail in the following sections. Installation and in-service inspection will be performed using UT methods and equipment as presented in Sections 11.3 through 11.7.

11.3 Ultrasonic Testing Background

UT is the NDE technique selected to examine the Electrosleeve™ repair. The probe is fabricated to define specific orientation angles for each transducer. The transducer orientations produce a normal beam as well as axial and circumferential shear waves.

11.3.1 Normal Beam Testing

Normal beam, or zero degree, testing directs sound energy at an incident angle normal to the tube ID wall. The ultrasonic sound wave travels through the couplant, impinges on the water/nickel interface, and a percentage of the energy propagates into the nickel. If the sleeve is bonded, the sound wave continues through the nickel/Alloy 600 interface and into the tube until it is reflected back to the transducer from the OD surface. If the sleeve is not bonded to the tube ID surface, the wave is reflected by the sleeve/tube interface. The TOF measurement is the time required for the sound to travel to a reflector and return to the transducer. The reflection may be from a discontinuity or from a surface of the material. If there are no material discontinuities (reflectors) within the combined sleeve/tube wall, the tube OD surface will reflect the sound energy. Material discontinuities such as disbond or pitting will produce a shorter TOF due to the reflection of the sound energy from a point closer than the tube OD.

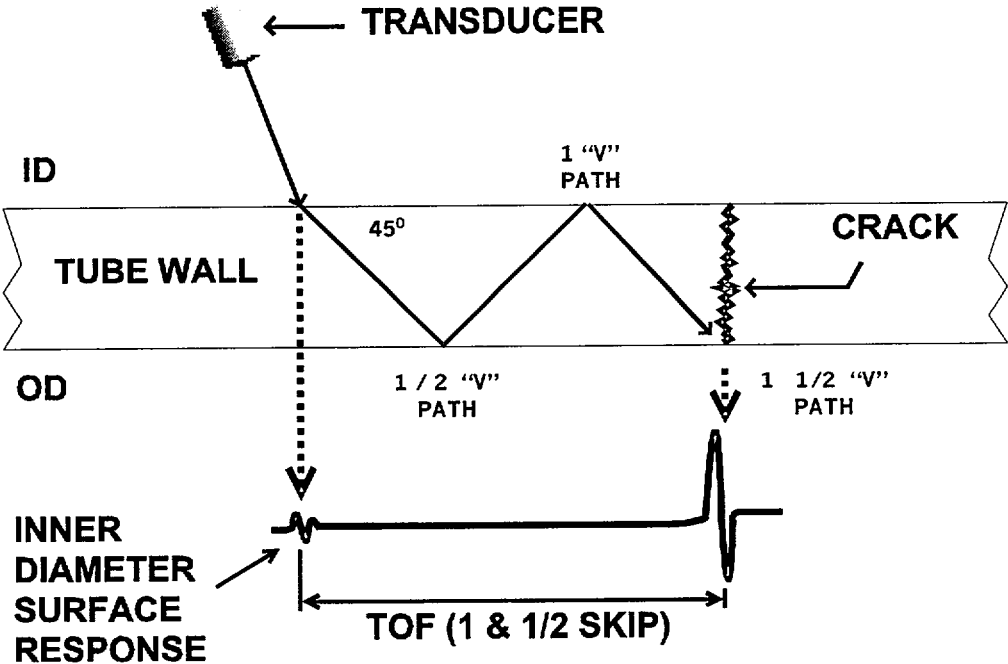
The TOF and the speed of sound in the material are used to determine the distance traveled. Thus, the material thickness may be calculated. The difference between the non-degraded material thickness TOF and a defect reflection TOF is used to define defect depth or size. In addition to bond determination, applications for zero degree examination include detection of volumetric wall thinning, pits, and IGA.

11.3.2 Angle Beam Testing

A transducer placed at an angle (Figure 11.3.1) produces a signal that enters the material along an incident angle greater than zero degree. The resultant sound propagation in the tube wall is termed a shear wave.

Angle beam, shear wave, testing differs from zero degree testing because the transmitted ultrasonic pulse is propagated at an angle (i.e., 45 degrees). As shown in Figure 11.3.1, the ultrasonic wave propagates within the wall in a path that resembles a "V". In this figure, the TOF is the time difference between the inner surface reflection and the corner reflector formed by the intersection of the crack and the tube OD.

FIGURE 11.3.1
UT WAVE "V" PATH



The detection of axial or circumferential crack-like indications is performed using shear wave testing. The shear wave detects cracks as well as volumetric type indications with sharp edges. Two separate transducers are required for the shear wave examination. One transducer is mounted to produce an axial propagation of ultrasonic energy (along the length of the tube) for the detection of circumferential flaws. A second transducer is mounted to propagate the ultrasonic energy in a circumferential direction for the detection of axially oriented flaws.

11.3.3 Summary of Inspection Transducers and Functions

Table 11.3.1 presents the required transducer for a given flaw type.

TABLE 11.3.1
TRANSDUCER AND FLAW TYPE COMPARISON

TRANSDUCER	FLAW TYPE
Axial Shear Wave, 45°	Circumferential Cracks
Circumferential Shear Wave, 45°	Axial Cracks
Normal Longitudinal Wave, 0°	Thickness, Volumetric Defects, Disbond

With each primary beam direction (axial or circumferential), it is possible to propagate the shear wave in two directions. For example, the axial shear wave could propagate either up or down a vertical tube segment. Similarly, the circumferential shear wave could propagate either clockwise or counterclockwise around the tube wall. Due to the typical morphology of thin wall tube crack-like flaws, there is little difference in response between the two beam directions (for the purpose of this document, thin wall is defined as wall thickness less than 0.125 inch). Flaws generally propagate normal to the originating tube surface and into the wall thickness. From the experimental data, it was concluded that the examination with two opposing beam directions for either the axial or circumferential direction is redundant and therefore unnecessary.

On this basis, single axial and single circumferential shear wave beams provide sufficient examination of the Electrosleeve™ repair.

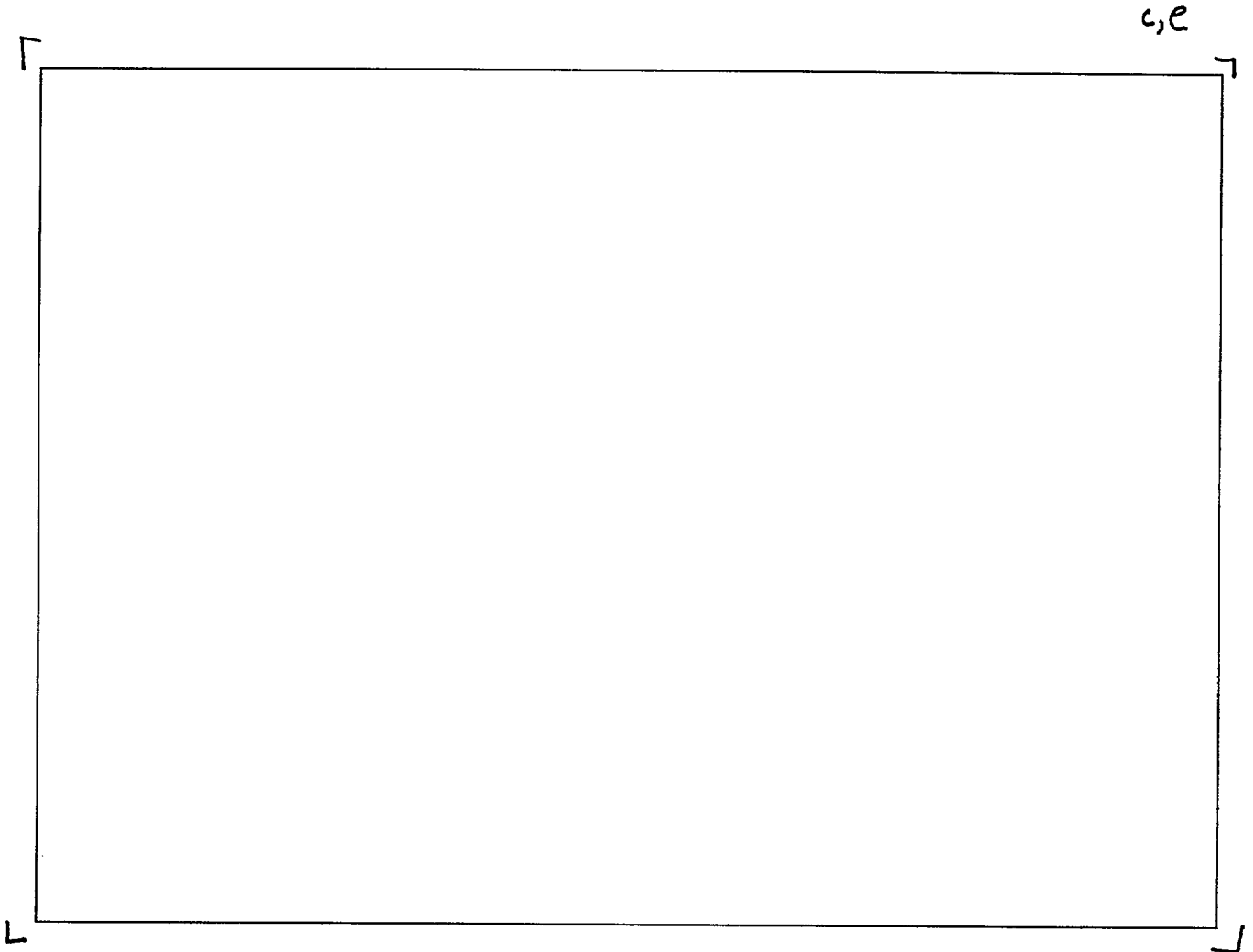
A 45 degree shear wave angle in the material was shown to be optimum for the detection of crack-like flaws in the Electrosleeve™ repair region. Angles less than 45 degrees reduce the reflected energy from crack-like flaws which propagate normal to the tube wall. This principle is illustrated by the normal beam (or zero degree) testing which is blind to tight, crack-like flaws. Angles greater than 45 degrees provide a longer transmission and attenuation path, a smaller reflected signal amplitude, and a reduced ability to separate closely spaced flaws.

Changes in tubing ID geometry affect the propagation of the sound energy. The tapered region causes some beam redirection and minor reduction in reflected signal amplitude. Testing with EDM notches and pulled tube samples that have been sleeved has shown that the UT system is capable of defect detection within the tapered region. The effect of beam redirection on the indicated defect axial location is minimal.

11.4 Ultrasonic System Description

The UT-360 system used to perform ultrasonic testing consists of both hardware and a computer system. The system is used to ultrasonically examine both the steam generator tube and the Electrosleeve™. The UT data acquisition equipment includes a UT probe head, probe motor unit, probe driver, water system, NDE Integrated Control (NIC) box, and the Hewlett-Packard (HP) computer station. The basic system diagram for a typical data acquisition station is shown in Figure 11.4.1.

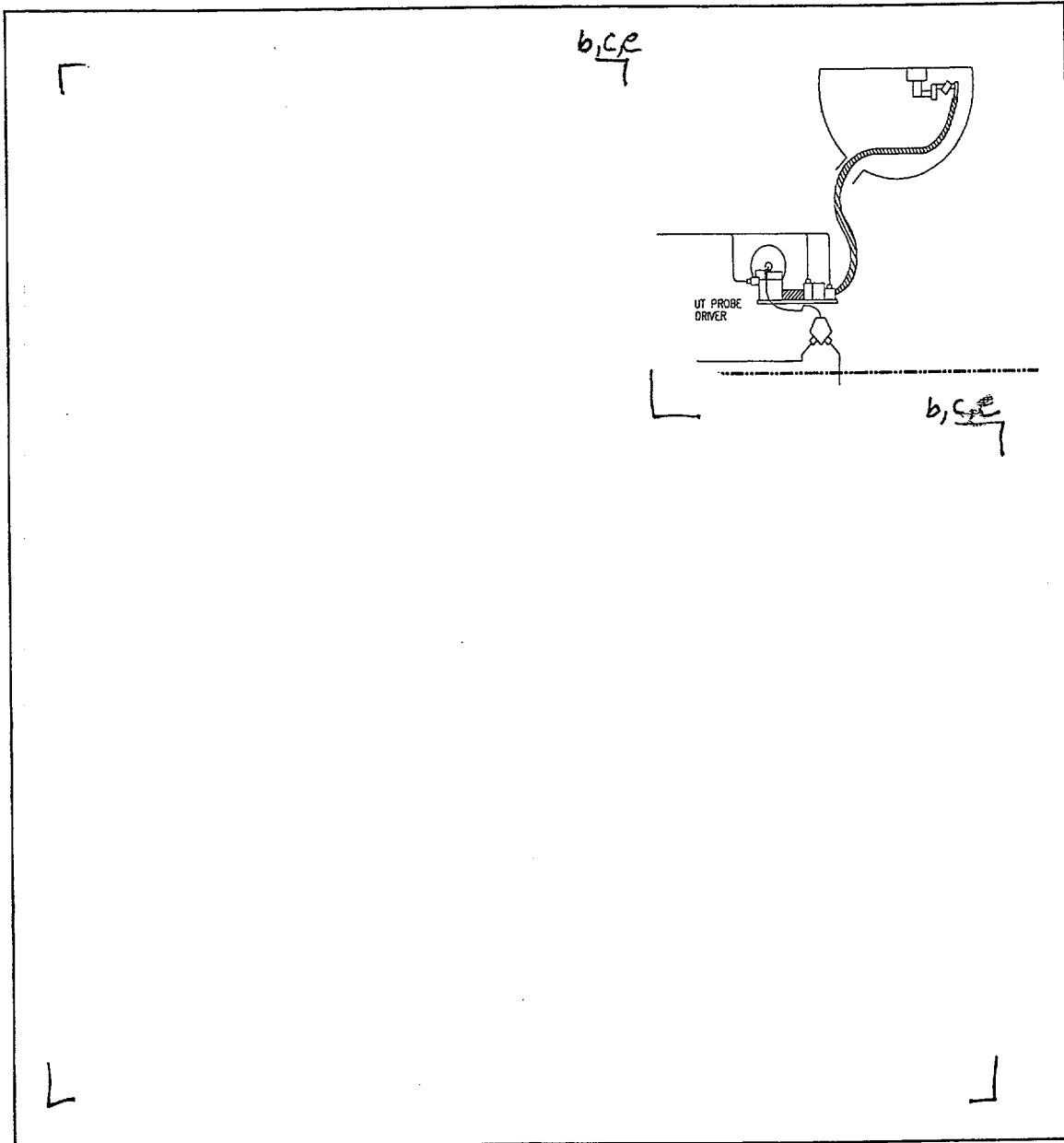
FIGURE 11.4.1
UT-360 SYSTEM DIAGRAM – DATA STATION



A typical UT-360 containment setup is shown in Figure 11.4.2.

The NIC box controller performs all acquisition functions, with the exception of the UT signal processing.

FIGURE 11.4.2
UT-360 SYSTEM DIAGRAM – CONTAINMENT



11.4.1 Controller and Data Acquisition

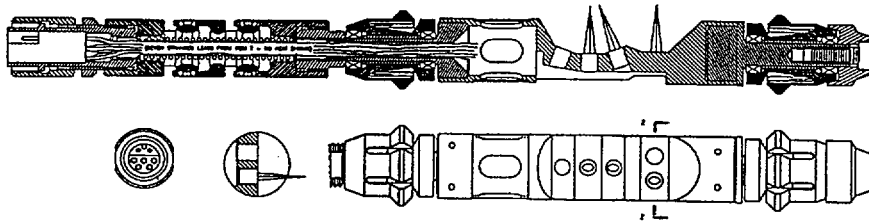
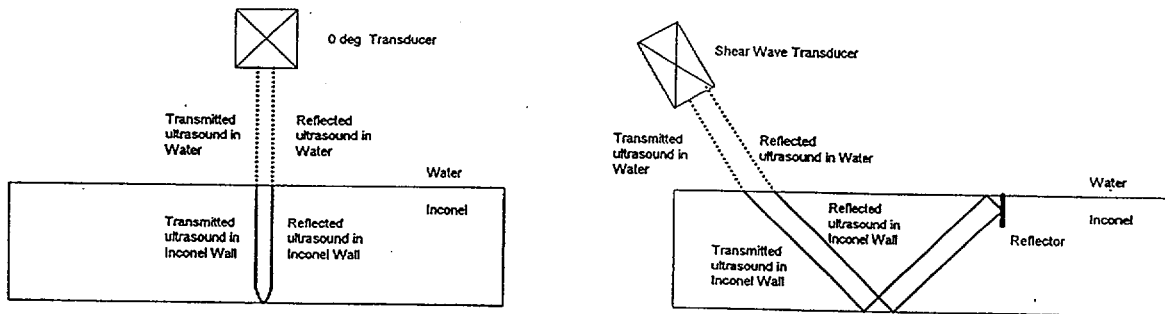
Communication cables connect the containment equipment to the control station. Fiber optic lines are used to transmit the UT waveforms, transmit the control signal used by the UT signal multiplex (MUX) system, and communicate with the NIC box. The computer processes, displays, and archives the data.

11.4.2 Probe Head and Motor Unit

The probe head has three ultrasonic transducers as shown in Figure 11.4.3. The motor unit contains a water seal, eddy current coils, the rotational encoder, and the motor to rotate the probe head. A probe driver inserts the UT probe into the tube. An axial position encoder is used to monitor the elevation (or motion) of the motor unit within the tube. The probe rotation, combined with the controlled pull of the motor unit, results in a helical scan path for the transducers. The probe driver is used to position the probe to the target elevation prior to scanning. ECT coils are used to locate support structures (TS and TSP). The axial position encoder is set to an elevation relative to the support structure.

FIGURE 11.4.3
UT-360 SYSTEM DIAGRAM – PROBE HEAD

- Rotating 3 Transducer Probe Head
 - 0 Degree (thickness / profilometry)
 - 45 Degree axial beam (circ cracks)
 - 45 Degree circ. beam (axial cracks)



The outside diameters of the UT probe and the plating anode prevent their use in severely dented tubes. For the tube sizes and plating thickness addressed in this document, the most restrictive condition is a single sided [^{b,c,e}] dent deformation in a [^{b,c}] tube with an average 0.031 inch Electrosleeve™. For this situation, the plating anode would not have sufficient free path for removal after the plating operation. The ultrasonic system has been qualified for profilometry and can be used to verify acceptable free path prior to plating. The dent deformation does not effect the ability of the ultrasonic system to detect cracking within the region surrounding the dent.

The probe is centered in the tube/sleeve by devices that operate over the entire range of inside diameters. The UT transducers require couplant to efficiently transmit the sound energy to and from the tube wall. The couplant is stored in the water system and is introduced through the motor unit by a small positive displacement pump. The couplant is retained in the tube by a water seal.

The motor unit connects to the signal multiplex (MUX) box. Signals to and from the three probe transducers are handled via the motor unit. The MUX box communicates signal information to the control system.

11.5 UT Acquisition Parameters

The following parameters and specifications summarize the UT system used to inspect an Electrosleeve™:

Transducers:	The transducers are spherical-focused, immersion transducers.
Transducer Frequency:	Operation frequency is approximately 10 MHz
Axial Pitch:	Approximately 0.015 inch (Range: 0.010 inch to 0.020 inch).
Circumferential Pitch:	Data samples approximately every 2 degrees.
Digitizer Frequency:	Shear Wave channels 100 MHz, (0.0012 inch per digitizer count resolution), Longitudinal (zero degree) channel 200 MHz, (0.0012 inch per digitizer count resolution), Target motion time of flight (TOF) is measured in digitizer counts. Target motion TOF in digitizer

counts is converted to microseconds by dividing the TOF (counts) by the digitization frequency.

The microseconds are converted to distance (depth) in the material by multiplying by the speed of sound for the specific propagation mode (shear or longitudinal).

Coverage: 100%

For example, with a 0.020 inch beam spot size and an axial pitch of 0.015 inch, the coverage percentage in the axial direction is 133%.

A circumferential coverage of approximately every 2 degrees is equivalent to a sample every 0.015 inch for 7/8" OD tubing. This provides a circumferential coverage of approximately 133%. Smaller tube diameters have larger percentage coverage for the same circumferential pitch of two degrees.

11.6 UT Data Presentation

The UT data is processed and displayed in several different modes for interpretation. These data displays assist the analyst in selecting waveform data to be evaluated in detail. Flaw detection, characterization, and sizing are performed using C-scans, D-scans, A-scans, and profilometry displays. The following discussion will define each presentation mode used for the analysis of the UT data.

11.6.1 C-Scan Maps

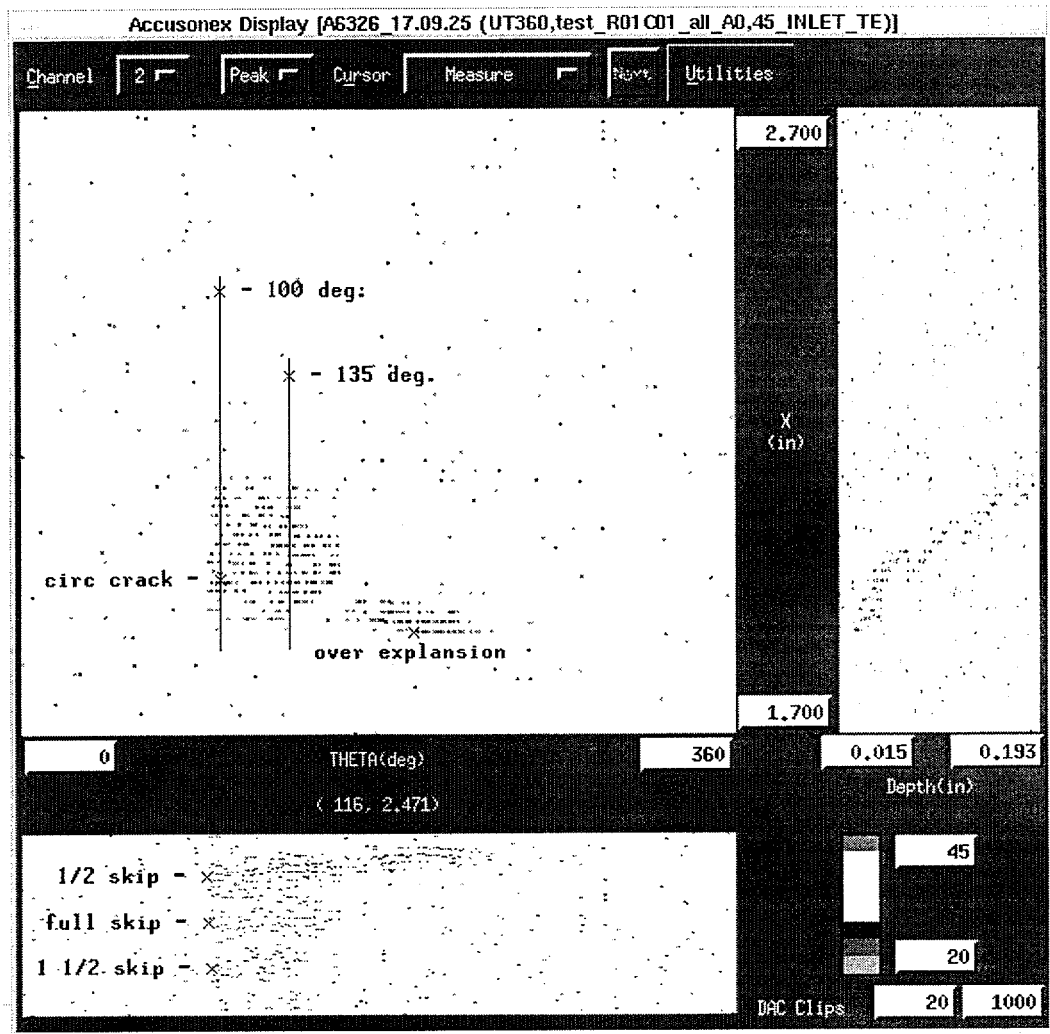
C-scan maps provide information pertaining to the strength (amplitude) and TOF of the returning signal. All acquired waveform peak values are displayed in a C-scan map. The C-scan maps provide three, two-dimensional views of the scanned region. The first, and largest, view is a plan view image with axial and circumferential scan dimensions. This view represents the surface of the tube cut axially and rolled flat. Each data point or pixel in this map represents returning signal amplitude. Each data point in the display is assigned a color based on the signal response amplitude. The color range is displayed in the legend of the C-scan map. Figure 11.6.1 shows a typical C-scan map, presented in gray-scale for ease of document reproduction.

In addition to the first view described in the previous paragraph, the C-scan map contains two additional views. The view to the right of the first view presents the returning signal strength information on a plot of axial scan length versus material depth. The axial scan length axis corresponds to the same axial scan length axis on the first view. The material depth axis corresponds to the TOF of the returning signal. The returning signal strength is plotted using the same color range as is used in the first view.

The third view in the C-scan map is below the first view. This view presents the returning signal strength information on a plot of circumferential scan dimension versus material depth. The circumferential scan axis corresponds to the same circumferential scan axis on the first view. The material depth axis corresponds to the TOF of the returning signal. The returning signal strength is plotted using the same color range as is used in the first view.

The two views described above are useful when the strength of the signal at a particular depth is important. The C-scan display allows the analyst to identify areas of amplitude fluctuations that may indicate the presence of ID pits, OD pits, nodules, and/or parent tube cracking.

FIGURE 11.6.1
TYPICAL C-SCAN MAP

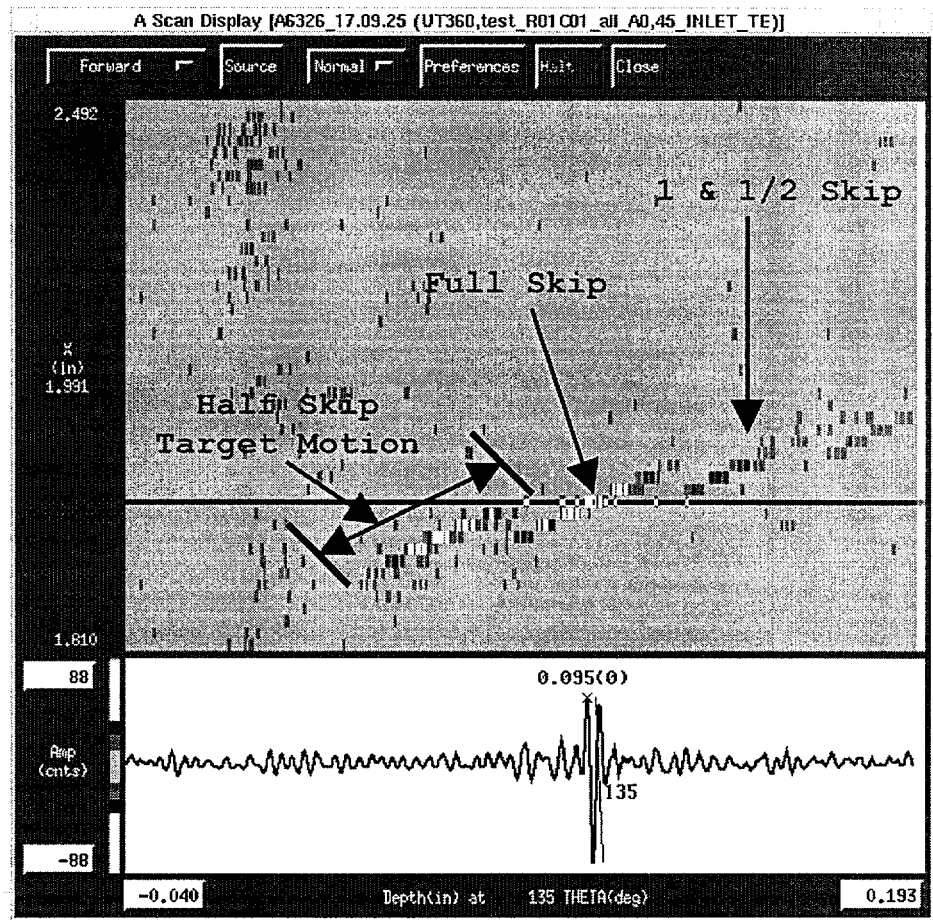


11.6.2 A-Scan Presentation

The A-scan data format provides a means to analyze the collected radio frequency (RF) waveforms. The A-scan data represents the entire returned RF waveform as acquired by a transducer. The full waveform allows the analyst to investigate low amplitude signal responses that might otherwise go undetected in the peak data presentation. The A-scan display plots the returning signal

amplitude as a function of time. The colors presented in the main display of the A-scan presentation indicate signal response amplitude. The A-scan presentation is the primary tool used to analyze signals for disbond, detect tube OD deposits, detect cracks, and evaluate volumetric indications. Using the A-scan display, the analyst determines thickness and measures detected flaw dimensions such as length, width and depth. Figure 11.6.2 is a typical A-scan presentation presented in gray-scale.

FIGURE 11.6.2
TYPICAL A-SCAN PRESENTATION



11.6.3 Profilometry Displays

The profilometry display is interpreted in the same manner as the C-scan display except that the pixel color represents the water path TOF. Using this display, the ID profile of the Electrosleeve™ surface can be presented. The analyst can use profilometry to determine the sleeve length and the internal diameter. Profilometry can display inner diameter contours of the sleeve and parent tube including denting and sleeve taper profiles. The format of the profilometry display is similar to the C-Scan shown in Figure 11.6.1.

11.7 UT Analysis Techniques

11.7.1 UT Probe Axial Location

Data from the eddy current (ECT) coils and an axial encoder are combined to establish the probe axial location prior to inspection of the Electrosleeve™. After the inspection is completed, the UT motor unit is moved until ECT detects the nearest TSP, and the axial position is confirmed.

11.7.2 UT Analysis Techniques for Normal (Zero Degree) Beam Testing

The normal (zero degree) beam TOF measurement is used to determine pit depth, disbond, and thickness. The transit time is measured from the time the ultrasonic wave is emitted to the time it returns to the transducer. By knowing the speed of sound through a given material (e.g., water, Alloy 600, or nickel), the depth can be determined.

The most common condition which can affect a UT-360 examination is the presence of tightly adhering deposits on the tube OD. These deposits occur at the sludge pile location, in

packed TSP crevices, or in freespan regions. These tightly adhering materials can attenuate ultrasonic signals. However, detection of volumetric flaws such as pits is not affected. As indicated before, volumetric flaw detection is accomplished by TOF measurements. Volumetric indications, by definition, reduce the amount of wall material whereas deposits increase the amount of apparent wall material. By observing the TOF values as compared to the known wall thickness, classification of deposits can be accomplished.

The base thickness of the tube wall beneath the Electrosleeve™ is established using the average of four measurements separated by 90 degrees above the Electrosleeve™ and four corresponding measurements below the Electrosleeve™. The resulting four base thickness values are used to calculate the sleeve minimum and average thickness. These measurements are taken in locations free of deposition.

11.7.3 UT Analysis Techniques for Shear Wave Testing

The shear wave examination is used to detect and size defects such as SCC. The primary signal characteristics used to size SCC are amplitude and TOF. As the probe shear wave transducer moves closer to a detected indication, the signal reflections will occur earlier in time and will change in amplitude. The technique initially locates the maximum amplitude of the signal with respect to the tube wall thickness in order to determine the origination surface. In addition, the presence of multiple reflectors from the same indication is noted. The flaw response signal characteristics will determine the appropriate method of sizing analysis.

The analysis of shear wave data uses three basic methods to determine the depth of a crack. The methods are tip sizing, shear wave Mode Converted Signal (MCS), and Full Skip Normalization (FSN).

Tip Sizing Method

Obtaining a reflection from the crack tip is considered [13.84] the most accurate method for crack depth sizing. Detection of a crack tip signal is indicated by a return signal that has a waveform reflection from the crack tip in addition to a waveform reflection from the corner reflector of the crack. The crack tip signal is difficult to observe for two reasons. The first reason is that the reflection amplitude from the tip is considerably less (6dB or 50%) than the amplitude of the corner reflection. This reduction in amplitude is proportional to the crack width (gap) at the tip. The second reason is that a tip reflection signal cannot be distinguished from the corner reflector signal until the crack depth of penetration exceeds one wavelength.

The waveform for the crack tip and the corner trap will overlap for small depth cracks. For a 10 MHz transducer, the depth of penetration equivalent to one wavelength is 0.012 inch. Therefore, to detect the crack tip, the penetration depth must be greater than 0.012 inch and there must be a sufficient gap between the crack faces. Typically, stress corrosion cracks in steam generator tubes are extremely tight (width less than 0.0005 inch); thus, even deep cracks may not be accurately sized using a tip signal.

As the depth of an outer diameter crack approaches the inner diameter surface, the tip signal may become masked by a signal known as a "near surface creeping wave". This signal is a longitudinal wave that propagates along the near surface (surface of sound incidence) at an angle of refraction between 75 and 90 degrees. The near surface creeping wave will produce a significant reflection from a crack tip that is within 0.012 inch of the inner diameter surface. Conventional tip sizing techniques treat this creeping wave reflection as a tip reflection with depth determination errors of less than 0.006 inch. For a tube examination prior to the application of an Electrosleeve™, the detection of the tip reflection would be expected for a crack with a

depth of penetration between 30% and 70% through wall. The near surface creeping wave reflection would be treated as a tip reflection for a crack with a depth of penetration between 70% and 100% through wall. After the application of the Electrosleeve, the tip reflection would be expected between 30% and 100% of the parent tube thickness.

Geometric calculations using the difference in the TOF between the tip reflection and the corner reflection are used to calculate the depth of the crack.

Mode Converted Signal Method

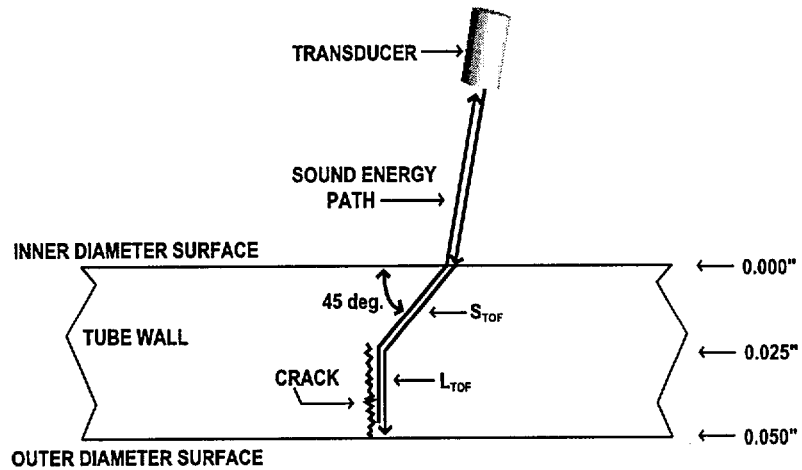
The primary signal characteristics used to size SCC are signal amplitude and TOF. As the probe shear wave transducer moves closer to a detected indication, the flaw response signal reflections will occur earlier in time and will change in amplitude. The detected extent of the target motion can be used to measure indication depth. Target motion is the apparent change in depth of an indication resulting from transducer motion.

The conventional TOF sizing technique requires certain assumptions to be made about the response signal target motion and TOF. Flaw examinations with subsequent destructive evaluations have indicated that these assumptions are partially incorrect for steam generator tube analysis.

With the assumption that crack responses are 45 degree shear wave returns, the transducer displacement from the location of the corner reflector to the crack tip reflection should correspond to the depth determined by the shear wave TOF. A significant discrepancy between the transducer displacement and the depth has been observed. As crack depth of penetration increases, the displacement versus depth discrepancy increases. One possible explanation for the displacement versus depth discrepancy is the existence of a mode converted signal [13.85].

A mode converted signal is defined as the conversion of the shear wave to a longitudinal wave at the point of incidence of the sound energy on the crack face [13.72]. Figure 11.7.1, with associated definitions and calculations, illustrates a mode converted signal for a tube wall thickness of 0.050 inch with a circumferential crack having a depth of penetration of 0.025 inch.

FIGURE 11.7.1
MODE CONVERSION METHOD EXAMPLE



In Figure 11.7.1, the symbols are defined as follows:

S_{TOF} = time of flight associated with the path distance of a shear wave traveling at a 45° angle in the tube wall to a depth of 0.025 inch at a shear wave velocity of 0.1188 in/ μ s.

L_{TOF} = time of flight associated with a longitudinal wave traveling at a 0° normal angle along the crack face to the outer diameter surface for a distance of 0.025 inch at a longitudinal velocity of 0.233 in/ μ s.

Solving for S_{TOF} and converting to microseconds,

$$S_{TOF} = [(0.025 \text{ in}) * (1 / \sin 45^\circ)] * (\mu\text{s} / 0.1188 \text{ in}) = 0.298 \mu\text{s}$$

The expected TOF for a pure shear wave reflection from the crack tip is 0.298 μ s.

Solving for L_{TOF} and converting to microseconds,

$$L_{TOF} = (0.025 \text{ in}) * (\mu\text{s} / 0.233 \text{ in}) = 0.107 \mu\text{s}$$

With mode conversion, L_{TOF} ($0.107 \mu s$) represents the resultant error introduced when a reflection TOF is assumed to consist only of a shear wave reflection.

Including the longitudinal wave component, the actual time of flight increases by the amount of L_{TOF} ,

$$TOTAL_{TOF} = 2*(S_{TOF} + L_{TOF}) = 2*(0.298\mu s + 0.107\mu s) = 0.810 \mu s$$

When determining $TOTAL_{TOF}$, two traversals of the sound energy path occur; thus, the sum of S_{TOF} and L_{TOF} is multiplied by two.

Solving for the Depth of Reflection (DOR) from the inner diameter surface,

$$DOR = 0.5*[(TOTAL_{TOF} \mu s)*(0.1188 \text{ in./} \mu s)]*(\sin 45^\circ)$$

When determining DOR, only a single traversal of the sound energy path is required; thus, the product is multiplied by 0.5.

Solving for the DOR for a fixed geometry condition,

$$DOR = 0.5*[(0.810 \mu s)*(0.1188 \text{ in./} \mu s)]*(\sin 45^\circ) = 0.034 \text{ in.}$$

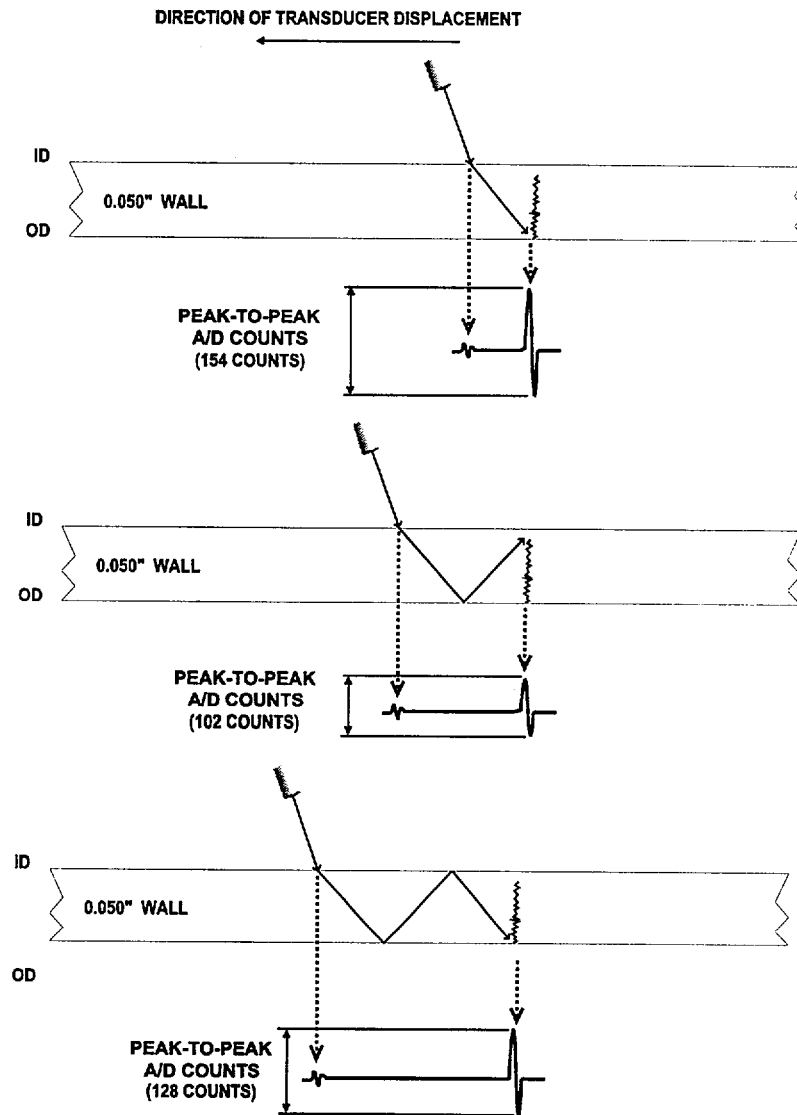
If a pure shear wave time of flight ($0.810 \mu s$) is assumed, the DOR would have been reported as 0.034 inch. This produces an apparent crack depth from the outer diameter of 0.016 inch ($0.050 - 0.034$). To correct the crack depth, the apparent crack depth is multiplied by 1.6. This results in a crack depth of 0.026 inch. This 1.6 correction multiplier assumes that the sound travels along the crack face and consequently is zero degree incident at the outer diameter surface, (Figure 11.7.1).

Full Skip Normalization

The Full Skip Normalization (FSN) sizing method compares the full skip return amplitude to the average of the outer diameter skip return amplitudes to yield improved depth of penetration determinations for deep ODSCC. This method provides a refinement of the depth determination when multiple skip information is available. As a crack propagates toward the ID, a full skip signal will develop. The FSN method is based on the observation that as crack depth of penetration increases, the full skip signal response amplitude increases and the characterization of the depth improves. The ratio of the full skip amplitude to the average of the outer diameter skip amplitudes produces a normalized result, with the benefit of eliminating the effect of the electronic system gain. The ratio was developed to use the full skip information to estimate the depth of a deep defect that propagates from the outer diameter surface.

This ratio can be used to provide an improved estimate of the depth of penetration of a crack propagating from the outer diameter of the tube. Figure 11.7.2 shows how this full skip amplitude is normalized to provide an estimate of crack depth.

FIGURE 11.7.2
FULL SKIP NORMALIZATION METHOD



Normalized Result – the ratio of the full skip amplitude to the average of the two outer diameter skips, (half skip and the 1 1/2 skip).

$$\text{Normalized Result} = 102 / [(0.5 * (154 + 128))] = 0.723$$

As crack depth increases, the FSN ratio increases. The FSN sizing method is independent of system gain, probe acquisition pitch, and signal saturation. A regression equation to correlate the FSN value to a crack depth has been developed for FSN values less than 1.0. In accordance with the crack depth sizing procedure, a FSN value greater than 1.0 is considered through wall. From the depth sizing qualification, this practice may result in as much as a 0.006 inch over call. For FSN values less than 1.0, the crack depth is computed using the regression and averaged with the tip and MCS depth values to determine the reported crack depth.

11.8 Qualification Program for Longitudinal Wave UT

As presented earlier, longitudinal wave UT is used for detection and sizing of volumetric flaws, disbonds, profilometry, and combined wall thickness. ASME Code Case N-504-1 [13.7] was used as a reference in developing the qualification of UT as a method of Electrosleeve™ inspection. Samples with manufactured flaws were used to study the capabilities of UT. The electro-deposition was performed to the nominal thickness values with tapers that were approximately 1/2 inch in length. The various longitudinal wave UT procedures were qualified using EPRI Appendix J peer reviews. Since the volumetric flaw and disbond qualifications require the technique to accurately measure combined wall thickness, a separate Appendix J peer review was not conducted for combined wall thickness. Combined wall thickness measurements from the destructive evaluation of the ODSCC sample set for crack depth sizing were used to develop an RSME for the combined wall thickness qualification.

11.8.1 Parent Tube OD Pits (Appendix J, ETSS 98-400 [13.76])

Definition

An OD pit is a localized wall loss on the OD of the parent tube. This defect mechanism may occur in the parent tube material behind a sleeve.

Inspection Requirement

Parent tube OD pitting must be detected and sized within Region C where the sleeve is the pressure boundary (Figure 11.1.1). The ultrasonic technique must demonstrate a high probability of detection (POD) of 40% through-wall parent tube OD pitting in Regions A and B (Figure 11.1.1) where the parent tube is all or part of the pressure boundary.

Sample Set Description

The sample set consisted of seven tubes each containing between two and six outer diameter pits. The 3/4" version of the three-channel probe was used to acquire the data. The reported actual depths were determined using a pin micrometer to a measurement uncertainty of ± 0.002 inch.

The remaining wall resolution (RWR) of the UT system for a 10 MHz transducer is 0.012 inch of remaining wall thickness. As the OD pit depth increases, the returning pit echo signal approaches the interface signal (inner diameter surface reflection). For deep pits, the pit reflection signal merges with the interface signal preventing an accurate measurement of the depth. Therefore, UT can not accurately measure thickness less than the RWR. Although deep pits with 0.012 inch or less of remaining wall cannot be accurately depth sized, detection is not affected.

When the signals merge, the UT analyst makes a call, which indicates that the pit is deep but that an accurate measurement of the pit depth is beyond the capability of the system. For a nominal 0.043 inch parent tube wall thickness, this would occur at a pit depth of $(0.043 - 0.012) = 0.031$ inch or 72% through-wall. Therefore, this limitation does not affect the ability to detect or size a 40% through-wall pit in the parent tube OD.

Data Set

The data set is presented in Table 11.8.1.

TABLE 11.8.1
PARENT TUBE OD PIT SAMPLE SET

Tube	Pit	Axial Location (inch)	Actual Measured Pit Depth (inch)
P6	A	5.500	0.012
	B	10.750	0.015
	C	11.125	0.010
	D	11.250	0.011
	E	12.500	0.009
	F	14.250	0.008
P35	A	2.250	0.017
	B	5.750	0.016
	C	8.500	0.016
	D	11.125	0.021
	E	13.630	0.025
	F	15.750	0.009
P38	A	2.000	0.018
	B	7.250	0.015
	C	14.630	0.008
P39	B	4.250	0.019
	C	7.000	0.020
	E	12.630	0.023
	G	15.250	0.012
P44	A	3.000	0.018
	B	14.750	0.013
P48	A	1.750	0.016
	B	4.250	0.010
	C	8.000	0.020
	D	11.250	0.020
	E	14.500	0.013
P51	A	3.750	0.016
	B	5.750	0.020
	C	8.690	0.023
	D	12.000	0.031
	E	14.440	0.018

Results

Table 11.8.2 summarizes the parent tube OD pit sizing analysis results for the thirty-one (31) indications presented in Table 11.8.1. The maximum under-calls from the analysis are reported under "Max Error".

TABLE 11.8.2
PARENT TUBE OD PIT SIZING RESULTS

PARENT TUBE OD PIT DEPTH RESULTS [3-CHANNEL CENTERED PROBE]					
TUBE SIZE: (3/4" x 0.043" wall)					
AXIAL PITCH (inch)	FTI UT ANALYST	AVERAGE ERROR (inch)	STANDARD DEVIATION (inch)	RMSE (inch)	MAX ERROR (inch)
0.010	1	0.000	0.003	0.003	-0.005
0.010	2	0.001	0.003	0.003	-0.005
0.015	1	0.000	0.003	0.003	-0.007
0.015	2	0.000	0.003	0.003	-0.006
0.020	1	-0.001	0.002	0.002	-0.007
0.020	2	0.000	0.003	0.003	-0.006

All OD pits were detected, which demonstrated a high POD for this defect mechanism.

11.8.2 Sleeve OD Pits (Appendix J, ETSS 98-402 [13.78])

Definition

A sleeve OD pit is a localized wall loss on the OD of the Electrosleeve™.

Inspection Requirement

Sleeve OD pits with a depth greater than 30% of the sleeve wall thickness exceed the conservatively selected plugging limit. In the

Electrosleeve™ region where the sleeve is the pressure boundary, sleeve OD pitting must be detected and depth sized.

Sample Set Description

The OD pit sizing evaluation was performed with tubes containing chemically induced pitting in the OD of the sleeve material. A method was devised to chemically generate pits on the OD surface of the Electrosleeve™. Two EDM notches, 0.010 inch wide, were made at each target location to form a cross. The depth, of each cross, terminated at the interface of the Electrosleeve™ and the Alloy 600. The pits were produced by injecting a chemical solution, consisting of various acids that attack only the nickel, into the center of each EDM cross. The process involved a series of chemical injections, holds, rinses, and differential focus optical (DFO) depth measurements to experimentally process each pit to a desired depth into the nickel. The DFO depth measurement technique has a reported error of ± 0.001 inch.

The sleeve OD pit sample set consists of seven 3/4" OD tubes and six 7/8" OD tubes each with three pit flaws. The following pit depths, as a percent through-wall based on DFO depth measurement technique, were achieved:

- Nine from 0% to 20% through-wall of the Electrosleeve™ as-built thickness,
- Twenty-two (22) from 21% to 60% through-wall of the Electrosleeve™ as-built thickness, and
- Eight from 61% to 90% through-wall of the Electrosleeve™ as-built thickness.

Two tubes, with a total of six pits, were destructively examined to provide information about the pitting evolution, diameter versus depth, and to validate the DFO technique. As a result they are excluded from the final data table.

The remaining wall resolution (RWR) of the UT system for a 10 MHz transducer is 0.012 inch of remaining wall thickness. As the OD pit depth increases, the returning pit echo signal approaches the interface signal (inner diameter surface reflection). For deep pits, the pit reflection signal merges with the interface signal preventing an accurate measurement of the depth. Therefore, UT can not accurately measure thickness less than the RWR. Although dip pits with 0.012 inch or less of remaining wall cannot be accurately depth sized, detection is not affected.

When the signals merge, the UT analyst makes a call that indicates that the pit is deep but an accurate measurement of the pit depth is beyond the capability of the system. For a nominal 0.031 inch sleeve wall thickness, this would occur at a pit depth of $(0.031 - 0.012) = 0.019$ inch or 61% through-wall of the sleeve. Therefore, this limitation does not affect the ability to detect or size a 30% through-wall service induced pit in the sleeve OD.

Data Set

The data set is presented in Table 11.8.3.

In Table 11.8.3, "UT combined thickness at pit center line" is the thickness of the sleeve and the parent tube measured at 0.1 inch above the centerline of each pit. "UT parent tube thickness" is the thickness of the parent tube measured above the centerline of each pit. The "measured pit depth" is the depth of the pit measured by an optical differential focus from the outer diameter of the parent tube. This depth includes the parent tube thickness in addition to the depth of penetration of the pit into the sleeve material. The "calculated sleeve pit depth" is the difference between the "measured pit depth" and the "UT parent tube thickness". This is the depth of penetration of the pit into the sleeve material.

TABLE 11.8.3
SLEEVE OD PIT DATA SET

Tube (size)	Pit	UT Combined Thickness at Pit Center Line (inch)	UT Parent Tube Thickness (inch)	Measured Pit Depth (inch)	Calculated Sleeve Pit Depth (inch)
081897-03M 3/4"	A	0.086	0.049	0.068	0.019
	B	0.086	0.049	0.055	0.006
	C	0.079	0.048	0.065	0.017
081897-04M 3/4"	A	0.080	0.050	0.056	0.006
	B	0.084	0.048	0.047	-0.001
	C	0.092	0.049	0.072	0.023
081897-05M 3/4"	A	0.085	0.048	0.060	0.012
	B	0.087	0.048	0.069	0.021
	C	0.085	0.049	0.066	0.017
081897-07M 3/4"	A	0.079	0.046	0.074	0.028
	B	0.089	0.049	0.065	0.016
	C	0.083	0.048	0.075	0.027
082597-02M 3/4"	A	0.084	0.043	0.065	0.022
	B	0.083	0.045	0.075	0.030
	C	0.078	0.042	0.042	0.000
091197-002 3/4"	A	0.080	0.043	0.065	0.022
	B	0.076	0.044	0.059	0.015
	C	0.082	0.043	0.074	0.031
041897-06 7/8"	A	0.087	0.049	0.056	0.007
	B	0.086	0.052	0.068	0.016
	C	0.090	0.051	0.078	0.027
042297-01 7/8"	A	0.084	0.051	0.056	0.005
	B	0.087	0.049	0.066	0.017
	C	0.097	0.052	0.074	0.022
042297-03 7/8"	A	0.085	0.051	0.077	0.026
	B	0.097	0.052	0.077	0.025
	C	0.087	0.049	0.070	0.021
042297-08 7/8"	A	0.090	0.051	0.058	0.007
	B	0.090	0.051	0.068	0.017
	C	0.085	0.049	0.069	0.020
082297-01S 7/8"	A	0.095	0.049	0.058	0.009
	B	0.094	0.051	0.070	0.019
	C	0.089	0.047	0.074	0.027

Results

Tables 11.8.4 and 11.8.5 summarize the sleeve OD pit sizing analysis results for the data set as presented in Table 11.8.3.

TABLE 11.8.4
SLEEVE OD PITTING RESULTS – 3/4" TUBE

CENTERED PROBE EXCLUDING DATA POINTS OUTSIDE SYSTEM RWR					
FTI UT ANALYST	NUMBER OF PITS	AVERAGE ERROR (inch)	STANDARD DEVIATION (inch)	RMSE (inch)	MAX ERROR (inch)
1	14	-0.001	0.002	0.002	-0.004
2	14	-0.001	0.002	0.002	-0.005

The maximum under-call errors for the sample set are reported as MAX ERROR in Table 11.8.4.

TABLE 11.8.5
SLEEVE OD PITTING RESULTS – 7/8" TUBE

CENTERED PROBE EXCLUDING DATA POINTS OUTSIDE SYSTEM RWR					
FTI UT ANALYST	NUMBER OF PITS	AVERAGE ERROR (inch)	STANDARD DEVIATION (inch)	RMSE (inch)	MAX ERROR (inch)
1	13	-0.001	0.003	0.003	-0.006
2	12	0.000	0.004	0.004	-0.005

The maximum under-call errors for the sample set are reported as MAX ERROR in Table 11.8.5. All sleeve OD pits were detected, which demonstrated a high POD for this damage mechanism.

11.8.3 Disbond (Appendix J, ETSS 98-403 [13.79])

Definition

A disbond region is an area where the nickel sleeve is not bonded to the ID of the parent tube. Disbond regions are considered to have neither volume nor material loss.

Inspection Requirement

The examination requirements specified in Section 6.A.2 of Reference 13.4 were used to select simulated disbond diameters. These requirements specifically state:

"Testing shall demonstrate that there are no nonbonded areas greater than 0.125 in. in width or length within the minimum required reinforcement length. Nonbonded areas greater than 0.125 in. and less than 0.250 in. may be evaluated by the Owner for acceptability. Nonbonded areas greater than 0.250 in. in any dimension are unacceptable."

To meet these requirements, the population of simulated disbond samples ranged from diameters less than 0.125 inch to diameters greater than 0.250 inch.

Sample Set Description

To simulate a disbond location between the Electrosleeve™ and Alloy 600, contoured-bottom EDM burns were used to install disbond patches of various diameters in the OD of Electrosleeve™ tubes. Each tube contained three outer diameter contoured-bottom holes with the target depth terminating at the interface of the Electrosleeve™ and Alloy 600. As a part of the disbond qualification, it was demonstrated that simulated disbond produces ultrasonic signal responses equivalent to actual process-induced disbond.

UT data was acquired at axial pitch values of 0.010, 0.015 and 0.020 inch. Pitch is the axial spacing between subsequent probe rotations. These three pitch values were required to demonstrate acceptable detection and extent sizing for the nominal 0.015 inch acquisition pitch.

It is necessary to measure two disbond edges when determining either axial or radial extent. A two-times-pitch error bound allowed for an error equal to one pitch at each edge. If an analyst chose the edge signals such that each edge determination contained an associated error of one pitch, the total error contained in the extent measurement would equal twice the pitch. As a result, for both axial and circumferential disbond extent measurements, an error not to exceed two times the relative pitch was considered an acceptable performance bound for the analysis. This error bound would result in a maximum error for any extent measurement of 0.040 inch, which falls well within the 0.125 inch requirement.

Data Set

Six tubes were used for the disbond qualification. The sample set consisted of three, 3/4" and three, 7/8" tubes with a total of eighteen (18) disbond regions (each contoured-bottom EDM represented the site of a single disbond region). Table 11.8.6 lists the disbond flaws that were fabricated to simulate process-induced disbond.

TABLE 11.8.6
DISBOND SAMPLE SET

TUBE (size)	DISBOND FLAW	ACTUAL DIAMETER (inch)
041897-006 7/8"	A	0.102
	B	0.072
	C	0.127
042297-01 7/8"	A	0.294
	B	0.330
	C	0.371
042297-08 7/8"	A	0.166
	B	0.207
	C	0.251
081897-03M 3/4"	A	0.101
	B	0.073
	C	0.126
081897-05M 3/4"	A	0.293
	B	0.331
	C	0.373
091197-002 3/4"	A	0.167
	B	0.206
	C	0.251

To ensure detection and adequate extent sizing, FTI acquires data with an average axial pitch of 0.015 inch and an average circumferential pitch of two degrees. The average circumferential pitch of two degrees can be converted to inches by the following equation:

$$\text{Circ. pitch (in.)} = [\text{Circ. pitch (}^\circ\text{)}] * [(3.14159 * \text{ID (in.)}) / 360^\circ]$$

Three axial pitches were acquired to demonstrate that variances of an average pitch of 0.015 inch would not produce an unacceptable extent determination. Table 11.8.7 provides the extent sizing bounds as a function of pitch.

TABLE 11.8.7
TWO PITCH EXTENT SIZING ERROR BOUNDS

AXIAL AND CIRC. EXTENT TOLERANCES					
TUBE SIZE (inch)	INSIDE DIAMETER (inch)	CIRC. PITCH (inch)	CIRC. EXTENT BOUND (inch)	AXIAL PITCH (inch)	AXIAL EXTENT BOUND (inch)
3/4"	0.654	0.011	0.022	0.010	0.020
				0.015	0.030
				0.020	0.040
7/8"	0.775	0.013	0.026	0.010	0.020
				0.015	0.030
				0.020	0.040

Results

Tables 11.8.8 and 11.8.9 summarize the sleeve disbond sizing analysis results for the data set presented in Table 11.8.6. The maximum under-call errors for each sample set are reported as MAX ERROR in the tables. The data includes two separate analyst results of three different axial pitch values.

Table 11.8.8 displays the results from comparing the UT circumferential extent measurements to the actual measured circumferential disbond extents. The maximum expected circumferential error bound for 3/4" and 7/8" samples was noted in Table 11.8.7 as 0.022 and 0.026 inch, respectively. All of the UT measured circumferential extents were within the expected bounds.

TABLE 11.8.8
DISBOND CIRCUMFERENTIAL EXTENT SIZING RESULTS

CIRCUMFERENTIAL EXTENT RESULTS [3-CHANNEL CENTERED PROBE]					
TUBE SIZE: 3/4"					
AXIAL PITCH (inch)	FTI UT ANALYST	AVERAGE ERROR (inch)	STANDARD DEVIATION (inch)	RMSE (inch)	MAX ERROR (inch)
0.010	1	-0.002	0.005	0.005	-0.012
0.010	2	-0.003	0.007	0.007	-0.012
0.015	1	0.001	0.011	0.011	-0.014
0.015	2	0.001	0.005	0.005	-0.006
0.020	1	0.003	0.006	0.006	-0.006
0.020	2	0.005	0.007	0.008	-0.006
TUBE SIZE: 7/8"					
0.010	1	0.001	0.010	0.009	-0.009
0.010	2	0.008	0.011	0.013	-0.016
0.015	1	0.004	0.007	0.008	-0.008
0.015	2	-0.009	0.009	0.012	-0.019
0.020	1	-0.001	0.011	0.010	-0.016
0.020	2	0.003	0.008	0.008	-0.006

Table 11.8.9 displays the results from comparing UT axial extent measurements to the actual measured axial disbond extents. The expected maximum extent bounds for axial pitch values of 0.010, 0.015, and 0.020 inch were noted in Table 11.8.7 as 0.020, 0.030, and 0.040 inch, respectively. All UT measured axial extents were within the expected bounds.

TABLE 11.8.9
DISBOND AXIAL EXTENT SIZING RESULTS

AXIAL EXTENT RESULTS [3-CHANNEL CENTERED PROBE]					
TUBE SIZE: 3/4"					
AXIAL PITCH (inch)	FTI UT ANALYST	AVERAGE ERROR (inch)	STANDARD DEVIATION (inch)	RMSE (inch)	MAX ERROR (inch)
0.010	1	0.008	0.004	0.009	0.000
0.010	2	0.005	0.012	0.013	-0.016
0.015	1	0.008	0.009	0.012	-0.006
0.015	2	-0.005	0.010	0.010	-0.016
0.020	1	0.011	0.012	0.016	-0.002
0.020	2	0.009	0.012	0.015	-0.006
TUBE SIZE: 7/8"					
0.010	1	0.007	0.008	0.010	-0.008
0.010	2	0.003	0.010	0.010	-0.012
0.015	1	0.001	0.010	0.009	-0.013
0.015	2	-0.006	0.008	0.009	-0.012
0.020	1	0.003	0.011	0.011	-0.012
0.020	2	0.006	0.011	0.012	-0.012

Both analysts detected all eighteen (18) disbond regions. The comparison of the UT measurements to the actual axial and circumferential disbond extent measurements demonstrates that the UT method is within the expected bound of two times the relative pitch. This indicates that distinct edge signals exist at disbond boundaries and contribute to the repeatability of sizing disbond extent within the expected bounds. The worst case root mean squared error (RMSE) and maximum error reported meet the 0.125 and 0.250 inch diametric disbond sizing requirements [13.7].

11.8.4 ID Pits (Appendix J, ETSS 98-404 [13.80])

Definition

ID pits may form on the inner diameter surface of the sleeve during the deposition process. Sleeve ID pits are typically less than 0.050 inch in diameter at the sleeve ID surface.

Inspection Requirement

UT is required to detect ID pits with diameters in excess of 0.050 inch. To ensure a high probability of detecting 0.050 diameter pits, the qualification testing must demonstrate the ability to detect ID pits of diameters greater than 0.025 inch.

UT is required to determine the location of the pit relative to the tube flaw. ID pits that are within one-half inch of a detected parent tube flaw are unacceptable. The reason for this criterion is that the propagation of the parent tube flaw could result in coincidence with the ID pit and produce a potential leak path.

ID pits are conservatively assumed to be 100% through the sleeve material; therefore, no depth sizing is required. ID pits with a depth greater than one wavelength (~0.006 inch for a 10MHz transducer and a 0.058 inch/ μ s speed of sound in water) can be

detected because at depths greater than 0.006 inch, there should be at least two distinct surface reflections.

Sample Set Description

A set of tubes with ID pits was selected from the process pre-qualification and training runs. This sample set consists of four sleeved 3/4" OD tubes with a total of twenty-five (25) ID pits. The tubes were examined with three axial pitch values. The tubes were split axially to characterize each pit location and diameter at the inner diameter surface.

Data Set

The qualification samples are presented in Table 11.8.10. Axial location is expressed in inches relative to the marked tube end. The circumferential location is expressed in degrees of rotation from an established zero degree reference mark located fourteen inches from the marked tube end. The circumferential locations were estimated and were used to correlate the data reported for pits in close proximity.

TABLE 11.8.10
ID PIT SAMPLE SET

Tube	Pit	Axial Location (inch)	Circ Location (degree)	Actual Pit Diameter (inch)
111396-02	1	11.70	250	0.038
	2	9.76	355	0.030
	3	6.75	290	0.014
	4	6.71	340	0.009
	5	6.69	290	0.015
	6	6.69	40	0.020
	7	6.66	50	0.017
112396-02	1	12.40	310	0.016
	2	9.13	190	0.020
	3	6.21	290	0.015
120196-03	1	9.92	315	0.042
	2	9.90	235	0.020
	3	9.66	240	0.025
	4	9.51	240	0.008
	5	9.42	235	0.010
	6	6.79	190	0.042
	7	6.68	310	0.027
010997-06	1	10.54	20	0.030
	2	8.25	155	0.043
	3	7.47	45	0.052
	4	7.22	320	0.050
	5	7.02	345	0.050
	6	6.78	325	0.047
	7	6.35	320	0.041
	8	5.72	355	0.032

Results

The UT data was analyzed by a single analyst to determine a probability of detection for ID pits in the range of diameters represented by the sample set. Table 11.8.11 presents the detection results for the three axial pitch values.

TABLE 11.8.11
ID PIT SAMPLE SET DETECTION RESULTS

Tube	Pit	Actual Pit Diameter (inch)	Detection At 0.010" Axial Pitch	Detection At 0.015" Axial Pitch	Detection At 0.020" Axial Pitch
111396-02	1	0.038	Y ⁽¹⁾	Y	Y
	2	0.030	Y	Y	Y
	3	0.014	Y	Y	Y
	4	0.009	Y	Y	Y
	5	0.015	Y	Y	Y
	6	0.020	Y	Y	Y
	7	0.017	Y	N ⁽²⁾	N
112396-02	1	0.016	N	N	N
	2	0.020	Y	Y	Y
	3	0.015	Y	Y	Y
120196-03	1	0.042	Y	Y	Y
	2	0.020	Y	Y	Y
	3	0.025	Y	Y	Y
	4	0.008	Y	Y	Y
	5	0.010	Y	Y	Y
	6	0.042	Y	Y	Y
	7	0.027	Y	Y	Y
010997-06	1	0.030	Y	Y	Y
	2	0.043	Y	Y	Y
	3	0.052	Y	Y	Y
	4	0.050	Y	Y	Y
	5	0.050	Y	Y	Y
	6	0.047	Y	Y	Y
	7	0.041	Y	Y	Y
	8	0.032	Y	Y	Y

NOTES:

- (1) Pit detected, "Y".
(2) Pit not detected, "N".

The analyst detected all ID pits with 0.025 inch or greater diameter. The two pits not detected had diameters less than 0.020 inch and depths less than 0.010 inch. From the Appendix J qualification, the ETSS presents an 87% POD @90%CL for ID pits with diameters greater than or equal to 0.020 inch acquired with a 0.015 inch axial pitch. Therefore there is a high probability that ID pits with diameters greater than 0.050 inch would be detected.

11.8.5 Inner Diameter Profilometry (Appendix J, ETSS 98-401 [13.77])

Definition

Inner diameter profilometry is used to detect and size dented regions located in the parent tube. This defect mechanism may occur in the area of a support structure.

Inspection Requirement

UT must be able to measure the dent deformation to sufficient accuracy to determine if the Electrosleeve operation can be performed. The profile measurement must be accurate to ± 0.002 inch to support the maximum dent determination of 0.023 inch. The 0.023 inch reduction in inner diameter represents the worst case free path restriction for an Electrosleeve™ anode.

Sample Set Description

A sample set of twenty-nine 7/8" OD tubes with a dent range of 0.002 inch to 0.031 inch was selected for this qualification. The tubes were examined with a 0.015 inch axial pitch.

Data Set

The qualification samples are presented in Table 11.8.12.

TABLE 11.8.12
ID PROFILOMETRY SAMPLE SET

Tube	Actual Dent (inch)
9-1	0.003
9-2	0.004
9-3	0.003
10-1	0.017
10-2	0.019
10-3	0.025
11-1	0.009
11-2	0.017
11-3	0.011
12-1	0.020
12-2	0.010
12-3	0.008
13-1	0.005
13-2	0.007
13-3	0.008
14-1	0.003
14-2	0.016
14-3	0.018
15-1	0.005
15-2	0.031
15-3	0.007
16-1	0.020
16-2	0.021
16-3	0.014
17-2	0.010
17-3	0.002
18-1	0.010
18-2	0.004
18-3	0.011

Results

The UT results from a single analyst were presented in the Appendix J peer review. Table 11.8.13 presents the results from the ETSS.

TABLE 11.8.13
ID PROFILOMETRY SAMPLE SET SIZING RESULTS

Tube	Actual Dent (inch)	UT Dent (inch)
9-1	0.003	0.003
9-2	0.004	0.004
9-3	0.003	0.004
10-1	0.017	0.016
10-2	0.019	0.018
10-3	0.025	0.024
11-1	0.009	0.009
11-2	0.017	0.017
11-3	0.011	0.011
12-1	0.020	0.018
12-2	0.010	0.009
12-3	0.008	0.009
13-1	0.005	0.005
13-2	0.007	0.005
13-3	0.008	0.007
14-1	0.003	0.002
14-2	0.016	0.014
14-3	0.018	0.018
15-1	0.005	0.004
15-2	0.031	0.030
15-3	0.007	0.008
16-1	0.020	0.019
16-2	0.021	0.020
16-3	0.014	0.014
17-2	0.010	0.010
17-3	0.002	0.002
18-1	0.010	0.011
18-2	0.004	0.004
18-3	0.011	0.010

The Appendix J qualification presented a 0.001 inch RMSE, which is sufficient for meeting the dent sizing accuracy for the Electrosleeve™ program.

11.8.6 Combined Wall Thickness

Definition

The combined wall thickness is the combination of the parent tube wall thickness and the sleeve wall thickness.

Inspection Requirement

The UT must be able to measure the combined wall thickness to sufficient accuracy to assure the sleeve wall meets the required minimum thickness. The thickness measurement must be accurate to 0.002 inch to support the minimum thickness requirements for sleeve installation.

Sample Set Description

The sample set consists of thickness measurements performed during the destructive evaluation of the ODSCC depth sizing sample set. From the ODSCC depth sizing sample set, nine axial and nine circumferential crack flaws were selected. Thickness measurements from the ultrasonic data analysis were compared to the thickness values determined by the destructive evaluation at each of the flaw locations.

Data Set

The destructive examination (DE) results are presented in Table 11.8.14.

TABLE 11.8.14
COMBINED WALL THICKNESS DATA SET

Flaw	Axial Location (inch)	Circ. Location (degree)	DE Thickness (inch)
A1	6.35	180	0.074
A2	4.30	180	0.077
A3	4.45	0	0.076
A4	4.30	0	0.076
A5	4.40	90	0.075
A8	6.15	0	0.077
A9	4.40	0	0.078
A10	6.15	220	0.076
A11	4.45	220	0.077
C1	6.15	170	0.081
C2	4.65	140	0.072
C3	4.65	90	0.075
C4	4.65	220	0.075
C5	4.75	10	0.076
C6	4.94	10	0.077
C7	4.65	120	0.080
C8	6.25	150	0.079
C9	4.95	180	0.078

Results

In accordance with the Appendix J qualified procedures for outer diameter pit depth measurement, the combined wall thickness was determined using the time of flight between successive back wall reflections of the longitudinal (thickness) waveform.

The results listed in Table 11.8.15 show that the maximum error and the RMSE are sufficient to meet the requirements for sleeve thickness examination.

TABLE 11.8.15
COMBINED WALL THICKNESS RESULTS

Flaw	Axial Location (inch)	Circ. Location (degree)	DE Thickness (inch)	UT Thickness (inch)	Delta
A1	6.35	180	0.074	0.075	0.001
A2	4.30	180	0.077	0.079	0.002
A3	4.45	0	0.076	0.077	0.001
A4	4.30	0	0.076	0.077	0.001
A5	4.40	90	0.075	0.076	0.001
A8	6.15	0	0.077	0.078	0.001
A9	4.40	0	0.078	0.080	0.002
A10	6.15	220	0.076	0.077	0.001
A11	4.45	220	0.077	0.078	0.001
C1	6.15	170	0.081	0.080	-0.001
C2	4.65	140	0.072	0.072	0.000
C3	4.65	90	0.075	0.074	-0.001
C4	4.65	220	0.075	0.075	0.000
C5	4.75	10	0.076	0.076	0.000
C6	4.94	10	0.077	0.076	-0.001
C7	4.65	120	0.080	0.080	0.000
C8	6.25	150	0.079	0.079	0.000
C9	4.95	180	0.078	0.078	0.000

MAX: 0.002
MIN: -0.001
RMSE: 0.001

11.8.7 Sleeve Nodules

A sleeve nodule is a localized build up of plating material on the ID of the sleeve. The UT system can detect and measure the nodule height. The detection and disposition of nodules is presented in the ETSS 98-404, Inner Diameter Pitting Analysis. Typically, nodules are less than 0.050 inch in diameter and do not impact probe operation. If the probe operation is impacted, the nodule height will be reduced by a suitable method.

11.9 Qualification Program for Shear Wave UT

Shear wave UT is used for detection and sizing of crack-like flaws in the parent tube. Samples with laboratory induced ODSCC were used to qualify the extent and depth sizing procedures. At present, there is no environmental technique available to induce corrosion cracking in the Electrosleeve™. Thus, the ODSCC was only in the parent tube material. The UT techniques have been shown to be effective in the detection and sizing of fatigue cracks propagated into the sleeve material

11.9.1 ODSCC Detection and Extent Sizing (Appendix J, ETSS 98-302 [13.81])

Definition

Primarily, parent tube cracking occurs in the form of outer diameter stress corrosion cracking (ODSCC), or primary water stress corrosion cracking (PWSCC). Cracks in thin wall tubing are planar in nature since a depth of penetration and an extent (length) are exhibited. These cracks propagate nearly perpendicular to their surface of origin. Since the Electrosleeve process removes the environment from PWSCC, the UT qualification focussed of the ODSCC, which may continue to propagate in depth and extent.

Inspection Requirement

Regions A and B (Figure 11.1.1) must be free of defects (based on ECT) at the time of sleeve installation. If parent tube cracking occurs in either of these regions, the tube will be plugged. In these regions, UT must demonstrate a high probability of detection of service induced cracks that have depths of penetration exceeding 40% through-wall of the parent tube.

Region C (Figure 11.1.1) contains one or more parent tube defects that have been covered by the Electrosleeve™. For those defects that are outer diameter cracks, the ultrasonic technique must detect the crack and determine the crack extent (length). The accuracy to which UT can measure crack extent determines the ability of the technique to determine if the crack has propagated into Region B, or to within 0.5 inch of a detected ID pit.

The goal of the qualification was to demonstrate that the technique could detect and extent size ODSCC cracks longer than 0.8 inch to an accuracy of 0.080 inch. Although the 0.8 inch length was established for a repair using a minimal Electrosleeve™ thickness based on burst pressure requirements for axial cracks within the tube support region, axial cracks of extent 0.8 to 1.5 inches are of interest to the structural Electrosleeve™ for certain adverse plant operational conditions.

Typically, axial cracks in the tube-sheet expansion transition region are less than 0.5 inch length and are not structurally challenging after the Electrosleeve™ repair. Long circumferential cracks at the expansion transition were chosen to demonstrate the ability of the technique to accurately extent size a circumferential crack after the application of the structural Electrosleeve™ repair.

Sample Set Description

The sample set consisted of eighteen axial (Table 11.9.1 and 11.9.2) and eighteen circumferential (Table 11.9.3 and 11.9.4) ODSCC cracks. The eighteen axial crack samples were 7/8" x 0.050" wall Alloy 600 tubes with dented tube support plate regions. The eighteen circumferential crack sample set was comprised of ten circumferential crack samples of 7/8" x 0.050" wall Alloy 600 tubes with dented tube support plate regions and eight circumferential crack samples of 3/4" x 0.043" wall Alloy 600 tubes with expansion transitions. The dented tube support samples were examined before and after the application of a thin Electrosleeve™ repair, (typical 0.012 inch). The expansion transition samples were examined before and after the application of a structural Electrosleeve repair, (typical 0.034 inch). The samples were examined in both scan directions for each process step, (before and after electro-deposition). Since there was no statistical difference resulting from scan direction, the Appendix J qualification presented the forward scan, normal probe operation, data only. Both pre-sleeve and post sleeve results were presented at the peer review to qualify the procedure for either condition.

Results

The outer diameter extent was determined by using the detection of the outer diameter skip target motion to locate the crack end points. Three analysts performed the analysis of the data.

TABLE 11.9.1
AXIAL ODSCC EXTENT SAMPLE SET PRE-SLEEVE RESULTS

tube	number	DE crack extent (inch)	analyst one crack extent (inch)	analyst three crack extent (inch)	delta DE analyst one (inch)	delta DE analyst three (inch)
009	1	0.362	0.398	0.398	0.036	0.036
009	3	0.630	0.577	0.577	-0.053	-0.053
011	3	1.051	1.074	1.074	0.023	0.023
012	3	0.720	0.708	0.695	-0.012	-0.025
013	2	0.762	0.801	0.828	0.039	0.066
017	1	0.360	0.372	0.372	0.012	0.012
020	1	0.666	0.676	0.707	0.010	0.041
021	1	1.458	1.422	1.452	-0.036	-0.006
023	1	1.110	1.146	1.160	0.036	0.050
025	3	1.259	1.301	1.301	0.042	0.042
027	1	1.303	1.323	1.338	0.020	0.035
028	1	0.930	0.954	0.967	0.024	0.037
030	1	1.244	1.271	1.301	0.027	0.057
031	1	1.017	0.979	0.993	-0.038	-0.024
032	2	1.429	1.404	1.434	-0.025	0.005
034	1	0.585	0.639	0.669	0.054	0.084
035	1	1.178	1.207	1.237	0.029	0.059
040	1	0.362	0.412	0.428	0.050	0.066

MIN: -0.053 -0.053
MAX: 0.054 0.084
AVE: 0.013 0.028
RMSE: 0.034 0.045

TABLE 11.9.2
AXIAL ODSCC EXTENT SAMPLE SET POST-SLEEVE RESULTS

tube	number	DE crack extent (inch)	analyst two crack extent (inch)	analyst three crack extent (inch)	delta DE analyst two (inch)	delta DE analyst three (inch)
009	1	0.362	0.415	0.397	0.053	0.035
009	3	0.630	0.551	0.551	-0.079	-0.079
011	3	1.051	1.072	1.072	0.021	0.021
012	3	0.720	0.725	0.694	0.005	-0.026
013	2	0.762	0.823	0.824	0.061	0.062
017	1	0.360	0.390	0.390	0.030	0.030
020	1	0.666	0.708	0.693	0.042	0.027
021	1	1.458	1.453	1.453	-0.005	-0.005
023	1	1.110	1.172	1.158	0.062	0.048
025	3	1.259	1.284	1.284	0.025	0.025
027	1	1.303	1.306	1.319	0.003	0.016
028	1	0.930	0.932	0.958	0.002	0.028
030	1	1.244	1.266	1.280	0.022	0.036
031	1	1.017	0.994	0.994	-0.023	-0.023
032	2	1.429	1.410	1.409	-0.019	-0.020
034	1	0.585	0.634	0.634	0.049	0.049
035	1	1.178	1.211	1.211	0.033	0.033
040	1	0.362	0.411	0.412	0.049	0.050

MIN: -0.079 -0.079
MAX: 0.062 0.062
AVE: 0.018 0.017
RMSE: 0.039 0.038

TABLE 11.9.3
CIRCUMFERENTIAL ODSCC EXTENT SAMPLE SET PRE-SLEEVE RESULTS

tube	number	DE crack extent (inch)	analyst one crack extent (inch)	analyst three crack extent (inch)	delta DE analyst one (inch)	delta DE analyst three (inch)
039	3	1.191	1.290	1.306	0.099	0.115
044	2	1.344	1.268	1.268	-0.076	-0.076
044	10	1.344	1.336	1.344	-0.008	0.000
044	14	1.161	1.130	1.130	-0.031	-0.031
046	1	1.039	1.008	1.023	-0.031	-0.016
053	1	1.527	1.497	1.481	-0.030	-0.046
063	1	1.466	1.481	1.489	0.015	0.023
064	1	1.214	1.222	1.237	0.008	0.023
070	1	1.558	1.527	1.520	-0.031	-0.038
072	1	1.405	1.466	1.481	0.061	0.076
013	8	1.571	1.584	1.623	0.013	0.052
013	9	0.327	0.360	0.367	0.033	0.040
022	14	1.636	1.590	1.603	-0.046	-0.033
022	15	1.047	1.041	1.034	-0.006	-0.013
023	16	1.571	1.532	1.545	-0.039	-0.026
023	17	0.851	0.831	0.825	-0.020	-0.026
024	18	0.785	0.805	0.818	0.020	0.033
024	19	0.785	0.753	0.759	-0.032	-0.026
				MIN:	-0.076	-0.076
				MAX:	0.099	0.115
				AVE:	-0.006	0.002
				RMSE:	0.041	0.047

TABLE 11.9.4
CIRCUMFERENTIAL ODSKC EXTENT SAMPLE SET
POST-SLEEVE RESULTS

tube	number	DE crack extent (inch)	analyst two crack extent (inch)	analyst three crack extent (inch)	delta DE analyst two (inch)	delta DE analyst three (inch)
039	3	1.191	1.290	1.290	0.099	0.099
044	2	1.344	1.283	1.260	-0.061	-0.084
044	10	1.344	1.344	1.329	0.000	-0.015
044	14	1.161	1.138	1.138	-0.023	-0.023
046	1	1.039	1.016	1.008	-0.023	-0.031
053	1	1.527	1.497	1.474	-0.030	-0.053
063	1	1.466	1.474	1.497	0.008	0.031
064	1	1.214	1.252	1.222	0.038	0.008
070	1	1.558	1.520	1.489	-0.038	-0.069
072	1	1.405	1.497	1.451	0.092	0.046
013	8	1.571	1.604	1.617	0.033	0.046
013	9	0.327	0.367	0.373	0.040	0.046
022	14	1.636	1.584	1.558	-0.052	-0.078
022	15	1.047	1.041	1.034	-0.006	-0.013
023	16	1.571	1.551	1.539	-0.020	-0.032
023	17	0.851	0.812	0.825	-0.039	-0.026
024	18	0.785	0.798	0.806	0.013	0.021
024	19	0.785	0.785	0.779	0.000	-0.006

MIN: -0.061 -0.084
MAX: 0.099 0.099
AVE: 0.002 -0.007
RMSE: 0.044 0.048

11.9.2 ODSCC Depth Sizing (Appendix J, ETSS 98-303 [13.82])

Definition

Primarily, parent tube cracking occurs in the form of outer diameter stress corrosion cracking (ODSCC), or primary water stress corrosion cracking (PWSCC). Cracks in thin wall tubing are typically planar in nature since a depth of penetration and an extent (length) are exhibited. These cracks propagate nearly perpendicular to their surface of origin. Since the Electrosleeve process removes the environment from PWSCC, the UT qualification focussed of the ODSCC, which may continue to propagate in depth and extent.

Inspection Requirement

Regions A and B (Figure 11.1.1) must be free of defects (based on ECT) at the time of sleeve installation. If parent tube cracking occurs in either of these regions, the tube will be plugged. In these regions, UT must demonstrate a high probability of detection of service induced cracks that have depths of penetration exceeding 40% through-wall of the parent tube.

Region C (Figure 11.1.1) contains one or more parent tube defects that have been covered by the Electrosleeve™. For those defects that are outer diameter cracks, the ultrasonic technique must monitor the crack depth. The accuracy to which UT can measure crack depth determines the ability of the technique to determine if the crack has propagated into the sleeve material.

The goal of the qualification was to demonstrate that the combination of the three depth sizing techniques, as presented in the procedure and section 11.7.3 of this document could accurately determine the crack depth of penetration to 0.011 inch. This accuracy would support the conservatively selected 30% sleeve degradation repair limit.

Sample Set Description

The sample set consists of twenty axial (Tables 11.9.5 and 11.9.6) and nineteen circumferential (Tables 11.9.7 and 11.9.8) ODSCC cracks. The crack samples are 3/4" x 0.043" wall Alloy 600 tubes with expansion transitions. The samples were examined before and after the application of a structural Electrosleeve repair, (typical 0.034 inch). The samples were examined in both scan directions for each process step, (before and after electro-deposition). Since there was no statistical difference resulting from scan direction, the Appendix J qualification presented the forward scan, normal probe operation, data only. Both pre-sleeve and post sleeve results were presented to the peer review to qualify the procedure for either condition.

Results

The maximum UT crack depth, as determined using the depth sizing procedure, was compared to the maximum crack depth as determined by destructive examination. Three analysts performed the analysis of the data.

TABLE 11.9.5
AXIAL ODSCC DEPTH SAMPLE SET PRE-SLEEVE RESULTS

tube RT-100	axial crack number	DE crack depth (inch)	analyst one crack depth (inch)	analyst three crack depth (inch)	delta DE analyst one (inch)	delta DE analyst three (inch)
-001	2	0.040	0.038	0.034	-0.002	-0.006
-003	3	0.039	0.042	0.042	0.003	0.003
	4	0.039	0.035	0.033	-0.004	-0.006
-004	5	0.043	0.043	0.042	0.000	-0.001
-007	8	0.040	0.035	0.034	-0.005	-0.006
	9	0.040	0.037	0.039	-0.003	-0.001
-011	10	0.042	0.043	0.044	0.001	0.002
	11	0.043	0.043	0.043	0.000	0.000
-012	12	0.011	0.022	0.014	0.011	0.003
	13	0.040	0.040	0.042	0.000	0.002
-015	14	0.040	0.042	0.043	0.002	0.003
	15	0.038	0.036	0.038	-0.002	0.000
-016	16	0.042	0.042	0.042	0.000	0.000
	17	0.026	0.021	0.018	-0.005	-0.008
-017	18	0.025	0.021	0.026	-0.004	0.001
	19	0.040	0.043	0.042	0.003	0.002
-018	20	0.012	0.013	0.008	0.001	-0.004
	21	0.041	0.042	0.043	0.001	0.002
-020	22	0.011	0.021	0.022	0.010	0.011
	23	0.041	0.041	0.043	0.000	0.002

MIN: -0.005 -0.008
MAX: 0.011 0.011
AVE: 0.000 0.000
RMSE: 0.004 0.004

TABLE 11.9.6
AXIAL ODSCC DEPTH SAMPLE SET POST-SLEEVE RESULTS

tube	axial crack number	DE crack depth (inch)	analyst one crack depth (inch)	analyst two crack depth (inch)	delta DE analyst one (inch)	delta DE analyst two (inch)
RT-100						
-001	2	0.040	0.044	0.039	0.004	-0.001
-003	3	0.039	0.042	0.040	0.003	0.001
	4	0.039	0.041	0.037	0.002	-0.002
-004	5	0.043	0.049	0.040	0.006	-0.003
-007	8	0.040	0.038	0.036	-0.002	-0.004
	9	0.040	0.037	0.035	-0.003	-0.005
-011	10	0.042	0.042	0.041	0.000	-0.001
	11	0.043	0.035	0.035	-0.008	-0.008
-012	12	0.011	0.020	0.019	0.009	0.008
	13	0.040	0.040	0.039	0.000	-0.001
-015	14	0.040	0.038	0.046	-0.002	0.006
	15	0.038	0.037	0.043	-0.001	0.005
-016	16	0.042	0.044	0.047	0.002	0.005
	17	0.026	0.026	0.031	0.000	0.005
-017	18	0.025	0.019	0.024	-0.006	-0.001
	19	0.040	0.039	0.042	-0.001	0.002
-018	20	0.012	0.018	0.014	0.006	0.002
	21	0.041	0.035	0.038	-0.006	-0.003
-020	22	0.011	0.017	0.018	0.006	0.007
	23	0.041	0.037	0.032	-0.004	-0.009

MIN: -0.008 -0.009
MAX: 0.009 0.008
AVE: 0.000 0.000
RMSE: 0.004 0.005

TABLE 11.9.7
CIRCUMFERENTIAL ODSCC DEPTH SAMPLE SET PRE-SLEEVE RESULTS

tube	circ. crack number	DE crack depth (inch)	analyst one crack depth (inch)	analyst three crack depth (inch)	delta DE analyst one (inch)	delta DE analyst three (inch)
RT-100						
-003	1	0.037	0.037	0.035	0.000	-0.002
-004	2	0.036	0.032	0.031	-0.004	-0.005
-005	3	0.027	0.042	0.027	0.015	0.000
	4	0.034	0.032	0.041	-0.002	0.007
-008	5	0.036	0.034	0.032	-0.002	-0.004
-009	6	0.039	0.038	0.042	-0.001	0.003
-010	7	0.026	0.030	0.035	0.004	0.009
-013	8	0.042	0.042	0.042	0.000	0.000
	9	0.041	0.042	0.042	0.001	0.001
-014	10	0.039	0.040	0.033	0.001	-0.006
	11	0.034	0.040	0.043	0.006	0.009
-021	12	0.042	0.041	0.042	-0.001	0.000
	13	0.034	0.037	0.034	0.003	0.000
-022	14	0.042	0.041	0.041	-0.001	-0.001
	15	0.042	0.040	0.042	-0.002	0.000
-023	16	0.043	0.042	0.042	-0.001	-0.001
	17	0.040	0.043	0.042	0.003	0.002
-024	18	0.041	0.041	0.042	0.000	0.001
	19	0.042	0.041	0.042	-0.001	0.000

MIN:	-0.004	-0.006
MAX:	0.015	0.009
AVE:	0.001	0.001
RMSE:	0.004	0.004

TABLE 11.9.8
CIRCUMFERENTIAL ODSCC DEPTH SAMPLE SET POST-SLEEVE RESULTS

tube RT-100	circ. crack number	DE crack depth (inch)	analyst one crack depth (inch)	analyst two crack depth (inch)	delta DE analyst one (inch)	delta DE analyst two (inch)
-003	1	0.037	0.049	0.052	0.012	0.015
-004	2	0.036	0.044	0.043	0.008	0.007
-005	3	0.027	0.049	0.048	0.022	0.021
	4	0.034	0.040	0.042	0.006	0.008
-008	5	0.036	0.038	0.038	0.002	0.002
-009	6	0.039	0.045	0.047	0.006	0.008
-010	7	0.026	0.030	0.030	0.004	0.004
-013	8	0.042	0.046	0.046	0.004	0.004
	9	0.041	0.044	0.045	0.003	0.004
-014	10	0.039	0.040	0.032	0.001	-0.007
	11	0.034	0.032	0.034	-0.002	0.000
-021	12	0.042	0.059	0.061	0.017	0.019
	13	0.034	0.034	0.029	0.000	-0.005
-022	14	0.042	0.058	0.056	0.016	0.014
	15	0.042	0.045	0.045	0.003	0.003
-023	16	0.043	0.044	0.043	0.001	0.000
	17	0.040	0.047	0.043	0.007	0.003
-024	18	0.041	0.046	0.053	0.005	0.012
	19	0.042	0.054	0.056	0.012	0.014

MIN: -0.002 -0.007
MAX: 0.022 0.021
AVE: 0.007 0.007
RMSE: 0.009 0.010

11.10 UT Qualification Results

This section summarizes the flaw detection and defect sizing capabilities of the UT system.

Detection

Table 11.10.1 presents a summary of flaw detection performance for the mechanisms covered in Sections 11.8 and 11.9. The "Lower Flaw Size" is the smallest dimension of interest detected. The "Upper Flaw Size" gives the largest flaw dimension in the sample set. The "Detection Ratio" represents the ratio of flaws detected to the total number of flaws in the samples. The "POD 95% LCL" (Lower Confidence Limit) is the "Detection Ratio" corrected for the statistical strength of the supporting data set. For each defect type, the POD value is computed for the sample range.

TABLE 11.10.1
SUMMARY OF FLAW DETECTION

FLAW TYPE	TABLE	LOWER FLAW SIZE (inch)	UPPER FLAW SIZE (inch)	NUMBER OF FLAWS	NUMBER DETECTED	DETECT RATIO	POD 95% LCL
Parent OD Pits	11.8.1	0.008 depth	0.031 depth	31	31	1.0	0.91
Sleeve OD Pits	11.8.3	None	0.031 depth	39	39	1.0	0.93
Disbond	11.8.6	0.072 dia.	0.373 dia.	18	18	1.0	0.85
Sleeve ID Pits	11.8.10	0.008 dia.	0.052 dia.	75 ⁽¹⁾	70	0.93	0.86
ODSCC Extent	11.9.1 through 11.9.4	0.33 extent	1.64 extent	36	36	1.0	0.92
ODSCC Depth	11.9.5 through 11.9.8	0.011 depth	0.043 depth	39	39	1.0	0.93
All SCC Detection	11.9.1 through 11.9.8	0.011 depth 0.33 Extent	0.051 depth 1.64 Extent	67 ⁽²⁾	67 ⁽²⁾	1.0	0.96

NOTES:

- (1) Twenty-five (25) flaws were acquired with three axial pitch values.
(2) Eight (8) circumferential ODSCC samples used for depth and extent.

Sizing Performance

Table 11.10.2 presents a summary of the sizing results for the flaw mechanisms in Sections 11.8 and 11.9. "Max Error" is the maximum under-call. The lower 95% confidence limit is calculated as follows:

Lower 95% Confidence Limit = Average Error - 1.645 x Error Standard Deviation

TABLE 11.10.2
SUMMARY OF SIZING PERFORMANCE

Flaw Type	Table	Comment	Average Error (inch)	Error STDEV (inch)	Max Error (inch)	RMSE (inch)	95 % LCL (inch)
Parent OD Pits	11.8.2	2 Analysts Centered Probe 3/4" Tube	0.000	0.003	-0.007	0.003	-0.005
Sleeve OD Pits	11.8.4 11.8.5	2 Analysts Centered Probe 3/4" and 7/8" Tube	-0.001	0.003	-0.006	0.003	-0.005
Disbond Circ	11.8.8	2 Analysts Centered Probe 0.015 inch pitch 3/4" and 7/8" Tube	-0.001	0.008	-0.019	0.009	-0.016
Disbond Axial	11.8.9	2 Analysts Centered Probe 0.015 inch pitch 3/4" and 7/8" Tube	0.000	0.009	-0.016	0.010	-0.017
Combined Wall Thickness	11.8.15	1 Analyst	0.000	0.001	-0.001	0.001	-0.001
ODSCC Extent Pre-Sleeve	11.9.1 11.9.3	2 Analysts Centered Probe 3/4" and 7/8" Tube	0.009	0.041	-0.076	0.042	-0.059
ODSCC Extent Post Sleeve	11.9.2 11.9.4	2 Analysts Centered Probe 3/4" and 7/8" Tube	0.007	0.042	-0.084	0.043	-0.062
ODSCC Depth Pre-Sleeve	11.9.5 11.9.7	2 Analysts Centered Probe 3/4" Tube	0.000	0.004	-0.008	0.004	-0.007
ODSCC Depth Post Sleeve	11.9.6 11.9.8	2 Analysts Centered Probe 3/4" Tube	0.004	0.007	-0.009	0.008	-0.008

Ultrasonic Examination Peer Review Summary

FTI has completed seven EPRI Appendix J peer reviews for the ultrasonic procedures used to detect and size the various pre and post installation defect mechanisms.

11.11 NDE Qualification Conclusions

The examination requirements were defined for the three sleeve regions of an installed Electrosleeve™. The sleeve structural pressure boundary is the primary NDE region of interest due to the need to determine if tube defects have propagated into the sleeve material.

Multiple NDE techniques were evaluated. While eddy current is a preferred technique for inspection of steam generator tubes, all available probe designs have encountered difficulties with sleeve examination. The primary eddy current problems are poor accuracy in depth sizing and inability to measure sleeve thickness and bond. The SCC detection capability and principles of UT provided the basis for UT as the selected NDE technology for examination. UT is the only technology with the proven capability to satisfy the sleeve installation examination requirements of thickness, positioning, and bond. In addition, UT inspection provides in-service monitoring of bond and flaw growth.

UT analysis procedures have been qualified using samples for combined wall thickness, tube OD pits, sleeve OD pits, sleeve ID pits, sleeve bond/disbond areas, and ODSCC cracks. The crack depth sizing accuracy provides satisfactory results.

Based on information provided in this topical report, UT has been qualified as the inspection method of the Electrosleeve™. The accuracy and detection capability of the UT technique provides NDE results to evaluate acceptable sleeve installation and to monitor the in-service integrity of the repaired pressure boundary of a steam generator tube.

12.0 PLUGGING LIMIT DEFINITION

To successfully disposition steam generator tube degradation and any potential accompanying sleeve degradation in accordance with Appendix B of 10 CFR Part 50, an in-service inspection process capable of performing the following tasks must be implemented:

- Detect indications of tube degradation,
- Characterize the indications by type, e.g., crack-like, wear, and pitting,
- Determine the orientation of crack-like degradation, and
- Accurately size the depth of degradation.

To meet these requirements, FTI implemented the Degradation-Specific Management (DSM) concept to establish inspection and repair criteria [13.75]. Section 11.0 presented the associated nondestructive examination methods that will be used, along with the qualification results. Section 12.0 combines the examination concepts described in Section 11.0 with the structural limits listed in Section 8.0 to define the Electrosleeve™ plugging limit. Thus, the Electrosleeve™ plugging limit was determined using a defect-specific structural limit with a reduction to account for combined flaw growth (during an inspection interval) and NDE sizing uncertainty. The postulated defects considered in the plugging limit evaluation included uniform thinning, OD and ID pitting, cracking, and disbond.

The following terms are used in Section 12.0:

Structural Limit: The maximum allowed reduction in the structural material by a specific degradation mechanism that meets the RG 1.121 requirements. This limit is determined using the minimum material properties at temperature.

Repair Limit: A defect limit below the structural limit that takes into account the NDE measurement uncertainty and the potential growth of a defect during the planned interval between inspections. If degradation in the sleeve reaches this repair limit, the sleeve must be removed from service to ensure that the defect will not exceed the structural limit during the next inspection interval.

Electrosleeve™ Plugging Limit: The amount of measured degradation that initiates an action to plug or repair an Electrosleeve™. This value encompasses all of the defects analyzed and currently encompasses all of the RSG tube sizes. This additional control limit provides added assurance that the measured degradation will not exceed the structural limit over the next inspection interval.

Growth: Flaw-specific expected degradation per inspection interval based on corrosion and/or fatigue properties. The total expected growth equals the degradation growth rate multiplied by the number of years in the inspection interval. The degradation growth rate is usually specified on a per-year basis.

95% Lower Confidence Limit (LCL): For a normal distribution of errors, the 95% lower confidence limit is calculated by subtracting 1.645 multiplied by the standard deviation from the average error.

RMSE: Root mean squared error.

Inspection Interval: The inspection interval used for the calculations in this section is a typical 18-month operating cycle.

12.1 Repair Limit for Uniform Thinning Degradation

The uniform thinning degradation mechanism can occur in the Electrosleeve™ material due to material wear or general corrosion. The structural limit calculations defined a maximum allowed structural degradation of 45% of the sleeve wall (Table 8.5.3). This calculation assumed 100% of the tube wall and 45% of the sleeve wall were removed by thinning (e.g., wear). The repair limit is determined by decreasing the allowed structural degradation to account for degradation growth and NDE uncertainty.

Per the definition in Section 9.3.4, a conservative upper limit of $\left[\begin{array}{c} b, c \end{array} \right]$ of the sleeve wall for general corrosion growth is used for a sleeve OD thinning degradation mechanism during a typical 18-month inspection interval. Actual growth will be considerably less due to the quality and corrosion resistance of the sleeve material and the expected operating environment, which is less harsh than the environment used in the corrosion testing.

The 95% LCL and UT sizing RMSE for wall thickness measurement associated with a normal beam examination (Table 11.10.2) are -0.001 inch and 0.001 inch, respectively. (Table 12.1.1 summarizes the repair limits for all sleeve nominal thicknesses based on the UT sizing RMSE.)

**TABLE 12.1.1
REPAIR LIMITS FOR UNIFORM THINNING
(Includes 100% Through-Wall Degradation in Tube)
BASED ON UT SIZING RMSE**

Tube OD x Thickness (inch)	Allowed Structural Degradation ⁽¹⁾ (Sleeve Wall)		UT RMSE (Sleeve Wall)		Growth During Inspection Interval ⁽²⁾ (Sleeve Wall)		Repair Limit (Sleeve Wall)	
	(%)	(mils)	(%)	(mils)	(%)	(mils)	(%)	(mils)
11/16 x 0.040	45	14.0	3.2	1	∩			4, 2, 27
3/4 x 0.042/0.043	45	15.3	2.9	1				
3/4 x 0.048	45	15.3	2.9	1				
7/8 x 0.050	45	17.1	2.6	1	L			1

NOTES:

- (1) Note that the circumferential extent for degradation at tubes adjacent to the TSP vertical supports (Figure 8.2.1) is limited as discussed in Section 8.5.
- (2) The inspection interval used in this table was 18 months.

12.2 Repair Limit for Sleeve Pitting and Disbond

12.2.1 Sleeve OD Pitting

The Electrosleeve™ nickel material is subject to pitting degradation in improbable environments for an operating steam generator. The structural limit calculations defined a maximum allowed structural degradation of 88.0% of the sleeve nominal thickness (Table 8.5.3) for a sleeve OD pit degradation mechanism. This calculation assumed 100% of the tube wall

was removed due to any form of degradation and that 88.0% of the sleeve wall was removed due to sleeve OD pitting.

The conservative upper limit of [^{b,c}] (see Section 9.3.4) of the sleeve wall for general corrosion growth is used for a sleeve OD pitting degradation mechanism during a typical 18-month cycle. Actual growth will be considerably lower due to the quality and corrosion resistance of the sleeve material and the expected operating environment, which is less harsh than the environment used in the pitting corrosion tests.

The 95% LCL and the upper limit UT sizing RMSE (Table 11.10.2) for pit sizing associated with a normal beam examination are -0.005 inch and 0.003 inch, respectively. (Table 12.2.1 summarizes the repair limits for all sleeve nominal thicknesses based on the UT sizing RMSE.)

**TABLE 12.2.1
REPAIR LIMITS FOR OD PITTING
(Includes 100% Through-Wall Degradation in Tube)
BASED ON UT SIZING RMSE**

Tube OD x Thickness (inch)	Allowed Structural Degradation ⁽¹⁾ (Sleeve Wall)		UT RMSE (Sleeve Wall)		Growth During Inspection Interval ⁽²⁾ (Sleeve Wall)		Repair Limit (Sleeve Wall)	
	(%)	(mils)	(%)	(mils)	(%)	(mils)	(%)	(mils)
11/16 x 0.040	7	4,627	9.7	3	7			4,627
3/4 x 0.042/0.043			8.8	3				
3/4 x 0.048			8.8	3				
7/8 x 0.050	8	5	7.9	3	8			5

NOTES:

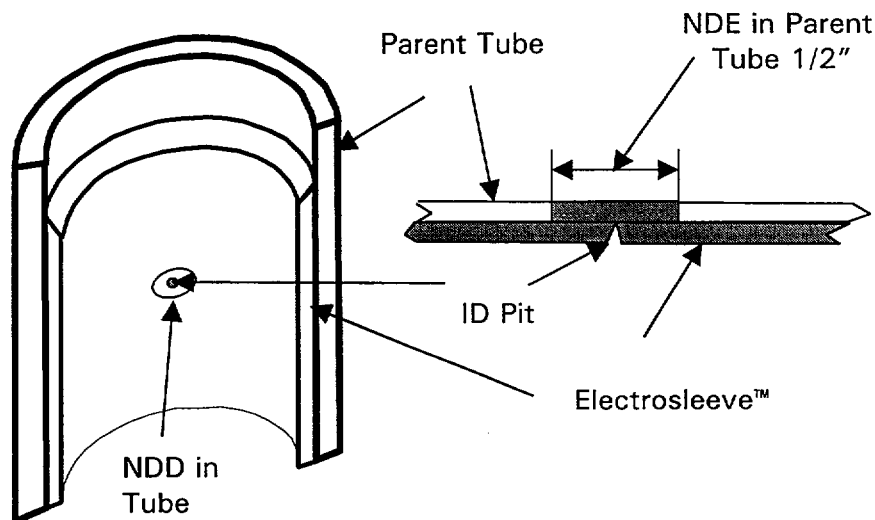
- (1) Note that the circumferential extent for degradation at tubes adjacent to the TSP vertical supports (Figure 8.2.1) is limited as discussed in Section 8.5.
- (2) The inspection interval used in this table was 18 months.

12.2.2 Sleeve ID Pitting

The electroforming process may produce an ID pit during Electrosleeve™ installation (Section 11.8.4). An ID pit is assumed to be 100% through the sleeve thickness. The inspection requirements for a sleeve ID pit specify a high probability (Table 11.10.1) of detection for pit diameters greater than []^{b,c}. A 1/4-inch bond width between any through-wall tube degradation and a sleeve ID pit is required to preclude the potential for any leakage. Figure 12.2.1 presents a schematic of an ID pit.

A sleeve with an ID pit will be plugged if a tube defect exists within 1/2 inch of the ID pit and the tube defect has the potential to become coincident with a sleeve ID pit. For example, a small circumferential crack at the TTS would be expected to grow circumferentially, but not axially. Table 12.4.2 lists the requirements for sleeve ID pits.

Figure 12.2.1 Schematic of ID Pit



12.2.3 Sleeve-to-Tube Disbond

Reference 13.4 specifies the installation NDE requirements for disbond. All disbond areas greater than []^{c,d,e} in any direction in Region B require an evaluation and concurrence from the plant owner for acceptability. Disbond areas greater than []^{c,d,e} in any direction in Region B are unacceptable. Table 12.4.2 lists the requirements for disbond.

12.3 Repair Limit for Cracking Degradation

The results of the Electrosleeve™ corrosion testing program and the use of nickel as a repair in Europe and Canada indicate the likelihood of a true crack-like flaw propagating into the sleeve material by corrosive attack is extremely low. However, plant safety requires validation of this low probability characteristic through in-service inspection. The most restrictive structural limit for a crack mechanism in the Electrosleeve™, as detailed in Table 8.5.3, is an axial crack greater than 0.75 inch long or a circumferential crack of 360° extent.

The assumed growth rate for postulated cracking degradation is 0% per cycle until detected, which is the same as the growth rates for other currently non-demonstrated (postulated) degradation modes. However, crack growth may occur due to fatigue. A conservative upper limit for fatigue crack growth, based on fracture mechanics analysis (Section 8.5), is 2.0% of the sleeve nominal thickness during an 18-month inspection interval. The 2.0% growth rate is used for all sleeve nominal thickness values.

The 95% LCL and the UT sizing RMSE (Table 11.10.2) for shear wave examination of a sleeved tube are -0.008 inch and 0.008 inch, respectively. The repair limits for a sleeve experiencing a cracking degradation mechanism, based on the RMSE and the 95% LCL are summarized in Tables 12.3.1 and 12.3.2, respectively.

TABLE 12.3.1
RMSE REPAIR LIMITS FOR
AXIAL CRACKS > 3/4"⁽²⁾ and 360° CIRCUMFERENTIAL CRACKS⁽¹⁾

Tube OD x Thickness (inch)	Allowed Structural Degradation (Sleeve Wall)		UT RMSE (Sleeve Wall)		Growth During Inspection Interval ⁽³⁾ (Sleeve Wall)		Repair Limit (Sleeve Wall)	
	(%)	(mils)	(%)	(mils)	(%)	(mils)	(%)	(mils)
11/16 x 0.040	17	4, e 7	25.8	8	17			4, e 7
3/4 x 0.042/0.043			23.5	8				
3/4 x 0.048			23.5	8				
7/8 x 0.050	L	J	21.1	8	L			J

NOTES:

- (1) Note that the circumferential extent for degradation at tubes adjacent to the TSP vertical supports (Figure 8.2.1) is limited as discussed in Section 8.5.
- (2) An additional reduction in the structural limit occurs when the axial crack length exceeds two inches.
- (3) The inspection interval used in this table was 18 months.

TABLE 12.3.2
95% LCL REPAIR LIMITS FOR
AXIAL CRACKS > 3/4"⁽²⁾ and 360° CIRCUMFERENTIAL CRACKS⁽¹⁾

Tube OD x Thickness (inch)	Allowed Structural Degradation (Sleeve Wall)		UT Error 95% LCL (Sleeve Wall)		Growth During Inspection Interval ⁽³⁾ (Sleeve Wall)		Repair Limit (Sleeve Wall)	
	(%)	(mils)	(%)	(mils)	(%)	(mils)	(%)	(mils)
11/16 x 0.040	17	4, e 7	25.8	8	17			4, e 7
3/4 x 0.042/0.043			23.5	8				
3/4 x 0.048			23.5	8				
7/8 x 0.050	L	J	21.1	8	L			J

NOTES:

- (1) Note that the circumferential extent for degradation at tubes adjacent to the TSP vertical supports (Figure 8.2.1) is limited as discussed in Section 8.5.
- (2) An additional reduction in the structural limit occurs when the axial crack length exceeds two inches.
- (3) The inspection interval used in this table was 18 months.

12.4 Electrosleeve™ Plugging Limits

The Electrosleeve™ plugging limit is conservatively set at 30% through-wall of the sleeve nominal thickness. The minimum repair limits for all tube and sleeve nominal thickness values, based on the UT uncertainty, from the conventional crack sizing and thickness UT techniques are listed in Table 12.4.1.

TABLE 12.4.1
MINIMUM REPAIR LIMITS USING EPRI APPENDIX J TECHNIQUES

CONVENTIONAL SIZING ERROR CALCULATION	MINIMUM REPAIR LIMIT (% THROUGH-WALL SLEEVE)	REFERENCED TABLE
Crack Sizing RMSE	49.3	12.3.1
Crack Sizing 95% LCL	49.3	12.3.2
Uniform Thinning 95% LCL	37.0	12.4.4

The minimum repair limit is 37.0% through-wall of the sleeve nominal thickness based on uniform thinning. Therefore, the Electrosleeve™ plugging limit of 30% through-wall of the sleeve nominal thickness has adequate margin to allow for both flaw growth and the UT 95% LCL. The 30% through-wall Electrosleeve™ plugging limit also applies to the tubes adjacent to the TSP vertical supports (Figure 8.2.1); however, the circumferential extent for any degradation is limited as discussed in Section 8.5.

The 30% plugging limit includes margin for the errors and growth associated with UT qualified sizing techniques.

Table 12.4.2 is a summary of the Electrosleeve™ plugging limits based on the criteria discussed in this section. Tables 12.4.3 and 12.4.4 summarize the repair limits for each tube size using the sizing RMSE and 95% LCL of the qualified UT techniques, respectively.

TABLE 12.4.2
ELECTROSLEEVE™ PLUGGING LIMITS

REGION ⁽⁴⁾	COMPONENT	ELECTROSLEEVE™ and TUBE PLUGGING LIMIT (Based on UT Measurement)
A	TUBE	<ul style="list-style-type: none"> Plant technical specification requirements
	SLEEVE ⁽¹⁾	<ul style="list-style-type: none"> All indications are acceptable⁽²⁾⁽³⁾
B	TUBE	<ul style="list-style-type: none"> Plant technical specification requirements
	SLEEVE ⁽¹⁾	<ul style="list-style-type: none"> Indication (except ID pit) $\geq 30\%$ through-wall Minimum bond [3%] Disbond [6%] in any dimension⁽²⁾⁽³⁾ Thickness (installation NDE only)⁽²⁾
C	TUBE	<ul style="list-style-type: none"> All Indications are acceptable <hr/> (Special Evaluation or Contingency Resolutions) ⁽²⁾ <ul style="list-style-type: none"> Plant technical specification requirements, see Appendix B.
	SLEEVE ⁽¹⁾	<ul style="list-style-type: none"> Indication (except ID pit) $> 30\%$ through-wall ID pit 100% through-wall and [3%] from any through-wall tube defect(s) whose growth may result in coincidence ID pit 100% through-wall without a [3%] bond between the pit and any through-wall tube defect(s) Thickness (installation NDE only)⁽²⁾

NOTES:

- (1) % through-wall corresponds to the Electrosleeve™ nominal thickness.
- (2) A non-conformance report (NCR) resolution with the concurrence of the plant owner is required to justify acceptability of sleeves for service with violations in the installation process, e.g., minimum thickness and disbond limit violations or the occurrence of ID pits or nodules in the sleeve.
- (3) Disbond growth detected during subsequent ISI inspection(s) requires a safety evaluation with the concurrence of the plant owner to justify continued service.
- (4) See Figure 11.1.1 for definition of Regions A, B and C.

TABLE 12.4.3
REPAIR LIMIT BASED ON UT SIZING RMSE

[^{b,c,e} 11/16" OD X 0.040" TUBE
] NOMINAL ELECTROSLEEVE™ THICKNESS

Electrosleeve™ Degradation Type (Includes 100% Through-Wall Degradation in Tube)	Allowed Structural Degradation (Sleeve Wall)		UT RMSE (Sleeve Wall)		Growth During Inspection Interval ⁽³⁾ (Sleeve Wall)		Repair Limit (Sleeve Wall)	
	(%)	(mils)	(%)	(mils)	(%)	(mils)	(%)	(mils)
Uniform Thinning ⁽¹⁾	45.0	14.0	3.2	1	✓			b,c,d,e
OD Pitting	✓	b,c,d,e	9.7	3				
Axial Crack ≤ 3/4"			25.8	8				
Axial Crack > 3/4" ⁽²⁾			25.8	8				
360° Circumferential Crack ⁽¹⁾	L	-1	25.8	8	L			-1

[^{b,c,e} 3/4" OD X 0.042"/0.043" TUBE
] NOMINAL ELECTROSLEEVE™ THICKNESS

Electrosleeve™ Degradation Type (Includes 100% Through-Wall Degradation in Tube)	Allowed Structural Degradation (Sleeve Wall)		UT RMSE (Sleeve Wall)		Growth During Inspection Interval ⁽³⁾ (Sleeve Wall)		Repair Limit (Sleeve Wall)	
	(%)	(mils)	(%)	(mils)	(%)	(mils)	(%)	(mils)
Uniform Thinning ⁽¹⁾	45.0	15.3	2.9	1	✓			b,c,d,e
OD Pitting	✓	b,c,d,e	8.8	3				
Axial Crack ≤ 3/4"			23.5	8				
Axial Crack > 3/4" ⁽²⁾			23.5	8				
360° Circumferential Crack ⁽¹⁾	L	J	23.5	8	L			J

NOTES:

- (1) Note that the circumferential extent for degradation at tubes adjacent to the TSP vertical supports (Figure 8.2.1) is limited as discussed in Section 8.5.
- (2) An additional reduction in the structural limit occurs when the axial crack length exceeds two inches.
- (3) The inspection interval used in this table was 18 months.

TABLE 12.4.3 (Cont'd)
REPAIR LIMIT BASED ON UT SIZING RMSE

[^{b,c,e} 3/4" OD X 0.048" TUBE
] NOMINAL ELECTROSLEEVE™ THICKNESS

Electrosleeve™ Degradation Type (Includes 100% Through-Wall Degradation in Tube)	Allowed Structural Degradation (Sleeve Wall)		UT RMSE (Sleeve Wall)		Growth During Inspection Interval ⁽³⁾ (Sleeve Wall)		Repair Limit (Sleeve Wall)	
	(%)	(mils)	(%)	(mils)	(%)	(mils)	(%)	(mils)
Uniform Thinning ⁽¹⁾	45.0	15.3	2.9	1	┌			^{b,c,d,e} ┐
OD Pitting	┌	^{b,c,d,e} ┐	8.8	3				
Axial Crack ≤ 3/4"			23.5	8				
Axial Crack > 3/4" ⁽²⁾			23.5	8				
360° Circumferential Crack ⁽¹⁾	└	┘	23.5	8	└			┘

[^{b,c,e} 7/8" OD X 0.050" TUBE
] NOMINAL ELECTROSLEEVE™ THICKNESS

Electrosleeve™ Degradation Type (Includes 100% Through-Wall Degradation in Tube)	Allowed Structural Degradation (Sleeve Wall)		UT RMSE (Sleeve Wall)		Growth During Inspection Interval ⁽³⁾ (Sleeve Wall)		Repair Limit (Sleeve Wall)	
	(%)	(mils)	(%)	(mils)	(%)	(mils)	(%)	(mils)
Uniform Thinning ⁽¹⁾	45.0	17.1	2.6	1	┌			^{b,c,d,e} ┐
OD Pitting	┌	^{b,c,d,e} ┐	7.9	3				
Axial Crack ≤ 3/4"			21.1	8				
Axial Crack > 3/4" ⁽²⁾			21.1	8				
360° Circumferential Crack ⁽¹⁾	└	┘	21.1	8	└			┘

NOTES:

- (1) Note that the circumferential extent for degradation at tubes adjacent to the TSP vertical supports (Figure 8.2.1) is limited as discussed in Section 8.5.
- (2) An additional reduction in the structural limit occurs when the axial crack length exceeds two inches.
- (3) The inspection interval used in this table was 18 months.

TABLE 12.4.4
REPAIR LIMIT BASED ON UT 95% LCL

[^{b,c,e} 11/16" OD X 0.040" TUBE
] NOMINAL ELECTROSLEEVE™ THICKNESS

Electrosleeve™ Degradation Type (Includes 100% Through-Wall Degradation in Tube)	Allowed Structural Degradation (Sleeve Wall)		UT 95% LCL (Sleeve Wall)		Growth During Inspection Interval ⁽³⁾ (Sleeve Wall)		Repair Limit (Sleeve Wall)	
	(%)	(mils)	(%)	(mils)	(%)	(mils)	(%)	(mils)
Uniform Thinning ⁽¹⁾	45.0	14.0	3.2	1	Γ			^{b,c,d,e} Γ
OD Pitting	Γ	^{b,c,d,e} Γ	16.1	5				
Axial Crack ≤ 3/4"			25.8	8				
Axial Crack > 3/4" ⁽²⁾			25.8	8				
360° Circumferential Crack ⁽¹⁾	L	↓	25.8	8	L			L

[^{b,c,e} 3/4" OD X 0.042"/0.043" TUBE
] NOMINAL ELECTROSLEEVE™ THICKNESS

Electrosleeve™ Degradation Type (Includes 100% Through-Wall Degradation in Tube)	Allowed Structural Degradation (Sleeve Wall)		UT 95% LCL (Sleeve Wall)		Growth During Inspection Interval ⁽³⁾ (Sleeve Wall)		Repair Limit (Sleeve Wall)	
	(%)	(mils)	(%)	(mils)	(%)	(mils)	(%)	(mils)
Uniform Thinning ⁽¹⁾	45.0	15.3	2.9	1				
OD Pitting	Γ	^{b,c,d,e} Γ	14.7	5				
Axial Crack ≤ 3/4"			23.5	8				
Axial Crack > 3/4" ⁽²⁾			23.5	8				
360° Circumferential Crack ⁽¹⁾	L	↓	23.5	8				

NOTES:

- (1) Note that the circumferential extent for degradation at tubes adjacent to the TSP vertical supports (Figure 8.2.1) is limited as discussed in Section 8.5.
- (2) An additional reduction in the structural limit occurs when the axial crack length exceeds two inches.
- (3) The inspection interval used in this table was 18 months.

TABLE 12.4.4 (Cont'd)
REPAIR LIMIT BASED ON UT 95% LCL

b, c, e 3/4" OD X 0.048" TUBE
] NOMINAL ELECTROSLEEVE™ THICKNESS

Electrosleeve™ Degradation Type (Includes 100% Through-Wall Degradation in Tube)	Allowed Structural Degradation (Sleeve Wall)		UT 95% LCL (Sleeve Wall)		Growth During Inspection Interval ⁽³⁾ (Sleeve Wall)		Repair Limit (Sleeve Wall)	
	(%)	(mils)	(%)	(mils)	(%)	(mils)	(%)	(mils)
Uniform Thinning ⁽¹⁾	45.0	15.3	2.9	1	┌			<i>b, c, d, e</i> ┐
OD Pitting	┌	<i>b, c, d, e</i> ┐	14.7	5				
Axial Crack ≤ 3/4"			23.5	8				
Axial Crack > 3/4" ⁽²⁾			23.5	8				
360° Circumferential Crack ⁽¹⁾	└	└	23.5	8	└			└

b, c, e 7/8" OD X 0.050" TUBE
] NOMINAL ELECTROSLEEVE™ THICKNESS

Electrosleeve™ Degradation Type (Includes 100% Through-Wall Degradation in Tube)	Allowed Structural Degradation (Sleeve Wall)		UT 95% LCL (Sleeve Wall)		Growth During Inspection Interval ⁽³⁾ (Sleeve Wall)		Repair Limit (Sleeve Wall)	
	(%)	(mils)	(%)	(mils)	(%)	(mils)	(%)	(mils)
Uniform Thinning ⁽¹⁾	45.0	17.1	2.6	1	┌			<i>b, c, d, e</i> ┐
OD Pitting	┌	<i>b, c, d, e</i> ┐	13.2	5				
Axial Crack ≤ 3/4"			21.1	8				
Axial Crack > 3/4" ⁽²⁾			21.1	8				
360° Circumferential Crack ⁽¹⁾	└	└	21.1	8	└			└

NOTES:

- (1) Note that the circumferential extent for degradation at tubes adjacent to the TSP vertical supports (Figure 8.2.1) is limited as discussed in Section 8.5.
- (2) An additional reduction in the structural limit occurs when the axial crack length exceeds two inches.
- (3) The inspection interval used in this table was 18 months.

13.0 REFERENCES

- 13.1 ASME Boiler and Pressure Vessel Code, Section II, 1989 Edition with 1989 Addenda.
- 13.2 ASME Boiler and Pressure Vessel Code, Section III and Section III Appendices, 1989 Edition with No Addenda.
- 13.3 ASME Boiler and Pressure Vessel Code, Section V, 1992 Edition with 1993 Addenda.
- 13.4 ASME Boiler and Pressure Vessel Code, Section XI, 1989 Edition with 1989 Addenda and Code Case N-569-1, "Alternative Rules for Repair by Electrochemical Deposition of Class 1 and 2 Steam Generator Tubing," Section XI, Division 1.
- 13.5 ASME Boiler and Pressure Vessel Code, Code Case N-47-33, "Class 1 Components in Elevated Temperature Service."
- 13.6 USNRC Draft Regulatory Guide 1.121, "Bases for Plugging Degraded PWR Steam Generator Tubes."
- 13.7 ASME Code Case N-504-1, "Alternative Rules for Repair of Class 1, 2, and 3 Austenitic Stainless Steel Piping."
- 13.8 F.P. Vacaro, et al, "Remedial Measures for Stress Corrosion Cracking of Alloy 600 Steam Generator Tubing," presented at Traverse City Third International Symposium on Environmental Degradation of Materials in Nuclear Power Systems - Water Reactors, September 1987.
- 13.9 J.E. Gutzwiller, S.W. Glass, "New Options for Improved Steam Generator U-Bend Integrity," presented at the SMIRT 9, post-conference seminar on Assuring Structural Integrity of Steel Reactor Pressure Boundary Components, Davos, Switzerland, August 1987.
- 13.10 EPRI Utility Experience Report, Electronucleaire Utility, Plants: Tihange 1, 2, 3, and Doel 1, 2, 3, 4, June 1987.
- 13.11 EPRI Steam Generator Tube Sleeving: Design, Specification and Procurement Checklist, Research Project S408-5, Topical Report December 1989.

- 13.12 EPRI TR-103824, Project 2859, Steam Generator Reference Book, Revision 1, December 1994.
- 13.13 ASTM E 8-93, "Standard Test Methods for Tension Testing of Metallic Materials."
- 13.14 ASTM E 21-92, "Standard Test Methods for Elevated Temperature Tension Testing of Metallic Materials."
- 13.15 ASTM E 111-82, "Standard Test Method for Young's Modulus, Tangent Modulus, and Chord Modulus."
- 13.16 ASTM E 606-92, "Standard Practice for Strain-Controlled Fatigue Testing."
- 13.17 ASTM E 466-82, "Standard Practice for Conducting Constant Amplitude Axial Fatigue Tests of Metallic Materials."
- 13.18 ASTM E 467-90, "Standard Practice for Verification of Constant Amplitude Dynamic Loads on Displacements in an Axial Load Fatigue Testing System."
- 13.19 ASTM E 468-90, "Standard Practice for Presentation of Constant Amplitude Fatigue Test Results for Metallic Materials."
- 13.20 ASTM E 290-92, "Standard Test Method for Semi-Guided Bend Test for Ductility of Metallic Materials."
- 13.21 ASTM B 489-85, "Standard Practice for Bend Test for Ductility of Electrodeposited and Autocatalytically Deposited Metal Coatings on Metals."
- 13.22 ASTM E 139-83, "Standard Practice for Conducting Creep, Creep-Rupture, and Stress-Rupture Tests of Metallic Materials."
- 13.23 ASTM E 92-82, "Standard Test Method for Vickers Hardness of Metallic Materials."
- 13.24 ASTM G 28-85, "Standard Test Methods of Detecting Susceptibility to Intergranular Corrosion in Wrought, Nickel-Rich, Chromium-Bearing Alloys."

- 13.25 ASTM G 35-88, "Standard Practice for Determining the Susceptibility of Stainless Steels and Related Nickel-Chromium-Iron Alloys to Stress-Corrosion Cracking in Polythionic Acids."
- 13.26 ASTM G 36-87, "Standard Practice for Evaluating Stress Corrosion Cracking Resistance of Metals and Alloys in a Boiling Magnesium Chloride Solution."
- 13.27 ASTM G 44-88, "Standard Practice for Evaluating Stress Corrosion Cracking Resistance of Metals and Alloys by Alternate Immersion in 3.5% Sodium Chloride Solution."
- 13.28 ASTM G 48-93, "Standard Test Methods for Pitting and Crevice Corrosion Resistance of Stainless Steels and Related Alloys by Use of Ferric Chloride Solution."
- 13.29 ASME TJ290.A716, 1976, "Criteria for Design of Elevated Temperature Class 1 Components in Section III, Division 1, of the ASME Boiler and Pressure Vessel Code."
- 13.30 L.N. Bystrov and A.B. Tsepelev, "Thermal Activation Analysis of Nickel Creep in the Temperature Range 200-500°C," *Izvestiya Akademii Nauk SSSR, Metally*, Allerton Press, Inc, No. 4, pp. 171-178, 1984.
- 13.31 Paul Shaninian and M.R. Achter, "Temperature and Stress Dependence of the Atmosphere Effect on Nickel-Chromium Alloy," pp. 244-250, *Transactions of American Society of Metals*, Vol LI, 1959. Ray T. Bayless, Editor, American Society of Metals, Cleveland, Ohio.
- 13.32 ANSYS Finite Element Code, Version 5.2.
- 13.33 Tibor Turi and Uwe Erb, "Thermal Expansion and Heat Capacity of Porosity-Free Nanocrystalline Materials," *Material Science & Engineering*, Volume A204, p. 34, 1995.
- 13.34 "Code for Pressure Piping, Nuclear Power Piping, USAS B31.7, DRAFT USA STANDARD," Published by ASME February 1968.
- 13.35 F.C. Monkman and N.J. Grant, "An Empirical Relationship Between Rupture Life and Minimum Creep Rate in Creep-Rupture Tests," *Proc. ASTM*, Volume 56, pp. 593-605, 1956.

- 13.36 H.R. Voohees, "Assessment and Use of Creep-Rupture Properties," Metals Handbook - Ninth Edition, Volume 8, Mechanical Testing, American Society for Metals, 1985.
- 13.37 D.B. Darling and J.A. Richards, III, "Nickel Plating of Pressurizer Heater Nozzles to Prevent PWSCC," Nuclear Plant Journal, November-December 1994.
- 13.38 R.K. Penny and D.L. Marriott, Design for Creep 2nd Edition, Chapman & Hall, 1995.
- 13.39 B. Michaut, F. Steltzlen, B. Sala, Ch. Laire, J. Stubbe, "Nickel Electroplating as a Remedy to Steam Generator Tubing PWSCC," Sixth International Symposium on Environmental Degradation of Materials in Nuclear Power Systems - Water Reactors, The Minerals, Metals, & Materials Society, 1993.
- 13.40 U. Erb, "Corrosion Behaviour of Nanocrystalline Materials - A Literature Review," 1996, Department of Materials & Metallurgical Engineering, Queens University, Kingston, Ontario, Canada.
- 13.41 PWR Secondary Water Chemistry Guideline - Revision 3, EPRI TR-102134 Revision 3, May 1993.
- 13.42 MULTEQ: Equilibrium of an Electrolytic Solution with Vapor-Liquid Partitioning and Precipitation, EPRI NP-5561-CCML, July 1992.
- 13.43 E. Pierson, J. Stubbe, "SCC Testing of Steam Generator Tubes Repaired by Welding Sleeves," Sixth International Symposium on Environmental Degradation of Materials in Nuclear Power Systems - Water Reactors, The Minerals, Metals & Materials Society, 1993.
- 13.44 M.H. Kaye, W.T. Thompson, "Nickel-Phosphorus Redox Potential-pH Diagrams," Centre for Computational Thermochemistry, Kingston, ON, Canada, 1996.
- 13.45 Z. Yang, T.H. Yip, R. Zhang and D.D. Perovic, "Effect of Grain Size on the Initiation and Growth of Fatigue Cracks in Nickel and Nickel-based Alloys."

- 13.46 Ning Wang, Zhirui Wang, K.T. Auld and U. Erb, *Aust. Acta Metall.*, "Effect of Grain Size on Mechanical Properties of Nanocrystalline Materials," Vol. 43, No. 2, 1995.
- 13.47 G. Palumbo, F. Gonzalez, V. Krstic and U. Erb, *Scripta Metall.*, "Geometric Considerations for the Creep Failure of Nanostructured Materials."
- 13.48 V. Sugimura, P.G. Lim, C.F. Shih and S. Suresh, *Acta Metallurgica*, 1995.
- 13.49 D. R. Diericks and W. J. Shack, "Technical Letter Report on Corrosion Behavior of Electrosleeve™ Repair Materials in Steam Generator Environments," Argonne National Laboratory, (Joseph Muscara, Program Manager, US NRC Office of Nuclear Reactor Research), July 1, 1998.
- 13.50 P. Marcus and O. Oda, "Influence du phosphore sur la dissolution et la passivation du nickel en milieu acide," *Mem. Sci. Rev. Metall.* 715, (1979).
- 13.51 F. Gonzalez and P. Spekkens, "Localized concentration processes and corrosion in nuclear steam generators," 9th International Congress on Metallic Corrosion v.3, p. 235 (1984).
- 13.52 F. Gonzalez and P. Spekkens. "Corrosion of Alloy 600 under Steam Generator Sludge Piles," 4th Symp. on Environ. Degr. of Mater. in Nucl. Power Systems Water Reactors, Jekyll Island 1989.
- 13.53 F. Gonzalez and P. King, "Corrosion Performance of Alloy 800 Tubing under CANDU Steam Generator Conditions," International Symposium Contribution of Materials Investigation to the Resolution of Problems Encountered in PWR Plants, Fontevraud, France, Sept 10-14, 1990.
- 13.54 F. Gonzalez and P. Spekkens, "Concentration processes under tubesheet sludge pile in nuclear steam generators," Proceedings of the Water Chemistry and Materials Performance Conference, Oct 21, 1986 Toronto, Canada, also published in *Nuclear Journal of Canada* 1, 129-140 (1987).
- 13.55 J.B. Lumsden, S.L. Jeanjaquet, A. McIlree, "Insights on Local Chemistry from Examination of Tubes," Imp. The Unstanding and Control of Corrosion on the Secondary Side of SG, October 9-13, 1995, Airlie, VA.

- 13.56 F. Larue, A. Gelpi, B. Michaut, "Nickel Plating S.G. Tubing Repair," Proceedings of the 1991 JAIF International Conference on Water Chemistry in Nuclear Power Plants, Japan Atomic Industrial Forum, Inc., April 1991, pp. 163-167.
- 13.57 M.G. Fontana, "Corrosion Engineering," McGraw Hill, Third Edition, 1986, pp. 134-135.
- 13.58 G.F. Nejedlik and E.G. Vargo, "Material Resistance to Mercury Corrosion," *Electrochemical Technology*, 3:250 (1965).
- 13.59 ASTM G 38-73 "Standard Practice for Making and Using C-Ring Stress Corrosion Test Specimens."
- 13.60 E.O. Hall, "The Deformation and Aging of Mild Steel: III Discussion of Results," *Proc. Phys. Soc. London* B64, pp. 747-753, (1951).
- 13.61 N.J. Petch, "The Cleavage Strength of Polycrystals," *Journal of the Iron and Steel Institute*, 174, pp. 25-28, (1953).
- 13.62 D. Osmola, P. Nolan, U. Erb, G. Palumbo, and K.T. Aust, "Microstructural Evolution at Large Driving Forces during Grain Growth of Ultrafine-Grained Ni-1.2wt%P," *Phys. Stat. Sol. (a)* 131, pp. 569-574, (1992).
- 13.63 K. Boylan, D. Ostrander, U. Erb, G. Palumbo, and K.T. Aust, "An In-Situ Tem Study of the Thermal Stability of Nanocrystalline Ni-P," *Scripta Metallurgica, et Materialia*, Vol. 25, pp. 2711-2716, (1991).
- 13.64 H.E. Kissinger, "Reaction Kinetics in Differential Thermal Analysis," *Analytical Chemistry*, Vol. 29, pp. 1702-1706, (1957).
- 13.65 S.C. Mehta, D.A. Smith, and U. Erb, "Study of grain growth in electrodeposited nanocrystalline nickel-1.2wt% phosphorus alloy," *Materials Science and Engineering*, A204, pp. 227-232, (1995).
- 13.66 M. Ratzker, D.S. Lashmore, and K.W. Pratt, "Electrodeposition and Corrosion Performance of Nickel-Phosphorus Amorphous Alloys," *Plating and Surface Finishing*, September 1986 pp. 74-82.

- 13.67 G.W. Dini, "Electrodeposition, The Materials Science of Coatings and Substrates," Noyes Publications, Park Ridge New Jersey, 1993.
- 13.68 R.F. Keating, P. Hernalsteen, and J.A. Begley, "EPRI Guidelines for Laboratory Measurements of the Burst Strength of Degraded Steam Generator Tubing."
- 13.69 Ch. Claire, E. Pierson, G. Strubbe "Belgium Experience on Repair of Steam Generator Tubes," EUROCORR '96, Nice, September 23, 1996.
- 13.70 C.F. Andreone, S. Yokell, Tubular Heat Exchanger Inspection, Maintenance and Repair, McGraw Hill, 1998, p. 311.
- 13.71 NUREG/CR-6227, PNNL-9433 "Performance Demonstration Tests for Eddy Current Inspection of Steam Generator Tubing," Pacific Northwest Laboratory, May 1996.
- 13.72 F.Krautkramer and H. Krautkramer, Ultrasonic Testing of Materials, 4th Edition, Springer-Verlag, 1990.
- 13.73 Draft EPRI Report TR-105505, "Burst Pressure Correlation for Steam Generator Tubes with Through-Wall Axial Cracks," February 1995.
- 13.74 C.S. Smith, "Grains, Phases, and Interfaces: An Interpretation of Microstructure," p. 47, Trans. AIME, 175, 15 (1948).
- 13.75 USNRC Draft Regulatory Guide DG-1074, "Steam Generator Tube Integrity."
- 13.76 ETSS#: 98-400, "FTI UT-360® Examinations. Detection and sizing of outer diameter pits located in seamless tubing," August 13, 1999.
- 13.77 ETSS#: 98-401, "FTI UT-360® Examinations. Detection and sizing of dented regions located in seamless tubing," August 13, 1999.
- 13.78 ETSS#: 98-402, "FTI UT-360® Examinations. Detection and sizing of outer diameter pits located in the Electrosleeve™," August 13, 1999..
- 13.79 ETSS#: 98-403, "FTI UT-360® Examinations. Detection and sizing of disbanded regions between Inconel 600 and Electrosleeve™," August 13, 1999.
- 13.80 ETSS#: 98-404, "FTI UT-360® Examinations. Detection of pitting located in the Electrosleeve™ ID surface," August 13, 1999.

- 13.81 ETSS#: 98-302, "FTI UT-360® Examinations. Detection and extent sizing of outer diameter stress corrosion cracking (ODSCC) in parent tubing," September 1, 2000.
- 13.82 ETSS#: 98-303, "FTI UT-360® Examinations. Detection and Depth sizing of outer diameter stress corrosion cracking (ODSCC) in parent tubing," December 5, 2000.
- 13.83 "Pressure and Leak-Rate Tests and Models for Predicting Failure of Flawed Steam Generator Tubes", prepared by Argonne National Laboratory for U.S. NRC, Office of Nuclear Regulatory Research, NUREG/CR-6664 ANL-99/23 August 2000.
- 13.84 ASNT, Nondestructive Testing Handbook, Ultrasonic Testing, Second Edition, Volume Seven, 1991, p. 578.
- 13.85 Ogilvy, J. A. and J. A. G. Temple, "Diffraction of Elastic Waves by Crack: Application to Time-of-Flight Inspection," Ultrasonic, November 1983, p. 260-269.

APPENDIX A

PWR DESIGN INFORMATION

TABLE A.1
W-D DESIGN INFORMATION

b,c,e
└

└

└

└

TABLE A.1 (Cont'd)
W-D DESIGN INFORMATION

b, c, e
└

└

└

└

TABLE A.1 (Cont'd)
W-D DESIGN INFORMATION

b, c, e
7

┌

└

└

TABLE A.1 (Cont'd)
W-D DESIGN INFORMATION

b, c, e }
}

┌

└

└

TABLE A.2
W-E DESIGN INFORMATION

b,c,e
└

└

L

└

TABLE A.2 (Cont'd)
W-E DESIGN INFORMATION

b, c, e
7

┌

L

└

TABLE A.2 (Cont'd)
W-E DESIGN INFORMATION

b,c,e

TABLE A.2 (Cont'd)
W-E DESIGN INFORMATION

b, c, e
7

┌

└

└

TABLE A.3
CE SYS 80 DESIGN INFORMATION

b, c, e

┌

└

┌

└

TABLE A.3 (Cont'd)
CE SYS 80 DESIGN INFORMATION

b, c, e

TABLE A.3 (Cont'd)
CE SYS 80 DESIGN INFORMATION

b, c, e
7

┌

└

└

TABLE A.4
WESTINGHOUSE 7/8" TUBING S/G DESIGN INFORMATION

b,c,e
└

└

L

└

TABLE A.4 (Cont'd)
WESTINGHOUSE 7/8" TUBING S/G DESIGN INFORMATION

b,c,e

┌

└

TABLE A.4 (Cont'd)
WESTINGHOUSE 7/8" TUBING S/G DESIGN INFORMATION

b, c, e

┌

└

└

TABLE A.4 (Cont'd)
WESTINGHOUSE 7/8" TUBING S/G DESIGN INFORMATION

b, c, e

┌

└

└

TABLE A.4 (Cont'd)
WESTINGHOUSE 7/8" S/G TUBING DESIGN INFORMATION

b,c,e
└

└

L

└

TABLE A.5
COMBUSTION ENGINEERING 3/4" x 0.048" TUBING S/G DESIGN INFORMATION

b,c,e
7

7

L

7

TABLE A.5 (Cont'd)
COMBUSTION ENGINEERING 3/4" x 0.048" TUBING S/G DESIGN INFORMATION

b,c,e
└

└

L

└

TABLE A.5 (Cont'd)
COMBUSTION ENGINEERING 3/4" x 0.048" TUBING S/G DESIGN INFORMATION

b,c,e
└

└

L

└

TABLE A.5 (Cont'd)
COMBUSTION ENGINEERING 3/4" x 0.048" TUBING S/G DESIGN INFORMATION

b,c,e
7

7

L

1

TABLE A.5 (Cont'd)
COMBUSTION ENGINEERING 3/4" x 0.048" TUBING S/G DESIGN INFORMATION

b,c,e
└

└

L

└

TABLE A.5 (Cont'd)
COMBUSTION ENGINEERING 3/4" x 0.048" TUBING S/G DESIGN INFORMATION

b, c, e
7

7

L

TABLE A.5 (Cont'd)
COMBUSTION ENGINEERING 3/4" x 0.048" TUBING S/G DESIGN INFORMATION

┌

b,c,e
└

┌

└

TABLE A.6
W-F DESIGN INFORMATION

b,c,e
└

└

L

└

TABLE A.6 (Cont'd)
W-F DESIGN INFORMATION

b, c, e

┌

└

└

TABLE A.6 (Cont'd)
W-F DESIGN INFORMATION

b,c,e 7

TABLE A.6 (Cont'd)
W-F DESIGN INFORMATION

b, c, e
7

┌

└

└

APPENDIX B

SITE SPECIFIC

LICENSING AMENDMENT REQUEST

SUMMARY

APPENDIX B**Site Specific Licensing Amendment Request Summary**

The design, structural analysis, installation process, corrosion resistance, inspection, and repair criteria for the Electrosleeve™ have been presented in this report for a range of tube sizes and plant operating conditions as defined in Section A. A Licensing Amendment Request (LAR) for a specific plant, which references this topical in the Technical Specification change request, may have unique conditions or plant considerations which have not been specifically addressed in this topical report. The following is a summary of these potential issues that must be considered in the Plant's LAR, if applicable.

- Locked Tube Loads: Allowable circumferential extent of uniform thinning is discussed in Section 8.5 with specific reference to vertical restraints, such as the TSP-to-wrapper support. Thermal transient conditions can produce axial loads in tubes that may be "locked-in" at the tube support due to corrosion products in the tube-to-tube support plate intersection. The tube support-to-wrapper attachment creates a restraint that accentuates the effects of normal thermal transients on tubes adjacent to the TSP support (see Figure 8.2.1). The effect of these loads on an installed Electrosleeve™ must be evaluated if plants plan to install an Electrosleeve™ in potentially locked tubes.
- Sleeve ID Pits Formed During Installation: The parent tube must be present for the installation of an Electrosleeve™. Therefore, the parent tube has some pressure boundary capability. If an Electrosleeve™ with fabrication induced ID sleeve pitting is left in service, it should be identified as a special interest inspection sleeve. The plugging criteria is defined in Section 12.2.2 and Table 12.4.2. Continued inspection of the sleeve is required in order to show that the plugging criteria continues to be satisfied, because of the potential for defect growth in the tube near the ID sleeve pit. Plant specific in-service inspection programs must address this special inspection issue.

- Sleeve Plugging Limits: Sleeve degradation plugging limits associated with OD cracking: The justification presented in Section 12 recommends a 30% OD crack depth into the sleeve wall as the plugging criteria for any installed sleeve, which is based on the worst case installation location allowed by this topical report. Plant specific recommendations may supplement this criteria based on location of the installed sleeve and the identified tube degradation mechanism.

For example; sleeve installations at the top-of-tubesheet have specific transition geometry and historical data relative to crack length which may be used to justify a higher plugging margin.

- Accident Conditions Beyond Design Basis: The design conditions for the Electrosleeve™ presented in this topical report are those that are currently recognized to be in the design basis for the applicable plants. Any potential plant specific accident conditions that are not in the current design basis must be evaluated separately.